

# On the genus *Polypedilum*, subgenus *Collartomyia*, with description of *P. (Col.) baishanzuensis* sp. nov. from Baishanzu Nature Reserve, China (Diptera, Chironomidae)

Chao Song<sup>1</sup>, Binqing Zhu<sup>2</sup>, Wei Liu<sup>3</sup>, Xin Qi<sup>1</sup>

**1** College of Life Sciences, Taizhou University, Taizhou, Zhejiang 318000, China **2** Nanjing Institute of Environmental Sciences, Ministry of Ecology and Environment, Nanjing 210042, Jiangsu, China **3** Lishui Baiyun Ecological Forest Farm, Lishui 323000, Zhejiang, China

Corresponding author: Xin Qi ([qixin0612@tzc.edu.cn](mailto:qixin0612@tzc.edu.cn))

Academic editor: Fabio L. da Silva | Received 18 June 2021 | Accepted 8 September 2021 | Published 22 October 2021

<http://zoobank.org/72D58C2C-3BD7-45EA-BDDE-2D03B9EA4673>

**Citation:** Song C, Zhu B, Liu W, Qi X (2021) On the genus *Polypedilum*, subgenus *Collartomyia*, with description of *P. (Col.) baishanzuensis* sp. nov. from Baishanzu Nature Reserve, China (Diptera, Chironomidae). ZooKeys 1065: 1–12. <https://doi.org/10.3897/zookeys.1065.69870>

## Abstract

A new species of the genus *Polypedilum* Kieffer, 1912 is described from Baishanzu Nature Reserve, China, based on molecular and morphological data. Molecular phylogenetic analysis based on standard barcode sequences confirmed a new clade of *Polypedilum* (*Collartomyia*) species. The new species is easily distinguished from its congeners by a combination of the following morphological characters: membrane of wing with a large spot occupying 70% of the proximal area; tergite without dark brown band pigmentation; tarsi I–V dark brown; superior volsella with three outer lateral setae and six long setae along inner base; inferior volsella with setose tubercles. An updated key to adult males of the subgenus *Collartomyia* is also provided.

## Keywords

Chironominae, *Collartomyia*, DNA barcode, key, morphology, new species, *Polypedilum*, taxonomy

## Introduction

*Polypedilum* Kieffer, 1912 is the largest chironomid genus, with more than 520 known species worldwide. Its subgeneric divisions and phylogeny have always been disputable and intractable (Sæther et al. 2010; Cranston et al. 2016; Yamamoto et al. 2016; Pinho and Silva 2020; Tang et al. 2021). Only two subgenera, *Collartomyia* Goetghebuer, 1936 and *Tripodura* Townes, 1945, form certain monophyletic groups. The subgenus *Collartomyia* was recently recognized by Tang et al. (2021) for the species having wing with a brownish band or dark spots, a well-developed gonocite bulb, split setae usually present on inner margin of gonostylus, including the previous subgenus *Cerobregma* Sæther & Sundal, 1998 and the monotypic genus *Yaethauma* Yamamoto, Yamamoto & Tang, 2018. The subgenus now includes 21 valid species recorded in the Afrotropical, Holarctic, and Oriental regions (Sæther and Sundal 1999; Kobayashi et al. 2003; Zhang and Wang 2005; Zhang et al. 2006; Moubayed-Breil 2007; Tang and Niitsuma 2017; Yamamoto et al. 2018; Lin et al. 2019; Qi et al. 2020; Liu et al. 2021).

DNA barcoding provides an effective and quick tool for species identification and delimitation, and has been proven successful in many different kinds of animals (Herbert et al. 2003). Chironomid researchers around the world have uploaded 3,310 species including 599,223 sequences in the Barcode of Life Database (BOLD) before 16 June, 2021. Barcode sequences are becoming a necessary character for chironomid species identification and new species descriptions (Song et al. 2016, 2018; Lin et al. 2018, 2020; Makarchenko et al. 2020; Qi et al. 2020).

Baishanzu National Nature Reserve is located in the south Zhejiang and north Fujian provinces of China; this region is well known for its high level of biodiversity and hot spots in Asia. It belongs to the tropical to warm temperate transitional zone. During field surveys in Baishanzu Nature Reserve, an unknown species of the genus *Polypedilum* were collected. Molecular data and morphological comparisons supported it as an undescribed taxon that we describe herein as a new species.

## Material and methods

The examined material was collected by light trap and then preserved in 75% ethanol at 4 °C in a refrigerator before final slide mounting. Tissues for total genomic DNA extraction were removed from the thorax and head of the adults. The extraction procedure followed the Qiagen DNeasy Blood and Tissue kit guide except for the use of an elution buffer quantity of 120 µl. After extraction, the exoskeletons were cleared and mounted on corresponding slides following the procedure described by Sæther (1969). Morphological terminology follows that of Sæther (1980). The photograph of the dorsal habitus was obtained with a DV500 5MP Digital Camera attached to a stereo microscope (Chongqing Optec SZ680). The photograph of the body parts was obtained using a Leica DMLS compound microscope. Photograph post-processing was done in Adobe photoshop and Illustrator (Adobe Inc., California, USA).

Abbreviations used are as follows:

<b>AR</b>	antennal ratio;	<b>MCu</b>	crossvein between media and cubitus;
<b>BR</b>	bristle ratio;	<b>OV</b>	outer verticals;
<b>BV</b>	beinverhältnisse;	<b>Pa</b>	prealars;
<b>Cu</b>	cubitus;	<b>Po</b>	post orbitals;
<b>Dc</b>	dorsocentrals;	<b>R</b>	radius;
<b>Fe</b>	femur;	<b>RM</b>	crossvein between radius and media;
<b>HR</b>	hypopygium ratio;	<b>Ta</b>	tarsomere;
<b>HV</b>	hypopygium value;	<b>Ti</b>	tibia;
<b>IV</b>	inner verticals;	<b>VR</b>	venarum ratio.
<b>LR</b>	leg ratio;		
<b>M</b>	media;		

The standard barcode region of COI-5P was amplified using the universal primers LCO1490 and HCO2198 (Folmer et al. 1994). PCR amplifications were carried out in a 25 µl volume including 12.5 µl 2 × Es Taq MasterMix (CoWin Biotech Co., Beijing, China), 0.625 µl of each primer, 2 µl of template DNA and 9.25 µl deionized H<sub>2</sub>O following Song et al. (2018). PCR products were electrophoresed in 1.0% agarose gel, purified, and sequenced in both directions using an ABI 3730XL capillary sequencer (Beijing Genomics Institute Co., Ltd., Hangzhou, China). Raw sequences were assembled into contigs and edited in BioEdit 7.2.5 (Hall 1999). The pairwise distances were calculated using the Kimura 2-Parameter (K2P) substitution model in MEGA 7 (Kumar et al. 2016). The neighbor joining tree was constructed using the K2P substitution model, 1,000 bootstrap replicates and the “complete deletion” option for missing data. Sequences, trace-files, and metadata of the new species were uploaded to the Barcode of Life Data Systems (BOLD) (Ratnasingham and Hebert 2013).

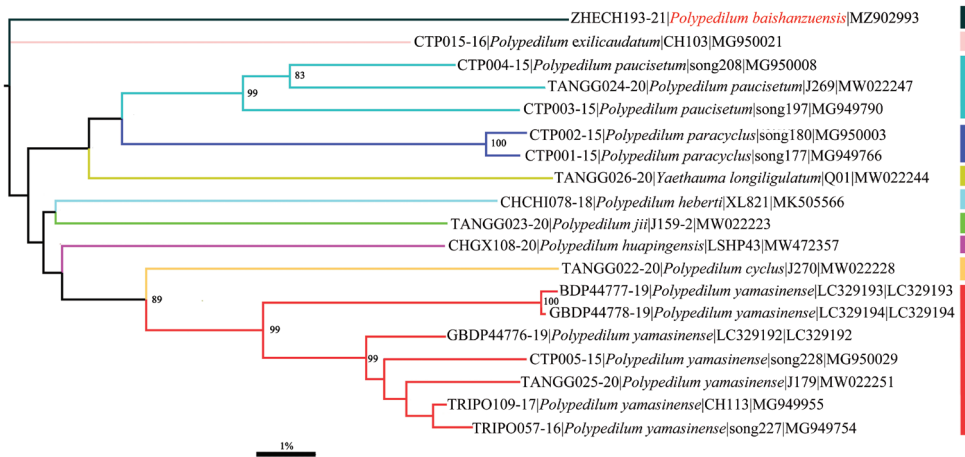
## Results

### Barcode analysis

The species was primarily blasted in GenBank and molecularly confirmed as a species of *Polypedilum*. Morphological characters support it belonging to the subgenus *Collartomyia*. All ten species with public COI sequences of *P. (Collartomyia)* species were used to construct the neighbor-joining tree based on COI barcode sequences and a distinct genetic branch suggests that our specimen belongs to a species new to science (Fig. 1). The minimum interspecific genetic distance within the subgenus *Collartomyia* is up to 14.8% divergence in partial COI sequences (Table 1), larger than the 5–8% threshold suggested by Song et al. (2016, 2018). The genetic divergence to the morphologically similar species *Polypedilum (Collartomyia) heberti* Lin & Wang, 2018 and *Polypedilum (Collartomyia) huapingensis* Liu & Lin, 2021 are up to 15.9% and 15.1% divergent, respectively.

**Table 1.** Kimura 2-parameter pairwise genetic distances based on COI barcodes of *Polypedium* (*Collartomyia*).

Species	Pairwise genetic distances																	
<i>P. baishanzuensis</i>  BSZ60																		
<i>P. cycclus</i>  MW022228	17.5																	
<i>P. exilicaudatum</i>  MG950021	14.8	15.6																
<i>P. heberti</i>  MK505566	15.8	15.2	13.6															
<i>P. huapingensis</i>  MW472357	14.8	13.0	13.0	13.0														
<i>P. jii</i>  MW022223	15.5	13.8	13.0	12.8	12.6													
<i>P. longiligulatum</i>  MW022244	16.9	16.6	14.7	16.0	14.4	14.0												
<i>P. paracyclus</i>  MG949766	17.3	16.0	13.4	14.2	13.8	14.2	14.4											
<i>P. paracyclus</i>  MG950003	17.1	15.1	14.4	14.4	13.8	14.4	14.6	1.2										
<i>P. paucisetum</i>  MW022247	17.7	15.6	13.2	15.6	14.7	14.2	13.4	13.2	13.8									
<i>P. paucisetum</i>  MG949790	17.3	13.8	13.2	15.2	15.3	14.8	13.2	12.0	12.2	9.0								
<i>P. paucisetum</i>  MG950008	14.8	14.0	11.6	14.2	14.0	12.4	12.2	10.7	11.1	6.5	7.4							
<i>P. yamasinense</i>  MG949955	16.0	11.5	13.4	12.8	12.2	12.2	13.4	13.8	14.0	14.5	14.4	14.1						
<i>P. yamasinense</i>  MW022251	16.2	13.0	13.0	14.2	13.0	13.4	14.6	15.8	15.8	16.2	16.0	15.1	2.7					
<i>P. yamasinense</i>  LC329192	15.4	11.6	13.2	12.4	11.8	12.8	13.4	13.6	13.8	15.4	13.8	13.8	2.0	3.5				
<i>P. yamasinense</i>  LC329193	18.5	12.0	13.8	15.0	14.5	14.4	15.6	14.2	13.8	16.8	16.2	15.8	6.7	8.1	7.4			
<i>P. yamasinense</i>  LC329194	18.3	11.8	13.6	14.8	14.3	14.2	15.4	14.0	14.0	16.6	16.0	15.5	6.5	7.9	7.2	0.3		
<i>P. yamasinense</i>  MG949754	16.2	12.4	13.6	13.0	12.4	12.8	14.2	14.4	14.6	15.6	15.0	14.8	0.8	2.5	2.2	7.6	7.4	
<i>P. yamasinense</i>  MG950029	16.2	12.6	13.9	14.2	13.2	13.2	15.4	15.6	15.4	14.9	15.4	14.3	3	4.7	4.0	8.9	8.7	2.8

**Figure 1.** Neighbor joining tree of 10 species of *Polypedium* (*Collartomyia*) COI barcodes based on K2P model. Numbers on branches represent bootstrap support (> 75%) based on 1,000 replicates, scale represents K2P genetic distance.

## Morphological description

### *Polypedium* (*Collartomyia*) *baishanzuensis* Song & Qi, sp. nov.

<http://zoobank.org/F43550CB-6444-4F86-9F41-09D2121DD6C1>

Figs 2–4

GenBank accession number: MZ902993.

**Type material.** *Holotype* (BOLD & TZU sample ID: ZJCH193; Field ID: BSZ60) 1 ♂, China, Zhejiang Province, Lishui City, Qingyuan county, Baishanzu National Nature Reserve, 27.76°N, 119.31°E, 11.VIII.2020, Qi X., light trap.



**Figure 2.** Holotype male of *Polypedilum (Collartomyia) baishanzuensis* Song & Qi, sp. nov.

**Table 2.** Lengths (in  $\mu\text{m}$ ) and proportions of legs of holotype male of *Polypedilum (Collartomyia) baishanzuensis* sp. nov. (n = 1).

	Fe	Ti	Ta <sub>1</sub>	Ta <sub>2</sub>	Ta <sub>3</sub>	Ta <sub>4</sub>	Ta <sub>5</sub>	LR	BV	SV	BR
P1	1300	1010	1250	850	660	550	265	1.24	0.65	1.85	3.03
P2	1450	1150	640	395	305	200	150	0.56	0.32	4.06	3.90
P3	1600	1260	960	550	430	280	160	0.77	0.37	2.98	2.90

The holotype is deposited in the collection of the College of Life Sciences, Taizhou University, Taizhou, China (TZU).

**Diagnostic characters.** The male adult can be distinguished from other *P. (Collartomyia)* species by the following combination of characters: most of the body yellowish; wing with distinct spots on 70% of the proximal part; tarsomeres dark brown; tergite without dark brown band pigmentation; superior volsella with six inner basal setae and three outer lateral setae; dorsal side of inferior volsella with three distinct setiferous tubercles.

**Etymology.** The specific name refers to the Baishanzu National Nature Reserve, where the holotype was collected.

Adult male (n = 1). Total length 4.40 mm; wing length 2.75 mm; total length / wing length 1.60; wing length / length of profemur 2.11.

**Coloration** (Fig. 2). Head, thorax and abdomen yellowish; palpomeres dark brown to blackish; femur, tibia and tarsomeres ta1–ta5 of P1 blackish; tarsomeres ta1–ta5 of P2 dark brown; tarsomeres ta3–ta5 of P3 dark brown; gonocoxite and proximal half of gonostylus dark brown.

**Head** (Fig. 3B). Frontal tubercle absent. Antenna with 13 flagellomeres, ultimate flagellomere 480  $\mu\text{m}$  long; AR 0.77. Temporal setae 16, including 8 inner verticals and

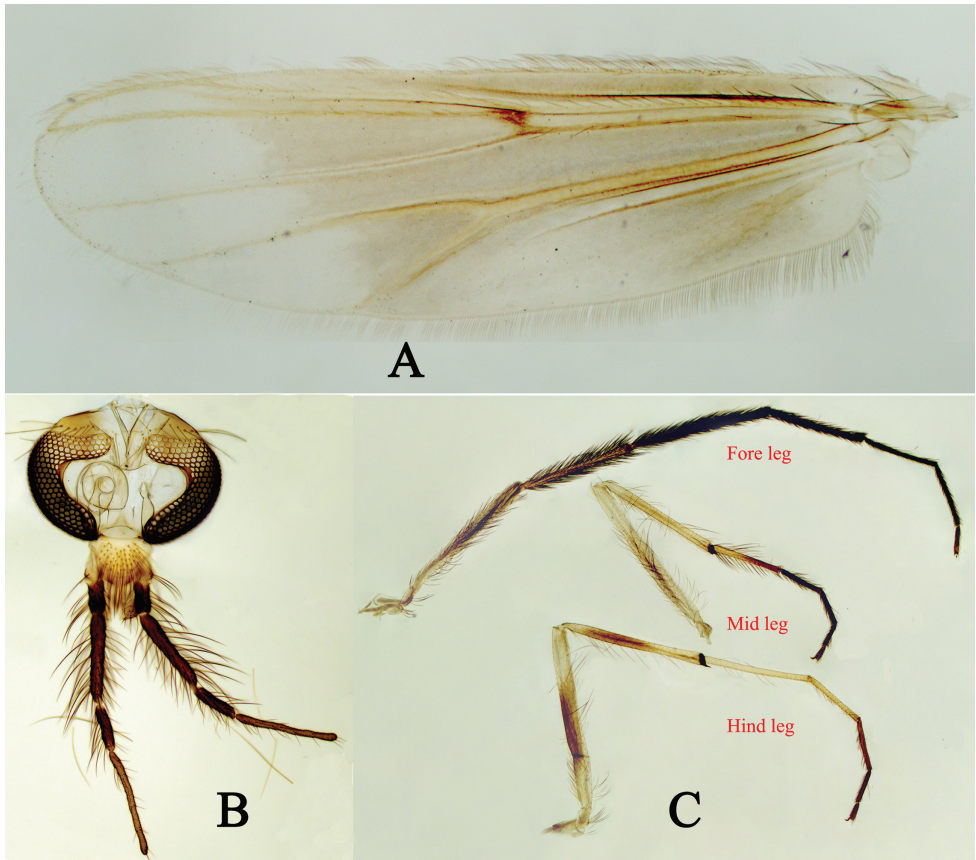


**Figure 3.** Holotype male of *Polypedilum (Collartomyia) baishanzuensis* Song & Qi, sp. nov. **A** wing **B** head **C** legs.

8 outer verticals; Clypeus with 57 setae; Palpomere lengths (in  $\mu\text{m}$ ): 70, 95, 277, 145, 330. Length of 5<sup>th</sup> palpomere / 3<sup>rd</sup> palpomere 1.19.

**Thorax.** Dorsocentrals 50; acrostichals 8; prealars 16; scutellum with 39 setae.

**Wing** (Fig. 3A). VR 1.14; Brachiolum without setae; R with 32 setae; R<sub>1</sub> with 44 setae; R<sub>4+5</sub> with 69 setae; Squama with 33 setae. Anal lobe moderately developed.

**Legs** (Fig. 3C). Terminal scale of fore tibia pointed, 37  $\mu\text{m}$  long. Spur of mid tibia 55  $\mu\text{m}$  long including 32 tooth comb, unspurred comb with 33 teeth. Spur of hind tibia 65  $\mu\text{m}$  long including 26 teeth, unspurred comb with 32 teeth. Lengths (in  $\mu\text{m}$ ) and proportions of legs as in Table 2.

**Hypopygium** (Figs 4–5). Basal part of abdominal segment VIII distinctly triangular and markedly pointed at base (Fig. 4A, 4E). Anal tergite with 27 median setae, laterosternite with 5 setae; Anal tergite bands strongly developed and sclerotized, forming a circle completely surrounding median setae. Anal point (Fig. 4B) 125  $\mu\text{m}$  long and 27.5  $\mu\text{m}$  wide at base, 5  $\mu\text{m}$  at apex; transverse sternapodeme 112  $\mu\text{m}$  long, phallopodeme 175  $\mu\text{m}$  long. Basal part of superior volsella (50  $\mu\text{m}$  long and 50  $\mu\text{m}$  wide)

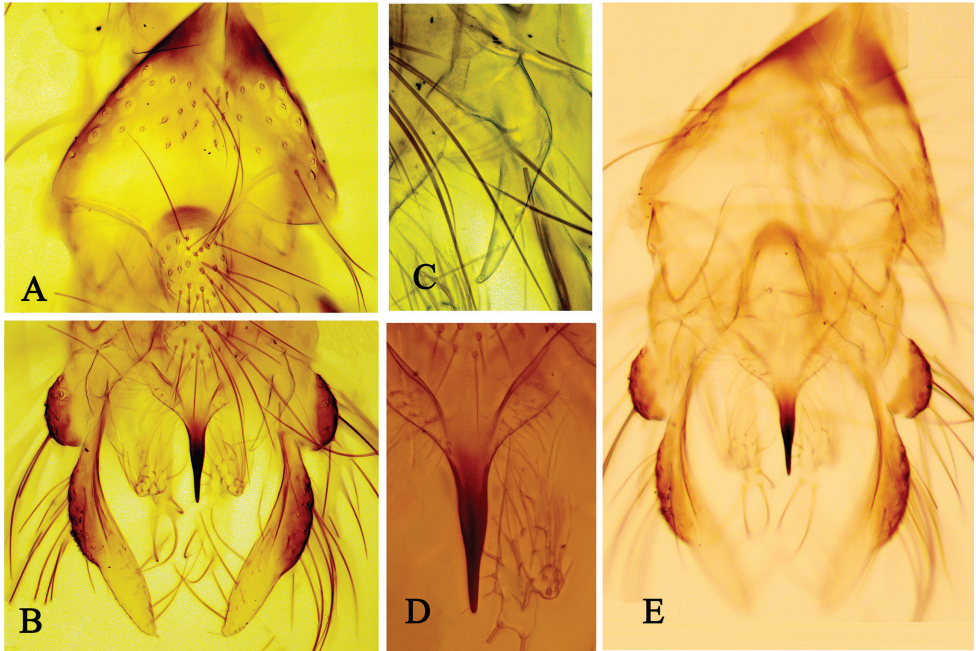


**Figure 4.** Holotype male of *Polypedilum (Collartomyia) baishanzuensis* Song & Qi, sp. nov. **A** tergite VIII **B** hypopygium, dorsal view **C** superior volsella **D** inferior volsella **E** hypopygium, ventral view.

covered with microtrichia and with 6 long setae along inner base and one long seta on outer side; projecting part of superior volsella 105  $\mu\text{m}$  long, with 2 long setae along the distal outer part (Fig. 4C). Inferior volsella (Fig. 4D) 217  $\mu\text{m}$  long, with 3 tubercle-like projections with strong macrosetae. Gonostylus 262  $\mu\text{m}$  long with macrosetae along distal inner margin. HR 1.0. HV 1.69.

Immatures and female unknown.

**Ecology.** Material composed of male adults was light-trapped from stones and boulders in a flowing mountain stream (Fig. 6), located at an altitude of 1,450 m.

**Distribution.** Only known from the type locality in Zhejiang province, China.

## Discussion

The morphological characters of the well-developed gonocoxite bulb of the new species clearly fit the subgeneric definition by Tang et al. (2021) and Sæther and Sundal (1998). The new species shows close morphological similarity with other *P. (Collartomyia)* species on the basis of the spotted wings, including those of *P. (C.) heberti* Lin & Wang, 2018 and *P. (C.) huapingensis* Liu & Lin, 2021, but can be clearly distinguished by tergite IX without a dark brown band or spots, tarsomeres of P1 dark brown, inferior volsella present, with three dorsal setiferous tubercles. Other differences are listed in Table 3.

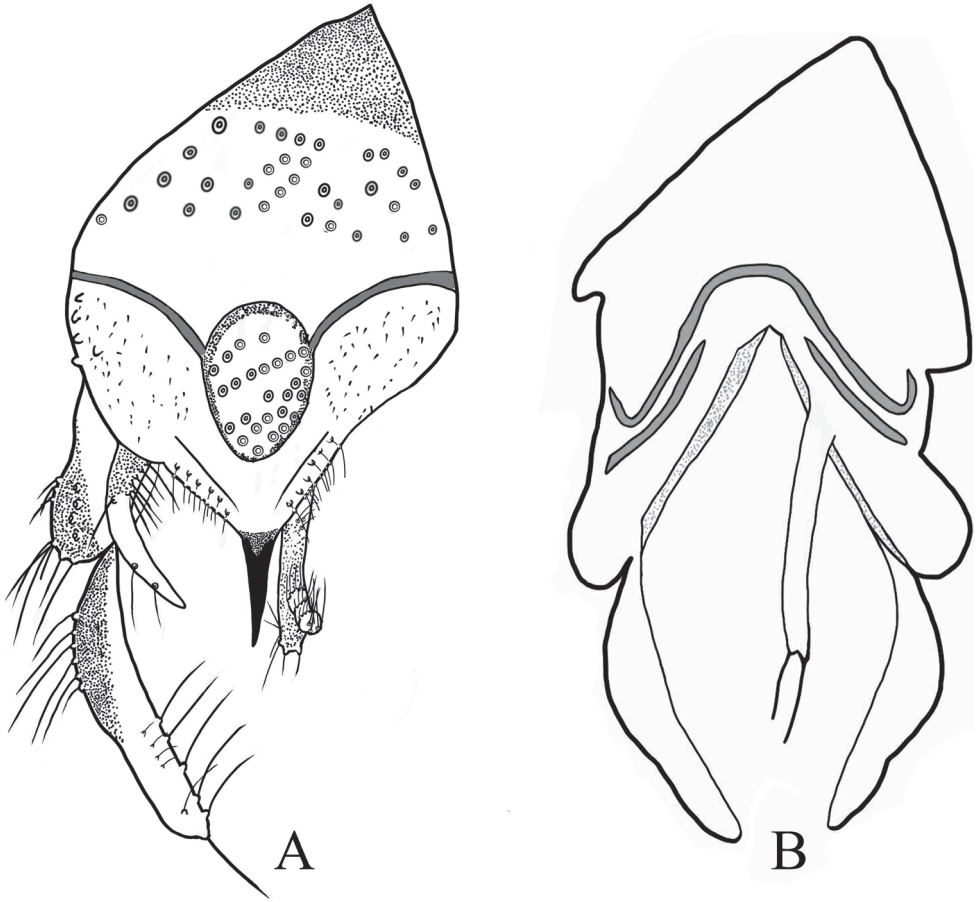


**Figure 5.** Holotype male of *Polypedilum (Collartomyia) baishanzuensis* Song & Qi, sp. nov. **A** hypopygium, dorsal view **B** hypopygium, ventral view.



**Figure 6.** Type locality of *Polypedilum (Collartomyia) baishanzuensis* Song & Qi sp. nov.

**Table 3.** Main differences between *P. (C.) heberti*, *P. (C.) huapingensis*, and *P. (C.) baishanzuensis* sp. nov.

Species	AR	LRI	Ta. of P1	Anal point	SVo	Ivo, dorsal side
<i>P. baishanzuensis</i>	0.77	1.24	dark brown	tapering	6 inner setae 3 outer setae	setose tubercles, present
<i>P. heberti</i>	0.51	1.02	yellow	tapering	5 inner setae outer setae	tubercles, absent
<i>P. huapingensis</i>	0.44	2.17	yellow	broadening	2 inner setae 1 outer seta	tubercles, absent

Key to known adult males of the *Polypedilum* (*Collartomyia*) modified from Lin et al. (2019) and Sæther and Sundal (1999)

- 1 Anteprenotal lobes reduced, with elongate scutal projection ..... 2
- Anteprenotal lobes narrowed dorsally and medially narrowly separated ..... 4
- 2 Maxillary palp reduced ..... *P. hirsutum* (Goetghebuer)
- Maxillary palp five-segmented..... 3
- 3 Anteprenotal lobe distinctly narrowed dorsally .....  
..... *P. longiligulatum* Yamamoto, Yamamoto & Tang
- Anteprenotal lobe reduced, with anteriorly elongate scutal projection .....  
..... *P. discaudatum* Amakye
- 4 Wing with dark spots..... 5
- Wing without spots ..... 11
- 5 Palpomeres reduced, palpomeres 4 and 5 combined about as long as palpomere 3; Sudan..... *P. brevipalpe* Sæther & Sundal
- Palpomeres five-segmented, fifth palpomere about twice as long as third palpomere ..... 6
- 6 Anteprenotum setose..... 7
- Anteprenotum bare ..... 8
- 7 Superior volsella with two outer setae; France, Italy .....  
..... *P. lotensis* Moubayed-Breil
- Superior volsella without outer setae; Ghana, Tanzania .....  
..... *P. volselligum* Sæther & Sundal
- 8 Wing with obvious spots; setae along inner margin of gonostylus strongly split ..... *P. ramiferum* Kieffer
- Wing with a large black spot on entire basal area; setae along inner margin of gonostylus not split..... 9
- 9 Anal point strong, mid-part contracted in a large inflated globe apically, with candle-like spine ..... *P. huapingensis* Liu & Lin
- Anal point strong and tapering ..... 10
- 10 Tergites II–VI brown with dark brown bands at middle.....  
..... *P. heberti* Lin & Wang
- Tergites II–VI pale brown without brown bands at middle .....  
..... *P. baishanzuensis* Song & Qi sp. nov.
- 11 Anteprenotum setose..... 12
- Anteprenotum bare ..... 15
- 12 Anal point broad, tapering towards apex; Canada and USA... *P. ontario* (Wally)
- Anal point narrow, parallel-sided ..... 13

13	Apical process of superior volsella without strong outer seta in apical half.....	<i>P. okigrandis</i> Sasa
–	Apical process of superior volsella with strong outer seta in apical half.....	14
14	Fore tibial scale pointed; tergite IX with strongly sclerotized circle; China ....	<i>P. cyclus</i> Zhang & Wang
–	Fore tibial scale rounded; tergite IX without strongly sclerotized circle; China and Japan.....	<i>P. yamasinense</i> (Tokunaga)
15	Scutum with a weak tubercle .....	16
–	Scutum without a tubercle.....	17
16	Superior volsella with one long outer seta; R <sub>2+3</sub> distinct; China .....	<i>P. jii</i> Zhang & Wang
–	Superior volsella without outer setae; R <sub>2+3</sub> evanescent; China .....	<i>P. exilicaudatum</i> Sæther & Sundal
17	Anal point broad, not parallel-sided; legs ringed with white.....	18
–	Anal point narrow, parallel-sided; legs not ringed.....	19
18	Anal point broad with strong median swelling and apical additional point; Ghana.....	<i>P. bulbocaudatum</i> Sæther & Sundal
–	Anal point awl-shaped, without an additional apical point; Ghana .....	<i>P. subulatum</i> Sæther & Sundal
19	Legs with dark patterns.....	<i>P. paracyclus</i> Qi & Song
–	Legs without dark patterns.....	20
20	AR 0.54–0.91; tergite IX with two setae; superior volsella short and broad; China .....	<i>P. paucisetum</i> Zhang
–	AR 1.15; tergite IX with more than 40 setae; superior volsella curved and tapered; France .....	<i>P. sætheri</i> Moubayed-Breil

## Acknowledgements

The authors are grateful to financial support from the National Natural Science Foundation of China (NSFC, Grant No. 32100353, 32070481), the Zhejiang Provincial Natural Science Foundation of China (Grant No. LY17C040001), the Science & Technology Project of Taizhou (Grant No. 1902gy23), and the Project of Biodiversity Survey in Lishui Municipality, Zhejiang Province of China.

## References

- Cranston PS, Martin J, Spies M (2016) Cryptic species in the nuisance midge *Polypedilum nubifer* (Skuse) (Diptera: Chironomidae) and the status of *Tripedilum* Kieffer. *Zootaxa* 4079(4): 429–447. <https://doi.org/10.11646/zootaxa.4079.4.3>
- Folmer O, Black M, Hoeh W, Lutz R, Vrijenhoek R (1994) DNA primers for amplification of mitochondrial cytochrome *c* oxidase subunit I from diverse metazoan

- invertebrates. *Molecular Marine Biology and Biotechnology* 3: 294–299. <https://doi.org/10.4028/www.scientific.net/DDF.7.460>
- Hall TA (1999) BioEdit: a user-friendly biological sequence alignment editor and analysis program for Windows 95/98/NT. *Nucleic Acids Symposium Series* 41: 95–98. <https://doi.org/10.1021/bk-1999-0734.ch008>
- Hebert PDN, Ratnasingham S, de Waard JR (2003) Barcoding animal life: cytochrome c oxidase subunit I divergences among closely related species. *Proceedings of the Royal Society B-Biological Sciences* 270: S96–99. <https://doi.org/10.1098/rsbl.2003.0025>
- Kobayashi T, Ohtaka A, Takahashi T (2003) The second record of ectoparasitic Chironomidae on Trichoptera from Japan, *Polypedilum (Cerobregma) kamotertium* Sasa, 1989 (Insecta, Diptera, Chironomidae, Chironomini). *Spixiana* 26: 83–91.
- Kodama A, Kawai K, Saito H (2018) A new species of *Tanytarsus* van der Wulp, 1874 (Diptera: Chironomidae) and the first Japanese record of *Tanytarsus ovatus* Johannsen, 1932 with DNA barcodes. *Zootaxa* 4422(4): 591–599. <https://doi.org/10.11646/zootaxa.4422.4.9>
- Kumar S, Stecher G, Tamura K (2016) MEGA7: Molecular Evolutionary Genetics Analysis Version 7.0 for Bigger Datasets. *Molecular Biology and Evolution* 33(7): 1870–1874. <https://doi.org/10.1093/molbev/msw054>
- Lin XL, Stur E, Ekrem T (2018) DNA barcodes and morphology reveal unrecognized species in Chironomidae (Diptera). *Insect Systematics & Evolution* 49(4): 329–398. <https://doi.org/10.1163/1876312X-00002172>
- Lin XL, Yu HJ, Wang Q, Bu WJ, Wang XH (2020) DNA barcodes and morphology confirm a new species of *Rheocricotopus (Psilocricotopus) orientalis* group (Diptera: Chironomidae). *Zootaxa* 4678(2): 282–290. <https://doi.org/10.11646/zootaxa.4768.2.9>
- Lin XL, Yu HJ, Zhang RL, Wang XH (2019) *Polypedilum (Cerobregma) heberti* sp. n. (Diptera: Chironomidae) from Gaoligong Mountains, Yunnan, China. *Zootaxa* 4571(2): 255–262. <https://doi.org/10.11646/zootaxa.4852.4.7>
- Liu WB, Yao Y, Yan CC, Wang XH, Lin XL (2021) A new species of *Polypedilum (Cerobregma)* (Diptera, Chironomidae) from Oriental China. *Zookeys* 1011: 139–148. <https://doi.org/10.3897/zookeys.1011.59554>
- Makarchenko EA, Semenchenko AA, Palatov DM (2020) Review of the genus *Shilovia* Makarchenko (Diptera: Chironomidae: Diamesinae: Boreoheptagiini) from the mountains of Central Asia, with morphological description and DNA barcoding of known species. *Zootaxa* 4895(2): 196–210. <https://doi.org/10.11646/zootaxa.4895.2.2>
- Moubayed-Breil J (2007) *Polypedilum (Cerobregma) lotensis*, new species, and *P. (C.) sætheri*, new species, from lowland streams and rivers in France (Diptera: Chironomidae). *Contributions to the systematics and ecology of aquatic Diptera-A tribute to Ole A. Sæther*. The Caddis Press, Columbus, 205–213.
- Pinho LC, Silva FLD (2020) Description of two new species of *Polypedilum (Asheum)* and immature stages of *Polypedilum (A.) curticaudatum* (Diptera: Chironomidae). *Zootaxa* 4759(2): 179–190. <https://doi.org/10.11646/zootaxa.4759.2.2>
- Qi X, Song C, Ge K, Wang XH (2020) *Polypedilum (Cerobregma) paracyclus* sp. n., a new species from Oriental China (Diptera: Chironomidae). *Zootaxa* 4881: 189–195. <https://doi.org/10.11646/zootaxa.4881.1.12>

- Ratnasingham S, Hebert PDN (2013) A DNA-based registry for all animal species: the barcode index number (BIN) system. *PLoS ONE* 8: e66213. <https://doi.org/10.1371/journal.pone.0066213>
- Sæther OA (1969) Some Nearctic Podonominae, Diamesinae, and Orthoclaadiinae (Diptera: Chironomidae). *Bulletin of the Fisheries Research Board of Canada* 170: 1–154.
- Sæther OA (1980) Glossary of chironomid morphology terminology (Diptera: Chironomidae). *Entomologica scandinavica Supplement* 14: 1–51.
- Sæther OA, Andersen T, Pinho LC, Mendes HF (2010) The problems with *Polypedilum* Kieffer (Diptera: Chironomidae), with the description of *Probolum* subgen. n. *Zootaxa* 2497: 1–36. <https://doi.org/10.5281/zenodo.195747>
- Sæther OA, Sundal A (1998) *Cerobregma*, a new subgenus of *Polypedilum* Kieffer, with a tentative phylogeny of subgenera and species groups within *Polypedilum* (Diptera: Chironomidae). *Journal of the Kansas Entomological Society* 71(3): 315–382.
- Song C, Wang Q, Zhang R, Sun B, Wang XH (2016) Exploring the utility of DNA barcoding in species delimitation of *Polypedilum* (*Tripodura*) non-biting midges (Diptera: Chironomidae). *Zootaxa* 4079(5): 534–550. <https://doi.org/10.11646/zootaxa.4079.5.2>
- Song C, Lin XL, Wang Q, Wang XH (2018) DNA barcodes successfully delimit morphospecies in a superdiverse insect genus. *Zoologica Scripta* 47: 311–324. <https://doi.org/10.1111/zsc.12284>
- Tang HQ, Cheng, QQ, Han W, Cranston PS (2021) Integrative taxonomy: molecular phylogenetics of *Polypedilum* (*Cerobregma*) and revisited morphology of *Yaethauma* and *Collartomyia* (Diptera: Chironomidae) reveals synonymy and supports new classification. *Zoological Journal of the Linnean Society*: zlaa187. <https://doi.org/10.1093/zoolinnean/zlaa187>
- Tang HQ, Niitsuma H (2017) Review of the Japanese *Microtendipes* (Diptera: Chironomidae: Chironominae), with description of a new species. *Zootaxa* 4320(3): 535–553. <https://doi.org/10.11646/zootaxa.4320.3.8>
- Yamamoto N, Yamamoto M, Hirowatari T (2016) Erection of a new subgenus in the genus *Polypedilum* Kieffer, 1912 (Diptera: Chironomidae) from Japan. *Japanese Society of Systematic Entomology* 22(2): 195–197.
- Yamamoto M, Yamamoto N, Tang HQ (2018) Two new chironomids bearing peculiar morphological features from Japan and China (Diptera: Chironomidae). *Journal of Limnology* 77: 40–49. <https://doi.org/10.4081/jlimnol.2018.1775>
- Zhang RL, Wang XH (2005) *Polypedilum* (*Cerobregma*) Sæther & Sundal from China (Diptera: Chironomidae). *Aquatic Insects* 27(1): 47–55. <https://doi.org/10.1080/01650420400019262>
- Zhang RL, Wang XH, Sæther OA (2006) Two unusual species of *Polypedilum* Kieffer (Diptera: Chironomidae) from Oriental China. *Zootaxa* 1282(1): 39–48. <https://doi.org/10.5281/zenodo.173435>

# The first Western Palearctic record of *Euprosthénops* Pocock (Araneae, Pisauridae), with description of a new species from Israel

Sergei Zonstein<sup>1</sup>, Yuri M. Marusik<sup>2,3</sup>

**1** Steinhardt Museum of Natural History, Klausner 12, 69978 Tel-Aviv, Israel **2** Institute for Biological Problems of the North RAS, Portovaya Str. 18, Magadan, Russia **3** Department of Zoology & Entomology, University of the Free State, Bloemfontein 9300, South Africa

Corresponding author: Sergei Zonstein ([znn@tauex.tau.ac.il](mailto:znn@tauex.tau.ac.il))

---

Academic editor: Shuqiang Li | Received 7 September 2021 | Accepted 22 September 2021 | Published 22 October 2021

---

<http://zoobank.org/59F58C75-DF68-4811-8981-742B4E1C82A5>

---

**Citation:** Zonstein S, Marusik YuM (2021) The first Western Palearctic record of *Euprosthénops* Pocock (Araneae, Pisauridae), with description of a new species from Israel. ZooKeys 1065: 13–27. <https://doi.org/10.3897/zookeys.1065.74119>

---

## Abstract

The primarily Afrotropical genus *Euprosthénops* Pocock, 1897 is recorded in the Western Palearctic for the first time. A diagnosis and an illustrated description of *E. insperatus* **sp. nov.**, based on a single male from southern Israel, are provided. Considering the structure of the male palp, the holotype of *E. insperatus* **sp. nov.** resembles males of two widespread African species, *E. australis* Simon, 1898 and *E. proximus* Lessert, 1916; it differs from them by colouration pattern as well as by the different shapes of the retrolateral tibial apophysis and the palpal sclerites. A short survey of the regional insect and spider genera of the paleotropical origin is also presented.

## Keywords

Afrotropical, Arava Valley, new species, paleotropical, spiders, taxonomy

## Introduction

The spider genus *Euprosthénops* Pocock, 1897 currently includes nine species and one subspecies distributed within the mainland Sub-Saharan Africa except one species known from India and Pakistan (WSC 2021). The genus is relatively well studied due to the surveys by Blandin (1974, 1975, 1976, 1978) and Silva and Sierwald (2014). However, little attention has been paid to the disjunct distribution of the genus, with

a wide gap between the ranges of Afrotropical and Indo-Malayan species. The present study is based on a quite unexpected occurrence of a single male congener in the Arava Valley, southernmost Israel. After examination, the male has been considered to represent a new species of *Euprosthénops*, which is diagnosed, described and illustrated herein.

## Material and methods

### Acronyms

**NMW** Naturhistorisches Museum Wien, Vienna, Austria;  
**SMNH** Steinhardt Museum of Natural History, Tel-Aviv, Israel.

Comparative material: *Euprosthénops* sp. aff. *australis* Simon, 1898 – 1♂ (NMW), NAMIBIA, Windhoek (no other data). *Euprosthénops proximus* Lessert, 1916 – 1♂ (SMNH), DR CONGO, *Bandundu Province*: Salonga Nat. Park, Lokoro River basin, about 110 km SSW Monkoto Village, 2°45.8'N, 20°19.3'E, alt. 400 m, 1.01–15.02.2018 (V. Kravchenko & G. Müller).

Photographs were taken using an Olympus SZX16 stereomicroscope with a Canon EOS 7D camera and prepared using the Helicon Focus 7.6.2 Pro (<http://www.helicon-soft.com>). Measurements were taken through the above-mentioned stereomicroscope to an accuracy of 0.01 mm. All measurements are given in millimetres.

### Abbreviations

<b>ALE</b>	anterior lateral eye(s);	<b>PLE</b>	posterior lateral eye(s);
<b>AME</b>	anterior median eye(s);	<b>PME</b>	median lateral eye(s).

Other used abbreviations are explained in the text and in the captions.

## Taxonomy

Family Pisauridae Simon, 1890

Genus *Euprosthénops* Pocock, 1897

**Type species.** *Podophthalma bayonianna* Brito Capello, 1867, by subsequent designation (Simon 1898).

**Diagnostic characters.** The genus and its characters were comprehensively described by Blandin (1976) and later redescribed by Silva and Sierwald (2014). Among the used characters (for their full set see Silva and Sierwald 2014), two are principal in distinguishing males from those of the closely related genus *Euprosthénopsis* Blandin,

1974. First, in males of *Euprostheno*s the palpal tibia is armed with a flattened and extended chisel-shaped retrolateral tibial apophysis (*Rta*; see Fig. 2C, D). Second, they possess a large lamellose distal tegular apophysis (*Dt*; Figs 2C, 4, 5). On the contrary, males of *Euprostheno*sis have a wide and concave retrolateral tibial apophysis as well as a short and rounded distal tegular apophysis (see Blandin 1974; Silva and Sierwald 2014).

**Composition and distribution.** According to WSC (2021) with the present addition, *Euprostheno*s includes ten species and one subspecies: ♂♀ *E. australis* Simon, 1898 (Senegal, Nigeria, Zambia, Botswana and South Africa), ♂♀ *E. bayaonianus* (Brito Capello, 1867) (West, Central and East Africa), ♀ *E. benoiti* Blandin, 1976 (Rwanda), ♂♀ *E. biguttatus* Roewer, 1955 (Congo, Namibia), ♂♀ *E. ellioti* (O. Pickard-Cambridge, 1877) (India, Pakistan?), ♂ *E. insperatus* sp. nov. (Israel), ♀ *E. pavesii* Lessert, 1928 (Central and East Africa), ♂♀ *E. proximus* Lessert, 1916 (Central, East and South Africa), ♂♀ *E. p. maximus* Blandin, 1976 (Ivory Coast), ♀ *E. schenkeli* (Roewer, 1955) (East Africa), ♂ *E. wuehlschi* Roewer, 1955 (Namibia). The record of a single female specimen of *E. ellioti* in the Pakistani Punjab by Dyal (1935) is doubtful, as there are no illustrations provided for this material and it is possible that even the generic assignment is not correct.

***Euprostheno*s *insperatus* sp. nov.**

<http://zoobank.org/21B8E295-1DE4-4B5D-9907-A413F3203AA4>

Figs 1, 2, 4A–D, 5A, C, 7, 8

**Type material.** *Holotype* ♂ (SMNH), ISRAEL, Southern District: Arava Valley, Hahal Shezaf 5 km S. Hazeva (Hatseva) Village, 30°43'N, 35°16'E, –120 m (below sea level), 26.03.2006 (S. Zonstein). The spider was collected within the Aqaba–Jordan section of the East African – Syrian rift zone, in a few kilometres to the west from the midline of fault. The holotype specimen is in a relatively good condition, only the left leg III is completely missed being evidently lost prior to sampling and preservation.

**Diagnosis.** The sole male of the new species most closely resembles the males of *E. australis* and *E. proximus* in a number of similarly shaped structures: the distal tegular apophysis (*Dt*), the tegular prolateral projection (*Pp*), the median apophysis (*Ma*) and the retrolateral tibial apophysis (*Ta*). *Euprostheno*s *insperatus* sp. nov. differs from these similar species in having relatively longer prolateral tegular projection (length of tegulum/length of projection ratio 1.4 to 1.5 vs. 1.6), in the localization of the embolus origin (posteriorly from posterior edge of distal tegular apophysis vs. anteriorly in *E. australis*), and in the shape of the distal part of the distal tegular apophysis, as well as by shorter palpal tibia (length/width ratio 1.5 vs. 1.6 to 1.7). Structure of male palp differs in many details from that in *E. proximus* and *E. australis* (Figs 2, 4A–F, 5A, C cf. Figs 3, 4E–G, 5B, D). From *E. schenkeli*, *E. pavesii* and *E. benoiti*, where the conspecific males remain unknown, *E. insperatus* sp. nov. can be distinguished by having a dissimilar dorsal abdominal pattern (Fig. 1B cf. Blandin 1976, figs 2, 3, 8).

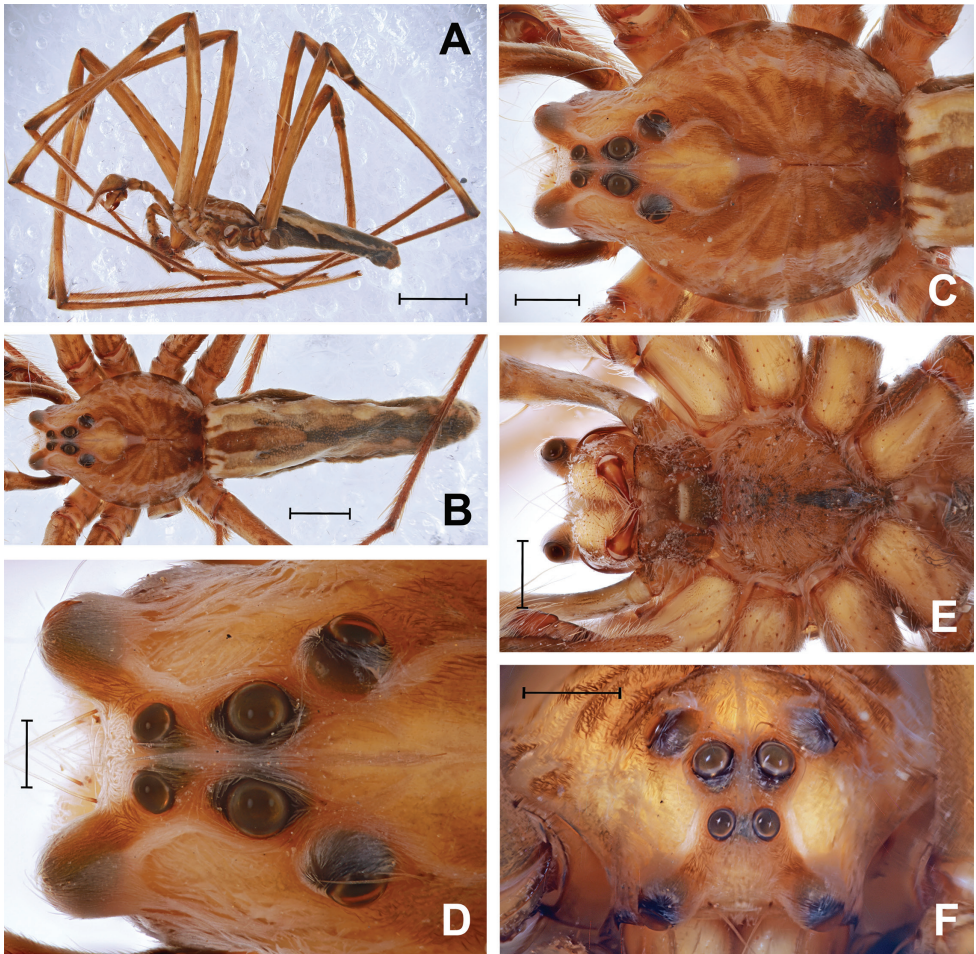


**Figure 1.** *Euprosthenoops insperatus* sp. nov., holotype male **A, B** habitus, dorsal and lateral **C, E** cephalothorax, dorsal and ventral **D, F** eye group, dorsal and frontal. Scale bars: 5 mm (**A**); 2 mm (**B**); 1 mm (**C, E, F**); 0.5 mm (**D**).

**Description. Male.** Habitus as in Fig. 1A, B. Total body length 13.75. Color in alcohol: cephalothorax, chelicerae, palps and legs mostly light to medium ginger brown; X-shaped eye group and radial thoracic grooves darkened; eyes encircled with narrow blackish areas; postocular area, chelicerae anteriorly and coxae I–IV ventrally light yellowish brown; maxillae and labium medium brown, sternum medium brown with short longitudinal dark brown band posteriorly; abdomen light brown anterodorsally, other parts of abdomen dark brown; carapace with two wide submarginal bands of adpressed whitish pubescence, abdomen with two similar longitudinal bands dorsally and with two very narrow light grey bands ventrally; all segments of palps and legs I–IV slightly to noticeably darkened proximally and subapically.

Carapace (Fig. 1C) 5.45 long, 4.21 wide. Clypeus and eye group as in Fig. 1D, F. Clypeus height 0.62. Eye diameters and interdistances: ALE 0.33, AME 0.22, PME

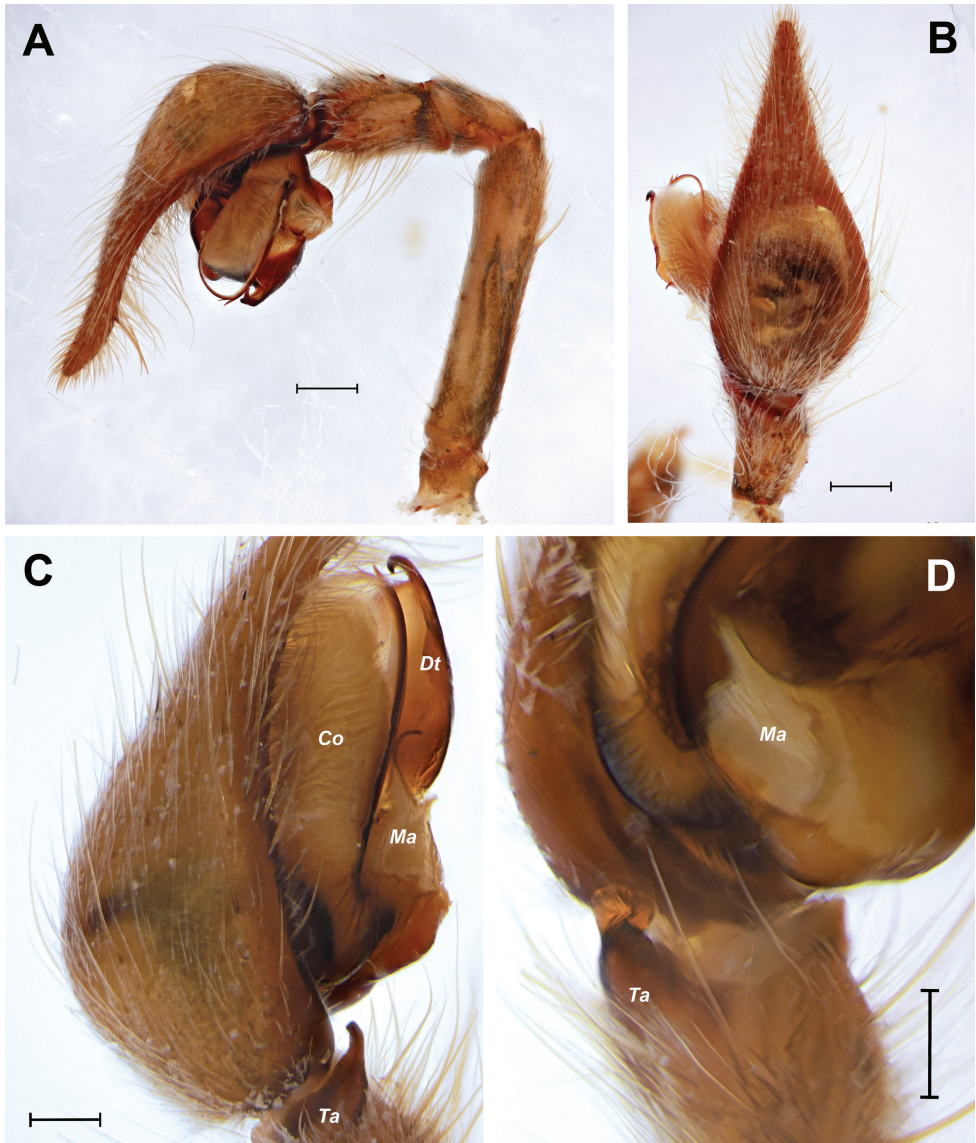


**Figure 2.** *Euprostenops insperatus* sp. nov., holotype male, structures of left (**A, B**) and right (**C, D**) palp **A** entire palp, retrolateral **B** palpal tibia and cymbium, dorsal **C, D** distal palpal tibia and basal embolus close up, retrolateral and ventral. Abbreviations: *Co* – conductor, *Dt* – distal tegular process, *Ma* – median apophysis, *Ta* – retrolateral tibial apophysis. Scale bars: 0.5 mm (**A, B**); 0.2 mm (**C, D**).

0.36, PLE 0.35, ALE–ALE 1.21, ALE–AME 0.75, AME–AME 0.16, AME–PME 0.33, ALE–PLE 1.64, PME–PME 0.23, PME–PLE 0.45, PLE–PLE 1.27. Cheliceral fang furrow: promargin and retromargin each armed with narrow row of 3 evenly disposed teeth, promargin with smaller uniformly sized and shaped teeth; within unevenly larger teeth of retromarginal row, median tooth largest. Sternum, labium and maxillae as in Fig. 1E. Labium 0.69 long, 0.86 wide. Sternum sharply nonagonal, 2.42 long, 2.43 wide.



**Figure 3.** *Euprostenops proximus* Lessert, 1916, male, structures of left palp **A** entire palp, retrolateral **B–E** palpal tibia and cymbium, dorsal, prolateral, ventral and retrolateral. Scale bars: 0.5 mm.

Ventral pairs of spines on tibiae I–IV: 4, 4, 3, 4, respectively. Paired claws on tarsi I–IV with 6–7 teeth each.

Palp and leg measurements as follows:

	Femur	Patella	Tibia	Metatarsus	Tarsus	Total
Palp	2.74	0.85	0.96	—	2.91	7.46
Leg I	11.31	2.90	11.84	12.77	5.66	44.48
Leg II	10.74	2.89	10.53	11.84	5.29	41.29
Leg III	9.13	2.18	7.98	8.27	3.71	31.27
Leg IV	11.28	2.54	11.01	11.15	4.89	40.87

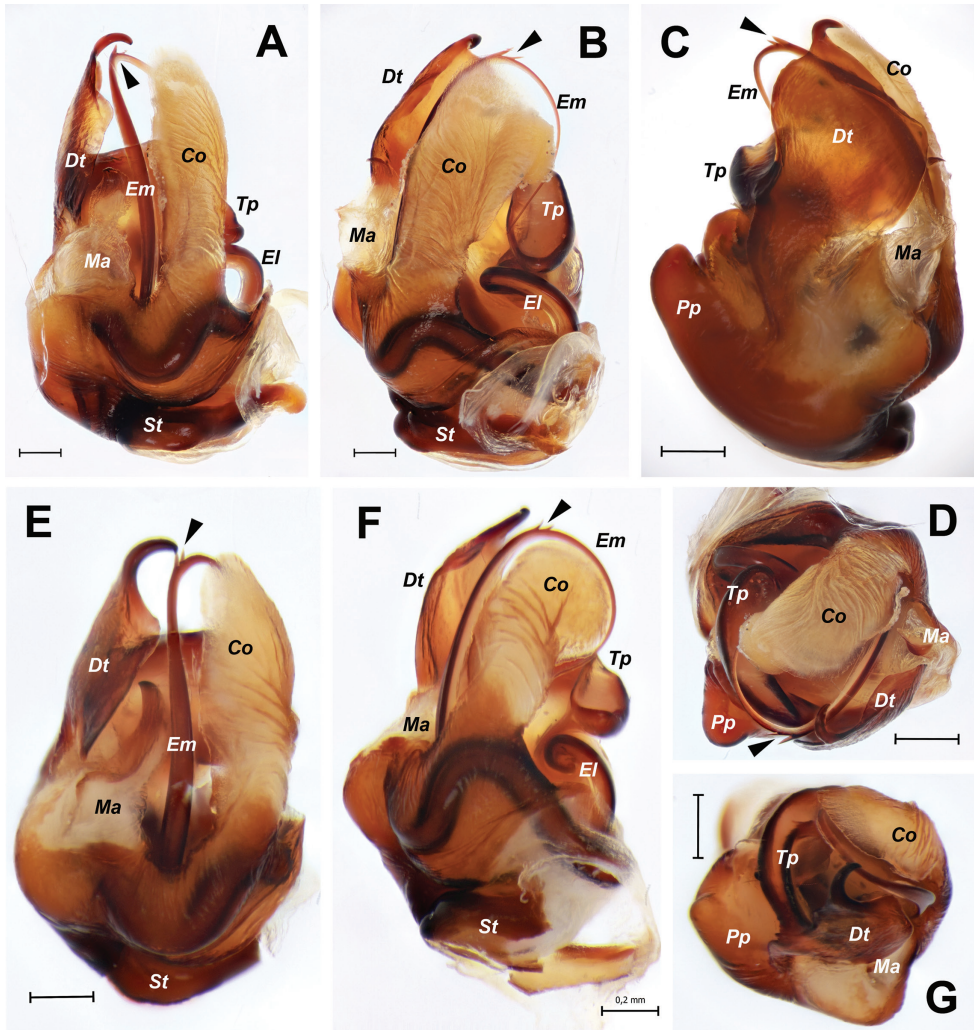


**Figure 4.** *Euprostheno insperatus* sp. nov., holotype male (**A–D**) and *E. proximus* Lessert, 1916, male (**E–G**), separated copulatory bulb **A, E** retrolateral **B, F** retrodorsal **C** ventral **D, G** frontal. Small teeth of embolus are indicated with arrows. Abbreviations: *Co* – conductor, *Dt* – distal tegular process, *El* – embolus loop, *Em* – embolus, *Ma* – median apophysis, *Pp* – prolateral projection, *St* – subtegulum, *Tp* – prolateral tegular pouch. Scale bars: 0.2 mm.

Male palp (Figs 2, 4A–D, 5A). Femur shorter than cymbium, 5 times longer than wide. Tibia slightly longer than patella with retrolateral apophysis (*Ta*) shorter than tibia's width. Cymbium 2.35 longer than wide, with long tip (about 0.25 of cymbium length). Subtegulum (*St*) moderately small and located retrolaterally. Tegulum with prolateral pouch (*Tp*) and distinct prolateral projection (*Pp*), height of projection (from base of tegulum to tip of projection) exceeds length of tegular distal apophysis (*Dt*).

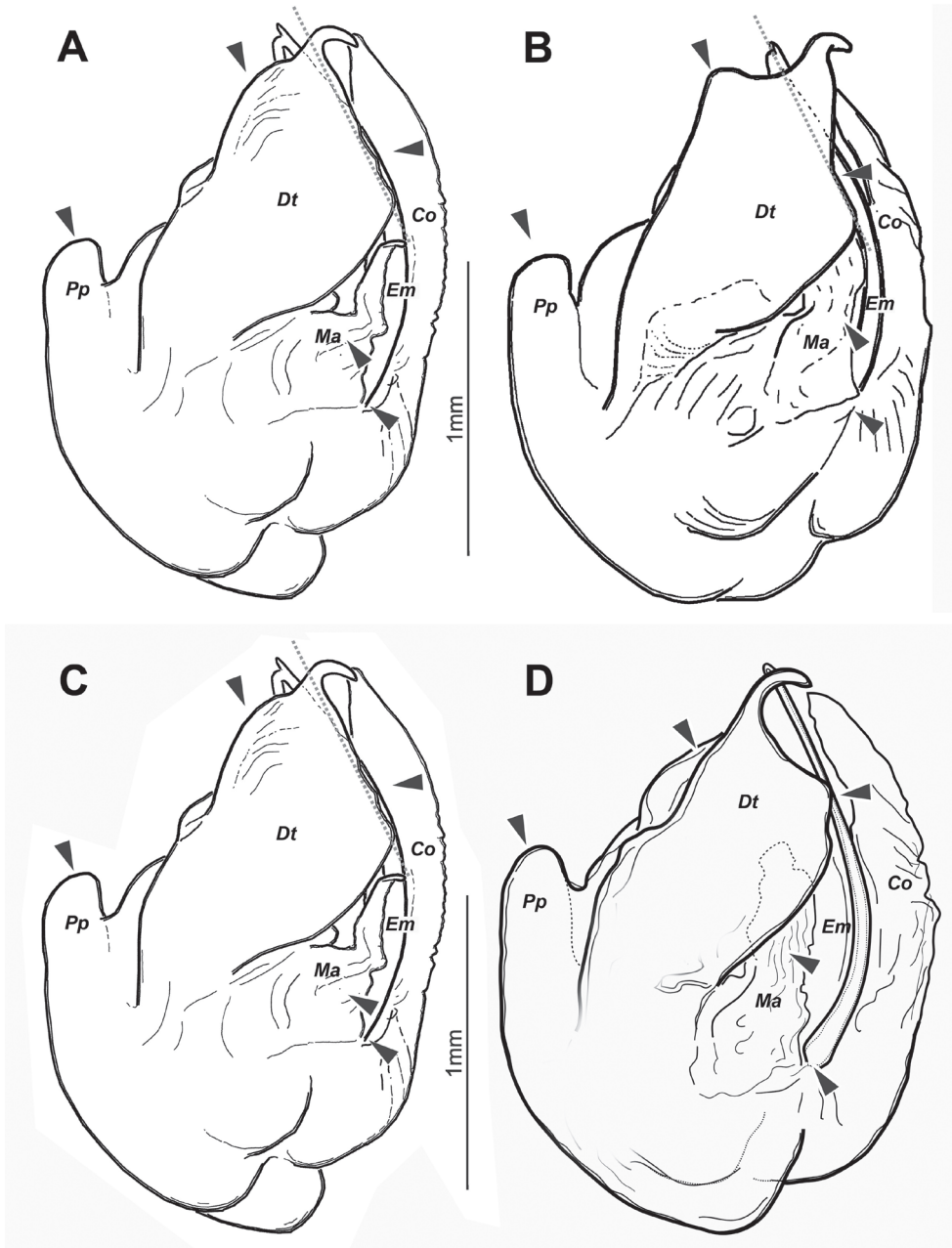


**Figure 5.** *Euprostenops insperatus* sp. nov., holotype male (A, C), and males of *E. australis* Simon, 1898 (B) and *E. proximus* Lessert, 1916 (D); comparison of copulatory bulbs schematically depicted in the same position. The differences in their structure are indicated with arrows. Abbreviations: Co – conductor, Dt – distal tegular process, Em – embolus, Ma – median apophysis, Pp – prolateral projection.

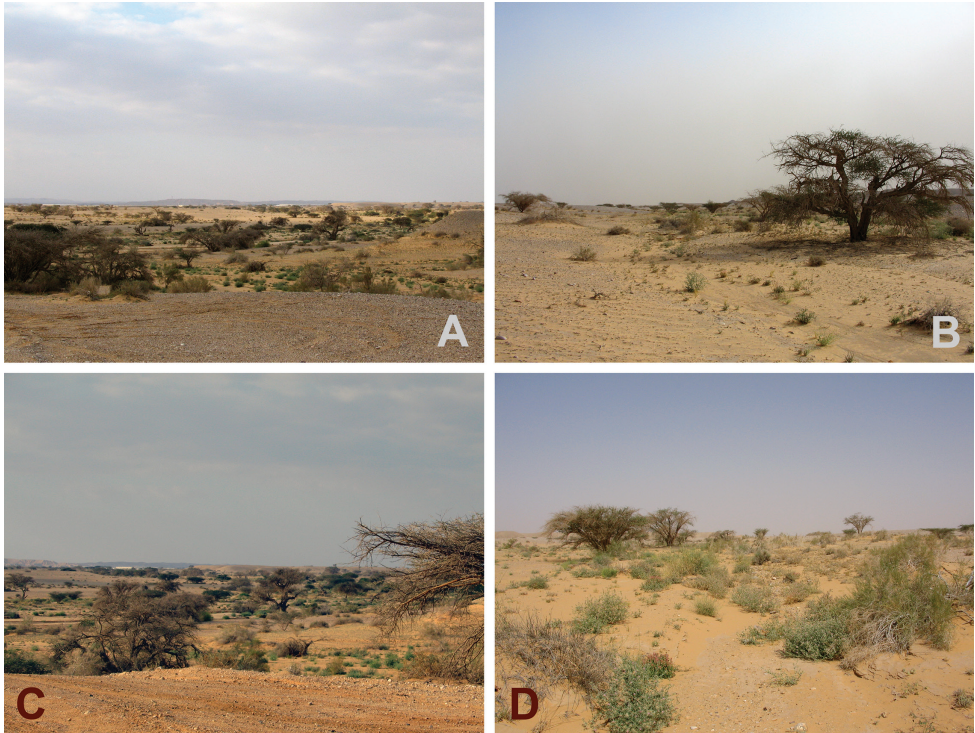


**Figure 6.** Surroundings of Nahal Shezaf, the type locality of *Euprostheno speratus* sp. nov. (A–D).

Distal apophysis with prolateral hook-shaped tip, anterior prolateral part slanting. Conductor (*Co*) large and long, weakly sclerotized. Embolus with 2 teeth on anterior loop.

**Female.** Unknown.

**Etymology.** From the Latin adjective of the masculine gender “*insperatus*” for “unforeseen”, alluding to the unexpected discovery of a species belonging to the previously paleotropical genus *Euprostheno*s in Israel.

**Ecology.** The holotype was found inside a small patch of shrubs and reeds growing close to a periodically wet riverbed that crosses the extremely arid desert biotopes (Fig. 6).

**Distribution.** Known only from the type locality (Fig. 7). The location of this sole record in relation to the records of other congeners lays far outside the previously known genus range (Fig. 8).

## Discussion

Since the 1960s, the territory belonging to the modern Israel is known as the “cross-roads” for different plant and animal taxa penetrating the country from the north, south and east (Zohary 1966; Danin et al. 1975; Furth 1975; Danin 1988; Freidberg



**Figure 7.** *Euprostenops insperatus* sp. nov., distribution record.

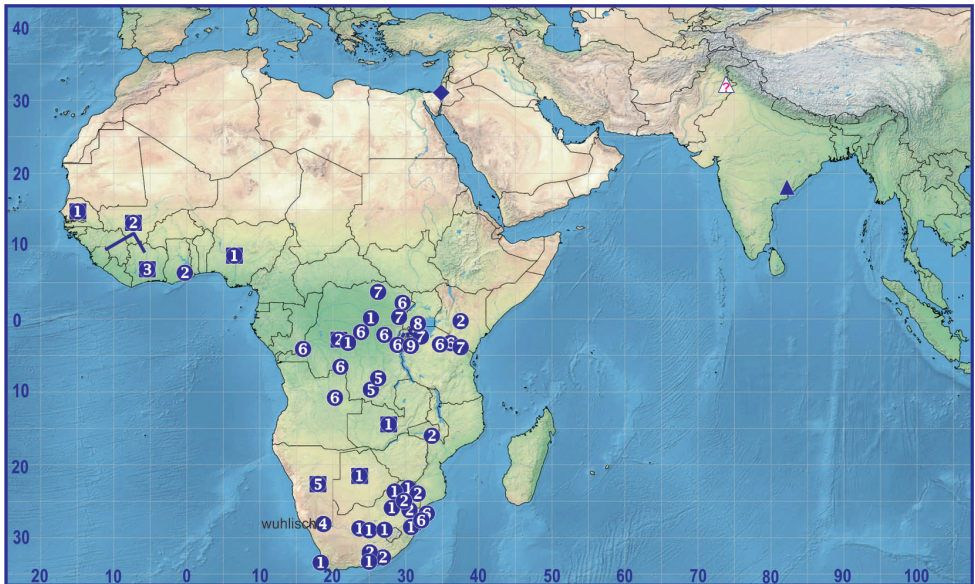


**Figure 8.** Distribution of *Euprostenops* spp. Records of Afrotropical congeners are presented as circles (localities) and quadrangles (country records) according to numbers: 1 *E. australis* Simon, 1898 2 *E. bayaonianus* (Brito Capello, 1867) 3 *E. proximus maximus* Blandin, 1976 4 *E. wuehlschi* Roewer, 1955 5 *E. biguttatus* Roewer, 1955 6 *E. proximus proximus* Lessert, 1916 7 *E. pavesii* Lessert, 1928 8 *E. schenkeli* (Roewer, 1955) 9 *E. benoiti* Blandin, 1976. Records of Asian *E. ellioti* (O. Pickard-Cambridge, 1877) and *E. insperatus* sp. nov. are indicated as triangles (? means questionable record) and diamond, respectively.

1988; Tchernov 1988). This biogeographical feature of the country can explain why species of paleotropical origin, primarily associated with the adjacent regions of East Africa, are presented here. The data listed below do not claim to be exhaustive; they are merely intended to show that a pattern of distribution, similar to the above-noted one, is neither frequent nor exclusive in relation to various groups of spiders and insects represented in Israel and adjacent Middle East countries.

Regarding the spiders (Araneae), the genus *Levymanus* Zonstein & Marusik, 2013 (Palpimanidae) originally was established as a monotypic taxon known only from the desert rift zone in south Israel (see Zonstein and Marusik 2013). Later, its type species was found in Saudi Arabia (El-Hennawy 2014) and UAE (Zonstein et al. 2017). Finally, two additional species were described from Ethiopia and south Iran (Zonstein et al. 2017; Zamani and Marusik 2020).

Two widespread paleotropical genera, *Calommata* Lucas, 1837 (Atypidae) and *Cambalida* Simon, 1909 (Corinnidae) are represented in Israel by a single species each (Levy 2007; personal unpublished data regarding the presence of *Cambalida* sp. in Israel). The shared range of all other species belonging to these genera extends from the Sub-Saharan Africa to south and eastern Asia (WSC 2021). Likewise, *Evipomma simoni* Alderweireldt, 1992 is a representative of the mostly paleotropical wolf spider genus *Evipomma* Roewer, 1959 (Lycosidae); this species, known previously from Sudan and Egypt, has been very recently found in southern regions of Israel (see Armiach Steinpress et al. 2021).

The similar situation is observed in two Afrotropical spider genera. Within eight species of *Festucula* Simon, 1901 (Salticidae) known from Sub-Saharan Africa, the genotype *E. vermiformis* Simon, 1901 has been recorded also in Sudan, Egypt and Israel (Azarkina and Foord 2014; WSC 2021). The same is true for *Pararaneus* Caporiacco, 1940 (Araneidae), where four of five species are limited in their distribution to either the mainland Africa or Madagascar, and only the trans-African *P. spectator* (Karsch, 1885) extends northward the genus range to Yemen, Sinai (Egypt) and Israel (Levy 1998; WSC 2021).

A similar disjunct distribution is recorded for the mostly Afrotropical huntsman spider genus *Pseudomicrommata* Järvi, 1912 (Sparassidae). Here, the distribution of four congeners is restricted to the western, eastern and southern regions of the mainland Africa (Moramand 2015). However, one species, *P. mocranica* Moramand, Zamani & Jäger, 2019 has been recently found in the Sistan & Baluchistan Province of Iran (see Moramand et al. 2019).

Among the insects (Hexapoda), the distribution of a paleotropical (predominantly, of an Afrotropical) taxon having its northernmost limit in Israel or very close to it can be observed in several insect orders. According to Blondi et al. (2017), the Afrotropical flea beetle genus *Calotheca* Heyden, 1887 (Coleoptera, Chrysomelidae) embraces 27 species distributed predominantly in central, southern and eastern regions of mainland Africa. One of them, *C. sacra* (Weise, 1897), is known mostly from East Africa (Eritrea, Ethiopia, Sudan), with one record in southwestern Saudi Arabia. However, this species considerably extends the genus range, penetrating the Great Rift Valley to the north as far as the northern coast of the Dead Sea (where it was originally described from).

In the tiger beetle subfamily Cicindelinae (Carabidae), East African *Cephalota litorea* (Forskål, 1775) spreads northward almost achieving the Egypt-Israeli border at the northwestern coast of the Gulf of Aqaba, while Asian records of *Habrodera nylotica* (Dejean, 1825) distributed throughout the mainland Africa and recorded also for the Canary Islands, are limited to the Sinai mountains (Matalin and Chikatunov 2016, fig. 5).

Within the weevil family Curculionidae, the paleotropical (and mostly Afrotropical) genus *Aorus* Schoenherr, 1835 is represented in Israel by *A. anthracinus* Brancsik, 1898, and this sole Palearctic record is the northernmost point of the genus distribution (Friedman 2018). A similar situation is observed in the African weevil genus *Bradybibastes* Heller, 1923, where one of species, *B. discoidalis* (Tournier, 1873), was found also in the southern part of Israel (see Friedman 2009). Inside the species-rich weevil genus *Merus* Gistel, 1857, *M. friedbergi* Friedman, 2019, recently described from south Israel, is the only Palearctic member of the *denticulatus* species group. So far, this species group has been considered to include 10 described and a few undescribed species from east, west, central and south regions of Africa, with the majority of the species concentrating along the Great Rift Valley (Friedman 2019). According to Friedman (2009), two apparently undescribed weevil species belonging to the Afrotropical genus *Cylindroides* Fairmaire, 1886 occur in southern Israel in the Rift Valley and in the Central and Southern Negev.

In the mayfly family Baetidae (Ephemeroptera), *Cloeon perkinsi* Barnard, 1932, previously known only from the western, eastern and southern regions of the mainland Africa, has been very recently found in Yemen, western Saudi Arabia and Israel (Yanai et al. 2020).

Among the taxa of Diptera, a disjunctive fruit fly genus *Hyalotephritis* Freidberg, 1979 includes only two species: *H. planiscutellata* (Becker, 1903), originally described from Egypt and then found in Ethiopia and Israel, and *H. complanata* (Munro, 1929) known from South and South-Western Africa (Freidberg 1979). The robber fly genus *Lamyra* Loew, 1851 (Asilidae), which has been recently revised and relimited to four species, is endemic to the Afrotropical Realm; however, one of these species, *L. vorax* Loew, 1858, extends into Israel, Yemen, UAE and Saudi Arabia in the Palearctic Region (Dikow and Londt 2000).

Similar paleotropical relations are also known for some Israeli taxa of moths and butterflies (Lepidoptera). Since description, the tiger moth genus *Olepa* Watson, 1980 (Erebidae, Arctiinae) has been considered as restricted to South and South-Eastern Asia (see Singh and Singh 2013). Several years ago, however, the first Palearctic species certainly belonging to the genus was described from Israel (Witt et al. 2005). Between 420 species of the butterfly family Noctuidae, registered in Israel by 2007, only two species of *Condica* Walker, 1856 follow this type of distribution (see Kravchenko et al. 2007). According to these data, *C. capensis* (Gueneé, 1852), widespread in the Old World tropical zone, penetrates Arabian Peninsula, Egypt and Israel, with the northernmost limit of its range in the Dead Sea area. While the mostly South Asian *C. palestinensis* (Staudinger, 1895) spreads northward along the rift zone to the Jordan Valley and Syria.

All the above-noted examples indicate that the disjunctive range of *Euprosthénops* is only a particular case of a more common pattern. In the future, either *E. insperatus* sp. nov. itself or related species, could well be found in Egypt, Yemen, Saudi Arabia and other regions of the Middle East. It is possible, however, that for various reasons, the former connections have disappeared and the gap will remain unfilled.

## Acknowledgements

We thank Alireza Zamani (currently at Zoological Museum, the University of Turku) who kindly checked an early version of the manuscript. We also appreciate Dragomir Dimitrov (University of Barcelona, Spain) and Xiaoqi Mi (Tongren University, China) for their constructive comments. Special thanks to Seppo Koponen who arranged our stay in Turku and provided us with the museum facilities. The senior co-author was supported by the Ministry of Absorption, Israel.

## References

- Armiach Steinpress I, Alderweireldt M, Cohen M, Chipman A, Gavish-Regev E (2021) Synopsis of the Evippinae (Araneae, Lycosidae) of Israel, with description of a new species. *European Journal of Taxonomy* 733: 87–124. <https://doi.org/10.5852/ejt.2021.733.1225>
- Azarkina GN, Foord SH (2014) A revision of the Afrotropical species of *Festucula* Simon, 1901 (Araneae: Salticidae). *African Invertebrates* 55(2): 351–375. <https://doi.org/10.5733/afin.055.0201>
- Blandin P (1974) Etudes sur les Pisauridae africaines II. Définition du genre *Euprosthénops* Pocock, 1897 et description du genre *Euprosthénopsis* n. gen. (Araneae – Pisauridae – Pisaurinae). *Revue de Zoologie Africaine* 81: 933–947. <https://doi.org/10.5962/bhl.part.76052>
- Blandin P (1975) Note sur *Euprosthénops ellioti* (Pickard-Cambridge O., 1877) (Araneae – Pisauridae – Pisaurinae). *Bulletin de la Société Zoologique de France* 100(4): 575–581.
- Blandin P (1976) Etudes sur les Pisauridae africaines IV. Les espèces du genre *Euprosthénops* Pocock, 1897 (Araneae – Pisauridae – Pisaurinae). *Revue Zoologique Africaine* 90(1): 63–88.
- Blandin P (1978) Le problème de l'espèce chez les araignées. Les problèmes de l'espèce dans le règne animal 2: 13–56.
- Blondi M, Frasca R, Grobbelaar E, D'Alessandro P (2017) Supraspecific taxonomy of the flea beetle genus *Blepharida* Chevrolat, 1836 (Coleoptera: Chrysomelidae) in the Afrotropical Region and description of *Afroblepharida* subgen. nov. *Insect Systematics & Evolution* 48: 97–155. <https://doi.org/10.1163/1876312X-48022152>
- Danin A (1988) Flora and vegetation of Israel and adjacent areas. In: Yom-Tov Y, Tchernov E (Eds) *The zoogeography of Israel*. Dr. W. Junk Publishers, Dordrecht, 129–158.
- Danin A, Orshan G, Zohary M (1975) The vegetation of the northern Negev and the Judean Desert of Israel. *Israel Journal of Botany* 24: 118–172.

- Dikow T, Londt JGH (2000) A review of *Lamyra* Loew (Diptera: Asilidae: Laphriinae). African Entomology 8(2): 189–200.
- Dyal S (1935) Fauna of Lahore. 4.–Spiders of Lahore. Bulletin of the Department of Zoology of the Panjab University 1: 119–252.
- El-Hennawy HK (2014) The first record of *Levymanus gershomi* in Saudi Arabia (Araneae, Palpimanidae). Serket 14(2): 97–101.
- Freidberg A (1979) The Afrotropical species assigned to *Terellia* R. D. (Diptera: Tephritidae). Journal of the Washington Academy of Sciences 69(4): 164–174.
- Freidberg A (1988) Zoogeography of Diptera in Israel. In: Yom-Tov Y, Tchernov E (Eds) The zoogeography of Israel. Dr. W. Junk Publishers, Dordrecht, 251–276.
- Friedman A-L-L (2009) Review of the biodiversity and zoogeographical patterns of the weevils (Coleoptera, Curculionoidea) in Israel. In: Neubert E, Amr Z, Taiti S, Gümüs B (Eds) Animal Biodiversity in the Middle East. Proceedings of the First Middle Eastern Biodiversity Congress, Aqaba, Jordan, 20–23 October 2008. ZooKeys 31: 133–148. <https://doi.org/10.3897/zookeys.31.123>
- Friedman A-L-L (2018) Review of the hygrophilous weevils in Israel (Coleoptera: Curculionoidea). Diversity 2018, 10(3): 1–48. <https://doi.org/10.3390/d10030077>
- Friedman A-L-L (2019) The first record of the genus *Merus* Gistel (Curculionidae: Molytinae: Mecysolobini) in the Western Palaearctic, with description of *Merus freidbergi* n. sp. from Israel. Israel Journal of Entomology 49(2): 351–364. <https://doi.org/10.5281/zenodo.3593312>
- Furth DG (1975) Israel, a great biogeographic crossroads. Discovery 11(1): 2–13.
- Kravchenko VD, Fibiger M, Hausmann A, Müller GC (2007) The Lepidoptera of Israel. Volume 2. Noctuidae. Pensoft Publishers, Sofia–Moscow, 320 pp.
- Levy G (1998) Twelve genera of orb-weaver spiders (Araneae, Araneidae) from Israel. Israel Journal of Zoology 43: 311–365.
- Levy G (2007) *Calommata* (Atypidae) and new spider species (Araneae) from Israel. Zootaxa 1551: 1–30. <https://doi.org/10.11646/zootaxa.1551.1.1>
- Matalin AV, Chikatunov VI (2016) The tiger beetles (Coleoptera, Carabidae, Cicindelinae) of Israel and adjacent lands. ZooKeys 578: 115–160. <https://doi.org/10.3897/zookeys.578.7383>
- Moradmand M (2015) Revision of the grass huntsman spider genus *Pseudomicrommata* Järvi, 1914 (Araneae: Sparassidae) in the Afrotropical Region. African Invertebrates 56(2): 425–443. <https://doi.org/10.5733/afin.056.0213>
- Moradmand M, Zamani A, Jäger P (2019) An Afrotropic element at the north-western periphery of the Oriental Region: *Pseudomicrommata mokranica* sp. nov. (Araneae: Sparassidae). Revue Suisse de Zoologie 126(2): 249–156. <http://doi.org/10.5281/zenodo.3463459>
- Silva ELC da, Sierwald P (2014) Description of the males of *Euprosthonops australis* Simon, 1898 and *Euprosthonopsis pulchella* (Pocock, 1902) (Araneae: Pisauridae). Zootaxa 3857(1): 137–150. <https://doi.org/10.11646/zootaxa.3857.1.8>
- Simon E (1898) Histoire naturelle des araignées. Deuxième édition, tome second. Roret, Paris, 193–380. <https://doi.org/10.5962/bhl.title.51973>

- Singh N, Singh J (2013) Review of the genus *Olepa* Watson (Lepidoptera: Erebiidae: Arctiinae). *Tinea* 22(4): 272–277.
- Tchernov E (1988) The paleobiogeographical history of the southern Levant. In: Yom-Tov Y, Tchernov E (Eds) *The zoogeography of Israel*. Dr. W. Junk Publishers, Dordrecht, 159–250.
- Witt TJ, Müller GC, Kravchenko VD, Miller MA, Hausmann A, Speidel W (2005) A new *Olepa* species from Israel (Lepidoptera: Arctiidae). *Nachrichtenblatt der Bayerischen Entomologen* 54(3/4): 101–115.
- WSC (2021) World Spider Catalog. Natural History Museum Bern. <http://wsc.nmbe.ch> [version 22.0, accessed on 5.05.2021]
- Yanai Z, Graf W, Terefe Y, Sartori M, Gattoliat J-L (2020) Re-description and range extension of the Afrotropical mayfly *Cloeon perkinsi* (Ephemeroptera, Baetidae). *European Journal of Taxonomy* 617: 1–23. <https://doi.org/10.5852/ejt.2020.617>
- Zamani A, Marusik YM (2020) New species of Filistatidae, Palpimanidae and Scytodidae (Arachnida: Araneae) from southern Iran. *Acta Arachnologica* 69(2): 121–126. <https://doi.org/10.2476/asjaa.69.121>
- Zohary M (1966) *Flora Palaestina*. Part I. The Israel Academy of Sciences and Humanities, Jerusalem, 364 pp.
- Zonstein S, Marusik YM (2013) On *Levymanus*, a remarkable new spider genus from Israel, with notes on the Chediminae (Araneae, Palpimanidae). *ZooKeys* 326: 27–45. <https://doi.org/10.3897/zookeys.326.5344>
- Zonstein SL, Marusik YM, Kovblyuk MM (2017) New data on the spider genus *Levymanus* (Araneae: Palpimanidae). *Oriental Insects* 51(3): 221–226. <https://doi.org/10.1080/00305316.2016.1275989>



# Twenty-eight new species of *Trigonopterus* Fauvel (Coleoptera, Curculionidae) from Central Sulawesi

Raden Pramesa Narakusumo<sup>1,2</sup>, Alexander Riedel<sup>1</sup>

**1** Museum of Natural History Karlsruhe, Erbprinzenstr. 13, D-76133 Karlsruhe, Germany **2** Museum Zoologicum Bogoriense, Research Center for Biology, Indonesian Institute of Sciences (LIPI), Jl. Raya Jakarta – Bogor, KM46, 16911, Indonesia

Corresponding author: Alexander Riedel ([riedel@smnk.de](mailto:riedel@smnk.de))

Academic editor: Miguel Alonso-Zarazaga | Received 16 July 2021 | Accepted 8 September 2021 | Published 22 October 2021

<http://zoobank.org/7454EAAA-72D4-4550-A676-586C840CDDCB>

**Citation:** Narakusumo RP, Riedel A (2021) Twenty-eight new species of *Trigonopterus* Fauvel (Coleoptera, Curculionidae) from Central Sulawesi. ZooKeys 1065: 29–79. <https://doi.org/10.3897/zookeys.1065.71680>

## Abstract

Here we present 28 new species of *Trigonopterus* from Central Sulawesi, mostly from Mt Dako and Mt Pompango: *Trigonopterus acutus* sp. nov., *T. ancora* sp. nov., *T. arcanus* sp. nov., *T. corona* sp. nov., *T. dakoensis* sp. nov., *T. daun* sp. nov., *T. ewok* sp. nov., *T. gundala* sp. nov., *T. hoppla* sp. nov., *T. kakimerah* sp. nov., *T. katopasensis* sp. nov., *T. matakensis* sp. nov., *T. moduai* sp. nov., *T. mons* sp. nov., *T. paramoduai* sp. nov., *T. pomberimbensis* sp. nov., *T. pompangeensis* sp. nov., *T. puspoi* sp. nov., *T. rosichoni* sp. nov., *T. rubidus* sp. nov., *T. sarinoi* sp. nov., *T. sutrisnoi* sp. nov., *T. tanah* sp. nov., *T. tejokusumoi* sp. nov., *T. toboliensis* sp. nov., *T. tolitoliensis* sp. nov., *T. tounaensis* sp. nov., *T. unyil* sp. nov. This fills important areas of distribution and brings the number of *Trigonopterus* species recorded from Sulawesi to 132.

## Keywords

Celebes, conservation, *cox1*, Cryptorhynchinae, DNA barcoding, endemism, hyperdiverse, integrative taxonomy, morphology, Southeast Asia, turbo-taxonomy, Wallacea

## Introduction

*Trigonopterus* is a hyperdiverse genus of flightless hidden-snout weevils (Cryptorhynchinae) ranging over the Indo-Australian-Melanesian archipelago. It originated in Northern Australia and rapidly diversified in New Guinea (Toussaint et al. 2017) before colonizing Sulawesi and dispersing further west to Sundaland (Tänzler et al. 2016; Letsch et al. 2020). Thus, Sulawesi acted as a hub for the dispersal to Borneo, Java and the Lesser

Sunda Islands. Currently, there are 451 described species (Riedel et al. 2013b, 2014; Riedel and Tänzler 2016; Narakusumo et al. 2019; Riedel and Narakusumo 2019), but discovery of new species is still far from approaching saturation, especially if new localities are being sampled. In the following, we report on 28 new species from Central Sulawesi Province, mostly based on two field trips to Mt Dako and Mt Pompangeo, plus four species from Mt Torompupu, Mt Katopasa, and Palu from the collection of “Museum Zoologicum Bogoriense”. Mt Dako with a maximum elevation of 2304 m was sampled between 700 and 2200 m. Mt Pompangeo with a maximum elevation of 2590 m was sampled between 1800 and 2000 m. The total of *Trigonopterus* species in Sulawesi and the adjacent islands was recently brought from a single one to 104 species (Riedel and Narakusumo 2019), and with the present paper to 132 species. We refrain from providing a key based on morphological characters for the same reasons as outlined previously (Riedel and Narakusumo 2019: p. 96). Until the number of described species approaches saturation, a traditional key would be incomplete and potentially highly misleading. Old museum specimens can be hard to identify based on *cox1* sequences using a PCR / Sanger sequencing workflow, but in many cases, fragments of degraded DNA will be sufficient to allow sequencing by NGS technologies (Staats et al. 2013). Thus, even dry specimens older than 100 years can be safely identified if deemed necessary.

Sulawesi is geologically complex (Hall 2009; Stelbrink et al. 2012) and its biogeography is currently the subject of a detailed study by us utilizing, among other taxa, the genus *Trigonopterus*. The purpose of this paper is to provide names to these species, especially as some of them had been part of an earlier study on mitogenomes (Narakusumo et al. 2020). While many additional new *Trigonopterus* species can be expected from Sulawesi, the species described herein fill an important gap in the distributional record (Fig. 29). Central Sulawesi is where the formerly separate geological terranes fused together (Hall 2009; Nugraha and Hall 2018), and its fauna may be one of the richest areas on this island.

## Materials and methods

This study is based on 866 specimens from Central Sulawesi Province. Holotypes were selected from 197 specimens for which the *cox1* gene had been sequenced. DNA was extracted nondestructively as described by Riedel et al. (2010). Genitalia of most specimens did not require extra maceration. They could be directly stained with an 0.01% alcoholic Chlorazol Black solution and stored in glycerol in microvials attached to the pin of the specimens. Genitalia of specimens with tissue not sufficiently digested after DNA extraction were macerated in a 10% KOH solution and rinsed in 5% acetic acid before staining. Illustrations of habitus and genitalia were prepared from holotypes. Finally, type series were supplemented with specimens stored in ethanol and older material from the dry collection. Long series of the sibling species *T. matakensis* sp. nov. and *T. pompangeensis* sp. nov. could not be assigned based on external characters and had to remain unidentified. Type depositories are cited using the following codens:

- MZB** LIPI Research Center of Biology, Division of Zoology, Museum Zoologicum Bogoriense, Widyasatwaloka, Cibinong, Indonesia.
- SMNK** Staatliches Museum für Naturkunde, Karlsruhe, Germany.

The methods applied for DNA sequencing and sequence analysis are the same as described by Riedel et al. (2010) and Tänzler et al. (2012), except for samples MZB0217-MZB0240 being sequenced only in reverse direction using the primer HCO. Morphological descriptions are limited to major diagnostic characters as outlined by Riedel et al. (2013a, b). Negative character states (i.e., the absence of a character) are only mentioned explicitly where it appears appropriate. In groups comprising hundreds of species enumerating the absence of rare character states leads to inflated descriptions that distract the reader from the important information, i.e., the diagnostic characters present in a given species.

The closest relatives of Central Sulawesi species were identified by creating an alignment of 773 *cox1* sequences representing ca. 185 species and generating a maximum likelihood reconstruction using the program IQTREE (Nguyen et al. 2015). The uncorrected p-distance was calculated using *dist.dna* function with parameter *model="raw"* and *pairwise.deletion="TRUE"*, in *ape* 5.0 package (Paradis and Schliep 2019) run on R 3.6.3 (R Core Team 2020). Morphological terminology follows Beutel and Leschen (2005) and Leschen et al. (2009), i.e., the terms “mesovertrite” / “metavertrite” are used instead of “mesosternite” / “metasternite” and “mesanepisternum” / “metanepisternum” instead of “mesepisternum” / “metepisternum”; “penis” is used instead of “aedeagus” as the tegmen is usually without useful characters in *Trigonopterus* and therefore omitted from species descriptions. Specimens were examined with a Leica MZ16 dissecting microscope and a fluorescent desk lamp for illumination. Measurements were taken with the help of an ocular grid. The length of the body was measured in dorsal aspect from the elytral apex to the front of the pronotum. Legs were described in an idealized laterally extended position; there is a dorsal / ventral and an anterior / posterior surface. Habitus illustrations were compiled using a DFC495 camera with L.A.S. 4.8.0 software adapted to a Z6 APO (all from Leica Microsystems, Heerbrugg, Switzerland). Photographic illustrations of genitalia were made using a DFC450 camera with L.A.S. 4.8.0 software adapted to an Axio Imager M2 microscope (Carl Zeiss Microscopy), with 5×, respectively 10× A-Plan lenses; resulting image stacks were compiled using the Helicon Focus 6.7.1 Pro software (Helicon Soft Ltd). For photography genitalia were temporarily embedded in glycerol gelatin as described by Riedel (2005), with their longitudinal axis somewhat lifted caudally, to adequately illustrate structures of the curved down apex. All photographs were enhanced using the programs Adobe Photoshop CS2 and CS6. However, care was taken not to obscure or alter any features of the specimens illustrated. Sequence data were submitted to GenBank of NCBI (National Center for Biotechnology Information) and the accession numbers are provided under each species, e.g., as “(GenBank OK481808)”.

## Taxonomy

### *Trigonopterus* Fauvel, 1862

*Trigonopterus* Fauvel, 1862 Type species: *Trigonopterus insignis* Fauvel, 1862, by monotypy.

**Diagnosis.** Fully apterous genus of Cryptorhynchinae. Length 1.5–6.0 mm. Rostrum in repose not reaching center of mesocoxa. Scutellar shield completely absent externally. Mesothoracic receptacle deep, posteriorly closed. Metanepisternum completely absent externally. Elytra with nine striae (sometimes superficially effaced). Tarsal claws minute. Usually body largely unclothed, without dense vestiture. For additional information, see <http://species-id.net/wiki/Trigonopterus>.

## Descriptions of the species

### 1. *Trigonopterus acutus* sp. nov.

<http://zoobank.org/BEA6B28C-CB9B-4C5F-934A-A10BB3611B07>

**Diagnostic description. Holotype. Male** (Fig. 1a). Length 2.50 mm. Color of antennae and legs ferruginous; remainder black. Body subovate; in dorsal aspect and in profile with constriction between pronotum and elytron. Rostrum dorsally with median costa, and pair submedian ridge; intervening furrows with rows of coarse punctures and small suberect scales; epistome indistinct, subglabrous with suberect setae. Pronotum with disk densely punctate; interspaces between punctures subglabrous; laterally in basal half impunctate. Elytra with striae marked by well-impressed lines and rows of punctures; intervals subglabrous, with sparse punctures. Meso- and metafemur with anteroventral ridge crenate-denticulate. Metafemur subapically with stridulatory patch. Metatibia basally subglabrous, in apical half with few long setae. Abdominal ventrites 1–2 concave, anteriorly microreticulate, partly with coarse punctures, center subglabrous; ventrite 5 flat, densely punctate, microreticulate. Penis (Fig. 1b) with sides of body converging, apex acuminate, without setae; with several endophallic sclerites, especially around the ostium; with pair of triangular sclerites reinforcing basal orifice laterally; apodemes 2.0× as long as body of penis; transfer apparatus dentiform, curved upwards; ductus ejaculatorius with indistinct bulbus. **Intraspecific variation.** Length 2.38–2.65 mm. Female rostrum slender, dorsally subglabrous, with rows of punctures.

**Material examined. Holotype** (MZB, Cole.173.053): MZB0160 (GenBank OK481878), Indonesia, C-Sulawesi, Toli-Toli, Gn. Dako, 01°02.977'N, 120°55.010'E to 01°03.210'N, 120°55.297'E, 1700–1800 m, 08–10-VII-2018, beaten. **Paratypes** (MZB, SMNK): Indonesia, C-Sulawesi, Toli-Toli, Gn. Dako: 5 exx, MZB0101 (GenBank OK481916), MZB0055 (GenBank OK481960), MZB0197 (GenBank OK481853), MZB0198 (GenBank OK481852), MZB0199 (GenBank OK481851), 01°02.977'N, 120°55.001'E to 01°03.210'N, 120°55.297'E, 1700–1800 m, 08–10-VII-2018, beaten; 4 exx, MZB0191 (GenBank OK481859), 01°03.782'N, 120°53.934'E to 01°02.977'N, 120°55.001'E, 1250–1750 m, 11-VII-2018, beaten.

**Distribution.** C-Sulawesi Prov. (Mt Dako). Elevation ca. 1700–1800 m.

**Biology.** On foliage in montane forest.

**Etymology.** The species name is the Latin adjective *acutus* -a -um (pointed, acute) and refers both to the elytral shape and the apex of the penis.

**Notes.** *Trigonopterus acutus* sp. nov. was coded as “*Trigonopterus* sp. 1207”. This species belongs to the *T. tatorensis*-group. It is closely related to *T. daun* sp. nov., from which it can be distinguished by the pointed apex of the penis.

## 2. *Trigonopterus ancora* sp. nov.

<http://zoobank.org/74813024-DE34-4E66-B8FD-8DD6C8EC33C3>

**Diagnostic description.** *Holotype*, male (Fig. 2a). Length 2.97 mm. Color of antennae ferruginous; legs dark ferruginous; remainder black. Body subovate; in dorsal aspect with weak constriction between pronotum and elytron; in profile dorsally convex. Rostrum dorsally with broad median costa and pair of submedian ridges; intervening furrows with sparse rows of recumbent setae; apical 1/3 subglabrous, with few punctures and with sparse setae. Pronotum with disk densely punctate with coarse punctures except along impunctate midline; interspaces between punctures subglabrous, subequal to or smaller than punctures' diameter. Elytra with striae marked by punctures and fine hairlines; basal margin bordered by transverse row; intervals flat, with few interspersed punctures. Femora edentate; anteroventral ridges simple. Metafemur dorsally with sparse, recumbent, silvery scales; dorsoposterior edge crenate; subapically with stridulatory patch. Metatibia in apical 1/2 with fringe of yellow setae. Abdominal ventrites 1–2 concave, subglabrous; sublaterally sparsely punctate, with sparse setae; ventrite 5 with deeply concave impression of subquadrate outline; lateral ridges and subapically densely punctate, sparsely setose. Penis (Fig. 2b) with sides of body subparallel; apex subtruncate, with median angulate extension, with sparse setae; ventrolaterally at middle with pair of knobs; apodemes 1.8× as long as body of penis; transfer apparatus spiniform, directed basad in repose, attached to anchor-shaped supporting sclerite; ductus ejaculatorius without bulb. **Intraspecific variation.** Length 2.28–2.97 mm. Female rostrum dorsally flattened, smooth, with sublateral furrows and submedian rows of small punctures. Female abdominal ventrite 5 flat, subglabrous, laterally with sparse punctures.

**Material examined.** *Holotype* (MZB, Cole.173.054): MZB0053 (GenBank OK481962), Indonesia, C-Sulawesi, Toli-Toli, Gn. Dako, 01°03.412'N, 120°54.126'E to 01°03.241'N, 120°54.328'E, 1200–1300 m, 07-VII-2018, beaten. *Paratypes* (MZB, SMNK): Indonesia, C-Sulawesi, Toli-Toli, Gn. Dako: 1 ex, MZB0251 (GenBank OK481802), same data as holotype; 24 exx, MZB0054 (GenBank OK481961), MZB0258 (GenBank OK481795), 01°03.782'N, 120°53.934'E to 01°03.574'N, 120°54.032'E, 970–1100 m, 05–06-VII-2018, beaten; 2 exx, 01°03.782'N, 120°53.934'E to 01°03.967'N, 120°53.692'E, 970–1000 m, 05-VII-2018, beaten; 4 exx, MZB0247 (GenBank OK481806), 01°03.782'N, 120°53.934'E, 970 m, 07-VII-2018, beaten; 5 exx, MZB0241 (GenBank OK481812), MZB0242 (GenBank OK481811), MZB0243 (GenBank OK481810), MZB0244 (GenBank OK481809), MZB0245 (GenBank OK481808),

01°03.782'N, 120°53.934'E to 01°03.574'N, 120°54.032'E, 970–1140 m, 06-VII-2018, beaten; 1 ex, MZB0057 (GenBank OK481958), 01°03.512'N, 120°54.054'E, 1100–1200 m, 13-VII-2018, sifted; 3 exx, MZB0250 (GenBank OK481803), MZB0256 (GenBank OK481797), MZB0257 (GenBank OK481796), 01°03.512'N, 120°54.054'E, 1100–1200 m, 06-VII-2018, beaten; 3 exx, same as holotype; 1 ex, MZB0248 (GenBank OK481805), 01°03.697'N, 120°53.991'E, 1030 m, 06-VII-2018, sifted; 1 ex, MZB0246 (GenBank OK481807), 01°03.574'N, 120°54.032'E to 01°03.181'N, 120°54.607'E, 1100–1400 m, 07-VII-2018, beaten; 4 exx, 01°03.241'N, 120°53.328'E to 01°03.181'N, 120°54.607'E, 1300–1400 m, 07-VII-2018, beaten; 1 ex, 01°03.014'N, 120°54.607'E to 01°02.977'N, 120°55.009'E, 1400–1750 m, 07-VII-2018, beaten.

**Distribution.** C-Sulawesi Prov. (Mt Dako). Elevation 970–1400 m.

**Biology.** On foliage and in leaf litter in montane forests.

**Etymology.** This epithet is the Latin noun *ancora* (anchor) in apposition and refers to the sclerite in the male transfer apparatus.

**Notes.** *Trigonopterus ancora* sp. nov. was coded as “*Trigonopterus* sp. 1114” (Narakusumo et al. 2020). The species belongs to the *T. satyrus*-group and is closely related to *T. rosichoni* sp. nov. from which it differs by the shape of the transfer apparatus and 9.4–9.6% p-distance of its *cox1* sequence.

### 3. *Trigonopterus arcanus* sp. nov.

<http://zoobank.org/88D3491B-F652-455A-80A4-CD8E683ACEDC>

**Diagnostic description. Holotype,** male (Fig. 3a). Length 2.40 mm. Color of antennae ferruginous; remainder black. Body subovate; in dorsal aspect with weak constriction between pronotum and elytron; in profile dorsally convex. Rostrum dorsally with median ridge and pair of submedian ridges; intervening furrows with sparse rows of narrow, recumbent scales; epistome in apical 1/4 indistinct, subglabrous, with sparse setae. Pronotum with disk punctate, each puncture containing short seta; median line impunctate; interspaces subglabrous. Elytra with striae marked by rows of small punctures; intervals subglabrous; near base with few slightly larger punctures. Femora edentate; anteroventral ridge weakly crenate, ending in apical 1/3; anterior surface densely punctate, each puncture with narrow recumbent scale. Metafemur dorsally rounded, subapically with extensive stridulatory patch. Metatibia with dorsal edge weakly denticulate. Abdominal ventrites 1–2 weakly concave, subglabrous; ventrite 5 with dense coarse punctures, covered with suberect scales. Penis (Fig. 3b) with body subparallel, apex asymmetrical with subangulate extension, with few setae; apodemes 2.0× as long as body of penis; transfer apparatus complex, asymmetrical, with subrotund capsule; ductus ejaculatorius without bulbus. **Intraspecific variation.** Length 2.13–2.80 mm. Female rostrum dorsally polished, with submedian and sublateral rows of punctures. Female abdominal ventrite 1 weakly concave with sparse minute punctures. Female abdominal ventrite 5 flat, medially weakly convex, punctate, with suberect scales.

**Material examined. Holotype** (MZB, Cole.173.055): MZB0060 (GenBank OK481955), Indonesia, C-Sulawesi, Toli-Toli, Gn. Dako, 01°3.574'N, 120°54.0322'E

to 01°03.180'N, 120°54.607'E 1100–1200 m, 06-VII-2018, beaten. **Paratype** (MZB, SMNK): Indonesia, C-Sulawesi, Toli-Toli, Gn. Dako: 2 exx, same data as holotype; 3 exx, MZB0195 (GenBank OK481855), 01°04.181'N, 120°53.565'E to 01°03.967'N, 120°53.692'E, 720–830 m, 01-VII-2018, beaten; 3 exx, 01°03.574'N, 120°54.032'E to 01°03.512'N, 120°54.054'E, 1100–1200 m, 06-VII-2018, beaten; 11 exx, 01°03.782'N, 120°53.934'E to 01°03.574'N, 120°54.032'E, 970–1100 m, 06-VII-2018, beaten; 3 exx, 01°03.782'N, 120°53.934'E to 01°03.574'N, 120°54.032'E, 970–1140 m, 06-VII-2018, beaten; 2 exx, 01°03.782'N, 120°53.934'E, 970 m, 04-VII-2018, beaten; 2 exx, MZB0281 (GenBank OK481775), 01°03.782'N, 120°53.934'E, 970 m, 07-VII-2018, beaten; 3 exx, 01°03.967'N, 120°53.692'E to 01°03.782'N, 120°53.934'E, 830–970 m, 01-VII-2018, beaten; 1 ex, MZB0192 (GenBank OK481858), 01°04.181'N, 120°53.565'E to 01°03.967'N, 120°53.692'E, 835–970 m, 01-VII-2018, beaten; 7 exx, 01°03.967'N, 120°53.692'E to 01°03.782'N, 120°53.934'E, 830–970 m, 05-VII-2018, beaten; 7 exx, MZB0282 (GenBank OK481774), 01°03.967'N, 120°53.692'E to 01°03.782'N, 120°53.934'E, 830–970 m, 03-VII-2018, beaten; 3 exx, 01°03.574'N, 120°54.032'E to 01°03.157'N, 120°54.195'E, 1100–1120 m, 06-VII-2018, beaten; 9 exx, MZB0058 (GenBank OK481957), MZB0090 (GenBank OK481927), MZB0196 (GenBank OK481854), 01°03.412'N, 120°54.126'E to 01°03.241'N, 120°54.328'E, 1200–1300 m, 07-VII-2018, beaten; 3 exx, MZB0061 (GenBank OK481954), MZB0091 (GenBank OK481926), MZB0280 (GenBank OK481776), 01°03.697'N, 120°53.991'E, 1030 m, 06-VII-2018, beaten; 13 exx, 01°03.697'N, 120°53.991'E, 1030 m, 06-VII-2018, sifted; 1 ex, 01°03.157'N, 120°54.195'E, 1120 m, 06-VII-2018, sifted; 1 ex, MZB0283 (GenBank OK481773), 01°03.157'N, 120°54.195'E, 1120 m, 13-VII-2018, sifted; 9 exx, 01°03.574'N, 120°54.032'E to 01°03.181'N, 120°54.607'E, 1100–1400 m, 07-VII-2018, beaten; 5 exx, 01°03.014'N, 120°54.607'E to 01°02.977'N, 120°55.009'E, 1400–1750 m, 01-VII-2018, beaten.

**Distribution.** C-Sulawesi Prov. (Mt Dako). Elevation 830–1400 m.

**Biology.** On foliage in montane forest.

**Etymology.** This epithet is based on the Latin adjective *arcanus* *-a, -um* (hidden) and it refers to its close similarity to its sibling species *T. ovatulus* Riedel and *T. pseudovatulus* Riedel.

**Notes.** *Trigonopterus arcanus* sp. nov. was coded as “*Trigonopterus* sp. 1187”. The species belongs to the *T. ovatulus*-group. It is closely related to *T. pseudovatulus* Riedel from which it can be distinguished by the absence of a metatibial supra-uncal tooth. Furthermore, it differs by 12.7–13.8% p-distances of its *cox1* sequence.

#### 4. *Trigonopterus corona* sp. nov.

<http://zoobank.org/67F09DA3-B2E0-4018-B8E7-45FB830B6D59>

**Diagnostic description.** **Holotype.** Male (Fig. 4a). Length 3.31 mm. Color of antennae, tarsi and elytra ferruginous; remainder black. Body subovate; in dorsal aspect with weak constriction between pronotum and elytron; in profile dorsally convex. Rostrum

dorsally with median ridge and indistinct pair of submedian ridges, separated by rows of coarse punctures; epistome indistinct, subglabrous. Pronotum with disk densely punctate with coarse punctures; almost reticulate, interspaces subglabrous. Elytra ferruginous, apex darkened; striae marked by rows of larger punctures; intervals with rows of smaller punctures; stria 8 along humerus with six coarse punctures, externally bordered by indistinct ridge. Femora edentate, anteroventral ridge simple, crenulate; anterior surface densely coarsely punctate. Metafemur dorsally with sparse, subrecumbent, silvery scales; dorsoposterior edge simple; subapically with stridulatory patch. Metatibia in apical 1/3 ventrally with rounded, blade-like extension, with sparse, long setae. Abdominal ventrites 1–2 concave, sparsely punctate with coarse punctures, each puncture with one suberect silvery scale; ventrite 5 densely coarsely punctate, with suberect silvery scales, with shallow median impression. Penis (Fig. 4b) with sides basally subparallel, near middle angulate, weakly converging; apex with median extension, with sparse setae; apodemes 2.3× as long as body; transfer apparatus flagelliform, ca. 3.4× as long as body of penis, subequal total length of penis; ductus ejaculatorius basally sclerotized, with indistinct bulb.

**Material examined.** *Holotype* (MZB, Cole.173.057): MZB0181 (GenBank OK481869), Indonesia, C-Sulawesi, Toli-Toli, Gn. Dako, 01°03.174'N, 120°55.272'E to 01°03.389'N, 120°55.524'E, 1800–1900 m, 10-VII-2018, beaten.

**Distribution.** C-Sulawesi Prov. (Mt Dako). Elevation ca. 1100–1200 m.

**Biology.** On foliage in montane forest.

**Etymology.** This epithet refers to the Corona virus (Sars-Cov2). The global pandemic led to the cancellation of field work, and a focus on this and other manuscripts. It is a noun in apposition.

**Notes.** *Trigonopterus corona* sp. nov. was coded as “*Trigonopterus* sp. 1235”. This species belongs to the *T. fulvicornis*-group and is related to *T. seticnemis* Riedel, from which it can be easily distinguished by the ferruginous elytra.

##### 5. *Trigonopterus dakoensis* sp. nov.

<http://zoobank.org/03951330-F918-48F9-A743-6E96205807C1>

**Diagnostic description.** *Holotype*, male (Fig. 5a). Length 2.58 mm. Color of antennae and legs ferruginous; remainder black. Body broad subovate; in dorsal aspect with weak constriction between pronotum and elytron, in profile dorsally convex, with very weak constriction. Rostrum dorsally with median costa and pair of submedian ridges; intervening furrows with sparse rows of suberect narrow scales; epistome short, subglabrous, with sparse setae. Pronotum densely punctate, with coarse punctures partly arranged in longitudinal rows; median line impunctate; each puncture bearing a seta; interspaces subglabrous; laterally in basal 1/3 impunctate. Elytra with striae marked by rows of punctures; basal margin bordered by transverse row of deeper, coarse punctures; interspaces subglabrous, with few small interspersed punctures; stria 8 along humerus with six coarse punctures; elytral apex subtruncate. Femora edentate; antero-

ventral ridge simple; anterior surface densely coarsely punctate, each puncture with recumbent scale. Metafemur with dorsoposterior edge denticulate, with silvery scales upcurved; subapically with stridulatory patch. Metatibia subapically at base of uncus with inward directed brush of yellowish setae. Abdominal ventrites 1–2 deeply concave, medially subglabrous, laterally covered with erect scales; ventrite 5 concave, at middle impunctate, surrounded by large, coarse punctures; apically with sharp, transverse ridge, forming oblique, subglabrous surface. Penis (Fig. 5b) with body in profile with constriction, its apical half swollen; apex, ventrally with acute median process, bordered by wide lobes bearing fringe of long setae; laterally with smaller pair of simple lobes; apodemes 2.4× as long as body of penis; transfer apparatus spiniform, contained by complex accessory sclerites; ductus ejaculatorius without bulbus. ***Intraspecific variation.*** Length 2.38–2.58 mm. Female unknown.

**Material examined.** ***Holotype*** (MZB, Cole.173.058): MZB0064 (GenBank OK481953), Indonesia, C-Sulawesi, Toli-Toli, Gn. Dako, 01°03.512'N, 120°54.054'E, 1100 m, 13-VII-2018, sifted. ***Paratype*** (SMNK): Indonesia, C-Sulawesi, Toli-Toli, Gn. Dako: 1 ex, MZB0065 (GenBank OK481952), 01°03.531'N, 120°54.052'E, 1100 m, 13-VII-2018, sifted.

**Distribution.** C-Sulawesi Prov. (Mt Dako). Elevation 1030–1200 m.

**Biology.** In leaf litter of mountain forest.

**Etymology.** This epithet is a Latinized adjective based on Mt Dako.

**Notes.** *Trigonopterus dakoensis* sp. nov. was coded as “*Trigonopterus* sp. 1189”. The species belongs to the *T. manadensis*-group. It is related to *T. manadensis* Riedel, from which it differs by the peculiar morphology of the penis and by the longitudinal rows of coarse punctures on the pronotum. The p-distance of their *cox1* sequences is 14.5–14.8%.

## 6. *Trigonopterus daun* sp. nov.

<http://zoobank.org/1FAC1195-2A80-44E5-9244-5AB006E919BA>

**Diagnostic description.** ***Holotype. Male*** (Fig. 6a). Length 2.28 mm. Color of antennae and legs ferruginous; remainder black. Body subovate, elongate; in dorsal aspect and in profile with weak constriction between pronotum and elytron. Rostrum dorsally with median costa and pair of submedian ridges; intervening furrows with sparse rows of subrecumbent setae; epistome indistinct. Pronotum with disk densely punctate; interspaces between punctures subglabrous. Elytra with striae marked by fine hairlines and rows of small punctures; basal margin bordered row of slightly larger punctures; sutural interval subglabrous, with few interspersed punctures. Profemur with anteroventral ridge weakly crenate. Meso- and metafemur with anteroventral ridge denticulate; anterior surface of femora coarsely punctate, each puncture with narrow recumbent scale. Metafemur with dorsoposterior edge indistinct; subapically with stridulatory patch. Metatibia ventrally with sparse row of long, stiff setae. Meso- and metaventrite with plumose scales. Abdominal ventrites 1–2 concave, microreticulate, with sparse punctures and plumose scales; ventrite 5 flat, densely punctate, microre-

ticulate. Penis (Fig. 6b) with sides of body converging, apex spatulate, truncate, without setae; ostium elongate; apodemes  $2.1\times$  as long as body of penis; transfer apparatus small, hook-shaped, directed basad in repose, without supporting sclerites; ductus ejaculatorius with indistinct bulbus. **Intraspecific variation.** Length 2.28–2.70 mm. Female rostrum subglabrous, with rows of small punctures. Female abdominal ventrite 5 anteriorly subglabrous, posterior half densely punctate.

**Material examined.** **Holotype** (MZB, Cole.173.059): MZB0099 (GenBank OK481918), Indonesia, C-Sulawesi, Toli-Toli, Gn. Dako,  $01^{\circ}03.697'N$ ,  $120^{\circ}53.991'E$ , 970 m, 07-VII-2018, beaten. **Paratypes** (MZB, SMNK): Indonesia, C-Sulawesi, Toli-Toli, Gn. Dako: 2 exx, MZB0100 (GenBank OK481917), MZB0278 (GenBank OK481778), same data as holotype; 1 ex,  $01^{\circ}03.967'N$ ,  $120^{\circ}53.692'E$  to  $01^{\circ}03.782'N$ ,  $120^{\circ}53.934'E$ , 830–970 m, 03-VII-2018, beaten; 2 exx, MZB0279 (GenBank OK481777),  $01^{\circ}03.967'N$ ,  $120^{\circ}53.692'E$  to  $01^{\circ}03.782'N$ ,  $120^{\circ}53.934'E$ , 830–970 m, 05-VII-2018, beaten; 1 ex,  $01^{\circ}03.782'N$ ,  $120^{\circ}53.934'E$ , 970 m, 05-VII-2018, beaten; 2 exx,  $01^{\circ}03.782'N$ ,  $120^{\circ}53.934'E$  to  $01^{\circ}03.574'N$ ,  $120^{\circ}54.032'E$ , 970–1100 m, 06-VII-2018, beaten; 1 ex, MZB0200 (PCR failed),  $01^{\circ}03.574'N$ ,  $120^{\circ}54.032'E$  to  $01^{\circ}03.181'N$ ,  $120^{\circ}54.607'E$ , 1100–1400 m, 07-VII-2018, beaten; 1 ex,  $01^{\circ}03.412'N$ ,  $120^{\circ}54.126'E$  to  $01^{\circ}03.241'N$ ,  $120^{\circ}54.328'E$ , 1200–1300 m, 07-VII-2018, beaten; 1 ex, MZB0254 (GenBank OK481799),  $01^{\circ}02.977'N$ ,  $120^{\circ}55.010'E$  to  $01^{\circ}03.782'N$ ,  $120^{\circ}53.934'E$ , 970–1740 m, 11-VII-2018.

**Distribution.** C-Sulawesi Prov. (Mt Dako). Elevation 970–1200 m.

**Biology.** On foliage in montane forest.

**Etymology.** This epithet is the Indonesian word for “leaf” and a noun in apposition. It refers to the species’ lifestyle on foliage.

**Notes.** *Trigonopterus daun* sp. nov. was coded as “*Trigonopterus* sp. 1116” (Narakusumo et al. 2020). This species belongs to the *T. tatorensis*-group. It is closely related to *T. acutus* sp. nov., from which it can be distinguished by the erect metatibial setae, and the truncated apex of the penis. The *cox1* p-distance is 10.0–10.5%.

## 7. *Trigonopterus ewok* sp. nov.

<http://zoobank.org/591D85E0-1EE1-4B4F-8619-B334A05B4C91>

**Diagnostic description.** **Holotype. Male** (Fig. 7a). Length 2.23 mm. Color ferruginous; thorax black. Body subovate; in dorsal aspect with moderate constriction between pronotum and elytron; in profile dorsally convex. Rostrum dorsally with median and pair of submedian ridges, separated by rows of coarse punctures containing subrecumbent yellow scales; epistome subglabrous, with sparse setae and minute punctures, posteriorly with transverse ridge. Pronotum with indistinct lateral edges subparallel to weak subapical constriction; disk with dense, partly confluent coarse punctures, with recumbent yellow scales; with subglabrous midline. Elytra with striae deeply impressed, containing rows of yellow or white scales; intervals costate, with rows of punctures and yellowish recumbent scales. Femora dentate, with acute tooth; anteroventral ridge weakly crenu-

late; dorsal and anterior surface with sparse white scales. Metafemur with dorsoposterior edge indistinct, weakly denticulate; subapically with extended stridulatory patch; dorsally with subrecumbent silvery scales. Dorsoposterior edge of tibiae subbasally angulate, denticulate. Abdominal ventrites 1–2 weakly concave, with dense coarse punctures, with sparse piliform scales; ventrite 5 with weak impression, densely punctate, with sparse suberect setae. Penis (Fig. 7b) with sides of body subparallel, apex subtruncate, with dense setae; apodemes 3.3× as long as body of penis; transfer apparatus flagelliform; ductus ejaculatorius basally sclerotized, with indistinct bulb. ***Intraspecific variation.*** Length 1.93–2.23 mm. Epistome of female rostrum posteriorly without transverse ridge. Female pronotum with yellow scales concentrated in sublateral bands. Elytra with scaling more or less extensive. Female abdominal ventrites 1–2 flat.

**Material examined.** **Holotype** (MZB, Cole.173.060): MZB0129 (GenBank OK481905), Indonesia, C-Sulawesi, Tojo Una-Una, Matako, Gn. Pompango, 01°35.215'S, 120°55.560'E to 01°35.079'S, 120°55.49'E, 1900 m, 28-II-2020, sifted. **Paratypes** (MZB, SMNK): Indonesia, C-Sulawesi, Tojo Una-Una, Matako, Gn. Pompango: 1 ex, MZB0128 (GenBank OK481906), 01°35.235'S, 120°55.679'E to 01°35.258'S, 120°55.588'E, 1900 m, 27-II-2020, sifted; 2 exx, MZB0130 (GenBank OK481904), 01°35.197'S, 120°55.658'E to 01°35.127'S, 120°55.622'E, 2000 m, 01-III-2020, sifted.

**Distribution.** C-Sulawesi Prov. (Mt Pompango). Elevation ca. 1900–2000 m.

**Biology.** In leaf litter of montane forest.

**Etymology.** This epithet is a noun in apposition based on the fictional character of small bear-like creatures from Star Wars VI movie.

**Notes.** *Trigonopterus ewok* sp. nov. was coded as “*Trigonopterus* sp. 1188” (Naraku-sumo et al. 2020). This species belongs to the *T. impressicollis*-group. It is closely related to *T. impressicollis* Riedel, which differs by the absence of longitudinal impressions on the pronotum, shorter setae on the apex of penis and 17.5–17.7% *cox1* p-distance.

## 8. *Trigonopterus gundala* sp. nov.

<http://zoobank.org/87D8C696-B01C-4E94-A1A8-28238FDC716F>

**Diagnostic description.** **Holotype.** Male (Fig. 8a). Length 2.75 mm. Color of antennae, elytra and legs ferruginous; head and thorax black. Body elongate subovate; in dorsal aspect and in profile with distinct constriction between pronotum and elytron. Rostrum dorsally with subglabrous median costa and pair of submedian ridges; intervening furrows with coarse punctures and subrecumbent setae; apical 1/3 subglabrous, with few punctures and with sparse suberect setae. Pronotum with disk reticulate-punctate; ridges between punctures subglabrous; laterally in basal 1/3 with sparser punctures. Elytra with striae deeply impressed; intervals costate, each with one row of greyish punctures containing minute seta; suture at middle weakly carinate. Femora edentate; with distinct anteroventral and posteroventral ridges simple; anterior surface densely coarsely punctate, each puncture with recumbent scale. Metafemur dor-

sally with row of confluent punctures, bordered by subglabrous line; subapically with stridulatory patch. Metatibia slender, with sparse suberect setae. Abdominal ventrites 1 and 2 flat with coarse punctures; ventrite 5, weakly concave towards apex, with dense small punctures. Penis (Fig. 8b) with sides of body subparallel; apex with median angulate extension and sparse long setae; apodemes 1.5× as long as body of penis; transfer apparatus spiniform, directed basad in repose; ductus ejaculatorius without bulb. **Intraspecific variation.** Length 2.55–2.76 mm. Female rostrum slender, subglabrous. Female ventrite 1 and 2 flat with dense small punctures. Female ventrite 5 flat.

**Material examined.** **Holotype** (MZB, Cole.173.061): MZB0079 (GenBank OK481938), Indonesia, C-Sulawesi, Toli-Toli, Gn. Dako, 01°03.389'N, 120°55.524'E to 01°03.567'N, 120°56.032'E, 1900–2200 m, 10-VII-2018, beaten. **Paratypes** (MZB, SMNK): Indonesia, C-Sulawesi, Toli-Toli, Gn. Dako: 2 exx, MZB0080 (GenBank OK481937), MZB0190 (GenBank OK481860), same data as holotype; 4 exx, MZB0082 (GenBank OK481935), MZB0186 (GenBank OK481864), MZB0187 (GenBank OK481863), MZB0188 (GenBank OK481862), 01°03.174N, 120°55.272'E to 01°03.389N, 120°55.524'E, 1800–1900 m, 10-VII-2018, beaten.

**Distribution.** C-Sulawesi Prov. (Mt Dako). Elevation ca. 1900–2200 m.

**Biology.** On foliage in montane forest.

**Etymology.** This epithet is a noun in apposition based on the fictional character of Indonesian comic superhero “Gundala, Son of Thunder”. The black and ferruginous colors of this species resemble Gundala’s movie costume.

**Notes.** *Trigonopterus gundala* sp. nov. was coded as “*Trigonopterus* sp. 1194”. It belongs to the *T. satyrus*-group and is closely related to *T. mons* sp. nov., but differs by the deeply striate elytra and a 8.2–8.7% *cox1* p-distance.

### 9. *Trigonopterus hoppla* sp. nov.

<http://zoobank.org/80388645-F13D-4FFC-9AB2-DC34EC40DFFB>

**Diagnostic description.** **Holotype. Male** (Fig. 9a). Length 2.75 mm. Color of antennae and legs ferruginous; elytra dark ferruginous, almost black; remainder black. Body subovate; in dorsal aspect and in profile with weak constriction between pronotum and elytron. Rostrum dorsally with median costa and pair of submedian ridges; intervening furrows with rows of coarse punctures, each puncture containing one subrecumbent seta; epistome indistinct. Pronotum with disk densely punctate-reticulate with coarse punctures. Elytra with striae deeply impressed; intervals costate, each with one row of punctures. Profemur with anteroventral ridge simple. Meso- and metafemur with anteroventral ridge crenate; anterior surface of femora coarsely punctate, each puncture with narrow recumbent scale. Metafemur with dorsoposterior edge indistinct; subapically with stridulatory patch. Metatibia ventrally with few long, stiff setae. Meso- and metaventrite with sparse plumose scales. Abdominal ventrites 1–2 concave, markedly microreticulate, with coarse punctures and sparse plumose scales; ventrite 5 flat, with shallow impression, densely punctate, microreticulate. Penis (Fig. 9b) with sides of body converging to pointed apex; ostium with complex sclerites; apodemes 2.4× as long as body of penis; transfer

apparatus spiniform, without supporting sclerites; ductus ejaculatorius with indistinct bulb. **Intraspecific variation.** Length 2.69–2.75 mm. Sculpture of paratype much less distinct; moderately to sparsely punctate, elytral striae weakly impressed.

**Material examined.** **Holotype** (MZB, Cole.173.062): MZB0201 (GenBank OK481850), Indonesia, C-Sulawesi, Toli-Toli, Gn. Dako, 01°02.977'N, 120°55.009'E to 01°03.210'N, 120°55.297'E, 1700–1800 m, 08–10-VII-2018, beaten. **Paratype** (SMNK): Indonesia, C-Sulawesi, Toli-Toli, Gn. Dako: 1 ex, MZB0277 (GenBank OK481779), 01°03.412'N, 120°54.126'E to 01°03.241'N, 120°54.328'E, 1200–1300 m, 07-VII-2018.

**Distribution.** C-Sulawesi Prov. (Mt Dako). Elevation 1300–1700 m.

**Biology.** On foliage in montane forest.

**Etymology.** This epithet is based on the German word “Hoppla”, an exclamation of surprise, comparable to the English “whoops”. It is to be treated as a noun in apposition.

**Notes.** *Trigonopterus hoppla* sp. nov. was coded as “*Trigonopterus* sp. 1232”. This species belongs to the *T. tatorensis*-group. It is closely related to *T. daun* sp. nov., from which it can be distinguished by the pointed apex of the penis and a *cox1* p-distance of 7.8%. The marked difference in sculpture between holotype and the single paratype is remarkable, and would usually indicate a separate species. However, genital morphology and *cox1* sequence of both specimens are almost identical, so either the coarse sculpture of the holotype, or the smooth sculpture of the paratype may be an aberration. Additional specimens are needed to clarify this matter.

#### 10. *Trigonopterus kakimerah* sp. nov.

<http://zoobank.org/4DA046DE-E058-4E96-BF43-DCD6FF75047E>

**Diagnostic description.** **Holotype. Male** (Fig. 10a). Length 2.30 mm. Color of antennae and legs ferruginous, remainder black. Body subovate; in dorsal aspect with weak constriction between pronotum and elytron; in profile dorsally convex. Rostrum punctate-rugose, in basal half with median and pair of submedian ridges, in apical half punctate. Pronotum with disk densely punctate, interspace subglabrous; median line impunctate. Elytra irregularly punctate with small punctures; interspaces subglabrous; along basal margin with denser punctures; stria 8 along humerus with five coarse punctures externally bordered by weak costa. Femora with anteroventral ridge crenulate, in metafemur shortened, forming blunt tooth. Metafemur dorsally with sparse slender scales; without distinct dorsoposterior edge; subapically with stridulatory patch. Abdominal ventrites 1–2 concave, subglabrous, sparsely punctate, microreticulate; ventrite 5 with shallow median impression, coarsely punctate, microreticulate. Penis (Fig. 10b) with sides of body subparallel to rounded apex; apodemes 2.0× as long as body of penis; endophallus with pair of elongate sclerites; transfer apparatus flagelliform, ca. 1.2× as long as body of penis, coiled up in apical portion of endophallus; ductus ejaculatorius without bulb. **Intraspecific variation.** Length 2.28–2.35 mm. Female rostrum slender, dorsally subglabrous, with submedian row of punctures. Female ventrite 5 without median impression.

**Material examined.** *Holotype* (MZB, Cole.173.063): MZB0207 (GenBank OK481846), Indonesia, C-Sulawesi, Tojo Una-Una, Matako, Gn. Pompangeo, 01°35.603'S, 120°55.437'E to 01°35.406'S, 120°55.547'E, 1800 m, 29-II-2020, beaten. *Paratype* (MZB, SMNK): Indonesia, C-Sulawesi, Tojo Una-Una, Matako, Gn. Pompangeo: 1 ex, MZB0208 (GenBank OK481845), 01°35.264'S, 120°55.588'E to 01°35.339'S, 120°55.599'E, 1900 m, 29-II-2020, beaten; 2 exx, MZB0209 (GenBank OK481844), MZB0210 (GenBank OK481843), 01°35.264'S, 120°55.588'E to 01°35.339'S, 120°55.599'E, 1900 m, 26–27-II-2020, beaten; 1 ex, MZB0154 (GenBank OK481884), 01°35.197'S, 120°55.658'E to 01°35.154'S, 120°55.507'E, 1900 m, 28-II-2020.

**Distribution.** C-Sulawesi Prov. (Mt Pompangeo). Elevation 1800–1900 m.

**Biology.** On foliage in montane forest.

**Etymology.** This epithet is the Indonesian term for “red legs”. It is a noun in apposition.

**Notes.** *Trigonopterus kakimerah* sp. nov. was coded as “*Trigonopterus* sp. 1202”. This species may belong to the *T. fulvicornis*-group. The *cox1* p-distance to other known species is above 14%.

### 11. *Trigonopterus katopasensis* sp. nov.

<http://zoobank.org/EFE5C4A8-8D53-4302-A54C-9E57C4165620>

**Diagnostic description.** *Holotype. Male* (Fig. 11a). Length 2.35 mm. Color of antennae and apical tarsomeres ferruginous; remainder black. Body subovate; in dorsal aspect with weak constriction between pronotum and elytron; in profile dorsally convex. Rostrum dorsally with median and pair of submedian carinae; intervening furrows with sparse rows of subrecumbent setae; epistome indistinct, subglabrous, subapically with sparse suberect setae. Pronotum with disk sparsely punctate with small punctures; interspaces subglabrous. Elytra sparsely punctate with irregular, minute punctures; interspaces subglabrous; striae indistinct; along basal margin with slightly denser row. Femora with anteroventral ridge crenulate; anterior surface microreticulate, dorsally and especially subapically coarsely punctate. Metafemur with dorsoposterior edge indistinct; subapically with stridulatory patch. Metatibia in apical half ventrally with sparse row of long, stiff setae; dorsal contour in apical third weakly emarginate. Abdominal ventrites 1–2 concave, subglabrous; ventrite 5 microreticulate, with subquadrate pit, bordered by subparallel lateral ridges. Penis (Fig. 11b) with sides of body subparallel; apex symmetrical, with angulate extension; with few setae; apodemes 2.2× as long as body of penis; transfer apparatus complex; ductus ejaculatorius with indistinct bulbus. **Intraspecific variation.** Length 1.98–2.68 mm. Female rostrum subglabrous, with distinct furrows, costae indistinct. Female abdominal ventrites 1–2 less concave; ventrite 5 flat.

**Material examined.** *Holotype* (MZB, Cole.173.064): MZB0108 (GenBank OK481912) Indonesia, C-Sulawesi, Tojo Una-Una, Ulubongka, Mire, Gn. Katopasa, 01°11.31'S, 121°27.348'E, 1380 m, 23–24-VII-2017, beaten. *Paratype* (MZB, SMNK): 27 exx, MZB0109 (GenBank OK481911) same data as holotype.

**Distribution.** C-Sulawesi Prov. (Mt Katopasa). Elevation ca. 1380 m.

**Biology.** On foliage in montane forest.

**Etymology.** This epithet is a Latinized adjective based on Mt Katopasa.

**Notes.** *Trigonopterus katopasensis* sp. nov. was coded as “*Trigonopterus* sp. 1190”. This species presumably belongs to the *T. barbipes*-group. From *T. barbipes* Riedel it differs by less distinct body sculpture, the structure of the penis, and a 18.5% *cox1* p-distance.

## 12. *Trigonopterus matakensis* sp. nov.

<http://zoobank.org/8F5E17E6-7640-4C26-81EF-B6CF87664D13>

**Diagnostic description. Holotype. Male** (Fig. 12a). Length 2.13 mm. Color of antennae ferruginous, legs dark ferruginous, remainder black. Body subovate; in dorsal aspect with weak constriction between pronotum and elytron; in profile dorsally convex, with very weak constriction between pronotum and elytron. Rostrum dorsally with median costa and with pair of irregular submedian ridges; intervening furrows with sparse rows of suberect setae, converging towards apex; epistome indistinct, subglabrous, with sparse erected setae. Pronotum with ovate punctures of transverse orientation; interspaces subglabrous. Elytra with striae marked by rows of small punctures; sutural interval with additional row, other intervals subglabrous, with sparse minute punctures; basal margin with transverse row of somewhat larger punctures. Femora dentate with small tooth; anterior surface punctate, microreticulate, each puncture with short recumbent seta. Meso- and metafemur with anteroventral ridge crenate. Metafemur subapically with stridulatory patch. Abdominal ventrites 1–2 concave, microreticulate, with sparse punctures; ventrite 5 punctate, microreticulate, with sparse setae, at middle with distinct impression. Penis (Fig. 12b) with body subparallel to rounded apex, with few short setae; apodemes 2.6× as long as body of penis; transfer apparatus spiniform, pointing apicad, held by subrotund sclerite; ductus ejaculatorius without bulbus. **Intraspecific variation.** Length 1.98–2.43 mm. Female rostrum smooth, subglabrous, with rows of small punctures. Female ventrite 5 flat, densely punctate, microreticulate.

**Material examined. Holotype** (MZB, Cole.173.065): MZB0159 (GenBank OK481879), Indonesia, C-Sulawesi, Tojo Una-Una, Matak, Gn. Pompangeo, 01°35.603'S, 120°55.437'E to 01°35.406'S, 120°55.547'E, 1800 m, 29-II-2020, beaten. **Paratypes** (MZB, SMNK): Indonesia, C-Sulawesi, Tojo Una-Una, Matak, Gn. Pompangeo: 1 ex, MZB0148 (GenBank OK481889), 01°35.215'S, 120°55.560'E to 01°35.079'S, 120°55.49'E, 1900 m, 28-II-2020, beaten; 1 ex, MZB0149 (GenBank OK481888), 01°35.603'S, 120°55.437'E to 01°35.406'S, 120°55.547'E, 1800 m, 29-II-2020, beaten; 4 exx, MZB0223 (GenBank OK481830), MZB0224 (GenBank OK481829), MZB0225 (GenBank OK481828), MZB0226 (GenBank OK481827), 01°35.359'S, 120°55.643'E to 01°35.581'S, 120°55.385'E, 1800 m, 29-II-2020, beaten; 2 exx, MZB0156 (GenBank OK481882), MZB0157 (GenBank OK481881), 01°35.359'S, 120°55.643'E to 01°35.581'S, 120°55.385'E, 1900 m, 29-II-2020, sifted; 3 exx, MZB0158 (GenBank OK481880), MZB0234 (GenBank OK481819), MZB0235 (GenBank OK481818), 01°35.235'S, 120°55.679'E to 01°35.258'S, 120°55.588'E, 1900

m, 26–27-II-2020, beaten; 2 exx, MZB0166 (GenBank OK481872), MZB0167 (GenBank OK481871), 01°35.603'S, 120°55.437'E to 01°35.406'S, 120°55.547'E, 1800 m, 29-II-2020, beaten; 5 exx, MZB0168 (GenBank OK481870), MZB0230 (GenBank OK481823), MZB0231 (GenBank OK481822), MZB0232 (GenBank OK481821), MZB0233 (GenBank OK481820), 01°35.197'S, 120°55.658'E to 01°35.154'S, 120°55.507'E, 1900 m, 28-II-2020, beaten; 10 exx, MZB0150 (GenBank OK481887), MZB0155 (GenBank OK481883), MZB0217 (GenBank OK481836), MZB0218 (GenBank OK481835), MZB0219 (GenBank OK481834), MZB0220 (GenBank OK481833), MZB0221 (GenBank OK481832), MZB0222 (GenBank OK481831), MZB0227 (GenBank OK481826), MZB0228 (GenBank OK481825), 01°35.197'S, 120°55.658'E to 01°35.127'S, 120°55.622'E, 2000 m, 01-III-2020, beaten.

**Distribution.** C-Sulawesi Prov. (Mt Pompangeo). Elevation 1800–2000 m.

**Biology.** On foliage and in leaf litter in montane forests.

**Etymology.** This epithet is a Latinized adjective based on Matakko village.

**Notes.** *Trigonopterus matakensis* sp. nov. was coded as “*Trigonopterus* sp. 1197”. This species belongs to the *T. ovalipunctatus*-group. It is closely related to *T. ovalipunctatus* Riedel, but differs by the subrotund shape of the supporting sclerites of the transfer apparatus and a 9.6–10.3% *cox1* p-distance.

### 13. *Trigonopterus moduai* sp. nov.

<http://zoobank.org/3A311395-FA62-492C-85CF-C5DFE56F1ED1>

**Diagnostic description. Holotype. Male** (Fig. 13a). Length 2.80 mm. Color of antennae and legs ferruginous; remainder black. Body subovate; in profile with weak constriction between pronotum and elytron. Rostrum at middle with constriction; dorsally coarsely punctate-rugose, in basal half with sublateral furrows containing rows of suberect setae; epistome indistinct, subglabrous with sparse setae. Pronotum with disk coarsely punctate-reticulate; interspaces between punctures subglabrous; each puncture with one minute seta. Elytra with striae marked by deep punctures each with one minute seta; intervals costate, subglabrous, with few interspersed punctures. Femora edentate; anteroventral ridges simple. Metafemur with dorsoposterior edge indistinct; subapically with stridulatory patch. Abdominal ventrites 1–2 concave, microreticulate, with coarse punctures; ventrite 5 with broad, shallow impression, microreticulate, with sparse small punctures. Penis (Fig. 13b) with sides of body subparallel, weakly converging, subapically with shallow constriction; apex setose, with median rounded extension; basal orifice ventrally with brace; apodemes 2.2× as long as body of penis; transfer apparatus flagelliform, looping S-shaped apicad, its tip emerging from apical orifice, ca. 3.5× as long as body of penis; ductus ejaculatorius without bulb. **Intraspecific variation.** Length 2.58–2.80 mm. Female rostrum more slender, punctures smaller. Female ventrites 1–2 almost flat.

**Material examined. Holotype** (MZB, Cole.173.066): MZB0072 (GenBank OK481945), Indonesia, C-Sulawesi, Toli-Toli, Gn. Dako, 01°02.977' N, 120°55.010' E to 01°03.210' N, 120°55.297' E, 1700–1800 m, 08–10-VII-2018, beaten. **Paratypes** (MZB,

SMNK): Indonesia, C-Sulawesi, Toli-Toli, Gn. Dako: 14 exx, MZB0071 (GenBank OK481946), MZB0073 (GenBank OK481944), MZB0165 (GenBank OK481873), same data as holotype; 1 ex, MZB0070 (GenBank FD03047006), 01°03.181'N, 120°54.607'E to 01°02.977'N, 120°55.001'E, 1400–1750 m, 07-VII-2018.

**Distribution.** C-Sulawesi Prov. (Mt Dako). Elevation ca. 1700–1800 m.

**Biology.** On foliage in montane forest.

**Etymology.** This epithet is a noun in apposition based on “Moduai”, a folk dance of people from Toli-Toli Regency.

**Notes.** *Trigonopterus moduai*, sp. nov. was coded as “*Trigonopterus* sp. 1201” and belongs to the *T. arachnobas*-group. It is very close to *T. paramoduai* sp. nov. (3.20–4.11% *cox1* p-distance) but can be distinguished by the darker elytral color, a slightly shorter rostrum, and the much longer flagellum of the male genital.

#### 14. *Trigonopterus mons* sp. nov.

<http://zoobank.org/CDF8BEDA-26ED-4254-9838-EA6285D263C1>

**Diagnostic description. Holotype. Male** (Fig. 14a). Length 2.81 mm. Color of antennae and legs ferruginous; elytra dark ferruginous; remainder black. Body subovate; in dorsal aspect with weak constriction between pronotum and elytron; in profile dorsally convex. Rostrum dorsally with flattened median costa and pair of submedian costae; intervening furrows with coarse punctures and suberect setae; apical 1/3 subglabrous, with suberect setae; epistome indistinct. Pronotum with disk densely punctate with coarse punctures; interspaces between punctures subglabrous; laterally in basal 1/3 subglabrous. Elytra with striae marked by punctures and fine hairlines; intervals subglabrous, with interspersed punctures. Femora edentate; anteroventral ridges simple. Metafemur with dorsoposterior edge simple; subapically with stridulatory patch. Abdominal ventrites 1–2 concave, medially subglabrous, laterally microreticulate, with coarse punctures; ventrite 5 with subquadrate pit, subglabrous, weakly microreticulate, subapically with short median carina; laterally punctate. Penis (Fig. 14b) with sides of body subparallel; apex subtruncate, with median triangular extension, with sparse long setae; apodemes 2.4× as long as body of penis; transfer apparatus flagelliform, looping apicad; support structures elongate lyriform; ductus ejaculatorius without bulbus. **Intraspecific variation.** Length 2.44–3.13 mm. Female rostrum more slender, subglabrous, with rows of punctures. Female ventrites 1–2 weakly concave. Female ventrite 5 flat, subglabrous, with sparse punctures.

**Material examined. Holotype** (MZB, Cole.173.067): Indonesia, C-Sulawesi, Toli-Toli, Gn. Dako, MZB0162 (GenBank OK481876), 01°03.181'N, 120°54.607'E to 01°02.977'N, 120°55.001'E, 1400–1750 m, 07-VII-2018, beaten. **Paratypes** (MZB, SMNK): Indonesia, C-Sulawesi, Toli-Toli, Gn. Dako: 3 exx, 01°03.782'N, 120°53.934'E to 01°02.977'N, 120°55.001'E, 1250–1750 m, 11-VII-2018, beaten; 13 exx, MZB0078 (GenBank OK481939), 01°03.389'N, 120°55.524'E to 01°03.567'N, 120°56.032'E, 1900–2200 m, 10-VII-2018, beaten; 16 exx, MZB0081 (GenBank OK481936), MZB0189 (GenBank OK481861), 01°03.174'N, 120°55.272'E to 01°03.389'N, 120°55.524'E, 1800–1900 m, 10-VII-2018, beaten; 16 exx,

MZB0083 (GenBank OK481934), MZB0084 (GenBank OK481933), 01°02.977'N, 120°55.001'E to 01°03.210'N, 120°55.297'E, 1700–1800 m, 10-VII-2018, beaten; 5 exx, MZB0163 (GenBank OK481875), same as holotype.

**Distribution.** C-Sulawesi Prov. (Mt Dako). Elevation 1700–1900 m.

**Biology.** On foliage in montane forest.

**Etymology.** This epithet is the Latin noun *mons* (mountain) in apposition.

**Notes.** *Trigonopterus mons* sp. nov. was coded as “*Trigonopterus* sp. 1195”. It belongs to the *T. satyrus*-group and is closely related to *T. gundala* sp. nov., which differs by the deeply striate elytra and a 8.2–8.7% *cox1* p-distance.

### 15. *Trigonopterus paramoduai* sp. nov.

<http://zoobank.org/639E9A24-FC23-49D7-B692-67D42B8F423B>

**Diagnostic description. Holotype. Male** (Fig. 15a). Length 2.56 mm. Color of antennae, legs and elytra ferruginous; remainder black. Body subovate; in profile with weak constriction between pronotum and elytron. Rostrum at middle with constriction; dorsally coarsely punctate-rugose, punctures containing rows of suberect setae; epistome indistinct, subglabrous with sparse setae. Pronotum with disk coarsely punctate-reticulate; interspaces between punctures subglabrous; each puncture with one minute seta. Elytra with striae marked by deep punctures each with one minute seta; intervals weakly costate, subglabrous. Femora edentate; anteroventral ridges simple. Metafemur with dorsoposterior edge indistinct; subapically with stridulatory patch. Abdominal ventrites 1–2 concave, with scattered coarse punctures; ventrite 5 with broad shallow impression, with sparse small punctures. Penis (Fig. 15b) with sides of body weakly concave, converging; apex setose, with distinct median extension; basal orifice ventrally with brace; apodemes 2.4× as long as body of penis; transfer apparatus flagelliform, curved, pointing basad, ca. 2.0× as long as body of penis; ductus ejaculatorius without bulbus. **Intraspecific variation.** Length 2.56–2.72 mm. Female rostrum more slender, punctures smaller. Female ventrites 1–2 almost flat.

**Material examined. Holotype** (MZB, Cole.173.068): MZB0183 (GenBank OK481867), Indonesia, C-Sulawesi, Toli-Toli, Gn. Dako, 01°03.389'N, 120°55.524'E to 01°03.567'N, 120°56.032'E, 1900–2200 m, 10-VII-2018, beaten. **Paratypes** (MZB, SMNK): Indonesia, C-Sulawesi, Toli-Toli, Gn. Dako: 3 exx, MZB0182 (GenBank OK481868), MZB0184 (GenBank OK481866), MZB0185 (GenBank OK481865), same as holotype; 2 exx, MZB0074 (GenBank OK481943), MZB0075 (GenBank OK481942), 01°03.174'N, 120°55.272'E to 01°03.389'N, 120°55.524'E, 1800–1900 m, 10-VII-2018, beaten; 2 exx, MZB0076 (GenBank OK481941), MZB0077 (GenBank OK481940), 01°03.389'N, 120°55.524'E to 01°03.567'N, 120°56.032'E, 1900–2200 m, 10-VII-2018, beaten.

**Distribution.** C-Sulawesi Prov. (Mt Dako). Elevation 1900–2200 m.

**Biology.** On foliage in montane forest.

**Etymology.** This epithet is based on the combination of the Greek prefix *para-* (next to; near by) and the sibling species *Trigonopterus moduai*, sp. nov..

**Notes.** *Trigonopterus paramoduai* sp. nov. was coded as “*Trigonopterus* sp. 1233” and belongs to the *T. arachnobas*-group. It is very close to *T. moduai* sp. nov. (3.20–4.11% *cox1* p-distance) from which it can be distinguished by the ferruginous elytral color, a slightly longer rostrum, and the shorter flagellum of the male genital.

**16. *Trigonopterus pomberimbensis* sp. nov.**

<http://zoobank.org/24840861-FE15-45AE-9FB7-9D33AEF4325B>

**Diagnostic description. Holotype. Male** (Fig. 16a). Length 1.98 mm. Color of antennae and tarsi ferruginous; remainder black. Body subovate; in dorsal aspect and in profile with weak constriction between pronotum and elytron. Rostrum dorsally with median and pair of submedian ridges; intervening furrows with sparse rows of suberect setae; epistome indistinct, subglabrous. Pronotum with disk densely punctate; interspaces between punctures subglabrous, subequal or smaller than punctures' diameter; laterally punctures coarse. Elytra with striae marked by weakly impressed rows of punctures; intervals subglabrous, with interspersed punctures. Femora with anteroventral ridge weakly crenate, ending with small acute tooth; anterior surface coarsely punctate, microreticulate. Metafemur with dorsoposterior edge simple; subapically with extended stridulatory patch. Metatibia ventrally with row of thin, erect setae. Abdominal ventrites 1–2 concave, densely punctate with coarse punctures and sparse plumose scales, interspaces microreticulate; ventrite 5 densely covered with erect to suberect plumose scales. Penis (Fig. 16b) with sides of body subparallel; apex subangular, medially extended into small tooth; with few long setae; apodemes 2.2× as long as body of penis; transfer apparatus spiniform, directed basad, held by anchor-shaped sclerites; ductus ejaculatorius without distinct bulbus. **Intraspecific variation.** Length 1.80–1.98. Female rostrum slender, dorsally subglabrous, with submedian row of punctures and sublateral furrows. Female abdominal ventrites 1–2 almost flat, with sparse suberect setae; ventrite 5 flat with sparse plumose scales.

**Material examined. Holotype** (MZB, Cole.173.069): MZB0132 (GenBank OK481902), Indonesia, C-Sulawesi, Tojo Una-Una, Matako, Gn. Pompangeo, 01°35.235'S, 120°55.679'E to 01°35.258'S, 120°55.588'E, 1900 m, 27-II-2020, sifted. **Paratypes** (MZB, SMNK): Indonesia, C-Sulawesi, Tojo Una-Una, Matako, Gn. Pompangeo: 5 exx, MZB0131 (GenBank OK481903), same data as holotype; 1 ex, 01°35.235'S, 120°55.679'E to 01°35.258'S, 120°55.588'E, 1900 m, 27-II-2020, beaten; 2 exx, MZB0153 (GenBank OK481885), 01°35.197'S, 120°55.658'E to 01°35.127'S, 120°55.622'E, 2000 m, 01-III-2020, beaten; 1 ex, 01°35.235'S, 120°55.679'E to 01°35.258'S, 120°55.588'E, 1900 m, 26–27-II-2020, beaten; 1 ex, MZB0143 (GenBank OK481894), 01°35.359'S, 120°55.643'E to 01°35.581'S, 120°55.385'E, 1900 m, 29-II-2020, sifted.

**Distribution.** C-Sulawesi Prov. (Mt Pompangeo). Elevation 1900–2000 m.

**Biology.** In leaf litter of montane forest.

**Etymology.** This epithet is a Latinized adjective based on Pomberimbe hill.

**Notes.** *Trigonopterus pomberimbensis* sp. nov. was coded as “*Trigonopterus* sp. 1191”. This species belongs to the *T. barbipes*-group. It is closely related to *T. viduus* Riedel, which differs by weakly impressed elytral striae and 19.7–21.2% *cox1* p-distance.

**17. *Trigonopterus pompangeensis* sp. nov.**

<http://zoobank.org/AD119D2E-9F79-4613-B54E-32B28582ADA4>

**Diagnostic description. Holotype. Male** (Fig. 17a). Length 2.16 mm. Color of antennae and legs ferruginous; remainder black. Body subovate; in dorsal aspect with weak constriction between pronotum and elytron; in profile dorsally convex. Rostrum dorsally with median costa and pair of somewhat irregular submedian ridges; epistome indistinct, subglabrous, apically with sparse suberect setae. Pronotum with ovate punctures of transverse orientation; interspaces subglabrous. Elytra with striae marked by rows of small punctures; sutural interval with additional row, other intervals subglabrous, with sparse minute punctures; basal margin with transverse row of denser punctures and wrinkles; stria 7 and 8 basally with somewhat coarser punctures. Femora dentate with small tooth; anterior surface densely punctate-rugose, microreticulate, each puncture with short recumbent seta. Meso- and metafemur with anteroventral ridge hardly crenate. Metafemur subapically with stridulatory patch. Abdominal ventrite 1–2 flat, subglabrous, with sparse punctures; ventrite 5 flat, densely punctate. Penis (Fig. 17b) with sides of body subparallel in basal half, converging in apical half, apex rounded, with few setae; apodemes 2.7× as long as body of penis; transfer apparatus spiniform, pointing apicad, held by pair of M-shaped sclerite; ductus ejaculatorius without bulbus. **Intraspecific variation.** Length 2.11–2.43. Female rostrum slender, dorsally subglabrous, with submedian row of punctures and sublateral furrows.

**Material examined. Holotype** (MZB, Cole.173.070): MZB0145 (GenBank OK481892), Indonesia, C-Sulawesi, Tojo Una-Una, Matak, Gn. Pompangeo, 01°35.603'S, 120°55.437'E to 01°35.406'S, 120°55.547'E, 1800 m, 29-II-2020, beaten. **Paratypes** (MZB, SMNK): Indonesia, C-Sulawesi, Tojo Una-Una, Matak, Gn. Pompangeo: 2 exx, MZB0239 (GenBank OK481814), MZB0240 (GenBank OK481813), same data as holotype; 1 ex, MZB0133 (GenBank OK481901), 01°35.235'S, 120°55.679'E to 01°35.258'S, 120°55.588'E, 1900 m, 27-II-2020, sifted; 3 exx, MZB0147 (GenBank OK481890), MZB0164 (GenBank OK481874), MZB0229 (GenBank OK481824), 01°35.197'S, 120°55.658'E to 01°35.154'S, 120°55.507'E, 1900 m, 28-II-2020, beaten; 1 ex, MZB0152 (GenBank OK481886), 01°35.359'S, 120°55.643'E to 01°35.581'S, 120°55.385'E, 1800 m, 29-II-2020, beaten; 1 ex, MZB0144 (GenBank OK481893), 01°35.235'S, 120°55.679'E to 01°35.258'S, 120°55.588'E, 1900 m, 26–27-II-2020, beaten; 4 exx, MZB0146 (GenBank OK481891), MZB0236 (GenBank OK481817), MZB0237 (GenBank OK481816), MZB0238 (GenBank OK481815), 01°35.197'S, 120°55.658'E to 01°35.127'S, 120°55.622'E, 2000 m, 01-III-2020, beaten.

**Distribution.** C-Sulawesi Prov. (Mt Pompangeo). Elevation 1800–2000 m.

**Biology.** On foliage in montane forest.

**Etymology.** This epithet is a Latinized adjective based on Mt Pompango.

**Notes.** *Trigonopterus pompangeensis* sp. nov. was coded as “*Trigonopterus* sp. 1198”. This species belongs to the *T. ovalipunctatus*-group. It is closely related to *T. ovalipunctatus* Riedel, but differs by a more densely punctate pronotum, the apically extended and converging penis, and 7.2–9.7% *cox1* p-distance.

**18. *Trigonopterus puspoi* sp. nov.**

<http://zoobank.org/9DFE5E8F-2010-4498-B534-FD4DD3265977>

**Diagnostic description.** *Holotype* (MZB). Male (Fig. 18a). Length 2.75 mm. Color of antennae ferruginous; legs dark ferruginous; remainder black. Body subovate; in dorsal aspect with weak constriction between pronotum and elytron; in profile dorsally convex. Rostrum with median and pair of submedian ridges; epistome distinct, posteriorly with subangulate ridge bearing five denticles. Pronotum with very weak subapical constriction; disk densely punctate; median line impunctate; interspaces between punctures subglabrous, subequal to punctures' diameter. Elytra with striae marked by rows of small punctures and fine hairlines; along basal margin with transverse row of denser punctures; stria 8 along humerus with seven coarse punctures; intervals subglabrous with interspersed punctures. Femora edentate, with distinct anteroventral ridge weakly crenate. Metafemur with dorsoposterior edge crenate; subapically with stridulatory patch. Posterior surface of metatibia with in apical half covered with long subrecumbent setae. Abdominal ventrites 1–2 concave, microreticulate, with sparse punctures; behind metacoxa with angular knob; ventrite 5 concave, subglabrous, sublaterally and subapically with sparse erect scales. Penis (Fig. 18b) with sides of body subparallel; apex symmetrical, with median triangular extension and sparse setae; apodemes 2.0× as long as body of penis; transfer apparatus U-shaped; ductus ejaculatorius without bulbus. **Intraspecific variation.** Length 2.48–3.36 mm. Female rostrum smooth and flat, epistome indistinct. Female metatibia subbasally dorsally somewhat widened, denticulate. Female abdominal ventrite 1 and 2 concave, subglabrous, laterally with few setae. Female abdominal ventrite 5 flat, medially glabrous, sublaterally and subapically punctate.

**Material examined.** *Holotype* (MZB, Cole.173.071): MZB0052 (GenBank OK481963), Indonesia, C-Sulawesi Prov, Toli-Toli, Gn. Dako, 01°03.967'N, 120°53.692'E to 01°03.782'N, 120°53.934'E, 840–970 m, 05-VII-2018, beaten. *Paratypes* (MZB, SMNK): Indonesia, Sulawesi Tengah, Toli-Toli, Gn. Dako: 1 ex, MZB0285 (GenBank OK481771), 01°03.967'N, 120°53.692'E to 01°03.782'N, 120°53.934'E, 840–970 m, 03-VII-2018, beaten; 1 ex, MZB0272 (GenBank OK481784), 01°04.1812'N, 120°53.5652'E to 01°3.9665'N, 120°53.6915'E, 720–830 m, 01-VII-2018, beaten; 2 exx, MZB0085 (GenBank OK481932), 01°03.574'N, 120°54.032'E to 01°03.323'N, 120°54.195'E, 1100–1200 m, 06-VII-2018, beaten; 1 ex, MZB0093 (GenBank OK481924), 01°03.574'N, 120°54.032'E to 01°03.782'N, 120°53.934'E, 830–1000 m, 05-VII-2018, beaten; 6 exx, MZB0260 (GenBank

OK481793), MZB0261 (GenBank OK481792), MZB0262 (GenBank OK481791), MZB0263 (GenBank OK481790), MZB0287 (PCR failed), MZB0288 (GenBank OK481770), 01°03.782'N, 120°53.934'E to 01°03.574'N, 120°54.032'E, 970–1140 m, 06-VII-2018, beaten; 2 exx, MZB0259 (GenBank OK481794), MZB0284 (GenBank OK481772, 01°03.782'N, 120°53.934'E to 01°03.574'N, 120°54.032'E, 970–1100 m, 06-VII-2018, beaten; 7 exx, MZB0264 (GenBank OK481789), 01°03.574'N, 120°54.032'E to 01°03.157'N, 120°54.195'E, 1100–1120 m, 06-VII-2018, beaten; 1 ex, MZB0286 (PCR failed), 01°03.782'N, 120°53.934'E to 01°02.977'N, 120°55.001'E, 1250–1750 m, 11-VII-2018.

**Distribution.** C-Sulawesi Prov. (Mt Dako). Elevation 830–1250 m.

**Biology.** On foliage in montane forest.

**Etymology.** This species is named in honor of Saleh Poespo, grandfather of the first author, and for his pioneering animal husbandry science in Indonesia. An invariable genitive.

**Notes.** *Trigonopterus puspoi* sp. nov. was coded as “*Trigonopterus* sp. 1113” (Narakusumo et al. 2020) and belongs to the *T. palopensis*-group. It is closely related to *T. tolitoliensis* sp. nov., from which it differs by its simple penis surface, the pubescence of the metatibia, and a 16.4–18.1% p-distance of its *cox1* sequence.

### 19. *Trigonopterus rosichoni* sp. nov.

<http://zoobank.org/B32661A6-A47A-40DE-8B3E-DBCE02563F99>

**Diagnostic description.** *Holotype*. **Male** (Fig. 19a). Length 2.40 mm. Color of antennae and legs ferruginous; remainder black. Body subovate; in dorsal aspect with weak constriction between pronotum and elytron; in profile dorsally convex. Rostrum dorsally with broad median costa and pair of submedian ridges; intervening furrows with sparse rows of subrecumbent setae; apical 1/3 subglabrous, with few punctures and with sparse suberect setae. Pronotum with disk densely punctate with coarse punctures; median line impunctate; interspaces between punctures subglabrous; laterally in basal 1/3 impunctate. Elytra with striae marked by rows of punctures and very fine hairlines; basal margin bordered by transverse row of punctures; intervals flat, with few interspersed punctures. Femora edentate; anteroventral ridges simple. Metafemur with dorsoposterior edge weakly crenate; subapically with stridulatory patch. Abdominal ventrites 1–2 concave, subglabrous; behind metacoxa with angular knob; ventrite 5 with deep subglabrous pit, subparallel lateral ridges and apical margin microreticulate, punctulate. Penis (Fig. 19b) with sides of body subparallel; apex with median angulate extension, with sparse setae; apodemes 2.6× as long as body of penis; transfer apparatus flagelliform; ductus ejaculatorius without bulbus. **Intraspecific variation.** Length 2.28–2.80 mm. Female rostrum dorsally smooth and flat. Female abdominal ventrite 5 flat, subglabrous, with sparse minute punctures.

**Material examined.** *Holotype* (MZB, Cole.173.072): MZB0094 (GenBank OK481923), Indonesia, C-Sulawesi, Toli-Toli, Gn. Dako, 01°03.782'N, 120°53.934'E

to 01°02.977'N, 120°55.001'E, 1250–1750 m, 11-VII-2018, beaten. **Paratypes** (MZB, SMNK): Indonesia, C-Sulawesi, Toli-Toli, Gn. Dako: 6 exx, MZB0193 (GenBank OK481857), MZB0194 (GenBank OK481856), MZB0249 (GenBank OK481804), same data as holotype; 3 exx, MZB0092 (GenBank OK481925), MZB0056 (GenBank OK481959), MZB0252 (GenBank OK481801), 01°03.181'N, 120°54.607'E to 01°02.977'N, 120°55.001'E, 1400–1750 m, 07-VII-2018, beaten; 2 exx, MZB0253 (GenBank OK481800), MZB0255 (GenBank OK481798), 01°02.977'N, 120°55.010'E to 01°03.782'N, 120°53.934'E, 970–1750 m, 11-VII-2018, beaten.

**Distribution.** C-Sulawesi Prov. (Mt Dako). Elevation ca. 1400–1750 m.

**Biology.** On foliage in montane forest.

**Etymology.** This species is named in honor of Rosichon Ubaidillah, curator and researcher of Hymenoptera at MZB. An invariable genitive.

**Notes.** *Trigonopterus rosichoni* sp. nov. was coded as “*Trigonopterus* sp. 1193”. It belongs to the *T. satyrus*-group and is closely related to *T. ancora* sp. nov. from which it differs by the shape of the transfer apparatus and 9.4–9.6% p-distance of its *cox1* sequence.

## 20. *Trigonopterus rubidus* sp. nov.

<http://zoobank.org/7464F2DE-28B8-4563-9EAF-C0501EFB4C93>

**Diagnostic description. Holotype. Male** (Fig. 20a). Length 2.50 mm. Color of antennae and elytra ferruginous; remainder black. Body subovate; in dorsal aspect with distinct constriction between pronotum and elytron, in profile dorsally convex. Rostrum dorsally with median and pair of submedian costae; intervening furrows with rows of coarse punctures and small setae; epistome indistinct, subglabrous with suberect setae. Pronotum with disk densely punctate; interspaces between large punctures subglabrous, subequal or smaller than punctures' diameter. Elytra with striae distinct, marked by rows of punctures; intervals subglabrous, with few scattered punctures; basal margin bordered by row of coarse, dense punctures. Meso- and metafemur with anteroventral ridge weakly crenate. Metafemur subapically with stridulatory patch. Meso- and metatibia subglabrous, with sparse erect setae. Abdominal ventrites 1–2 concave, subglabrous, with coarse punctures; ventrite 5 with shallow impression, densely punctate. Penis (Fig. 20b) with sides of body subparallel; apex broadly angulate, with sparse setae; apodemes 3.0× as long as body of penis; transfer apparatus flagelliform, curved, pointing basad, basally supported by pair of L-shaped sclerites; ductus ejaculatorius basally markedly sclerotized and somewhat swollen, curving around apodeme tips, then becoming thin and membranous. **Intraspecific variation.** Length 2.16–2.93 mm; elytral coloration orange to dark ferruginous. Female rostrum more slender, dorsally subglabrous, with rows of punctures. Female abdominal ventrites 1–2 weakly concave, punctate. Female abdominal ventrite 5 flat, densely punctate.

**Material examined. Holotype** (MZB, Cole.173.073): MZB0161 (GenBank OK481877), Indonesia, C-Sulawesi, Toli-Toli, Gn. Dako, 01°03.389'N, 120°55.524'E to 01°03.567'N, 120°56.032'E, 1900–2200 m, 10-VII-2018, beaten. **Paratypes**

(MZB, SMNK): Indonesia, C-Sulawesi, Toli-Toli, Gn. Dako: 40 exx, MZB0216 (GenBank OK481837), same as holotype; 5 exx, MZB0066 (GenBank OK481951), 01°03.782'N, 120°53.934'E to 01°02.977'N, 120°55.001'E, 1250–1750 m, 11-VII-2018, beaten; 18 exx, 01°02.977'N, 120°55.967'E to 01°03.210'N, 120°55.297'E, 1700–1800 m, 08–10-VII-2018, beaten; 6 exx, MZB0067 (GenBank OK481950), MZB0068 (GenBank OK481949), 01°03.174'N, 120°55.272'E to 01°03.389'N, 120°55.524'E, 1800–1900 m, 10-VII-2018, beaten; 31 exx, MZB0069 (GenBank OK481948), 01°03.174'N, 120°55.272'E to 01°03.389'N, 120°55.524'E, 1800–1900 m, 10-VII-2018, beaten; 5 exx, 01°03.174'N, 120°55.272'E to 01°03.389'N, 120°55.524'E, 1800–1900 m, 08–10-VII-2018, beaten.

**Distribution.** C-Sulawesi Prov. (Mt Dako). Elevation 1700–1900 m.

**Biology.** On foliage in montane forest.

**Etymology.** This epithet is the Latin adjective *rubidus*, *-a*, *-um* (reddish) referring to the elytral color.

**Notes.** *Trigonopterus rubidus* sp. nov. was coded as “*Trigonopterus* sp. 1199”. This species belongs to the *T. tatorensis*-group. It is closely related to *T. tatorensis* Riedel, from which it differs by denser pronotal punctures, its reddish elytral color and 9.5–9.9% *cox1* p-distance.

## 21. *Trigonopterus sarinoi* sp. nov.

<http://zoobank.org/863640D7-FD62-4CF6-9A97-264A73A7C09F>

**Diagnostic description. Holotype. Male** (Fig. 21a). Length 2.40 mm. Color of antennae and elytral base ferruginous; legs dark ferruginous; head, thorax and elytral sides black. Body subovate; in dorsal aspect with distinct constriction between pronotum and elytron; in profile dorsally convex. Rostrum at base dorsally swollen, markedly bent ventrad; with lateral flanges in front of eyes; dorsally with distinct median carina and pair of submedian ridges; intervening furrows each with row of erect, clavate scales; epistome indistinct. Pronotum with distinct subapical constriction; disk densely punctate; interspaces subglabrous; with subglabrous median costa; in apical half with erect, clavate scales. Elytra irregularly punctate; striae indistinct; interspaces subglabrous; some punctures with suberect, piliform to subclavate scale, in some areas missing or abraded. Meso- and metafemur with anteroventral ridge crenate, ending with small tooth; anterior surface coarsely punctate-reticulate, with erect subclavate scales. Metafemur with dorsoposterior edge serrate; subapically with stridulatory patch. Metatibia with dorsal edge serrate. Abdominal ventrites 1–2 concave, subglabrous, with few scattered erect scales; ventrite 5 almost flat, with broad shallow impression, microreticulate, with sparse suberect scales. Penis (Fig. 21b) with sides of body diverging; apex medially with subangular extension, without setae; apodemes 2.0× as long as body of penis; transfer apparatus flagelliform, forming a full coil, basally held by lyriform sclerite; ductus ejaculatorius with indistinct bulb.

**Material examined.** *Holotype* (MZB, Cole.173.074): MZB0106 (GenBank OK481913), Indonesia, C-Sulawesi, Sigi, Kolagi, Namu, Gn. Torompupu, 01°24.637'S, 119°57.597'E, 800 m, 15–27-XI-2017, sifted. Right thorax and elytron cracked, right mid- and hind leg glued separately to card.

**Distribution.** C-Sulawesi Prov. (Gn. Torompupu). Elevation ca. 800 m.

**Biology.** In leaf litter.

**Etymology.** This species is named in honor of Sarino, technician working at the Coleoptera collection of LIPI-MZB. An invariable genitive.

**Notes.** *Trigonopterus sarinoi* sp. nov. was coded as “*Trigonopterus* sp. 1208”. This species belongs to the *T. lampros*-group. It is closely related to *T. yoda* Riedel, which differs by its black-bronze elytral color and a 19.3% *cox1* p-distance.

## 22. *Trigonopterus sutrisnoi* sp. nov.

<http://zoobank.org/963BE7BE-53F4-4473-9485-CCE33EC99E53>

**Diagnostic description.** *Holotype. Male* (Fig. 22a). Length 2.88 mm. Color of antennae ferruginous, legs dark ferruginous, remainder black. Body subrhomboid; in profile dorsally convex. Rostrum with median and pair of submedian carinae; intervening furrows with rows of suberect scales; epistome indistinct, sparsely setose; profile in basal 1/3 dorsally swollen, markedly convex to forehead. Pronotum with disk densely punctate, interspace subglabrous; median line impunctate. Elytra irregularly punctate with small punctures; interspaces subglabrous; striae 2–5 marked by fine hairlines. Femora edentate; with anteroventral ridge crenate. Metafemur dorsally with suberect silvery scales, dorsoposterior edge denticulate; subapically with stridulatory patch. Metatibia with dorsal edge very weakly denticulate, subapically with constriction; ventrally with sparse row of long setae. Meso- and metathorax ventrally densely squamose with erect plumose scales. Abdominal ventrites 1–2 concave, subglabrous, almost impunctate, sublaterally with sparse suberect scales; ventrite 5 flat, densely punctate, punctures with dense erect scales, interspaces microreticulate. Penis (Fig. 22b) with sides of body subparallel, near middle with very shallow constriction; apex with median extension, with sparse setae; apodemes 2.0× as long as body of penis; transfer apparatus long spiniform, pointing basad, with complex supporting sclerites; basal sclerite elongate V-shaped; ductus ejaculatorius with bulbus. **Intraspecific variation.** Length 2.48–2.88 mm. Female rostrum slender, in apical half dorsally subglabrous, with submedian row of punctures and sublateral furrows. Female abdominal ventrite 5 flat, sparsely punctate, with sparse scales.

**Material examined.** *Holotype* (MZB, Cole.173.075): MZB0203 (GenBank OK481848), Indonesia, C-Sulawesi, Toli-Toli, Gn. Dako, 01°04.181'N, 120°53.565'E to 01°03.967'N, 120°53.692'E, 835–970 m, 03-VII-2018, beaten. *Paratype* (SMNK): MZB0097 (GenBank OK481920), Indonesia, C-Sulawesi, Toli-Toli, Gn.

Dako, 01°04.1812'N, 120°53.5652'E to 01°3.9665'N, 120°53.6915'E, 720–830 m, 01-VII-2018, beaten.

**Distribution.** C-Sulawesi Prov. (Mt Dako). Elevation ca. 720–970 m.

**Biology.** On foliage in lower montane forest.

**Etymology.** This epithet is named in honor of Hari Sutrisno, curator of moths and researcher at MZB. An invariable genitive.

**Notes.** *Trigonopterus sutrisnoi* sp. nov. was coded as “*Trigonopterus* sp. 1206”. This species belongs to the *T. toraja*-group. It is related to *T. toboaliensis* sp. nov., which differs by its lateral extensions of the penis and a *cox1* p-distance of 15.3–15.5%.

### 23. *Trigonopterus tanah* sp. nov.

<http://zoobank.org/E32B51C0-0A96-49D3-9442-3D0513B57B40>

**Diagnostic description. Holotype. Male** (Fig. 23a). Length 2.13 mm. Color of antennae yellowish; legs ferruginous; remainder black. Body subovate; in dorsal aspect with weak constriction, in profile with marked constriction between pronotum and elytron. Rostrum dorsally with median costa and pair of submedian ridges; intervening furrows filled with rows of coarse punctures containing each one indistinct seta; epistome simple, subglabrous. Pronotum with disk dorsally swollen, densely coarsely punctate-reticulate; interspaces between punctures subglabrous. Elytra with striae impressed, with dense rows of deep punctures; sutural interval with row of minute punctures, other intervals subglabrous, costate; basal margin bordered by transverse row of punctures. Profemur with anteroventral ridge simple; meso- and metafemur with denticle in apical 1/2; anterior surface of femora with longitudinal wrinkles, weakly punctate. Metafemur subapically with stridulatory patch. Abdominal ventrites 1–2 microreticulate, concave, with coarse punctures; ventrite 5 almost flat, microreticulate, sparsely punctate. Penis (Fig. 23b) with sides of body subparallel; apex rounded, sublaterally with sparse setae; apodemes 2.3 X as long as body of penis; transfer apparatus dentiform, directed basad in repose, flanked by pair of small sclerites; ductus ejaculatorius with indistinct bulbus.

**Material examined. Holotype** (MZB, Cole.173.056): MZB0202 (GenBank OK481849), Indonesia, C-Sulawesi, Toli-Toli, Gn. Dako, 01°03.512'N, 120°54.054'E, 1100–1200 m, 13-VII-2018, sifted.

**Distribution.** C-Sulawesi Prov. (Mt Dako). Elevation ca. 1100–1200 m.

**Biology.** In leaf litter of montane forest.

**Etymology.** This epithet is the Indonesian word for “soil” and a noun in apposition. It refers to the species’ lifestyle on the ground among leaf litter.

**Notes.** *Trigonopterus tanah* sp. nov. was coded as “*Trigonopterus* sp. 1234”. It is closely related to *T. darwini* Riedel, from which it can be distinguished by its coarser sculpture, and the subparallel body of the penis. The *cox1* p-distance of both species is 10.8%.

**24. *Trigonopterus tejokusumoi* sp. nov.**

<http://zoobank.org/7AD6A5C2-873A-467B-98CD-220501419A60>

**Diagnostic description. *Holotype*. Male** (Fig. 24a). Length 2.90 mm. Color of antennae and tarsi ferruginous, remainder black. Body subovate; in dorsal aspect with weak constriction between pronotum and elytron; in profile dorsally convex. Rostrum dorsally with median costa and pair of submedian ridges; intervening furrows with sparse rows of suberect scales; epistome indistinct, subglabrous. Eyes medially approximate. Pronotum with disk densely punctate, laterally punctures larger; interspaces subglabrous. Elytra densely irregularly punctate with small punctures; striae indistinct; hardly visible; interspaces subglabrous; stria 8 along humerus with row of six coarse punctures. Femora edentate; anterior and dorsal surface coarsely punctate, reticulate, each puncture containing silvery elongate scale. Meso- and metafemur with anteroventral ridge crenate; metafemur subapically with stridulatory patch. Metatibia in apical half ventrally with fringe of long setae. Abdominal ventrites 1–2 concave, dull, with sparse punctures, each bearing suberect scale; ventrite 5 with shallow impression, microreticulate, dull, with sparse suberect scales. Penis (Fig. 24b) with sides of body subparallel; apex asymmetrical, obtuse median extension shifted to the left, with sparse setae; apodemes 2.1× as long as body of penis; transfer apparatus spiniform, supported by plate-like sclerite; ductus ejaculatorius with indistinct bulbus. ***Intraspecific variation***. Length 2.38–3.00 mm. Female body more slender. Female rostrum slender, dorsally subglabrous, with submedian row of punctures and sublateral furrows. Female abdominal ventrite 5 flat, punctate, with suberect scales.

**Material examined. *Holotype*** (MZB, Cole.173.076): MZB0137 (GenBank OK481897), Indonesia, C-Sulawesi, Tojo Una-Una, Matako, Gn. Pompangeo, 01°35.215'S, 120°55.560'E to 01°35.079'S, 120°55.49'E, 1900 m, 28-II-2020, beaten. ***Paratypes*** (MZB, SMNK): Indonesia, C-Sulawesi, Tojo Una-Una, Matako, Gn. Pompangeo 7 exx, same data as holotype; 13 exx, MZB0139 (GenBank OK481895), MZB0206 (GenBank OK481847), 01°35.603'S, 120°55.437'E to 01°35.406'S, 120°55.547'E, 1800 m, 29-II-2020, beaten; 15 exx, MZB0266 (PCR failed), MZB0267 (PCR failed), MZB0268 (PCR failed), 01°35.359'S, 120°55.643'E to 01°35.581'S, 120°55.385'E, 1800 m, 29-II-2020, beaten; 8 exx, 01°35.264'S, 120°55.588'E to 01°35.339'S, 120°55.599'E, 1900 m, 27-II-2020, beaten; 12 exx, 01°35.264'S, 120°55.588'E to 01°35.339'S, 120°55.599'E, 1900 m, 26–27-II-2020, beaten; 4 exx, MZB0211 (GenBank OK481842), MZB0212 (GenBank OK481841), 01°35.074'S, 120°55.467'E to 01°35.154'S, 120°55.507'E, 1900 m, 28-II-2020, beaten; 26 exx, MZB0138 (GenBank OK481896), MZB0265 (GenBank OK481788), 01°35.197'S, 120°55.658'E to 01°35.127'S, 120°55.622'E, 2000 m, 01-III-2020, beaten; 1 ex, 01°35.197'S, 120°55.658'E to 01°35.127'S, 120°55.622'E, 2000 m, 01-III-2020, sifted.

**Distribution.** C-Sulawesi Prov. (Mt Pompangeo). Elevation 1800–2000 m.

**Biology.** On foliage in montane forest.

**Etymology.** This species is named in honor of Slamet Tedjokoesoemo, pioneer of veterinary science in Indonesia and grandfather of the first author. An invariable genitive.

**Notes.** *Trigonopterus tejokusumoi* sp. nov. was coded as “*Trigonopterus* sp. 1200”. This species belongs to the *T. barbipes*-group. It is most closely related to *T. barbipes* Riedel, but differs by smaller and more irregular elytral punctures, a peculiar obtuse apex of the penis and a 16% *cox1* p-distance.

## 25. *Trigonopterus toboliensis* sp. nov.

<http://zoobank.org/3CD000BF-2C7C-4FA4-85B0-3174D02272D4>

**Diagnostic description. Holotype. Male** (Fig. 25a). Length 2.90 mm. Color of antennae ferruginous, legs dark ferruginous, remainder black. Body subrhomboid; in profile dorsally convex. Rostrum with median and pair of submedian carinae; intervening furrows with rows of suberect scales; epistome indistinct, sparsely setose; profile in basal 1/3 dorsally swollen, markedly convex to forehead. Pronotum with disk densely punctate, interspace subglabrous; median line impunctate. Elytra irregularly punctate with small punctures; interspaces subglabrous; striae 2–6 marked by fine hairlines. Femora edentate; with anteroventral ridge crenulate. Metafemur dorsally with suberect silvery scales, dorsoposterior edge denticulate; subapically with stridulatory patch. Metatibia with dorsal edge very weakly denticulate, subapically with constriction. Abdominal ventrites 1–2 concave, subglabrous, almost impunctate, with sparse suberect scales; ventrite 5 flat, densely punctate, punctures with suberect scales, interspaces microreticulate. Penis (Fig. 25b) with sides of body subparallel, near middle body with lateral flanges; apex with median triangular extension, without setae; apodemes 2.2× as long as body of penis; transfer apparatus spiniform; ductus ejaculatorius with indistinct bulb. **Intraspecific variation.** Length 2.90–3.09 mm. Female rostrum slender, in apical half dorsally subglabrous, with submedian row of punctures and sublateral furrows. Female ventrite 5 flat, sparsely punctate, subapically with sparse scales.

**Material examined. Holotype** (MZB, Cole.173.077): MZB0126 (GenBank OK481908), Indonesia, C-Sulawesi, Palu, Donggala – Toboli, Kebun Kopi, 00°43.256'S, 119°56.759'E, 850 m, 03-III-2020, beaten. **Paratypes** (MZB, SMNK): MZB0127 (GenBank OK481907), MZB0213 (GenBank OK481840), MZB0214 (GenBank OK481839), MZB0215 (GenBank OK481838), same data as holotype; 4 exx, ARC7157 (GenBank OK481769), Palu, Palolo, Kamarora, trail to waterfall, ca. 01°12.541'S, 120°09.648'E, 700 m, 23–27-VIII-1997, beaten.

**Distribution.** C-Sulawesi Prov. (Palu, Palolo). Elevation 700–850 m.

**Biology.** On foliage in montane forest.

**Etymology.** This epithet is a Latinized adjective based on Toboli village.

**Notes.** *Trigonopterus toboliensis* sp. nov. was coded as “*Trigonopterus* sp. 1192”. This species belongs to the *T. toraja*-group. It is closely related to *T. ampanensis* Riedel from which it differs by the shape and position of the lateral extensions of the penis and a *cox1* p-distance of 14.5–14.7%.

**26. *Trigonopterus tolitoliensis* sp. nov.**

<http://zoobank.org/0E1883D2-0FCF-446C-BC9A-8B0BB603DDDF>

**Diagnostic description. Holotype. Male** (Fig. 26a). Length 3.00 mm. Color of antennae ferruginous; legs dark ferruginous; remainder black. Body subovate; in dorsal aspect with weak constriction between pronotum and elytron; in profile dorsally convex. Rostrum dorsally with median and pair of submedian costae separated by row of coarse punctures; epistome with surface subglabrous and suberect setae, posteriorly with three denticles. Pronotum with weak subapical constriction; disk densely punctate; median line impunctate; interspaces between punctures subglabrous, subequal to punctures' diameter. Elytra subglabrous, with striae marked by rows of small punctures and fine hairlines; along basal margin with transverse row of denser punctures; stria 8 along humerus with six coarse punctures; intervals subglabrous. Femora edentate, with distinct anteroventral ridge. Metafemur with dorsoposterior edge crenate; subapically with stridulatory patch. Posterior surface of metatibia with rows of long suberect spatulate scales. Abdominal ventrites 1–2 concave, dull-shagreened, with sparse punctures; behind metacoxa with angular knob; ventrite 5 concave, subglabrous, sublaterally with sparse erect scales. Penis (Fig. 26b) with sides of body subparallel; apex symmetrical, with median subangular extension and sparse setae; dorsally body in front of middle with pair of brushes of long setae; apodemes 1.9× as long as body of penis; transfer apparatus Y-shaped; ductus ejaculatorius without bulbus. **Intraspecific variation.** Length 2.08–3.16 mm. Female rostrum in apical half slender, dorsally subglabrous, with submedian rows of punctures and sublateral furrows; female epistome indistinct. Female abdominal ventrites 1–2 weakly concave, with sparse minute punctures; female ventrite 5 weakly concave, with scattered punctures and setae.

**Material examined. Holotype** (MZB, Cole.173.078): MZB0050 (GenBank OK481965), Indonesia, C-Sulawesi Prov., Toli-Toli, Gn. Dako, Base camp 1, 01°03.782'N, 120°53.934'E to 01°03.574'N, 120°54.032'E, 970–1100 m, 05–06-VII-2018, beaten. **Paratypes** (MZB, SMNK): Indonesia, C-Sulawesi Prov., Toli-Toli, Gn. Dako: 52 exx, same as holotype; 1 ex, 01°04.181'N, 120°53.565'E to 01°03.967'N, 120°53.692'E, 720–830 m, 01-VII-2018, beaten; 1 ex, 01°03.967'N, 120°53.692'E to 01°03.782'N, 120°53.934'E, 830–970 m, 01-VII-2018, beaten; 1 ex, 01°03.967'N, 120°53.692'E to 01°03.782'N, 120°53.934'E, 830–970 m, 05-VII-2018, beaten; 3 exx, 01°03.967'N, 120°53.692'E to 01°03.782'N, 120°53.934'E, 830–970 m, 03-VII-2018, beaten; 1 ex, MZB0271 (GenBank OK481785), 01°03.782'N, 120°53.934'E, 970 m, 04-VII-2018, beaten; 23 exx, MZB0095 (GenBank OK481922), MZB0098 (GenBank OK481919), MZB0096 (GenBank OK481921), MZB0273 (GenBank OK481783), MZB0274 (GenBank OK481782), MZB0275 (GenBank OK481781), 01°03.697'N, 120°53.991'E, 970 m, 07-VII-2018, beaten; 12 exx, MZB0086 (GenBank OK481931) 01°03.574'N, 120°54.032'E to 01°03.782'N, 120°53.934'E, 830–1000 m, 05-VII-2018, beaten; 7 exx, 01°03.782'N, 120°53.934'E to 01°03.967'N, 120°53.692'E, 970–1000 m, 05-VII-2018, beaten; 66 exx, MZB0087 (GenBank OK481930), MZB0088 (GenBank OK481929),

MZB0089 (GenBank OK481928), same data as holotype; 6 exx, 01°03.782'N, 120°53.934'E to 01°03.574'N, 120°54.032'E, 970–1140 m, 06-VII-2018, beaten; 14 exx, 01°03.574'N, 120°54.032'E to 01°03.157'N, 120°54.195'E, 1100–1120 m, 06-VII-2018, beaten; 7 exx, 01°03.574'N, 120°54.032'E to 01°03.512'N, 120°54.054'E, 1100–1120 m, 06-VII-2018, beaten; 1 ex, MZB0059 (GenBank OK481956), 01°03.512'N, 120°54.054'E, 1100–1200 m, 13-VII-2018, sifted; 7 exx, 01°03.512'N, 120°54.054'E, 1100–1200 m, 06-VII-2018, beaten; 50 exx, MZB0051 (GenBank OK481964), 01°03.574'N, 120°54.032'E to 01°03.181'N, 120°54.607'E, 1100–1400 m, 07-VII-2018, beaten; 15 exx, 01°03.697'N, 120°53.991'E, 1030 m, 06-VII-2018, sifted; 3 exx, MZB0276 (GenBank OK481780), 01°03.412'N, 120°54.126'E to 01°03.241'N, 120°54.328'E, 1200–1300 m, 07-VII-2018, beaten; 3 exx, MZB0049 (GenBank OK481966), MZB0269 (GenBank OK481787), MZB0270 (GenBank OK481786), 01°03.782'N, 120°53.934'E to 01°02.977'N, 120°55.001'E, 1250–1750 m, 11-VII-2018, beaten.

**Distribution.** C-Sulawesi Prov. (Mt Dako). Elevation 830–1250 m.

**Biology.** On foliage in montane forests.

**Etymology.** This epithet is a Latinized adjective based on Toli-Toli regency.

**Notes.** *Trigonopterus tolitoliensis* sp. nov. was coded as “*Trigonopterus* sp. 1186”. The species belongs to the *T. palopensis*-group. It is closely related to *T. puspoi* sp. nov. from which it differs by the setose brushes on the dorsal surface of the penis, the scaling of the metatibia, and a 16.4–18.1% p-distance of its *cox1* sequence.

## 27. *Trigonopterus tounensis* sp. nov.

<http://zoobank.org/B5125BF4-0D58-495C-B570-1B0717AF4809>

**Diagnostic description. Holotype. Male** (Fig. 27a). Length 2.58 mm. Color of antennae ferruginous; remainder black. Body subovate; in dorsal aspect with weak constriction between pronotum and elytron; in profile dorsally convex. Rostrum dorsally with median costa and pair of submedian ridges; intervening furrows each with sparse row of erect scales; epistome subglabrous with sparse suberect setae, posteriorly with five denticles. Pronotum with disk densely punctate with coarse punctures; almost reticulate, interspaces subglabrous; each puncture containing single, minute seta; medially with impunctate line. Elytra densely irregularly punctate with small punctures; striae indistinct; interspaces between punctures subglabrous; striae 7–9 with larger punctures; stria 8 along humerus with seven large, coarse punctures. Femora edentate, anteroventral ridge simple; anterior surface densely coarsely punctate, each puncture with suberect scale. Metafemur with dorso-posterior edge weakly denticulate; subapically with stridulatory patch; dorsally with rows of silvery scales. Posterior face of metatibia in apical 1/2 with dense yellowish setae. Abdominal ventrites 1–2 concave, densely punctate with coarse

punctures and sparse erect scales, sublaterally each with blunt tooth; in profile ventrite 2 subangularly projecting; ventrite 5 densely coarsely punctate, with median impression. Penis (Fig. 27b) with sides of body subparallel; apex with short median angulate extension, with sparse setae; apodemes  $2.9\times$  as long as body; transfer apparatus complex; ductus ejaculatorius with distinct bulbus. **Intraspecific variation.** Length 2.38–2.58 mm. Female rostrum flat, dorsally with median costa and row of punctures, and pair of submedian costae; epistome simple, subglabrous with sparse punctures and suberect setae. Female abdominal ventrites 1–2 with shallow impression, surface with sparse coarse punctures; ventrite 5 flat, with dense punctures and suberect setae.

**Material examined. Holotype** (MZB, Cole.173.079): MZB0110 (GenBank OK481910), Indonesia, C-Sulawesi, Tojo Una-Una, Ulubongka, Mire, Gn. Katopasa,  $01^{\circ}11.31'S$ ,  $121^{\circ}27.348'E$ , 1380 m, 23–24-VII-2017, beaten. **Paratype** (MZB, SMNK): 3 exx, MZB0111 (GenBank OK481909), same data as holotype.

**Distribution.** C-Sulawesi Prov. (Mt Katopasa). Elevation ca. 1380 m.

**Biology.** On foliage in montane forest.

**Etymology.** This epithet is a Latinized adjective based on the Indonesian abbreviation of Tojo Una-Una “Touna” and refers to the type locality.

**Notes.** *Trigonopterus tounensis*, sp. nov. was coded as “*Trigonopterus* sp. 1115” (Narakusumo et al. 2020). This species belongs to the *T. posoensis*-group. It is closely related to *T. obelix* Riedel, which differs by 15.2–16% *cox1* p-distance.

## 28. *Trigonopterus unyil* sp. nov.

<http://zoobank.org/74F11B0E-6885-4F20-8886-7484D5C6EF03>

**Diagnostic description. Holotype. Male** (Fig. 28a). Length 1.52 mm. Color largely ferruginous; thorax, sides of elytra and patch at the middle of intervals 2–3 black. Body subovate; in dorsal aspect and in profile with moderate constriction between pronotum and elytron. Rostrum dorsally with dense coarse punctures, areolate-reticulate; with sparse suberect setae; epistome, subglabrous, apically with sparse setae, posteriorly with transverse angulate ridge forming median denticle. Pronotum subapically with weak constriction; disk coarsely punctate, reticulate; each puncture bearing a suberect, clavate, apicad directed, yellowish scale; medially with subglabrous costa, subapically shortened. Elytra with striae marked by rows of suberect subclavate scales; intervals costate, glabrous; basal margin bordered by simple ridge. Femora dentate; anterior surface dull, rugose, but without distinct punctures; with sparse suberect scales. Metafemur dorsally rounded; subapically with stridulatory patch. Abdominal ventrites 1–2 flat, dull, with coarse punctures, with sparse suberect scales; ventrite 5 flat, microreticulate, dull. Penis (Fig. 28b) with sides of body subparallel, towards apex rounded, medially pointed, with sparse setae;

apodemes 2.1× as long as body of penis; transfer apparatus denticulate, held by pair of brace-shaped sclerites; ductus ejaculatorius with distinct bulb. **Intraspecific variation.** Length 1.38–1.70. Female rostrum subglabrous, with submedian rows of punctures.

**Material examined.** *Holotype* (MZB, Cole.173.080): MZB0134 (GenBank OK481900), Indonesia, C-Sulawesi, Tojo Una-Una, Matakko, Gn. Pompangeo, 01°35.235'S, 120°55.679'E to 01°35.258'S, 120°55.588'E, 1900 m, 27-II-2020, sifted. *Paratypes* (MZB, SMNK): Indonesia, C-Sulawesi, Tojo Una-Una, Matakko, Gn. Pompangeo: 6 exx, MZB0135 (GenBank OK481899), same data as holotype; 4 exx, MZB0136 (GenBank OK481898), 01°35.197'S, 120°55.658'E to 01°35.127'S, 120°55.622'E, 2000 m, 01-III-2020, sifted.

**Distribution.** C-Sulawesi Prov. (Mt Pompangeo). Elevation ca. 1900–2000 m.

**Biology.** In leaf litter of montane forest.

**Etymology.** This epithet is a noun in apposition based on the Indonesian hand puppet character from “Si Unyil” TV series.

**Notes.** *Trigonopterus unyil* sp. nov. was coded as “*Trigonopterus* sp. 1196”. Presumably, this species belongs to the *T. nanus*-group.

## Discussion

Relatively short field trips to two mountains in Sulawesi (i.e. five days at Mt Pompangeo and 14 days at Mt Dako) resulted in the discovery of 25 out of 28 *Trigonopterus* species newly described herein. Only a single species, *T. toboliensis* sp. nov. from Palu, respectively Palolo had been collected earlier. This exemplifies what great positive impact dedicated field work can have to species-discovery of neglected arthropod taxa, especially in montane areas. While the more conspicuous species of birds, mammals, butterflies, larger beetles or plants may have been collected on earlier surveys (Bebber et al. 2010; Troudet et al. 2017), the great majority of small-sized beetles of less than 3 mm body size is usually neglected and not sufficiently represented in unidentified museum collections.

It is noteworthy that in some localities pairs of sister species have been discovered: *T. moduai* sp. nov., and *T. paramoduai* sp. nov. are both found in narrowly separated elevation zones of Mt Dako. Although genetically very close (3.20–4.11% *cox1* p-distance) they are very distinct morphologically. Other such species pairs are morphologically very hard or impossible to separate, but very divergent genetically, i.e. *T. matakensis* sp. nov. and *T. pompangeensis* sp. nov. from Mt Pompangeo or the allopatric *T. ovatulus* Riedel and *T. pseudovatulus* Riedel from mountains north of Lake Poso (Riedel and Narakusumo 2019). It would be interesting to explore factors of their speciation in detail.

Mt Dako is a nature reserve, and forests above 800 m are largely intact. On the other hand, Mt Pompangeo is without any conservation status and has been logged ex-

tensively between 1970 m and 2000 m. Patches of rainforest remaining in the steeper areas are still at risk being affected by regular forest fires. Both Mt Dako and Mt Pom-pangeo harbour endemic *Trigonopterus* species, and presumably additional ones could be discovered if longer field trips are conducted in the remaining forest patches. These forest patches among the Sulawesi rainforest still hold the largely unknown diversity of *Trigonopterus* and other arthropod species. They should be of greater concern to conservation despite or rather because of their fragmentation.

## Provisional catalogue of species groups of *Trigonopterus* in Sulawesi

**subgenus *Mimidotasia* Voss:** *T. pauper* Riedel, *T. luwukensis* Riedel, *T. selayarensis* Riedel, *T. wangiwangiensis* Riedel.

***T. abnormis*-group:** *T. abnormis* Riedel, *T. kolakensis* Riedel

***T. analis*-group:** *T. analis* Riedel, *T. pagaranganensis* Riedel, *T. pseudanalis* Riedel

***T. arachnobas*-group:** *T. arachnobas* Riedel, *T. darwini* Riedel, *T. gracilipes* Riedel, *T. idefix* Riedel, *T. moduai* sp. nov., *T. paramoduai* sp. nov., *T. pumilus* Riedel, *T. rudis* Riedel, *T. tanah* sp. nov., *T. tenuipes* Riedel.

***T. barbipes*-group:** *T. barbipes* Riedel, *T. ejaculatorius* Riedel, *T. katopasensis* sp. nov., *T. pomberimbensis* sp. nov., *T. tejokusumoi* sp. nov., *T. vicinus* Riedel, *T. viduus* Riedel.

***T. bornensis*-group:** *T. rotundatus* Riedel.

***T. collaris*-group:** *T. collaris* Riedel, *T. klabatensis* Riedel, *T. paracollaris* Riedel.

***T. crenulatus*-group:** *T. costatulus* Riedel, *T. crenulatus* Riedel, *T. humilis* Riedel, *T. squalidulus* Riedel.

***T. curtus*-group:** *T. procurtus* Riedel, *T. pseudosimulans* Riedel, *T. scitulus* Riedel.

***T. dimorphus*-group:** *T. reticulatus* Riedel, *T. scabripes* Riedel, *T. pendolensis* Riedel.

***T. fulvicornis*-group:** *T. celebensis* Riedel, *T. corona* sp. nov., *T. fulvicornis* (Pascoe, 1885), *T. kakimerah* sp. nov., *T. pseudofulvicornis* Riedel, *T. seticnemis* Riedel.

***T. honestus*-group:** *T. inhonestus* Riedel.

***T. incendium*-group:** *T. incendium* Riedel.

***T. impressicollis*-group:** *T. adpersus* Riedel, *T. castaneipennis* Riedel, *T. ewok* sp. nov., *T. impressicollis* Riedel, *T. mesai* Riedel, *T. serripes* Riedel, *T. suturatus* Riedel.

***T. laevigatus*-group:** *T. invalidus* Riedel, *T. jasmineae* Riedel, *T. laevigatus* Riedel.

***T. lampros*-group:** *T. artemis* Riedel, *T. carinirostris* Riedel, *T. curvipes* Riedel, *T. lampros* Riedel, *T. sarinoid* sp. nov., *T. yoda* Riedel.

***T. manadensis*-group:** *T. ambangensis* Riedel, *T. armipes* Riedel, *T. cirripes* Riedel, *T. dakoensis* sp. nov., *T. heberti* Riedel, *T. mahawuensis* Riedel, *T. manadensis* Riedel, *T. modoindingensis* Riedel, *T. pseudomanadensis* Riedel, *T. volcanorum* Riedel.

***T. minabassae*-group:** *T. indigenus* Riedel, *T. minabassae* Riedel, *T. prismae* Riedel, *T. sampunensis* Riedel, *T. silvicola* Riedel.

***T. nanus*-group:** *T. hirsutus* Riedel, *T. nanus* Riedel, *T. unyil* sp. nov..

***T. nitidulus*-group:** *T. cricki* Riedel, *T. nitidulus* Riedel.

- T. ovalipunctatus*-group:** *T. lompobattangensis* Riedel, *T. matakensis* sp. nov., *T. ovalipunctatus* Riedel, *T. pompangeensis* sp. nov., *T. pseudovalipunctatus* Riedel.
- T. ovatulus*-group:** *T. arcanus* sp. nov., *T. ovatulus* Riedel, *T. pseudovatulus* Riedel.
- T. palopensis*-group:** *T. asterix* Riedel, *T. fuscipes* Riedel, *T. kotamobagensis* Riedel, *T. latipennis* Riedel, *T. matalibaruensis* Riedel, *T. moatensis* Riedel, *T. palopensis* Riedel, *T. puspoi* sp. nov., *T. rhombiformis* Riedel, *T. rufipes* Riedel, *T. tolitoliensis* sp. nov..
- T. politus*-group:** *T. allotopus* Riedel, *T. pseudallotopus* Riedel.
- T. posoensis*-group:** *T. obelix* Riedel, *T. posoensis* Riedel, *T. tounensis* sp. nov..
- T. relictus*-group:** *T. mangkutanensis* Riedel
- T. rotundulus*-group:** *T. rotundulus* Riedel, *T. watsoni* Riedel
- T. saltator*-group:** *T. bonthainensis* Riedel
- T. satyrus*-group:** *T. ancora* sp. nov., *T. gundala* sp. nov., *T. mons* sp. nov., *T. rosichoni* sp. nov., *T. satyrus* Riedel.
- T. sampuragensis*-group:** *T. sampuragensis* Riedel.
- T. tatorensis*-group:** *T. acutus* sp. nov., *T. daun* sp. nov., *T. hoppla* sp. nov., *T. hypocrita* Riedel, *T. incognitus* Riedel, *T. rubidus* sp. nov., *T. sulawesiensis* Riedel, *T. tatorensis* Riedel, *T. tomohonensis* Riedel.
- T. toraja*-group:** *T. ampanensis* Riedel, *T. rantepao* Riedel, *T. scaphiformis* Riedel, *T. sutrisnoi* sp. nov., *T. toboliensis* sp. nov., *T. toraja* Riedel.

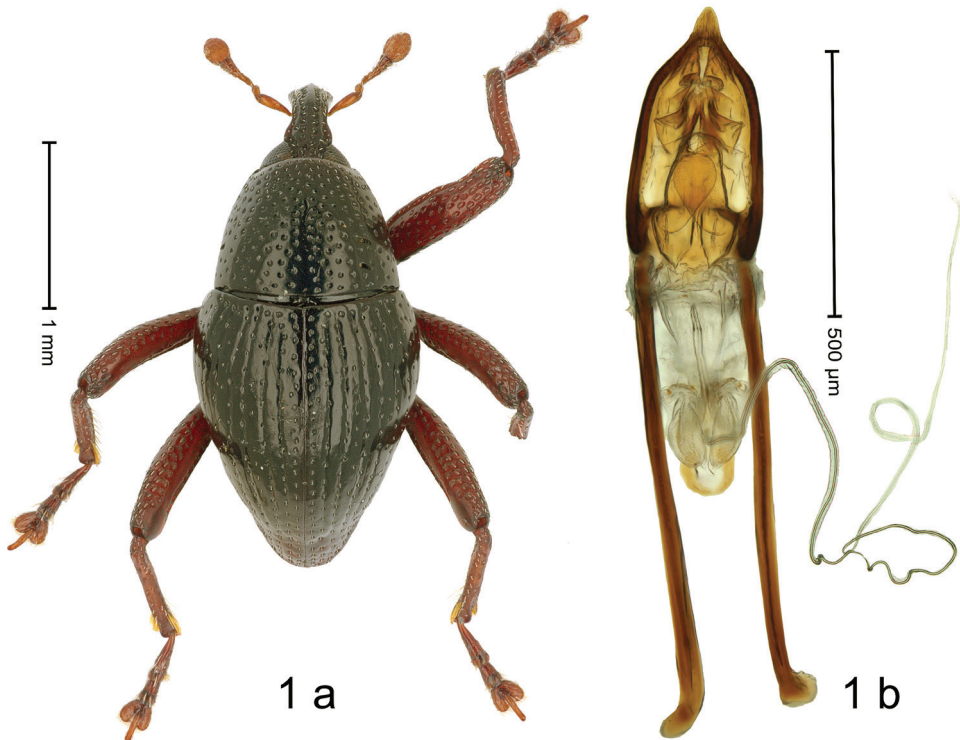


**Figure 1.** *Trigonopterus acutus* sp. nov., holotype **a** habitus **b** penis.

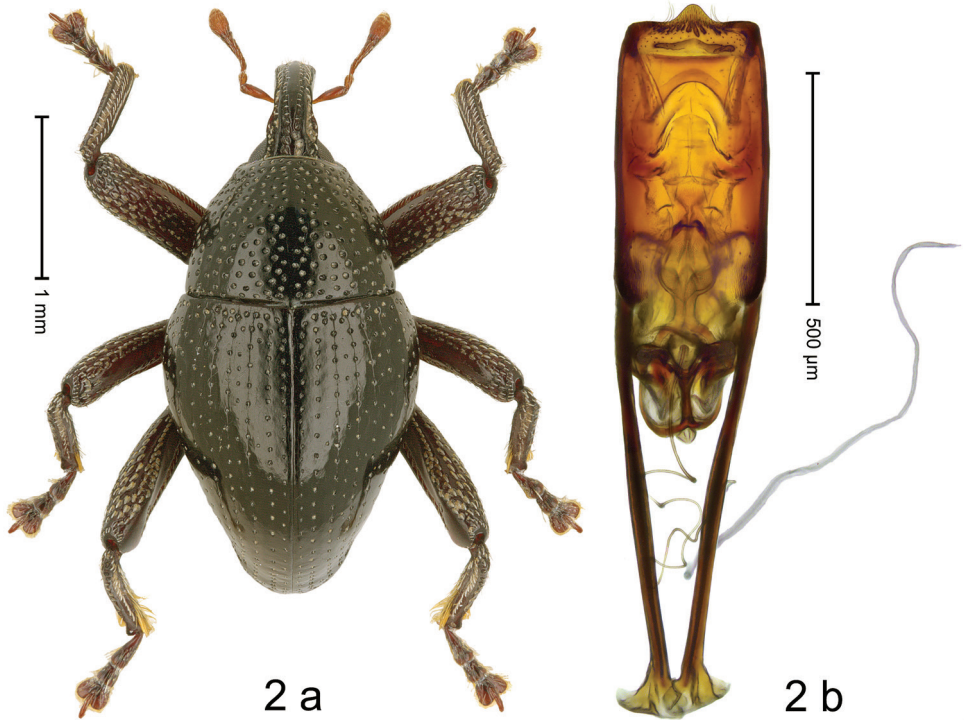


**Figure 2.** *Trigonopterus ancora* sp. nov., holotype **a** habitus **b** penis.

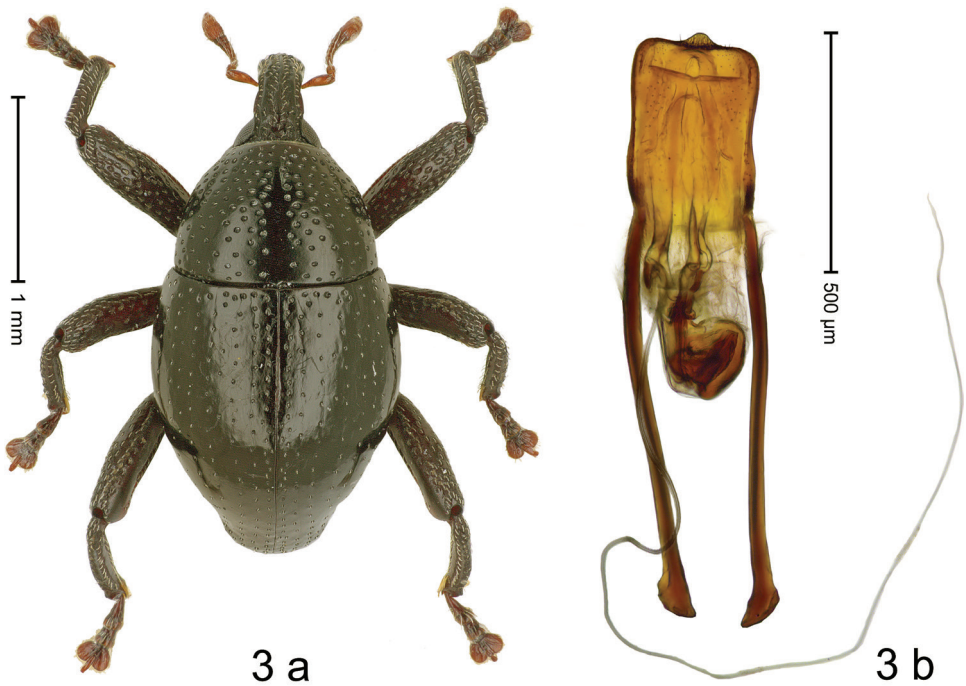


**Figure 3.** *Trigonopterus arcanus* sp. nov., holotype **a** habitus **b** Penis.

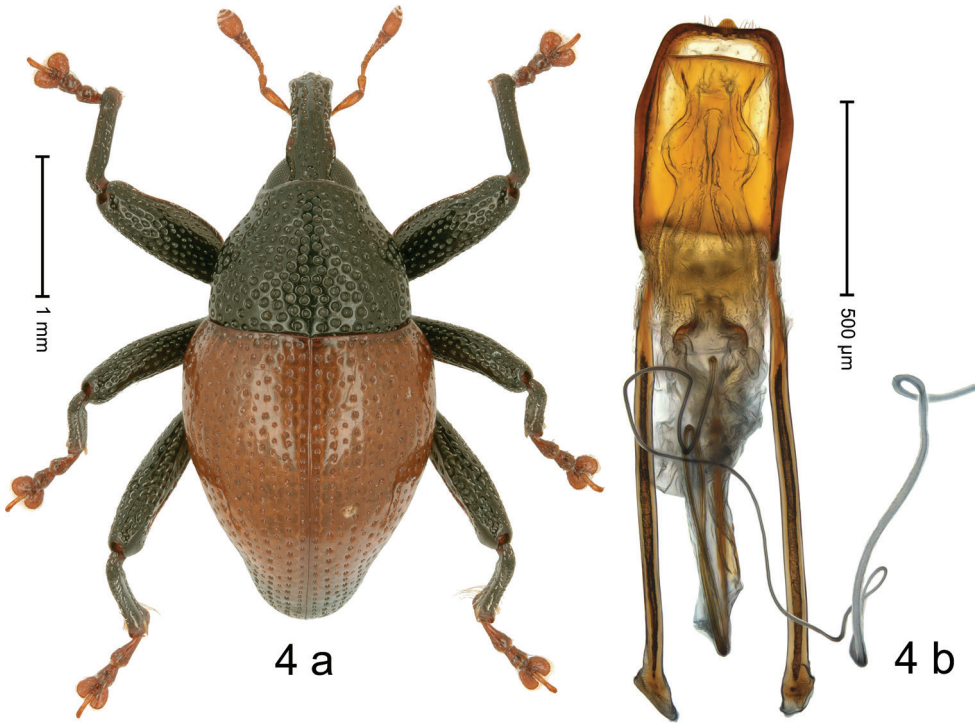


Figure 4. *Trigonopterus corona* sp. nov., holotype **a** habitus **b** penis.

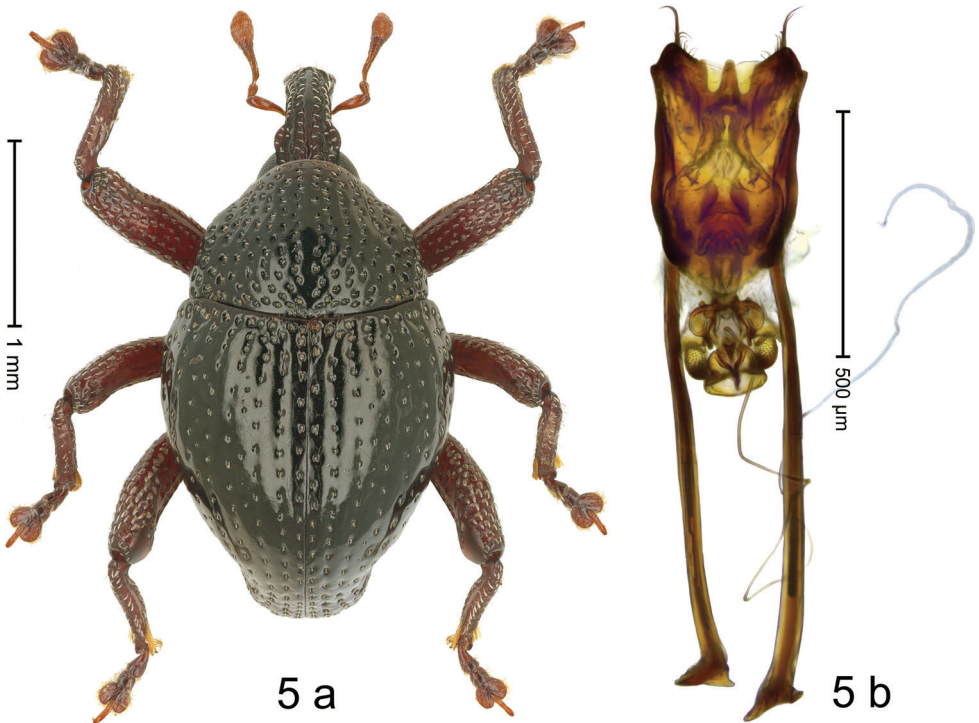
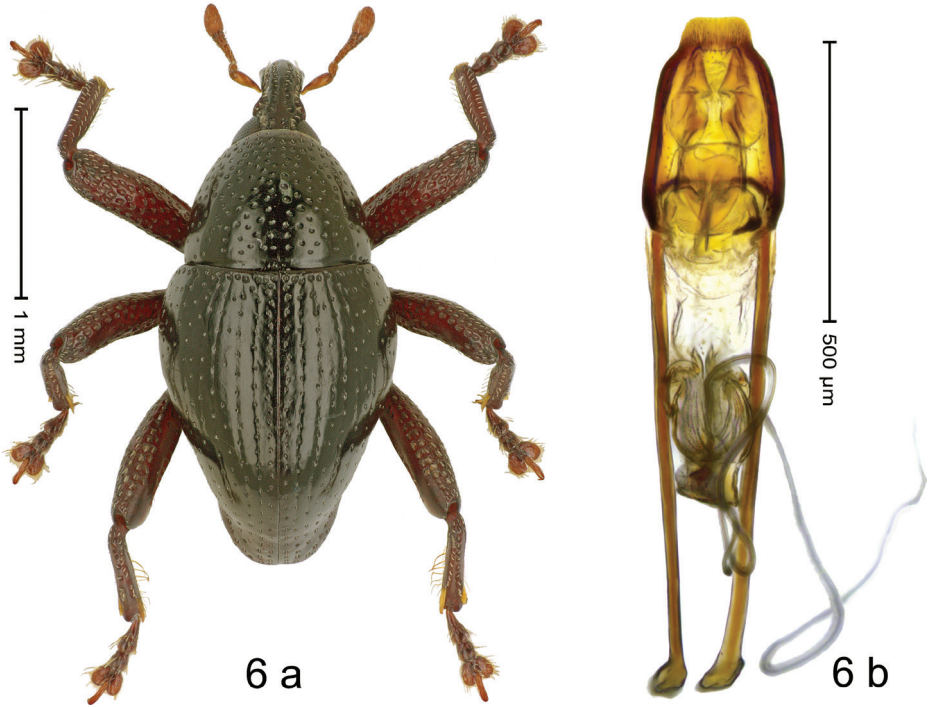
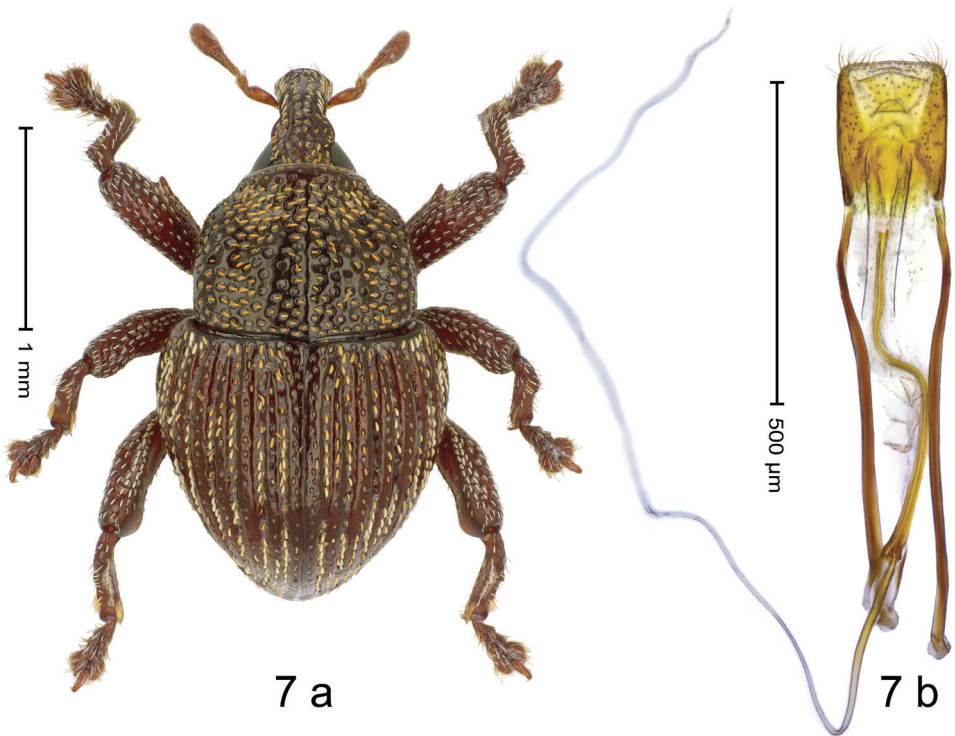


Figure 5. *Trigonopterus dakoensis* sp. nov., holotype **a** habitus **b** penis.



**Figure 6.** *Trigonopterus daun* sp. nov., holotype **a** habitus **b** penis.



**Figure 7.** *Trigonopterus ewok* sp. nov., holotype **a** habitus **b** penis.

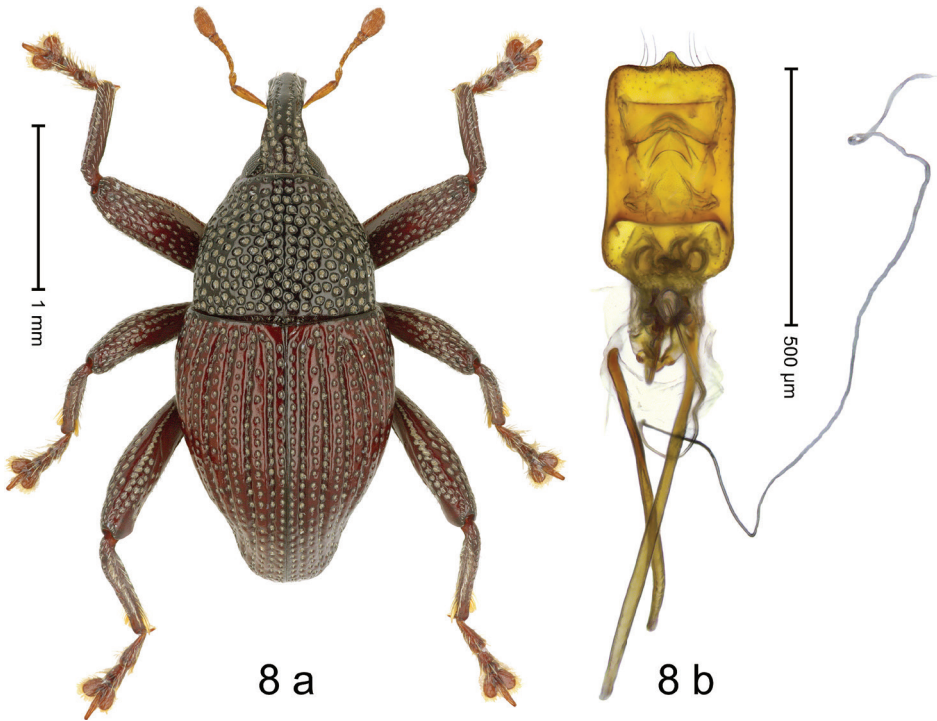


**Figure 8.** *Trigonopterus gundala* sp. nov., holotype **a** habitus **b** penis.

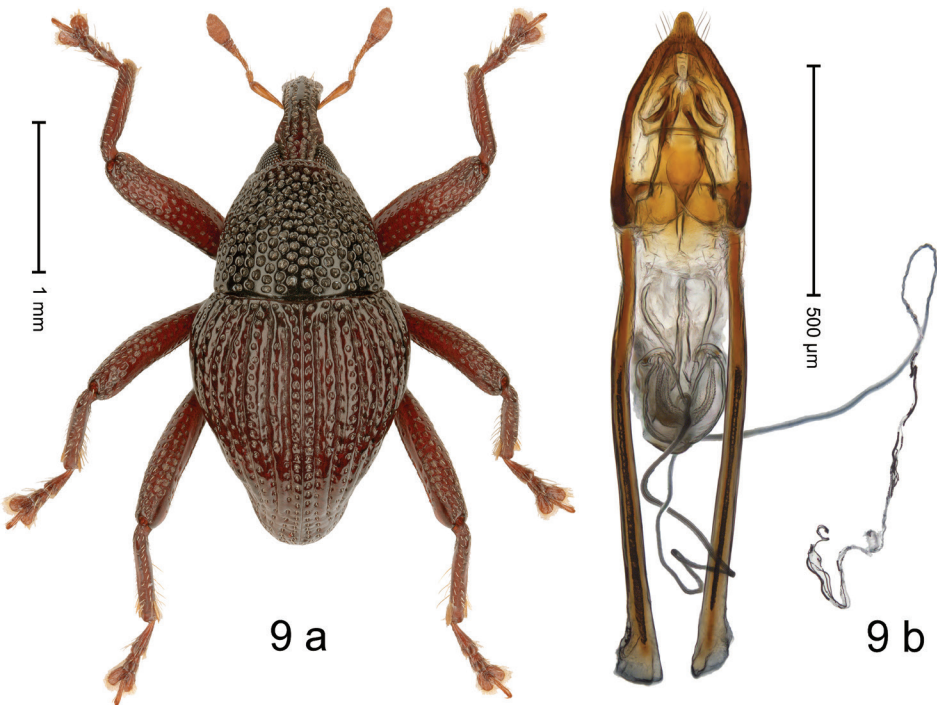


**Figure 9.** *Trigonopterus hoppla* sp. nov., holotype **a** habitus **b** penis.

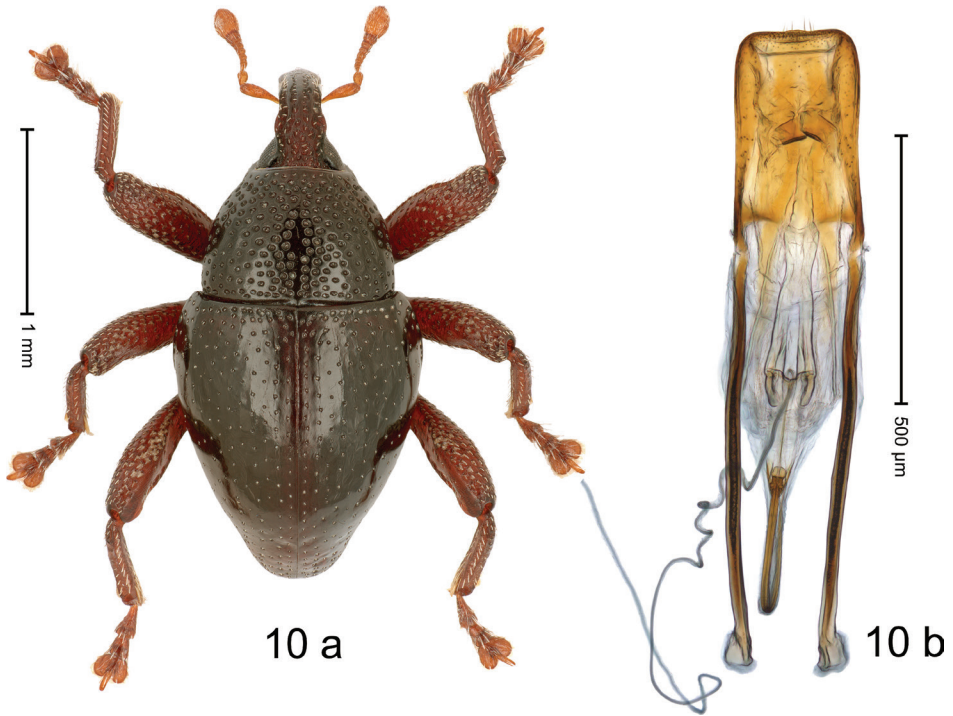


**Figure 10.** *Trigonopterus kakimerah* sp. nov., holotype **a** habitus **b** penis.

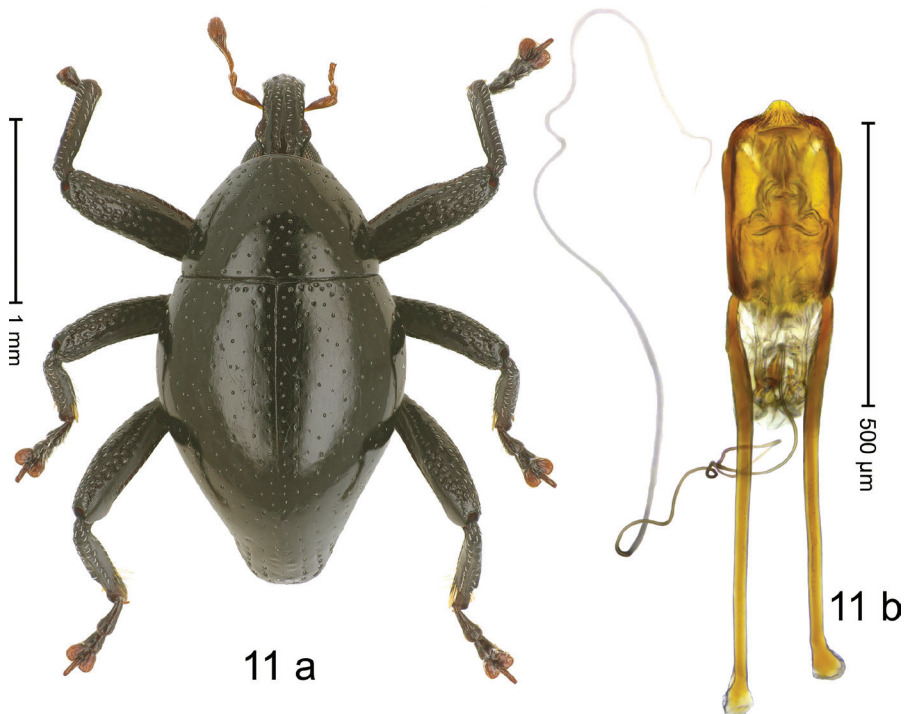


**Figure 11.** *Trigonopterus katopasaensis* sp. nov., holotype **a** habitus **b** penis.

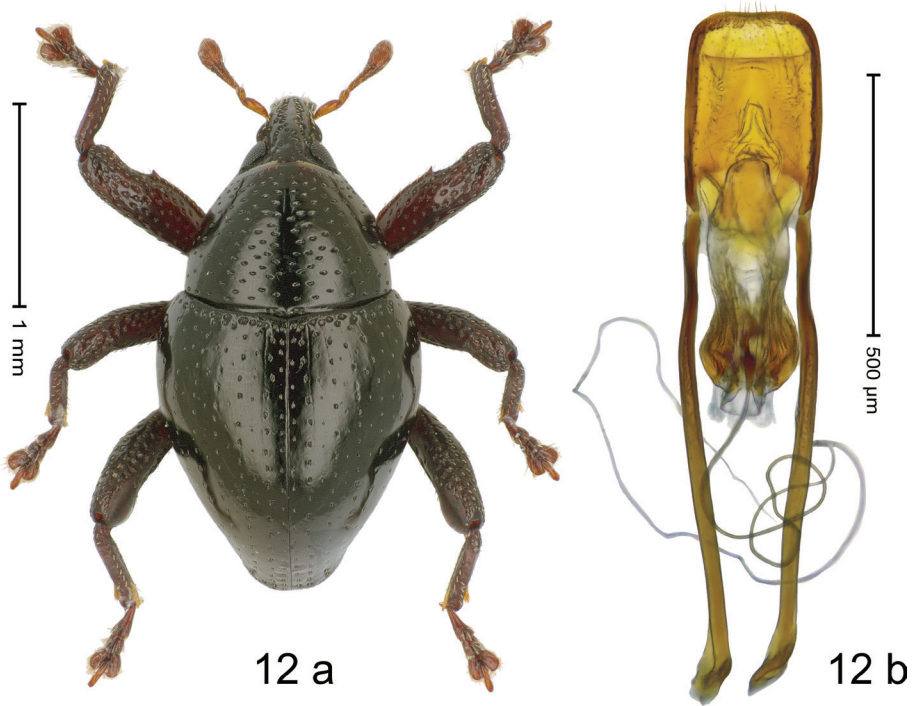


**Figure 12.** *Trigonopterus matakensis* sp. nov., holotype **a** habitus **b** penis.

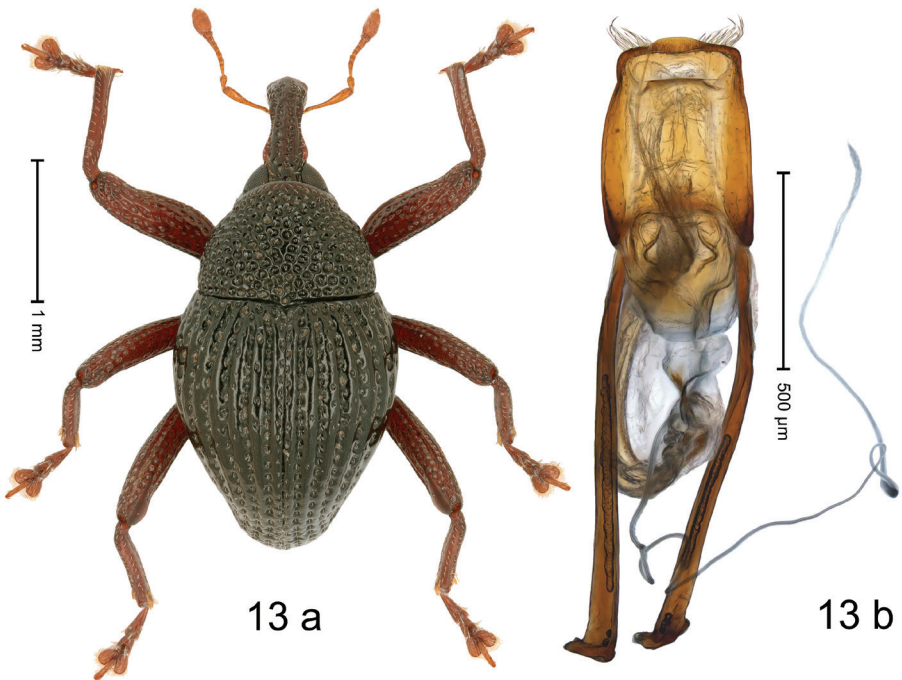


**Figure 13.** *Trigonopterus moduai* sp. nov., holotype **a** habitus **b** penis.

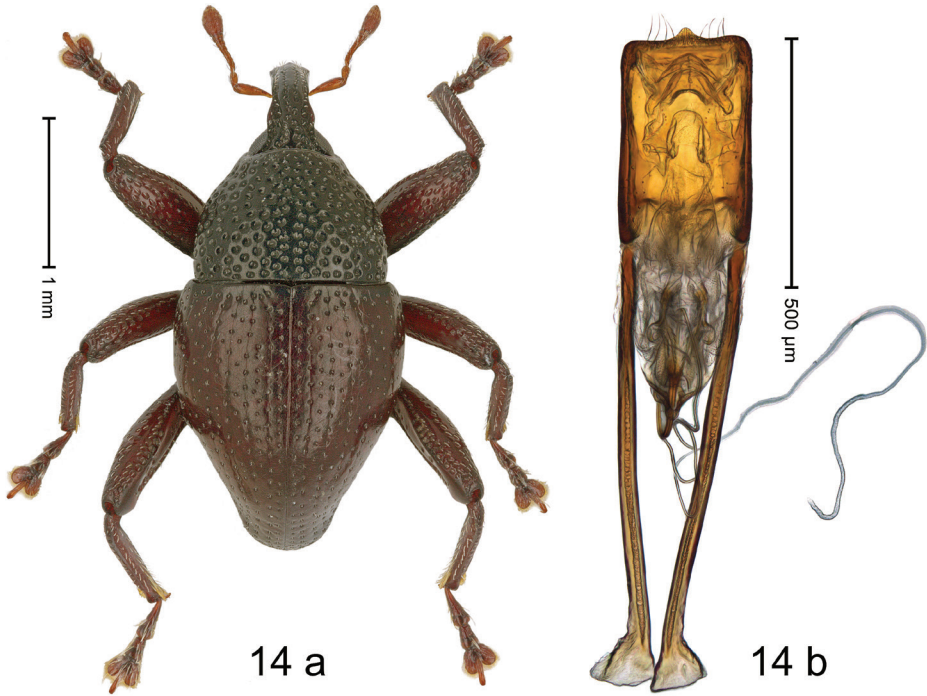


**Figure 14.** *Trigonopterus mons* sp. nov., holotype **a** habitus **b** penis.

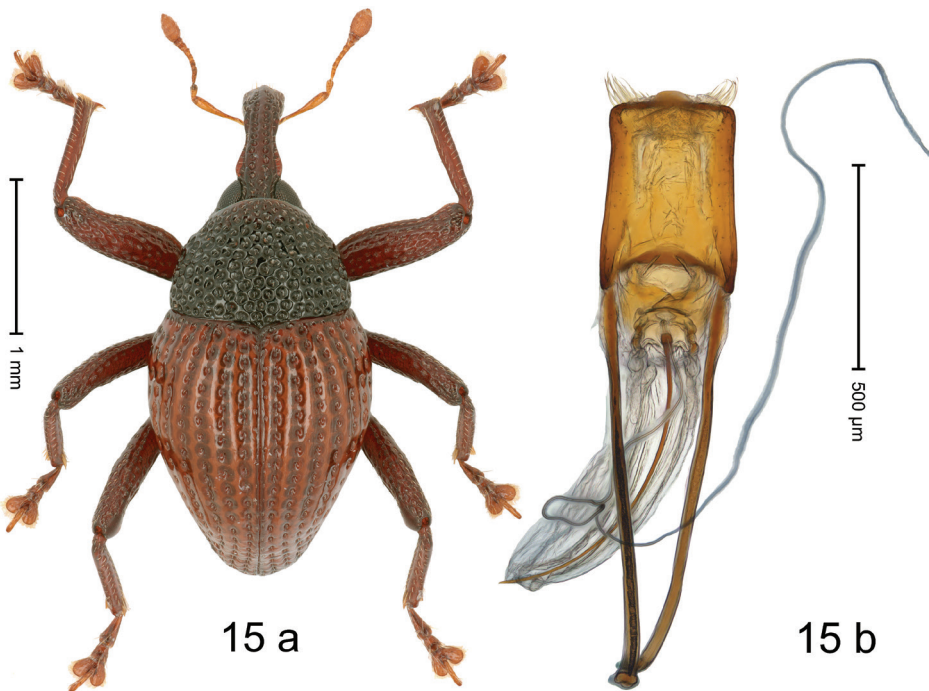


**Figure 15.** *Trigonopterus paramoduai* sp. nov., holotype **a** habitus **b** penis.

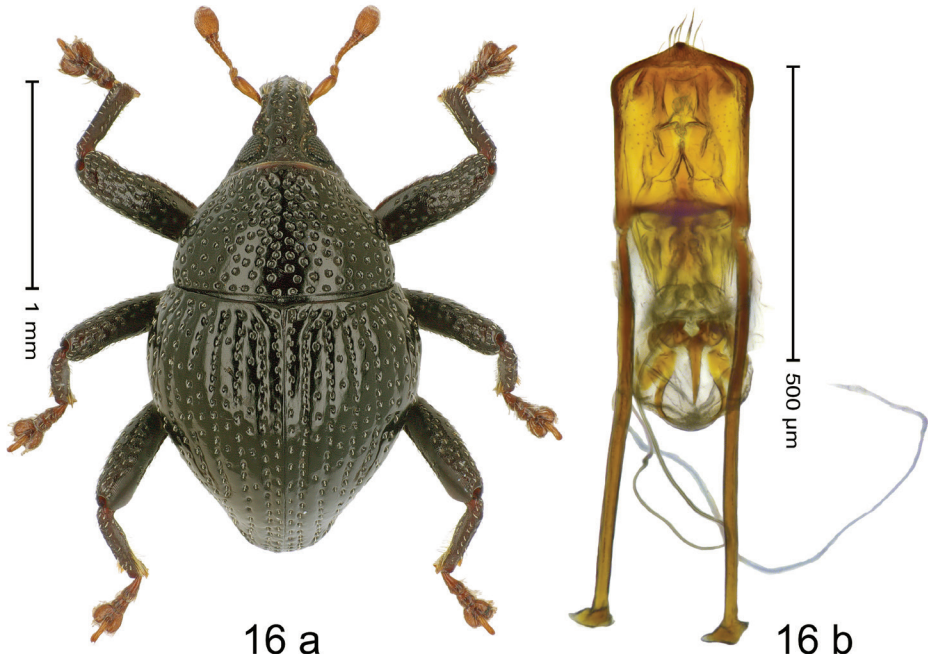


**Figure 16.** *Trigonopterus pomberimbensis* sp. nov., holotype **a** habitus **b** penis.

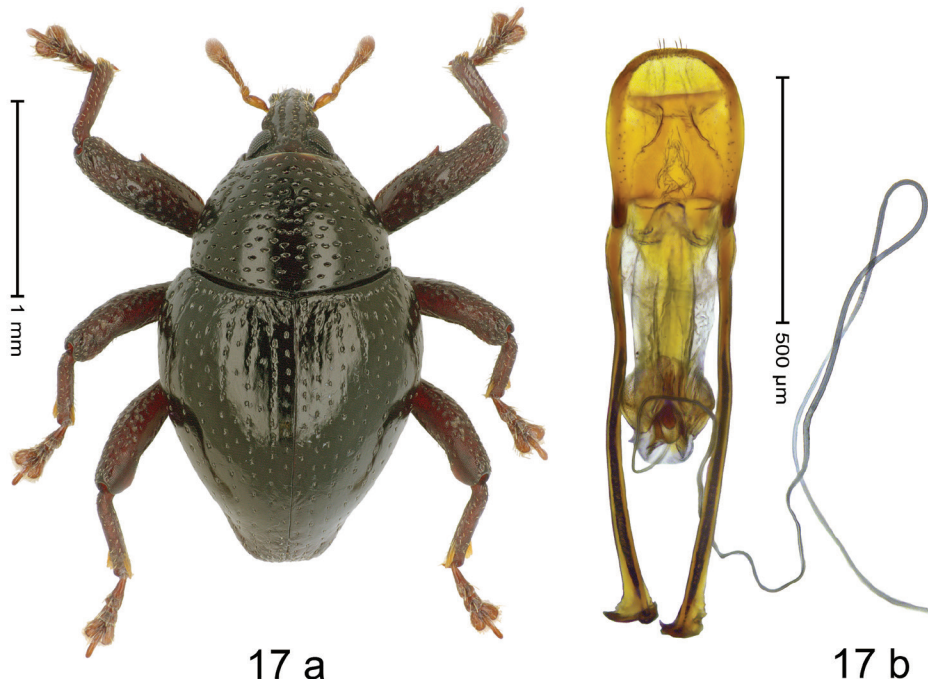


**Figure 17.** *Trigonopterus pompangeensis* sp. nov., holotype **a** habitus **b** penis.

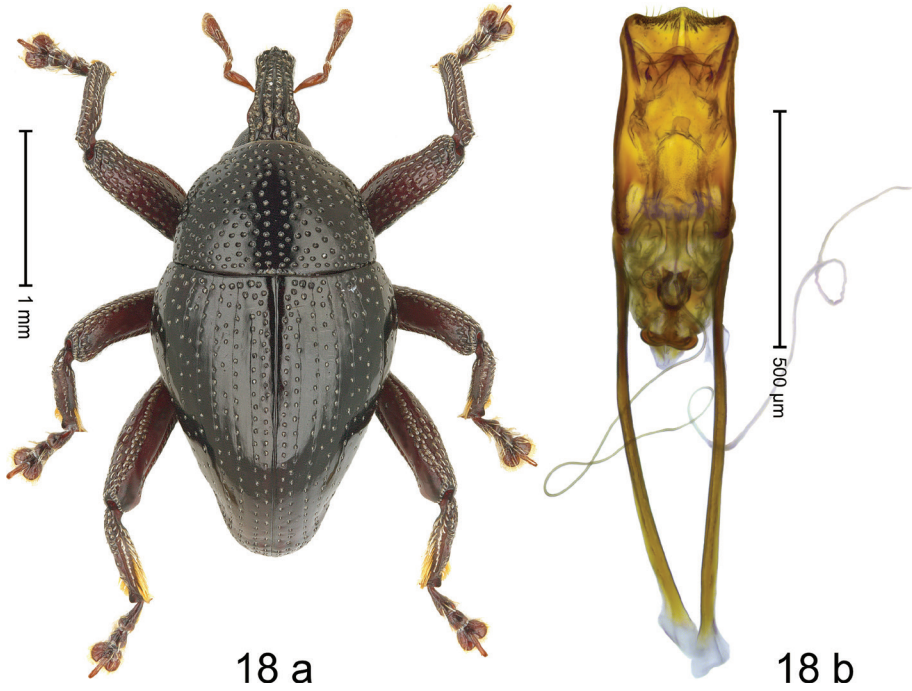


**Figure 18.** *Trigonopterus puspoi* sp. nov., holotype **a** habitus **b** penis.

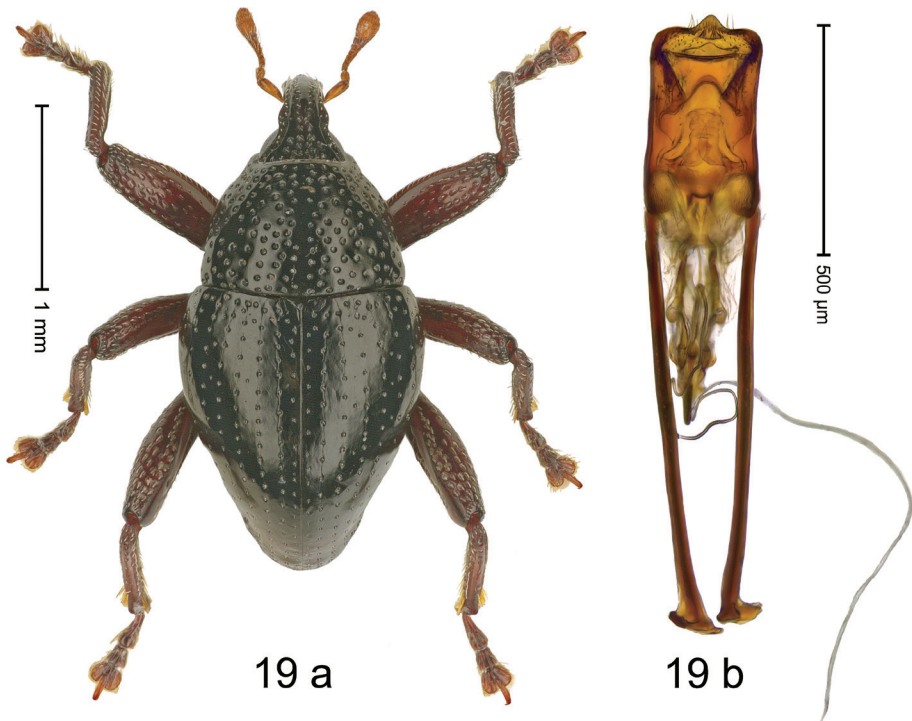


**Figure 19.** *Trigonopterus rosichoni* sp. nov., holotype **a** habitus **b** penis.

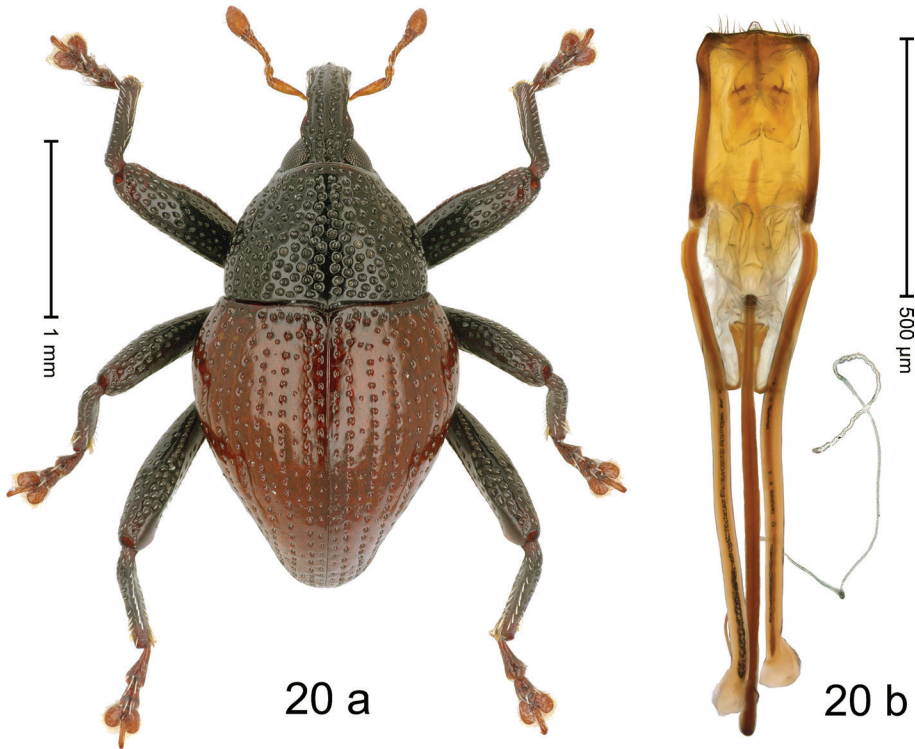


**Figure 20.** *Trigonopterus rubidus* sp. nov., holotype **a** habitus **b** penis.

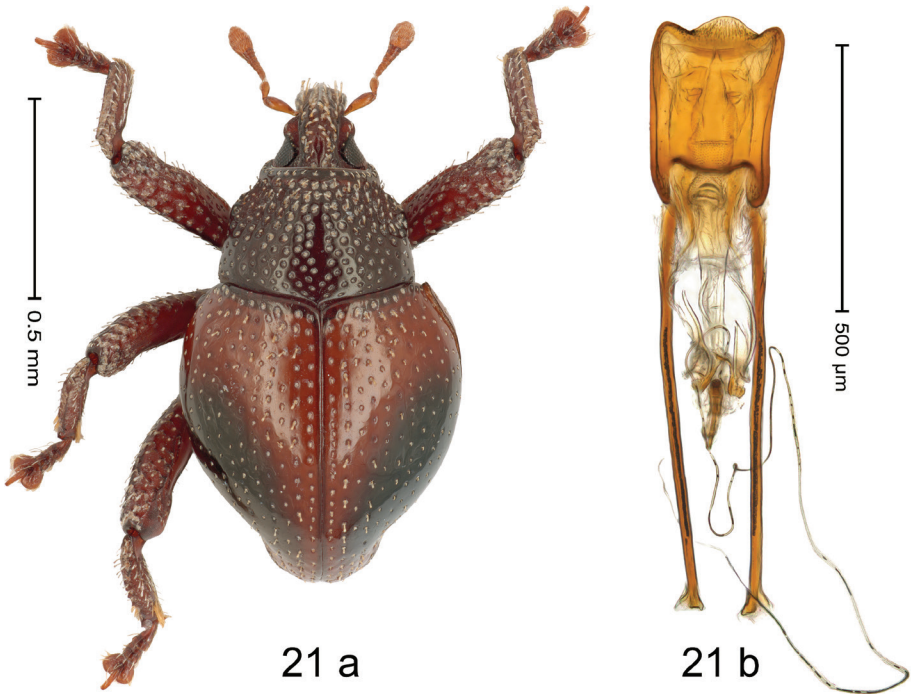


**Figure 21.** *Trigonopterus sarinoides* sp. nov., holotype **a** habitus **b** penis.

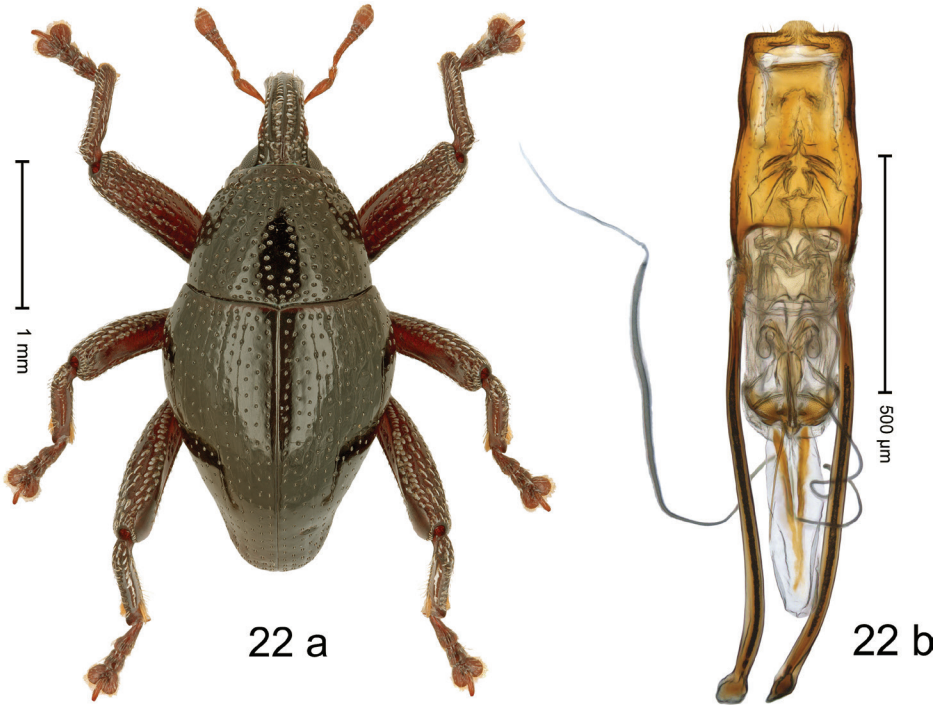


**Figure 22.** *Trigonopterus sutrisnoi* sp. nov., holotype **a** habitus **b** penis.

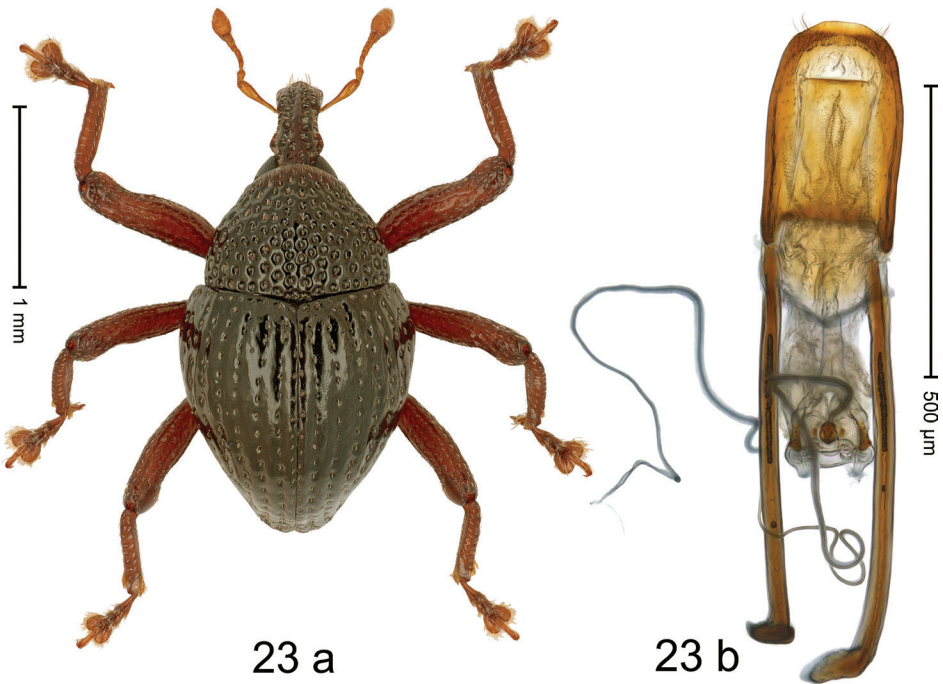


**Figure 23.** *Trigonopterus tanah* sp. nov., holotype **a** habitus **b** penis.

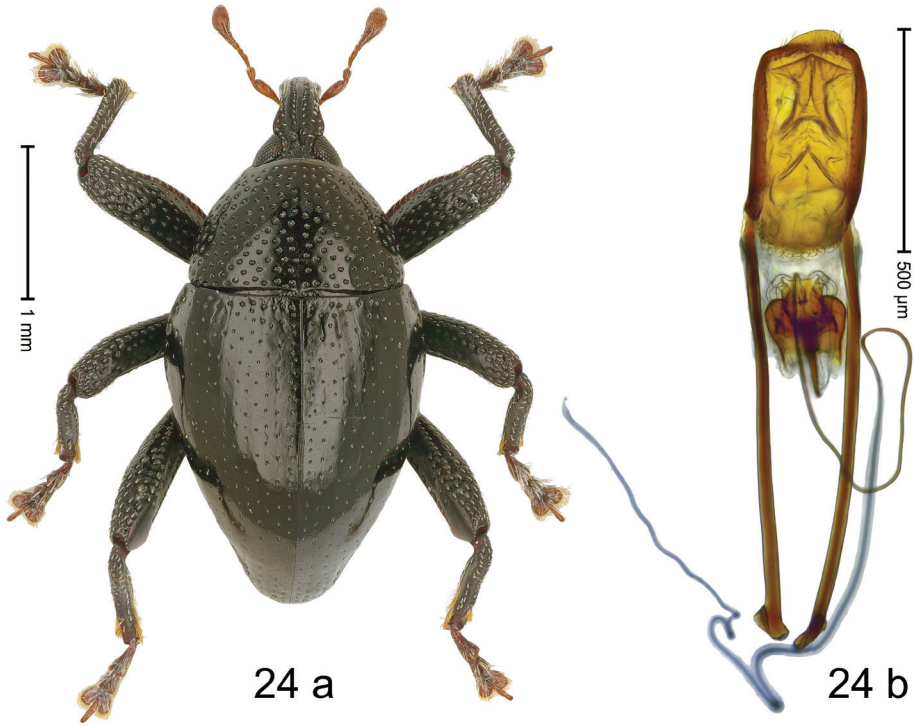


**Figure 24.** *Trigonopterus tejokusumoi* sp. nov., holotype **a** habitus **b** penis.

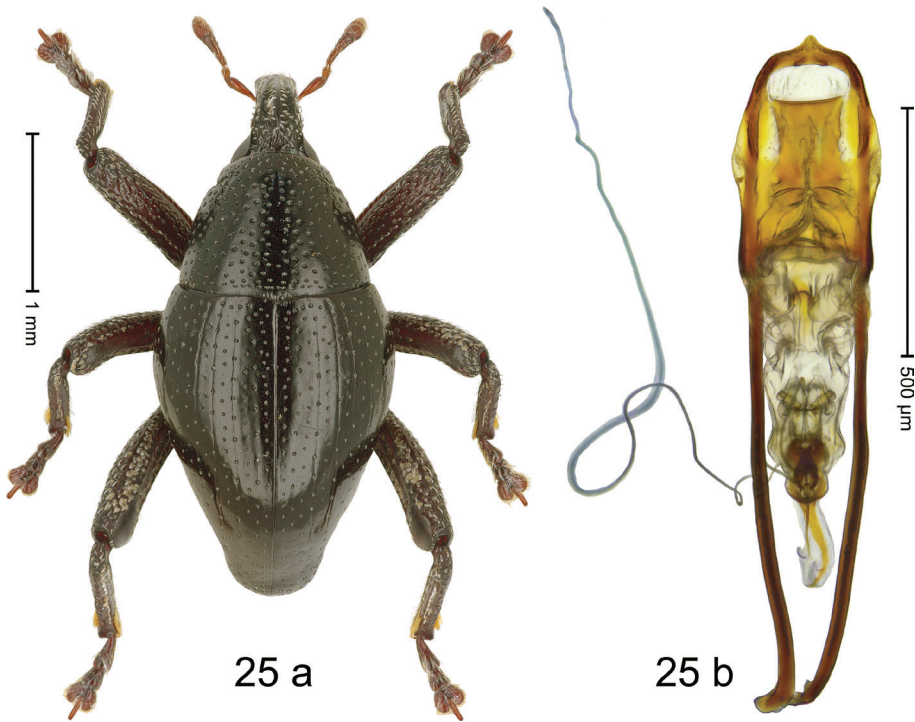


**Figure 25.** *Trigonopterus toboliensis* sp. nov., holotype **a** habitus **b** penis.

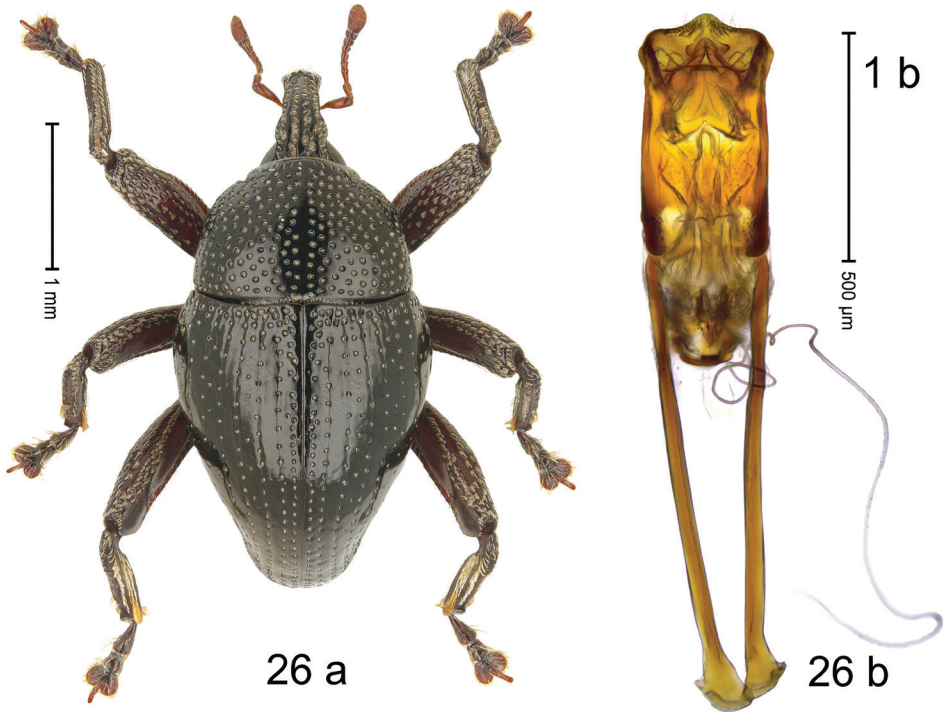


**Figure 26.** *Trigonopterus tolitoliensis* sp. nov., holotype **a** habitus **b** penis.

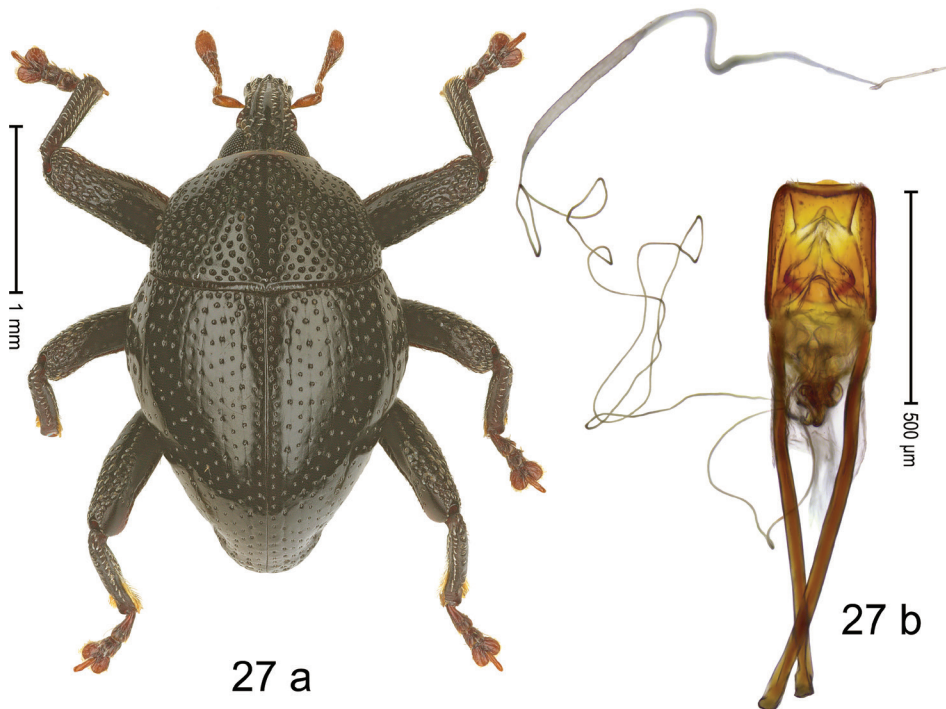


**Figure 27.** *Trigonopterus tounensis* sp. nov., holotype **a** habitus **b** penis.

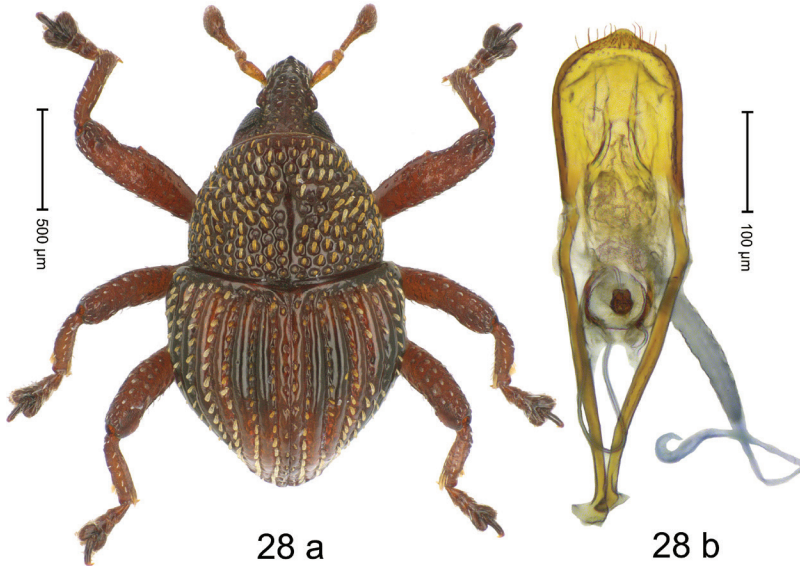


**Figure 28.** *Trigonopterus unyil* sp. nov., holotype **a** habitus **b** penis.

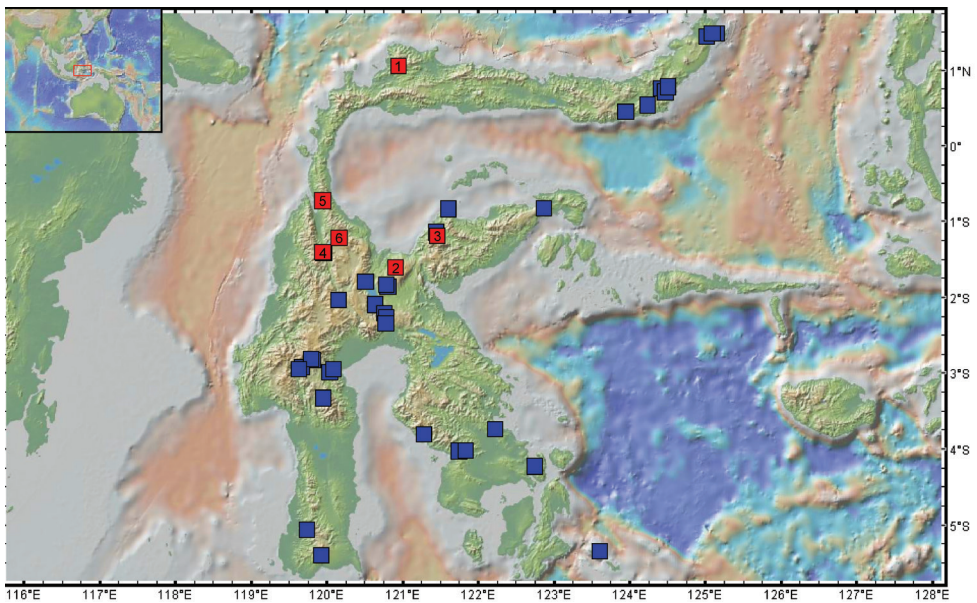


**Figure 29.** Map of *Trigonopterus* records across Sulawesi and adjacent islands. Blue dots from Riedel and Narakusumo (2019); white dots from present study. Prepared using GeoMapApp ([www.geomapapp.org](http://www.geomapapp.org); Ryan et al. 2009); 1 = Mt Dako (*T. acutus* sp. nov., *T. ancora* sp. nov., *T. arcanus* sp. nov., *T. corona* sp. nov., *T. dakoensis* sp. nov., *T. daun* sp. nov., *T. gundala* sp. nov., *T. hoppla* sp. nov., *T. moduai* sp. nov., *T. mons* sp. nov., *T. paramoduai* sp. nov., *T. puspoi* sp. nov., *T. rosichoni* sp. nov., *T. rubidus* sp. nov., *T. sutrisnoi* sp. nov., *T. tanah* sp. nov., *T. tolitoliensis* sp. nov.); 2 = Mt Pompango (*T. ewok* sp. nov., *T. kakimerah* sp. nov., *T. matakensis* sp. nov., *T. pomberimbensis* sp. nov., *T. pompangeensis* sp. nov., *T. tejokusumoi* sp. nov., *T. unyil* sp. nov.); 3 = Mt Katopasa (*T. katopasensis* sp. nov., *T. tounensis* sp. nov.); 4 = Mt Torompupu (*T. sarinoi* sp. nov.); 5 = Palu (*T. toboliensis* sp. nov.); 6 = Palolo (*T. toboliensis* sp. nov.).

## Acknowledgements

We thank LIPI (Indonesian Institute of Sciences), RISTEK (Ministry of State for Research and Technology, Indonesia) and the Indonesian Department of Forestry for providing relevant permits. The field work in Indonesia would not have been possible without the generous hospitality and help of many local people from Matakko, Enrekang, Teluk Bone, Kinapasan villages and we thank all of them very warmly. Thanks to Anang Setiawan Achmadi (MZB) for letting the first author join his expedition to Mt Dako, I Nyoman Sumerta (InaCC), Fahri (Tadulako University Palu), Evan, Mursalim, Jusman and Ali for companionship during the field trips. Finally, MA Alonso-Zarazaga (Madrid), CHC Lyal (London), and GP Setliff (Kutztown) are thanked for their helpful comments on the manuscript. This work was funded by the German Research Foundation DFG (RI 1817/1-1, 3-1, 3-3, 3-4, 5-1 to A.R.) and the German Academic Exchange Service DAAD (91654661 to R.P.N.).

## References

- Bebber DP, Carine MA, Wood JR, Wortley AH, Harris DJ, Prance GT, Davidse G, Paige J, Pennington TD, Robson NKB, Scotland RW (2010) Herbaria are a major frontier for species discovery. *Proceedings of the National Academy of Sciences*, 107(51): 22169–22171. <https://doi.org/10.1073/pnas.1011841108>
- Beutel RG, Leschen RAB (2005) *Handbook of Zoology*, Vol. IV, Part 38, Coleoptera, Beetles. Vol. 1: Morphology and Systematics (Archostemata, Adephaga, Myxophaga, Polyphaga partim). Walter de Gruyter, Berlin, 567 pp. <https://doi.org/10.1515/9783110904550>
- Hall R (2009) Southeast Asia's changing palaeogeography. *Blumea - Biodiversity, Evolution and Biogeography of Plants* 54: 148–161. <https://doi.org/10.3767/000651909X475941>
- Leschen RAB, Beutel RG, Lawrence JF, Slipinski A (2009) *Handbook of Zoology*, Vol. IV, Part 38, Coleoptera, Beetles. Vol. 2: Morphology and Systematics (Elateroidea, Bostrichiformia, Cucujiformia partim). Walter de Gruyter, Berlin, 786 pp.
- Letsch H, Balke M, Toussaint EFA, Narakusumo RP, Fiedler K, Riedel A (2020) Transgressing Wallace's Line brings hyperdiverse weevils down to earth. *Ecography* 43(9): 1329–1340. <https://doi.org/10.1111/ecog.05128>
- Narakusumo RP, Balke M, Riedel A (2019) Seven new species of *Trigonopterus* Fauvel (Coleoptera, Curculionidae) from the Tanimbar Archipelago. *Zookeys* 888: 75–93. <https://doi.org/10.3897/zookeys.888.38642>
- Narakusumo RP, Riedel A, Pons J (2020) Mitochondrial genomes of twelve species of hyperdiverse *Trigonopterus* weevils. *PeerJ* 8: e10017. <https://doi.org/10.7717/peerj.10017>
- Nguyen LT, Schmidt HA, von Haeseler A, Minh BQ (2015) IQ-TREE: A fast and effective stochastic algorithm for estimating Maximum-Likelihood phylogenies. *Molecular Biology and Evolution* 32:268–274. <https://doi.org/10.1093/molbev/msu300>
- Nugraha AMS, Hall R (2018) Late cenozoic palaeogeography of Sulawesi, Indonesia. *Palaeogeography, Palaeoclimatology, Palaeoecology*, 490: 191–209. <https://doi.org/10.1016/j.palaeo.2017.10.033>

- Paradis E, Schliep K (2019) ape 5.0: an environment for modern phylogenetics and evolutionary analyses in R. *Bioinformatics*, 35(3): 526–528. <https://doi.org/10.1093/bioinformatics/bty633>
- R Development Core Team (2019) R: A Language and Environment for Statistical Computing. R Foundation for Statistical Computing.
- Riedel A (2005) Digital imaging of beetles (Coleoptera) and other three-dimensional insects. In: Häuser C, Steiner A, Holstein J, Scoble MJ (Eds) *Digital Imaging of Biological Type Specimens. A Manual of Best Practice. Results from a study of the European Network for Biodiversity Information*, Stuttgart, 222–250.
- Riedel A, Daawia D, Balke M (2010) Deep *cox1* divergence and hyperdiversity of *Trigonopterus* weevils in a New Guinea mountain range (Coleoptera, Curculionidae). *Zoologica Scripta* 39(1): 63–74. <https://doi.org/10.1111/j.1463-6409.2009.00404.x>
- Riedel A, Sagata K, Suhardjono YR, Tänzler R, Balke M (2013a) Integrative taxonomy on the fast track – towards more sustainability in biodiversity research. *Frontiers in Zoology* 10: 1–15. <https://doi.org/10.1186/1742-9994-10-15>
- Riedel A, Sagata K, Surbakti S, Tänzler R, Balke M (2013b) One hundred and one new species of *Trigonopterus* weevils from New Guinea. *ZooKeys* 280: 1–150. <https://doi.org/10.3897/zookeys.280.3906>
- Riedel A, Tänzler R, Balke M, Rahmadi C, Suhardjono YR (2014) Ninety-eight new species of *Trigonopterus* weevils from Sundaland and the Lesser Sunda Islands. *ZooKeys* 467: 1–162. <https://doi.org/10.3897/zookeys.467.8206>
- Riedel A, Tänzler R (2016) Revision of the Australian species of the weevil genus *Trigonopterus* Fauvel. *ZooKeys* 556: 97–162. <https://doi.org/10.3897/zookeys.556.6126>
- Riedel A, Narakusumo RP (2019) One hundred and three new species of *Trigonopterus* weevils from Sulawesi. *ZooKeys* 828: 1–153. <https://doi.org/10.3897/zookeys.828.32200>
- Ryan WBF, Carbotte SM, Coplan J, O’Hara S, Melkonian A, Arko R, Weissel RA, Ferrini V, Goodwillie A, Nitsche F, Bonczkowski J, Zemsky R (2009), Global Multi-Resolution Topography (GMRT) synthesis data set, *Geochemistry, Geophysics, Geosystems* 10: Q03014. <https://doi.org/10.1029/2008GC002332>.
- Staats M, Erkens RH, van de Vossen B, Wieringa JJ, Kraaijeveld K, Stielow B, Geml J, Richardson JE, Bakker FT (2013) Genomic treasure troves: complete genome sequencing of herbarium and insect museum specimens. *PLoS ONE* 8(7): e69189
- Stelbrink B, Albrecht C, Hall R, von Rintelen R (2012) The biogeography of Sulawesi revisited: is there evidence for a vicariant origin of taxa on Wallace’s “anomalous island”? *Evolution* 66: 2252–2271. <https://doi.org/10.1111/j.1558-5646.2012.01588.x>
- Tänzler R, Sagata K, Surbakti S, Balke M, Riedel A (2012) DNA barcoding for community ecology – how to tackle a hyperdiverse, mostly undescribed Melanesian fauna. *PLoS ONE* 7(1): e28832. <https://doi.org/10.1371/journal.pone.0028832>
- Tänzler R, Van Dam MH, Toussaint EFA, Suhardjono YR, Balke M, Riedel A (2016) Macroevolution of hyperdiverse flightless beetles reflects the complex geological history of the Sunda Arc. *Scientific Reports* 6: e18793. <https://doi.org/10.1038/srep18793>

- Toussaint EFA, Tänzler R, Balke M, Riedel A (2017) Transoceanic origin of microendemic and flightless New Caledonian weevils. *Royal Society Open Science* 4(6): 160546. <https://doi.org/10.1098/rsos.160546>
- Troudet J, Grandcolas P, Blin A, Vignes-Lebbe R, Legendre F (2017) Taxonomic bias in biodiversity data and societal preferences. *Scientific Reports* 7: 9132. <https://doi.org/10.1038/s41598-017-09084-6>



# On the brink of extinction: a new freshwater amphipod *Jesogammarus acalceolus* (Anisogammaridae) from Japan

Ko Tomikawa<sup>1</sup>, Naoya Kimura<sup>2</sup>

**1** Hiroshima University, Graduate School of Humanities and Social Sciences, 1-1-1 Kagamiyama, Higashihiroshima, Hiroshima, 739-8524, Japan **2** Tokiwazaka 1-7-18, Hirosaki, Aomori, 036-8263, Japan

Corresponding author: Ko Tomikawa ([tomikawa@hiroshima-u.ac.jp](mailto:tomikawa@hiroshima-u.ac.jp))

---

Academic editor: Rachael Peart | Received 16 July 2021 | Accepted 19 August 2021 | Published 26 October 2021

---

<http://zoobank.org/629D364D-946E-4F18-B5E0-DC12C40E7F98>

---

**Citation:** Tomikawa K, Kimura N (2021) On the brink of extinction: a new freshwater amphipod *Jesogammarus acalceolus* (Anisogammaridae) from Japan. ZooKeys 1065: 81–100. <https://doi.org/10.3897/zookeys.1065.71687>

---

## Abstract

Freshwater habitats, especially cold springs, are environments in which the risk of extinction faced by organisms remains high due to human activities. To conserve endangered species, it is important to describe and name them. Here, a new, endangered freshwater anisogammarid amphipod species, *Jesogammarus (Jesogammarus) acalceolus* **sp. nov.**, found in a spring in Aomori Prefecture, Japan, is described which is potentially the sole remaining habitat of this species. Both morphological and molecular phylogenetic results strongly support the nesting of the new species within *Jesogammarus*. *Jesogammarus (J.) acalceolus* **sp. nov.** is the first species of genus *Jesogammarus* that was found to lack a calceolus, a sensory organ located on male antenna 2. Thus, the diagnostic criteria for this genus required amendment. A reconstruction of ancestral calceoli, based on a molecular phylogenetic tree, revealed that the common ancestor of *Jesogammarus* possessed calceoli, which were secondarily lost in *J. (J.) acalceolus* **sp. nov.** Our results indicate that this new species, which is key to clarifying the evolution of the calceolus, is of high conservation significance.

## Keywords

Ancestral state reconstruction, molecular phylogeny, systematics

## Introduction

Fresh water is indispensable to human life. It is also an important habitat for many aquatic organisms. Fresh water accounts for ca. 2.5% of all water on Earth (Lehner

and Döll 2004). Approximately 9.5% of all known species live in fresh water (Balian et al. 2008). Deterioration of freshwater environments due to human activities remains a worldwide issue (Martínuzzi et al. 2014; Reid et al. 2019). Species inhabiting freshwater habitats are reported to be at a greater risk of extinction compared to marine and terrestrial species (Dudgeon et al. 2006; Collen et al. 2009, 2014).

Spring water is ground water that collects in soil due to rain and snow in mountainous areas. Recently, deterioration of spring water environments, leading to the depletion of spring water, caused by an inflow of domestic drainage and agricultural chemicals. Additionally, excessive pumping of groundwater for drinking and agricultural purposes has become an issue of worldwide proportions. Therefore, of the species inhabiting freshwater habitats, those that depend on spring water are considered to be at an even higher risk of extinction (Fluker et al. 2010). However, currently available taxonomic data on invertebrates inhabiting spring water appear to be insufficient, with many species remaining undescribed (Murphy et al. 2009). Although the discovery rate of species appears to be increasing, many species go unrecognized before becoming extinct (Mora et al. 2011). Thus, conducting taxonomic studies as well as naming and describing species is essential for conserving endangered species (Stork 1993; McKinney 1999; Giam et al. 2012; Coleman 2015; Costello et al. 2015).

The order Amphipoda comprises peracarid crustaceans belonging to the class Malacostraca. Of the more than 10,000 amphipod species that have been described globally, ca. 20% occur in freshwater (Väinölä et al. 2008; Horton et al. 2021). Freshwater amphipods generally prefer cool environments (Väinölä et al. 2008), and cold spring water and flowing spring water are the best habitats for them. Springs in the Japanese archipelago reportedly harbour diverse endemic amphipods (Tomikawa and Morino 2003; Tomikawa et al. 2003; Tomikawa 2017). The anisogammarid genus, *Jesogammarus* Bousfield, 1979, is the most diverse group among Japanese freshwater amphipods. *Jesogammarus* was established by Bousfield (Bousfield 1979), with *Anisogammarus jesoensis* Schellenberg, 1937 as the type species. In the same paper as that which described this type species, Bousfield established *Annanogammarus* Bousfield, 1979 and *Ramellogammarus* Bousfield, 1979 with *Gammarus annandalei* Tattersall, 1922 and *Gammarus ramellus* Weckel, 1907 as type species, respectively. *Annanogammarus* was later classified as a subgenus under *Jesogammarus* (Morino 1985). At present, *Jesogammarus* is known to contain 22 species from the Japanese Archipelago, the Korean Peninsula, and the Chinese mainland (Tomikawa et al. 2017). *Jesogammarus* is morphologically similar to *Ramellogammarus*, which is endemic to North American coastal fresh waters; these genera are considered to be closely related (Bousfield 1979, 1981). The former is distinguished from the latter mainly by having an antennal sensory organ termed the calceolus (Morino 1985; Bousfield and Morino 1992). However, though molecular phylogenetic studies have been conducted previously on Anisogammaridae, the phylogenetic relationship between *Jesogammarus* and *Ramellogammarus* has not yet been fully clarified (Macdonald III 2005; Tomikawa et al. 2010; Li et al. 2020).

Recently, a population of *Jesogammarus* species, lacks a calceolus on male antenna 2, was found in a spring in the Aomori Prefecture of Japan, which is potentially the sole

remaining habitat of this species (Fig. 1). We describe this species as *J. (J.) acalceolus* sp. nov. Describing and naming this species, as have been done here, can be considered important first steps leading to its conservation. In addition, we investigated the evolution of calceoli in *Jesogammarus* species with molecular phylogenetic analyses and ancestral state reconstruction.

## Materials and methods

### Sample collection

Specimens of *J. (J.) acalceolus* sp. nov. were collected from Haguro Shrine Spring, Hiro-saki, Aomori Prefecture, Japan (40.6153°N, 140.3854°E). Amphipods were collected by a fine-mesh hand net from fallen leaves and mosses. Specimens were fixed in 99% ethanol on the site.

### Morphological observation

Appendages of the examined amphipods were dissected using needles under a stereomicroscope (Olympus SZX7) and mounted in gum-chloral medium on glass slides. Prepared specimens were examined by a light microscope (Nikon Eclipse Ni) and illustrated using the aid of a camera lucida attached to the light microscope. The body length was measured from the tip of the rostrum to the base of the telson along the dorsal curvature to the nearest 0.1 mm following Tomikawa et al. (2017). The specimens have been deposited in the Tsukuba Collection Center of the National Museum of Nature and Science, Tokyo (NSMT).

### PCR and DNA sequencing

Genomic DNA was extracted from the pleopod muscle of the specimens following procedures detailed by Tomikawa et al. (2014). The primer sets for PCR and cycle sequencing reactions used in this study were as follows: for 28S rRNA (28S), 28SF and 28SR (Tomikawa et al. 2012); for cytochrome *c* oxidase subunit I (COI), Am-COI-H and Am-COI-T (Tomikawa 2015); and for 16S rRNA (16S), 16STf (Macdonald III 2005) and 16Sbr (Palumbi 1996). PCR and DNA sequencing were performed using the method detailed by Tomikawa (2015). The newly obtained DNA sequence has been deposited in the International Nucleotide Sequence Database Collaboration (IN-SDC) through the DNA Data Bank of Japan (DDBJ) (Table 1).

### Molecular phylogenetic analyses

The phylogenetic analyses were conducted based on sequences of nuclear 28S rRNA and mitochondrial COI and 16S rRNA genes. The alignment of COI was trivial, as no indels were observed. The sequences of 28S and 16S were aligned using the Muscle

**Table 1.** Samples used for molecular analyses with voucher/isolate number, collection locality, and NCBI GenBank accession number. Sequences marked with an asterisk (\*) were obtained for the first time in this study.

Species	Voucher or isolate #	Locality	NCBI GenBank acc. nos.		
			28S rRNA	COI	16S rRNA
<i>Anisogammarus pugettensis</i>	G1500	Akkeshi Bay, Hokkaido, Japan	LC624749*	LC624757*	LC624742*
<i>Barrowgammarus macginitiei</i>	G37	Akkeshi Bay, Hokkaido, Japan	LC624750*	LC624758*	LC624743*
<i>Eogammarus kygi</i>	G1	Naibetsu River, Hokkaido, Japan	LC214759	LC052229	LC052250
<i>E. posjeticus</i>	G3	Lake Akkeshi, Hokkaido, Japan	LC214760*	LC052230	LC052251
<i>Jesogammarus (Annanogammarus) annandalei</i>	G1162	Lake Biwa, Shiga, Japan	LC214786	LC052248	LC052269
<i>J. (A.) debilis</i>	IZCAS-I-A0325	Fangshan, Beijing, China	EF582997		EF582846
<i>J. (A.) fluviatilis</i>	G83	Samegai, Shiga, Japan	LC214766	LC052236	LC052257
<i>J. (A.) koreaensis</i>	G1376	Deoksin-ri, Onsan-eup, Ulju-gun, Ulsan, Korea	LC624751*	LC624759*	
<i>J. (A.) naritai</i>	G1167	Lake Biwa, Shiga, Japan	LC214787	LC052249	LC052270
<i>J. (A.) suwaensis</i>	G88	Lake Suwa, Nagano, Japan	LC214767	LC052237	LC052258
<b><i>Jesogammarus (Jesogammarus) acalceolus sp. nov.</i></b>	NSMT-Cr 29008 (G1625)	Haguro Shrine Spring, Aomori, Japan	LC624752*	LC624760*	LC624744*
<b><i>J. (J.) acalceolus sp. nov.</i></b>	NSMT-Cr 29005 (G1845)	Haguro Shrine Spring, Aomori, Japan	LC624753*	LC624761*	LC624745*
<i>J. (J.) bousfieldi</i>	KUZ Z1799	Aburato, Tsuruoka, Yamagata, Japan	LC214778	LC214538	LC214795
<i>J. (J.) fujinoi</i>	G17	Yamagata, Japan	LC214762	LC052232	LC052253
<i>J. (J.) hebeiensis</i>	IZCAS-I-A0294	Yanqing, Beijing, China	EF582998		EF582847
<i>J. (J.) hinumensis</i>	G52	Lake Hinuma, Ibaraki, Japan	LC214765	LC052235	LC052256
<i>J. (J.) hokurikuensis</i>	G1838	Shimizucho, Fukui, Japan	LC624754*	LC624762*	LC624746*
<i>J. (J.) ikiensis</i>	G515	Iki, Nagasaki, Japan	LC214772	LC052242	LC052263
<i>J. (J.) jesoensis</i>	G164	Sapporo, Hokkaido, Japan	LC214769	LC052239	LC052260
<i>J. (J.) mikadoi</i>	G13	Rokugo, Akita, Japan	LC214761	LC052231	LC052252
<i>J. (J.) paucisetulosus</i>	G1037	Mito, Ibaraki, Japan	LC214780	LC052247	LC052268
<i>J. (J.) shonaiensis</i>	G192	Sakata, Yamagata, Japan	LC214770	LC052240	LC052261
<i>J. (J.) spinopalpus</i>	G32	Onjuku, Chiba Prefecture, Japan	LC214763	LC052233	LC052254
<i>J. (J.) uchiyamaryui</i>	KUZ Z1803	Tanie River, Iki, Nagasaki, Japan	LC214773	LC214533	LC214790
<i>Ramellogammarus oregonensis</i>	G1537	Willamette River, Corvallis, Oregon, USA	LC624755*		
<i>R. similimanus</i>	G1540	Alice Springs, Portland, Oregon, USA	LC624756*		
<i>Spasskogammarus spasskii</i>	G35	Akkeshi Bay, Hokkaido, Japan	LC214764*	LC052234	LC052255
<i>Gammarus mukudai</i>	G858	Iki, Nagasaki, Japan	AB893234	LC624763*	LC624747*
<i>G. nipponensis</i>	G797	Kiyotaki, Kyoto, Japan	AB893232	LC624764*	LC624748*

algorithm implemented in MEGA X (Kumar et al. 2018). Phylogenetic relationships were reconstructed via Maximum Likelihood (ML) and Bayesian Inference (BI). The best evolutionary models were selected based on the corrected Akaike Information Criterion (AIC) for ML and Bayesian Information Criterion (BIC) for BI using MEGA X (Kumar et al. 2018). ML phylogenies were conducted using MEGA X (Kumar et al. 2018) under the substitution model GTR+G+I, and 1,000 bootstrap replications (Felsenstein 1985) were performed to estimate statistical support for branching patterns. BI analyses were estimated using MrBayes v3.2.6 (Ronquist et al. 2012) under the substitution model GTR+G+I, with Markov chains of 10 million generations. Parameter estimates and convergence were checked using Tracer v1.7.1 (Rambaut et al. 2018), and the first 1 million trees were discarded as burn-in. Two gammarid species, *Gammarus mukudai* Tomikawa, Soh, Kobayashi & Yamaguchi, 2014 and *G. nipponensis* Uéno, 1966, were included in the analyses as outgroup taxa.

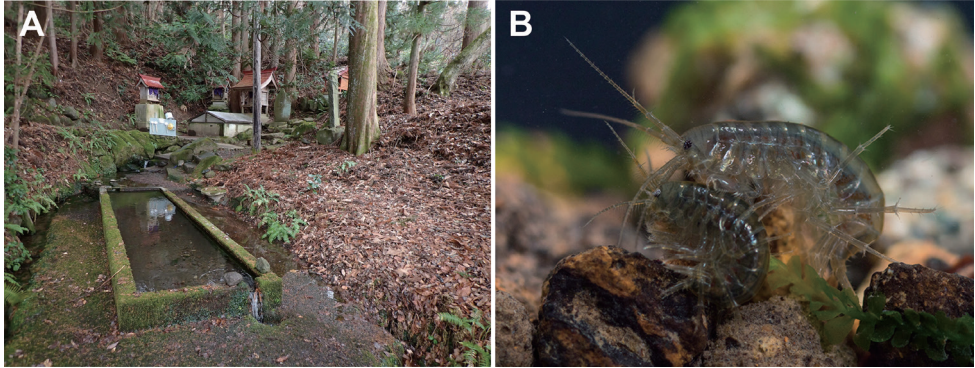


**Figure 1.** Habitat and live specimens of *Jesogammarus (Jesogammarus) acalceolus* sp. nov. **A** the type locality, Haguro Shrine Spring, Hirosaki, Aomori Prefecture, Japan **B** mate guarding pair, male is upper and female is lower, photographed by Ryu Uchiyama.

## Ancestral state reconstruction

The ancestral states of the calceolus on male antenna 2 were reconstructed on the tree (Fig. 2) via the likelihood model using Mesquite v3.61 (Maddison and Maddison 2019). The Markov K-state 1 parameter model was used for likelihood reconstruction at each ancestral node with equal probability for all particular character state changes.

## Results

### Molecular phylogenetic analyses

The monophyly of *Jesogammarus* was inferred with maximum (100% bootstrap support [BS]) and relatively low (0.85 posterior probability [PP]) support values in the maximum likelihood (ML) and Bayesian inference tree (BI) trees, respectively (Fig. 2). Although *Jesogammarus* formed a sister group with *Barrowgammarus* Bousfield, 1979 (87% BS), their relationship was not supported by BI analyses. The new species collected in this study, *J. (J.) acalceolus*, was nested within *Jesogammarus* and clustered with *J. (J.) hinumensis* Morino, 1993 and *J. (J.) ikiensis* Tomikawa, 2015. In this study, the phylogenetic position of *J. (A.) koreaensis* Lee & Seo, 1990 was also clarified for the first time: this species formed a sister group with *J. (A.) debilis* Hou & Li, 2005, with high support values (98% BS, 1.0 PP). Of the 22 species of *Jesogammarus*, 20, excluding *J. (J.) fontanus* Hou & Li, 2004 and *J. (J.) ilhoii* Lee & Seo, 1992, were included in the molecular phylogenetic analyses of this study.

### Ancestral state reconstruction

The likelihood reconstruction (Fig. 2) demonstrated that the calceolus on male antenna 2 was an ancestral character state of the most recent common ancestor (MRCA) of the *Jesogammarus* species, with 0.96 proportional likelihood (PL). The character



setae. Female gnathopods 1 and 2 strongly dissimilar. Coxal gills on gnathopod 2 and pereopods 3–7, gills 2–5 each with 2 accessory lobes, gills 6 and 7 each with 1 accessory lobe. Uropods 1 and 2, rami extending beyond peduncle of uropod 3. Uropod 3, inner ramus not longer than 0.4 times of that of outer ramus; terminal article distinct. Brood plate 2 of female broadly expanded anteroproximally.

**Remarks.** The presence of a calceolus on the flagellum of male antenna 2 is a major diagnostic feature of *Jesogammarus*, which distinguishes it from *Ramellogammarus* (Bousfield 1979; Morino 1985). However, the discovery of the new species, *J. acalceolus*, which lacks a calceolus, indicated that the calceolus was not critical for diagnosis. The genus *Jesogammarus* is distinguishable from *Ramellogammarus* by the dissimilar female gnathopods 1 and 2 and the expanded brood plates of the female. The genus *Jesogammarus* shares a similar coxal gill type with marine *Locustogammarus* Bousfield, 1979 and *Spasskogammarus* Bousfield, 1979 but differs from these two genera in terms of the following features (features of *Locustogammarus* and *Spasskogammarus* in parentheses): from *Locustogammarus*, in terms of longer antenna 1 than antenna 2 (subequal in *Locustogammarus*), dissimilar female gnathopods 1 and 2 (similar in *Locustogammarus*), uropods 1 and 2 with rami extending beyond the peduncle of uropod 3 (not extending in *Locustogammarus*), and a distinct terminal article of uropod 3 (very small in *Locustogammarus*); from *Spasskogammarus*, in terms of dorsal margins of pleonites with slender setae (lacking in *Spasskogammarus*), longer antenna 1 than antenna 2 (subequal in *Spasskogammarus*), and slender pereopods 5–7 (short in *Spasskogammarus*).

***Jesogammarus (J.) acalceolus* sp. nov.**

<http://zoobank.org/43EABC71-3F5A-48ED-9982-6320B94C6CAC>

[New Japanese name: Shitsuko-yokoebi]

Figures 1B, 3–5

**Material examined. Holotype:** male (7.4 mm, NSMT-Cr 29003), Haguro Shrine Spring, Hirosaki, Aomori Prefecture, Japan (40.6153°N, 140.3854°E), collected by A. Ohtaka, N. Kimura, and K. Tomikawa on 10 December 2020. **Paratypes:** two females (7.3 mm, NSMT-Cr 29004; 6.7 mm, NSMT-Cr 29005 [G1845]), two male (7.7 mm, NSMT-Cr 29006; 7.5 mm, NSMT-Cr 29007 [G1844]), data same as for the holotype; male (6.8 mm, NSMT-Cr 29008 [G1625]), same locality of the holotype, collected by A. Ohtaka on 23 December 2018; 3 males (7.3–7.6 mm, NSMT-Cr 29009) and three females (6.4–7.3 mm, NSMT-Cr 29009), same locality of the holotype, collected by A. Ohtaka on 17 June 2018; 3 males (5.8–8.0 mm, NSMT-Cr 29009) and three females (5.3–6.4 mm, NSMT-Cr 29009), same locality of the holotype, collected by N. Kimura on 23 December 2018; seven males (7.6–8.8 mm, NSMT-Cr 29009) and three females (5.6–6.6 mm, NSMT-Cr 29009), same locality of the holotype, collected by N. Kimura on 10 December 2020; 10 males (6.9–9.9 mm, NSMT-Cr 29009) and 11 females (5.9–8.3 mm, NSMT-Cr 29009), same locality of the holotype, collected by N. Kimura on 12 December 2020.

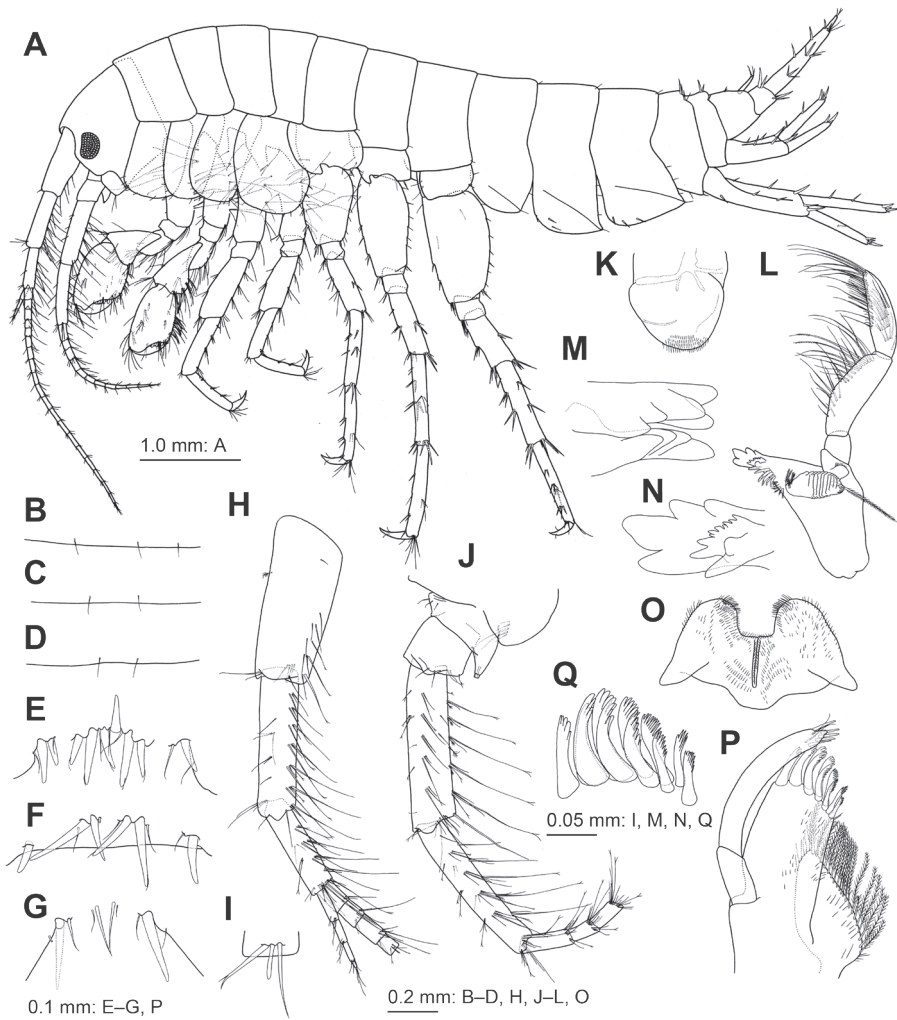


**Figure 3.** *Jesogammarus (Jesogammarus) acalceolus* sp. nov., male (7.4 mm), NSMT-Cr 29003 **A** habitus, lateral view **B–D** dorsal margins of pleonites 1–3, respectively, dorsal views **E–G** dorsal margins of urosomites 1–3, respectively, dorsal views **H** peduncular articles 1–3, accessory flagellum, and flagellar articles 1–4 of antenna 1, medial view **I** aesthetasc and associate setae on the flagellum of antenna 1, medial view **J** peduncular articles 1–5 and flagellar articles 1–3 of antenna 2, medial view **K** upper lip, posterior view **L** right mandible, medial view **M–N** incisor and lacinia mobilis of left and right mandibles, medial views **O** lower lip, ventral view **P** maxilla 1, medial view **Q** serrate robust setae on outer plate of maxilla 1, medial view.

**Diagnosis.** Dorsal surface of pereonites smooth. Pleonites 1–3 each with fewer than three dorsal setae. Antenna 1 without robust seta on posterodistal corner of peduncular article 1. Male antenna 2 without calceoli. Mandible with palp article 1 lacking setae. Uropod 3 without plumose setae on outer ramus.

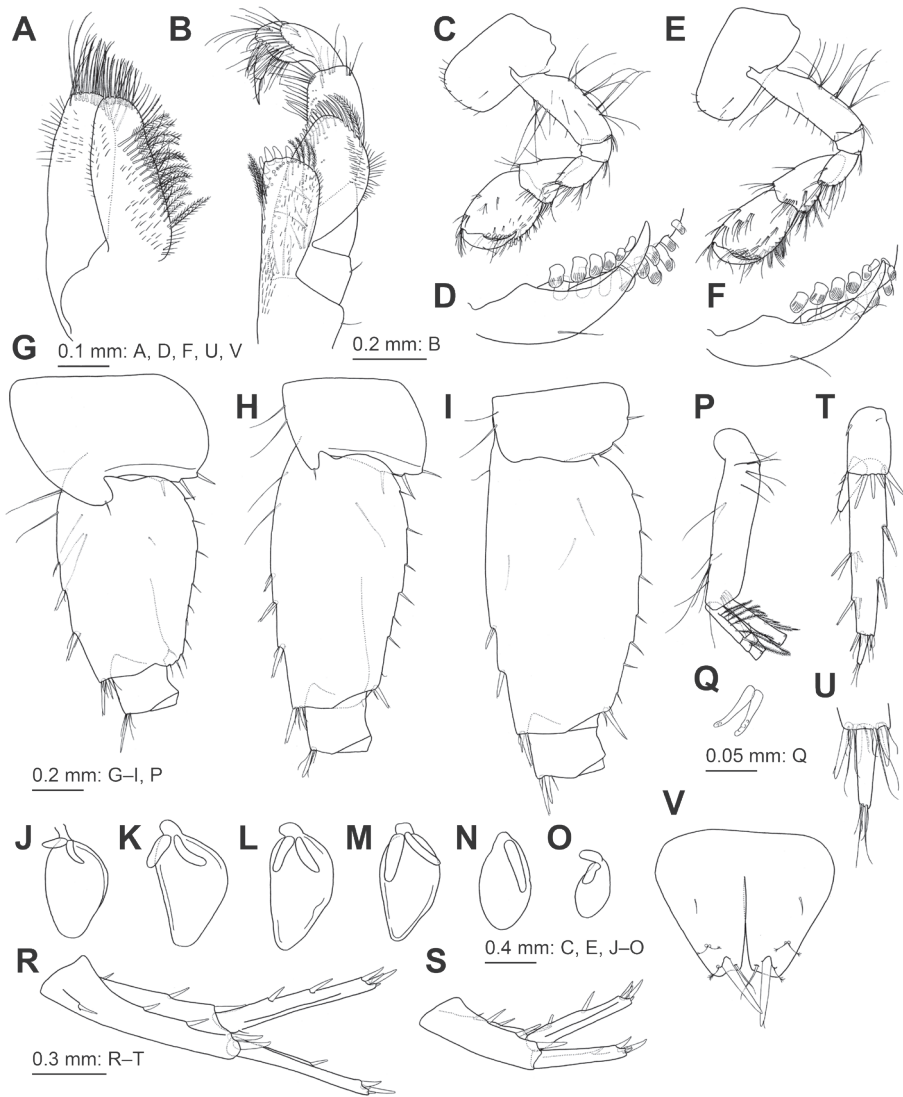


**Figure 4.** *Jesogammarus (Jesogammarus) acalceolus* sp. nov., male (7.4 mm), NSMT-Cr 29003 **A** maxilla 2, medial view **B** maxilliped, dorsal view **C** gnathopod 1, medial view **D** palmar margin of propodus and dactylus of gnathopod 1, medial view, some setae omitted **E** gnathopod 2, medial view **F** palmar margin of propodus and dactylus of gnathopod 2, medial view, some setae omitted **G–I** coxa-ischium of pereopods 5–7, respectively, lateral views **J–O** coxal gills on gnathopod 2–pereopod 7, respectively, lateral views **P** pleopod 1, lateral view, distal parts of rami omitted **Q** retinacula on peduncle of pleopod 1, lateral view **R–S** uropods 1–2, respectively, dorsal views **T** uropod 3, ventral view **U** distal part of proximal article and terminal article of outer ramus of uropod 3, ventral view **V** telson, dorsal view.

**Description. Male** [7.4 mm, NSMT-Cr 29003].

**Body.** Head (Fig. 3), rostrum short; lateral cephalic lobe with ventral margin weakly concave; antennal sinus rounded; eyes small, subreniform, major axis  $0.3 \times$  head height. Pereonites, dorsal surfaces smooth (Fig. 3). Pleonites 1–3 (Fig. 3B–D), dorsal margins each with three, two, and two setae. Epimeral plate 1 with rounded posterior margin bearing seta, seta on posteroventral corner (Fig. 3A); epimeral plate 2 with posterior margin almost straight bearing three setae, seta on weakly produced posteroventral corner, two and one robust setae on ventral margin and submargin, respectively (Fig. 3A); epimeral plate 3 with posterior margin almost straight bearing three setae, seta on quadrate posteroventral corner, three robust setae on ventral margin (Fig. 3A). Urosomite 1 (Fig. 3E) with dorsal margin bearing a pair of lateral robust setae and a middle cluster of robust setae; urosomite 2 (Fig. 3F) with dorsal margin bearing a pair of lateral robust setae and clusters of robust setae; urosomite 3 (Fig. 3G) with dorsal margin bearing a pair of robust setae.

**Antennae.** Antenna 1 (Fig. 3H)  $0.6 \times$  length of body; length ratio of peduncular articles 1–3 in  $1.0 : 0.9 : 0.6$ ; peduncular article 1 with posterodistal corner lacking robust seta, posterior margin with three pairs of setae and single seta; peduncular article 2 with posterior margin bearing six clusters of setae; peduncular article 3 with posterior margin bearing four clusters of setae; accessory flagellum comprising four articles; primary flagellum comprising 20 articulate, aesthetasc on each article. Antenna 2 (Fig. 3J)  $0.7 \times$  length of antenna 1; article 4 of peduncular  $1.1 \times$  article 5; peduncular articles 4 and 5 with posterior margins each bearing five setal clusters; flagellum comprising 12 articles, calceoli absent.

**Mouth parts.** Upper lip (Fig. 3K) with fine seta on rounded distal margin. Mandibles (Fig. 3L–N), left and right incisors comprising five and four teeth, respectively, left lacinia mobilis comprising four teeth, right lacinia mobilis bifid with many denticles; molar process triturative with plumose seta; left and right mandibles with seven and five blade-like setae on accessory setal rows, respectively; palp comprising 3 articles with length ratio of  $1.0 : 3.3 : 2.8$ ; article 1 of palp without setae; article 2 with 25 setae; article 3 bearing pair of setae on inner surface, three clusters of setae and single seta on outer surface. Lower lip (Fig. 3O), outer lobes broad, inner lobes indistinct. Maxilla 1 (Fig. 3P) with medial margin of inner plate bearing 20 plumose setae; eleven serrate robust setae on outer plate apically (Fig. 3Q); palp comprising 2 articles, article 1 marginally bare, apical margin of article 2 with five robust setae and two slender seta. Maxilla 2 (Fig. 4A) with inner plate bearing oblique inner row of 17 plumose setae. Maxilliped (Fig. 4B) with inner plate bearing three apical and two inner marginal robust setae; outer plate, apical margin with plumose setae and inner margin with robust setae; palp comprising four articles, inner margin and submargin of article 2 with rows of setae, article 3 bearing facial setae, slightly curved article 4 with slender nail.

**Gnathopods.** Gnathopod 1 (Fig. 4C, D) with coxa bearing marginal setae ventrally; basis with long setae on anterior and posterior margins; length of carpus  $1.4 \times$  width, with seta on anterior margin; length of propodus  $1.3 \times$  carpus and  $1.4 \times$  width, bearing two clusters of setae on anterior margin, propodus with oblique and weakly convex palmar margin bearing six medial and ten lateral peg-like robust

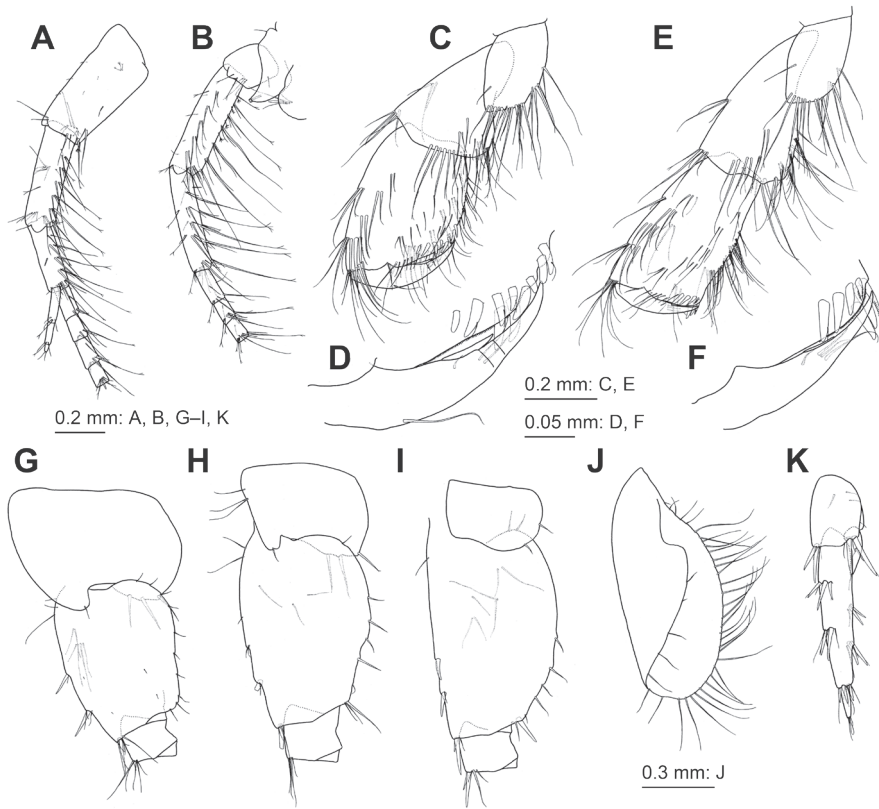


**Figure 5.** *Jesogammarus (Jesogammarus) acalceolus* sp. nov., female (7.3 mm), NSMT-Cr 29004 **A** peduncular articles 1–3, accessory flagellum, and flagellar articles 1–4 of antenna 1, medial view **B** peduncular articles 1–5 and flagellar articles 1–3 of antenna 2, medial view **C** ischium-dactylus of gnathopod 1, medial view **D** palmar margin of propodus and dactylus of gnathopod 1, medial view, some setae omitted **E** ischium-dactylus of gnathopod 2, medial view **F** palmar margin of propodus and dactylus of gnathopod 2, medial view, some setae omitted **G–I** coxa-ischium of pereopods 5–7, respectively, lateral views **J** brood plate on gnathopod 2, lateral view **K** uropod 3, ventral view.

setae; dactylus weakly curved, as long as palmar margin. Gnathopod 2 (Fig. 4E, F) with coxa bearing marginal setae ventrally; basis with anterior and posterior margins bearing long setae; length of carpus  $1.8 \times$  width, bearing setae on anterior margin; length of propodus  $1.1 \times$  carpus and  $1.6 \times$  width, respectively, with two clusters of setae on anterior margin, propodus with oblique and weakly convex anterior margin bearing eight medial and five lateral peg-like robust setae; dactylus weakly curved, as long as palmar margin.

**Pereopods.** Pereopods 3 and 4 (Fig. 3A) similar, coxa of pereopod 3 subrectangular with ventral setae; coxa of pereopod 4 expanded with posterior concavity, anterodistal corner and ventral margin with setae. Pereopod 5 (Figs 3A, 4G) with bilobed coxa bearing apical seta on anterior lobe, two robust setae on ventral margin of posterior lobe, posterodistal corner of posterior lobe rounded with robust

seta; basis with weakly expanded posterior margin bearing setae, posterodistal corner not lobate. Pereopod 6 (Figs 3A, 4H) with bilobed coxa bearing anteroproximal setae and apical seta on anterior lobe, two robust setae on ventral margin of posterior lobe, posterodistal corner of posterior lobe quadrate with robust seta; basis with weakly expanded posterior margin bearing setae, posterodistal corner not lobate. Pereopod 7 (Figs 3A, 4I) with weakly concave coxa in ventral margin bearing setae; basis with weakly expanded posterior margin bearing setae, posterodistal corner not lobate with robust and slender setae.

**Coxal gills** (Fig. 4J–O) with two accessory lobes on gills 2–5, posterior lobes longer than or equal to anterior ones, one accessory lobe on gills 6 and 7.

**Pleopods 1–3** (Fig. 4P) with peduncle bearing paired retinacula (Fig. 4Q) on inner margin; inner ramus with inner basal margin bearing bifid plumose setae.

**Uropods.** Uropod 1 (Fig. 4R) with peduncle bearing basofacial robust seta, two robust setae on inner and outer margins, one and two robust setae on inner and outer distal corners, respectively; length of inner ramus  $0.8 \times$  that of peduncle, inner margin of inner ramus with two robust setae; length of outer ramus  $0.9 \times$  that of inner ramus, inner margin of outer ramus with robust seta. Uropod 2 (Fig. 4S) with peduncle bearing two robust setae on inner and outer margins, respectively, and robust seta on inner and outer distal corners; length of inner ramus  $0.9 \times$  that of peduncle, inner margin of inner ramus with two robust seta; length of outer ramus  $0.8 \times$  that of inner ramus, inner margin of outer ramus with robust seta. Uropod 3 (Fig. 4T, U) with peduncle length  $0.3 \times$  that of outer ramus; length of inner ramus  $0.3 \times$  that of outer ramus, inner ramus with slender setae on inner margin and setae apically; outer ramus comprising two articles, proximal article with two clusters of setae on inner and outer margins, some of which robust, lacking plumose setae, length of terminal article  $0.2 \times$  that of proximal article, apical part of terminal article with simple setae.

**Telson** (Fig. 4V)  $0.8$  times as long as wide, cleft for 67% of length, with robust seta and slender setae on each lobe.

**Female** [7.3 mm, NSMT-Cr 29004].

**Antennae.** Antenna 1 (Fig. 5A), length ratio of peduncular articles 1–3 in  $1.0 : 0.8 : 0.6$ ; peduncular article 1 with pair of setae and single seta on posterior margin; peduncular article 2 with five clusters of setae on posterior margin; accessory flagellum comprising three articles; primary flagellum comprising 17 articles. Antenna 2 (Fig. 5B) with peduncular article 4 bearing six clusters or single setae on posterior margin; peduncular article 5 with five clusters or single setae on posterior margin; flagellum comprising eleven articles, lacking calceoli.

**Gnathopods.** Gnathopod 1 (Fig. 5C, D) with carpus bearing cluster of setae on anterior margin; length of propodus  $1.2 \times$  that of carpus and  $1.5 \times$  width; propodus with eight medial and two lateral robust setae on palmar margin. Gnathopod 2 (Fig. 5E, F) with carpus bearing cluster of setae on anterior margin; propodus and carpus approximately the same length, propodus with three medial and two lateral robust setae and one medial and one lateral pectinate robust setae on palmar margin.

**Pereopods 5–7** with more expanded posterior margin of bases than those of male (Fig. 5G–I).

**Brood plates** (= oostegites) (Fig. 5J) wide, with numerous setae on its margins.

**Uropod 3** (Fig. 5K), length of peduncle  $0.4 \times$  that of outer ramus; length of inner ramus  $0.2 \times$  that of outer ramus.

**Variations.** Although almost all specimens have a pleonite 1 with a pair of setae on the dorsal margin, a few specimens have three setae. Some specimens have a urosomite 1 with a pair of lateral robust setae and a pair of clusters of robust setae on its dorsal margin. The numbers of setal clusters on the posterior margins of the peduncular articles 1–3 of antenna 1 ranged from two to four, six or seven, and two to four, respectively. The number of setal clusters on the posterior margins of the peduncular articles 4 and 5 ranged from five or six and four or five, respectively. Some specimens have robust setae on the outer margin of the outer ramus of uropod 1 and lack robust setae on the inner margin of the outer ramus of uropod 2. Some specimens have a telson with 2 robust setae on each lobe. The number of eggs is up to 9.

**Etymology.** The new specific name derived from the absence of calceolus.

**Remarks.** *Jesogammarus (J.) acalceolus* sp. nov. differs from its congeners by lacking a calceolus on the flagellum of antenna 2 in male. This new species is similar to *J. (J.) bousfieldi* Tomikawa, Hanzawa & Nakano, 2017 and *J. (J.) paucisetulosus* Morino, 1984 in having the following features: eyes are small; antenna 1 lacks robust setae on the posterodistal corner of the peduncular article 1; antennae 1 and 2 have many long setae on the posterior margins of the peduncular articles; maxilla 1 lacks setae on the outer margin of the palp article 2; and gnathopods 1 and 2 have few setae on the ventral margins of the coxae in female. In addition to the absence of a calceolus, *J. (J.) acalceolus* sp. nov. is distinguished from *J. (J.) bousfieldi* by the pleonites 1–3 each with less than three setae on the dorsal margins (vs. more than four setae in *J. (J.) bousfieldi*).

**Assessment of conservation status.** *Jesogammarus (J.) acalceolus* sp. nov. was found in a spring located 120 m above sea level, on the slope of the volcanic Mt. Iwaki, Aomori Prefecture, Japan. Although we conducted an intensive survey of inland waters at more than 400 sites in the Aomori Prefecture, this new species was present only in this one spring described above and not found in any others (unpublished data). In most of the freshwater habitats that were investigated, *J. (J.) jesoensis* Schellenberg, 1937, which is distributed in Hokkaido and northern Honshu, was present. Because *J. (J.) acalceolus* sp. nov. and *J. (J.) jesoensis* are not closely related (Fig. 2), it is expected that the current distributions of both species are a result of different evolutionary processes. As a positive aspect, the type locality of *J. (J.) acalceolus* sp. nov. is in the precincts of the Iwaki Haguro Shrine, built in AD 807, as a result of which this type locality has been treated with care by locals for more than 1,000 years (Sasaki 1995). Therefore, the environment of this spring has been preserved in good condition, allowing the present *J. (J.) acalceolus* sp. nov. population to survive. At present, this spring has an abundance of water ( $60 \text{ m}^3/\text{day}$ ) (Yamamoto 1994), and its environment is stable. However, amphipods are known to be highly sensitive to chemicals, such as pesticides (Schulz 2003; Nyman et al 2013). This species inhabits only a few meters of a spring brooklet surrounded by apple plantations. Therefore, the deterioration of its habitat due to an inflow of agricultural chemicals into spring water may lead to its extinction.

Key to species of *Jesogammarus* based on Tomikawa et al. (2017)

- 1 Accessory lobes of coxal gills on gnathopod 2 and pereopods 3–5 well developed, both anterior and posterior lobes subequal in length or posterior lobe longer than anterior one; palmar margin of propodus of female gnathopod 2 with pectinate setae..... **2 (subgenus *Jesogammarus*)**
- Accessory lobes of coxal gills on gnathopod 2 and pereopods 3–5 weakly developed, anterior and posterior lobes unequal in length, often posterior lobe rudimentary; palmar margin of propodus of female gnathopod 2 without pectinate setae..... **13 (subgenus *Annanogammarus*)**
- 2 Article 1 of mandibular palp with setae..... **3**
- Article 1 of mandibular palp without setae..... **6**
- 3 Dorsal margin of pleonites 1–3 each with 1–2 setae; eye large; article 1 of mandibular palp with 1 robust seta; female pereopods densely setose.....  
..... ***J. hinumensis* Morino, 1993**
- Dorsal margin of pleonites 1–3 each with more than 4 setae; eye small to medium; article 1 of mandibular palp with 2 or 3 robust setae; female pereopods not densely setose ..... **4**
- 4 Peduncular article 1 of antenna 1 with robust seta on posterodistal corner....  
..... ***J. spinopalpus* Morino, 1985**
- Peduncular article 1 of antenna 1 with slender seta on posterodistal corner ..... **5**
- 5 Inner ramus of uropod 3 length  $1/4 \times$  outer ramus; inner margin of outer ramus of uropod 3 with 4–6 plumose setae..... ***J. fontanus* Hou & Li, 2004**
- Inner ramus of uropod 3 length  $1/3 \times$  outer ramus; inner margin of outer ramus of uropod 3 with ca. 10 plumose setae.....  
..... ***J. hebeiensis* Hou & Li, 2004**
- 6 Male antenna 2 without calceoli ..... ***J. acalceolus* sp. nov.**
- Male antenna 2 with calceoli..... **7**
- 7 Dorsal margin of pereonites 1–3 each with 2 long setae .....  
..... ***J. mikadoi* Tomikawa, Morino & Mawatari, 2003**
- Dorsal margin of pereonites 1–3 without setae ..... **8**
- 8 Posterodistal corner of peduncular article 1 of antenna 1 without robust seta; posterior margin of peduncular article 2 of antenna 1 with more than 5 setae and/or setal bundles; outer margin of palp article 2 of maxilla 1 without setae..... **9**
- Posterodistal corner of peduncular article 1 of antenna 1 with robust seta (occasionally lacking); posterior margin of peduncular article 2 of antenna 1 with less than 4 setae and/or setal bundles; outer margin of palp article 2 of maxilla 1 with setae..... **10**
- 9 Dorsal margins of pleonites 1–3 each with more than 4 setae .....  
..... ***J. bousfieldi* Tomikawa, Nakano & Hanzawa, 2017**
- Dorsal margins of pleonites 1–3 each with 0–3 setae .....  
..... ***J. paucisetulosus* Morino, 1984**

- 10 Accessory lobes of coxal gills on gnathopod 2 and pereopods 3–5 short and straight ..... ***J. uchiyamaryui* Tomikawa, Nakano & Hanzawa, 2017**
- Accessory lobes of coxal gills on gnathopod 2 and pereopods 3–5 long and curved..... **11**
- 11 Dorsal margins of pleonites 1–3 each with 2 or 3 setae; posterior margin of peduncular article 2 of antenna 1 with 3 or 4 setae and/or setal bundles.....  
..... ***J. ikiensis* Tomikawa, 2015**
- Dorsal margins of pleonites 1–3 each with more than 7 setae; posterior margin of peduncular article 2 of antenna 1 with 2 setae and/or setal bundles..... **12**
- 12 Palmar margin of propodus of male gnathopod 2 without pectinate setae.....  
..... ***J. jesoensis* complex** [see Tomikawa et al. (2016)]
- Palmar margin of propodus of male gnathopod 2 with pectinate setae.....  
..... ***J. ilhoii* Lee & Seo, 1992**
- 13 Dorsal margin of pleonite 3 with robust setae; posterior margin of peduncular articles 4 and 5 each with more than 5 long-setal bundles.....  
..... ***J. naritai* Morino, 1985**
- Dorsal margin of pleonite 3 without robust setae; posterior margin of peduncular articles 4 and 5 each with less than 3 short-setal bundles..... **14**
- 14 Posterodistal corner of bases of pereopods 5–7 with long setae.....  
..... ***J. annandalei* (Tattersal, 1922)**
- Posterodistal corner of bases of pereopods 5–7 without short setae ..... **15**
- 15 Dorsal margins of pleonites 1–3 each with 2–4 setae .....  
..... ***J. fluvialis* Morino, 1985**
- Dorsal margins of pleonites 1–3 each with more than 10 setae ..... **16**
- 16 Posterodistal corner of peduncular article 1 of antenna 1 with robust seta; palmar margin of propodus of female gnathopod 2 with simple setae only ...  
..... ***J. koreaensis* Lee & Seo, 1990**
- Posterodistal corner of peduncular article 1 of antenna 1 without robust seta; palmar margin of propodus of female gnathopod 2 with weakly pectinate setae..... ***J. debilis* Hou & Li, 2005**

## Discussion

Among freshwater habitats, springs have an especially high risk of extinction of species (Fluker et al. 2010). The highly diverse genus *Jesogammarus*, which is found in spring water habitats of the Japanese Archipelago, has a sensory organ termed the calceolus on male antenna 2. We described a new endangered freshwater amphipod species, *Jesogammarus (Jesogammarus) acalceolus* sp. nov., found in a spring in Aomori Prefecture, Japan, which is potentially the sole remaining habitat of this species.

Although the calceolus is thought to be a sensory organ, its function and evolution are not well understood (Lincoln and Hurley 1981; Godfrey et al. 1988; Read and Williams 1990; Dunn 1998). Therefore, the discovery of *J. (J.) acalceolus* sp. nov.,

which lacks calceoli, provides important clues regarding the function and evolution of calceoli. An ancestral reconstruction of calceoli via the molecular phylogenetic tree generated during this study revealed that the common ancestor of *Jesogammarus* possessed calceoli, which were secondarily lost in *J. (J.) acalceolus* sp. nov. (Fig. 2). Since *Jesogammarus* carried calceoli only on the flagellum of antenna 2 of males, it is considered that calceoli have a reproductive function (Bousfield and Shih 1994). Females of amphipods lay eggs just after moulting when the exoskeleton is soft. Therefore, some species display a reproductive behaviour termed “precopula”, in which a male holds and guards a female for a couple of days till the female’s moulting and subsequent laying eggs. Dunn (1998) reported that calceoli can be used to evaluate the moulting interval of females to find suitable females for mate guarding. In this study, *J. (J.) acalceolus* sp. nov., the males of which lack calceoli, was also found to practice precopulatory guarding, which suggested that calceoli are not always necessary for precopulatory guarding in *J. (J.) acalceolus* sp. nov.

The calceolus is a typically club- or paddle-shaped structure found on the antennae of amphipods (Schmitz 1992). Although structures similar to the calceolus are also found in the antennal articles of Anaspidacea and Mysida, these are not considered to be homologous to amphipod calceoli (Bousfield and Shih 1994). Calceoli are used mainly as a taxonomic character in the higher taxa of amphipods (Lincoln and Hurley 1981; Holsinger 1992; Bousfield and Shih 1994). In Anisogammaridae, the presence or absence of calceoli is used as a genus-level taxonomic feature (Bousfield 1979). However, the molecular phylogenetic tree generated in this study confirmed that the non-calceolate species, *J. (J.) acalceolus* sp. nov., is nested in *Jesogammarus*, and not in *Anisogammarus*, *Ramellogammarus* or *Spasskogammarus*, the other Anisogammaridae with non-calceolate species (Fig. 2). These results indicated that the calceolus should no longer be used as a diagnostic feature of *Jesogammarus* and the genus needs to be redefined. Therefore, in this study, we have amended the diagnosis of *Jesogammarus*. In *Gammarus*, the seasonal variation of the presence or absence of calceoli was known (Karaman and Pinkster 1977), but *J. (J.) acalceolus* sp. nov., lacks calceoli year-round, suggesting that male antenna 2 lacking calceoli is a stable taxonomic feature.

Freshwater amphipods have low dispersal ability, and there thus exists a high tendency for endemic species to be distributed throughout each region (Tomikawa 2017). In addition, our taxonomic studies revealed a considerable presence of *Jesogammarus* fauna in the Japanese Archipelago (Tomikawa and Morino 2003; Tomikawa et al. 2003, 2017; Tomikawa 2015). For these reasons, it is unlikely that *J. (J.) acalceolus* sp. nov. will be found outside type localities, thereby limiting the current habitat of this species to a great extent. In the past, there have been many cold springs in Hirosaki with the type locality of this new species. However, recent, rapid urbanization has led to a depletion of such springs (Sasaki 1995). Besides, the habitat of this species may have been lost due to the disappearance of springs and/or environmental pollution caused by the use of agrochemicals, both of which were associated with apple plantations that flourished in this region. Thus, to conserve what is possibly the only remaining population of *J. (J.) acalceolus* sp. nov., it will be necessary to conduct further investigations into

risk factors and develop a conservation plan with the cooperation of local communities and policymakers. In conclusion, our results indicate that this new species, which is key to clarifying the evolution of the calceolus, is of high conservation significance.

## Acknowledgements

We greatly appreciate Dr. Akifumi Ohtaka for his support in field surveys and his continuous support of this study. We thank Dr. Chi-Woo Lee for providing materials of *J. (A.) koreaensis* and Ryu Uchiyama for providing photographs of specimens of the new species. This work was partly supported by the Japan Society for the Promotion of Science KAKENHI grants JP17K15174 and JP17H00820 to KT.

## References

- Balian EV, Segers H, Levéque C, Martens K (2008) The freshwater animal diversity assessment: an overview of the results. *Hydrobiologia* 595: 627–637. <https://doi.org/10.1007/s10750-007-9246-3>
- Bousfield EL (1979) The amphipod superfamily Gammaroidea in the northeastern Pacific region: systematics and distributional ecology. *Bulletin of the Biological Society of Washington* 3: 297–357.
- Bousfield EL (1981) Evolution in North Pacific coastal marine amphipod crustaceans In: Reveal JL, Scudder GGE (Eds) *Evolution today*, Proceedings of the Second International Congress of Systematic and Evolutionary Biology. Hunt Institute for Botanical Documentation, 68–89.
- Bousfield EL, Morino H (1992) The amphipod genus *Ramellogammarus* in fresh waters of western North America: systematics and distributional ecology. *Contributions to Natural Science, British Columbia Museum* 17: 1–21.
- Bousfield EL, Shih C (1994) The phylogenetic classification of amphipod crustaceans: problems in resolution. *Amphipacifica* 1: 76–134.
- Coleman CO (2015) Taxonomy in times of the taxonomic impediment – examples from the community of experts on amphipod crustaceans. *Journal of Crustacean Biology* 35: 729–740. <https://doi.org/10.1163/1937240X-00002381>
- Collen B, Loh J, Whitmee S, McRae L, Amin R, Baillie JEM (2009) Monitoring change in vertebrate abundance: the Living Planet Index. *Conservation Biology* 23: 317–327. <https://doi.org/10.1111/j.1523-1739.2008.01117.x>
- Collen B, Whitton F, Dyer EE, Baillie JEM, Cumberlidge N, Darwall WRT, Pollock C, Richman NI, Soulsby A, Böhm M (2014) Global patterns of freshwater species diversity, threat and endemism. *Global Ecology and Biogeography* 23: 40–51. <https://doi.org/10.1111/geb.12096>
- Costello MJ, Vanhoorne B, Appeltans W (2015) Conservation of biodiversity through taxonomy, data publication, and collaborative infrastructures. *Conservation Biology* 29: 1094–1099. <https://doi.org/10.1111/cobi.12496>

- Dudgeon D, Arthington AH, Gessner MO, Kawabata Z, Knowler DJ, Lévêque C, Naiman RJ, Prieur-Richard A, Soto D, Stiassny MLJ, Sullivan CA (2006) Freshwater biodiversity: importance, threats, status and conservation challenges. *Biological reviews of the Cambridge Philosophical Society* 81: 163–182. <https://doi.org/10.1017/S1464793105006950>
- Dunn AM (1998) The role of calceoli in mate assessment and precopula guarding in *Gammarus*. *Animal Behaviour* 56: 1471–1475. <https://doi.org/10.1006/anbe.1998.0916>
- Felsenstein J (1985) Confidence limits on phylogenies: an approach using the bootstrap. *Evolution* 39: 783–791. <https://doi.org/10.2307/2408678>
- Fluker BL, Kuhajda BR, Lang NJ, Harris PM (2010) Low genetic diversity and small long-term population sizes in the spring endemic watercress darter, *Etheostoma nuchale*. *Conservation Genetics* 11: 2267–2279. <https://doi.org/10.1007/s10592-010-0111-y>
- Giam X, Scheffers BR, Sodhi NS, Wilcove DS, Ceballos G, Ehrlich PR (2012) Reservoirs of richness: least disturbed tropical forests are centres of undescribed species diversity. *Proceedings of the Royal Society B* 279: 67–76. <https://doi.org/10.1098/rspb.2011.0433>
- Godfrey RB, Holsinger JR, Carson KA (1988) Comparison of the morphology of calceoli in the fresh water amphipods *Crangonyx richmondensis* sens. lat. (Crangonyctidae) and *Gammarus minus* (Gammaridae). *Crustaceana Supplement* 13: 115–121.
- Holsinger JR (1992) Sternophysingidae, a new family of subterranean amphipods (Gammaridea: Crangonyctoidea) from South Africa, with description of *Sternophysinx calceoli*, new species, and comments on phylogenetic and biogeographic relationships. *Journal of Crustacean Biology* 12: 111–124. <https://doi.org/10.2307/1548726>
- Horton, T, Lowry J, De Broyer C, et al. (2021) World Amphipoda Database. <http://www.marinespecies.org/amphipoda>
- Karaman GS, Pinkster S (1977) Freshwater Gammarus species from Europe, North Africa and adjacent regions of Asia (Crustacea–Amphipoda) Part 1. *Gammarus pulex*-group and related species. *Bijdragen tot de Dierkunde* 47: 1–97. <https://doi.org/10.1163/26660644-04701001>
- Kumar S, Stecher G, Li M, Knyaz C, Tamura K (2018) MEGA X: Molecular Evolutionary Genetics Analysis across computing platforms. *Molecular Biology and Evolution* 35: 1547–1549. <https://doi.org/10.1093/molbev/msy096>
- Lehner B, Döll P (2004) Development and validation of a global database of lakes, reservoirs and wetlands. *Journal of Hydrology* 296: 1–22. <https://doi.org/10.1016/j.jhydrol.2004.03.028>
- Li Y, Li S, Liu H, Kurenschikov DK, Hou Z (2020) Eocene-Oligocene sea-level fall drove amphipod habitat shift from marine to freshwater in the Far East. *Zoologica Scripta* 49: 357–365. <https://doi.org/10.1111/zsc.12409>
- Lincoln RJ, Hurley DE (1981) The calceolus, a sensory structure of gammaridean amphipods (Amphipoda: Gammaridea). *Bulletin of the British Museum, Natural history, Zoology* 40: 103–116.
- Macdonald III KS, Yampolsky L, Duffy JE (2005) Molecular and morphological evolution of the amphipod radiation of Lake Baikal. *Molecular Phylogenetics and Evolution* 35: 323–343. <https://doi.org/10.1016/j.ympev.2005.01.013>

- Maddison WP, Maddison DR (2019) Mesquite: a modular system for evolutionary analysis. Version 3.61. <http://www.mesquiteproject.org>
- Martínuzzi S, Januchowski-Hartley SR, Pracheil BM, McIntyre PB, Plantinga AJ, Lewis DJ, Radeloff VC (2014) Threats and opportunities for freshwater conservation under future land use change scenarios in the United States. *Global Change Biology* 20: 113–124. <https://doi.org/10.1111/gcb.12383>
- McKinney M (1999) High rates of extinction and threat in poorly studied taxa. *Conservation Biology* 13: 1273–1281.
- Mora C, Tittensor DP, Adl S, Simpson AGB, Worm B (2011) How many species are there on earth and in the ocean? *PLoS Biology* 9: e1001127. <https://doi.org/10.1371/journal.pbio.1001127>
- Morino H (1985) Revisional studies on *Jesogammarus-Annanogammarus* (Gammaroidea: Amphipoda) from central Japan. *Publications of Itako Hydrobiological Station* 2: 9–55.
- Murphy NP, Adams M, Austin AD (2009) Independent colonization and extensive cryptic speciation of freshwater amphipods in the isolated groundwater springs of Australia's Great Artesian Basin. *Molecular Ecology* 18: 109–122. <https://doi.org/10.1111/j.1365-294X.2008.04007.x>
- Nyman A, Hintermeister H, Schirmer K, Ashauer R (2013) The insecticide imidacloprid causes mortality of the freshwater amphipod *Gammarus pulex* by interfering with feeding behavior. *PLoS ONE* 8: e62472. <https://doi.org/10.1371/journal.pone.0062472>
- Palumbi SR (1996) Nucleic acids II: The polymerase chain reaction. In: Hillis DM, Moritz C, Mable BK (Eds) *Molecular Systematics*. Second Edition. Sinauer Associates, Inc., 205–247.
- Rambaut A, Teslenko M, van der Mark P, Ayres DL, Darling A, Höhna S, Larget B, Liu L, Suchard MA, Huelsenbeck JP (2018) Posterior Summarization in Bayesian Phylogenetics Using Tracer 1.7. *Systematic Biology* 67: 901–904. <https://doi.org/10.1093/sysbio/sys029>
- Read AT, Williams DD (1990) The role of the calceoli in precopulatory behaviour and mate recognition of *Gammarus pseudolimnaeus* Bousfield (Crustacea, Amphipoda). *Journal of Natural History* 24: 351–359. <https://doi.org/10.1080/00222939000770261>
- Reid AJ, Carlson AK, Creed IF, Eliason EJ, Gell PA, Johnson PTJ, Kidd KA, MacCormack TJ, Olden J, Ormerod SJ, Smol JP, Taylor WW, Tockner K, Vermaire JC, Dudgeon D, Cooke SJ (2019) Emerging threats and persistent conservation challenges for freshwater biodiversity. *Biological reviews of the Cambridge Philosophical Society* 94: 849–873. <https://doi.org/10.1111/brv.12480>
- Ronquist F, Teslenko M, van der Mark P, Ayres DL, Darling A, Höhna S, Larget B, Liu L, Suchard MA, Huelsenbeck JP (2012) MRBAYES 3.2: efficient Bayesian phylogenetic inference and model selection across a large model space. *Systematic Biology* 61: 539–542. <https://doi.org/10.1093/sysbio/sys029>
- Sasaki S (1995) Visit to valuable water springs (31) Valuable water springs in Aomori Prefecture. *Journal of Groundwater Hydrology* 37: 317–328. <https://doi.org/10.5917/jagh1987.37.317>

- Schmitz EH (1992) Chapter 10: Amphipoda In: Harrison FW, Humes AG (Eds) *Microscopic Anatomy of Invertebrates*, volume 9 Crustacea. Wiley-Liss, New York, 443–528.
- Schulz R (2003) Using a freshwater amphipod in situ bioassay as a sensitive tool to detect pesticide effects in the field. *Environmental Toxicology and Chemistry* 22: 1172–1176. <https://doi.org/10.1002/etc.5620220529>
- Stork NF (1993) How many species are there? *Biological Conservation* 2: 215–232. <https://doi.org/10.1007/BF00056669>
- Tomikawa K, Morino H (2003) Two new freshwater species of the genus *Jesogammarus* (Crustacea: Amphipoda: Anisogammaridae) from northern Japan. *Zoological Science* 20: 229–241. <https://doi.org/10.2108/zsj.20.229>
- Tomikawa K (2015) A new species of *Jesogammarus* from the Iki Island, Japan (Crustacea, Amphipoda, Anisogammaridae). *ZooKeys* 530: 15–36. <https://doi.org/10.3897/zookeys.530.6063>
- Tomikawa K (2017) Species Diversity and Phylogeny of Freshwater and Terrestrial Gammaridean Amphipods (Crustacea) in Japan. In: Motokawa M, Kajihara H (Eds) *Species Diversity of Animals in Japan*. Springer, 249–266. [https://doi.org/10.1007/978-4-431-56432-4\\_9](https://doi.org/10.1007/978-4-431-56432-4_9)
- Tomikawa K, Kobayashi N, Mawatari SF (2010) Phylogenetic relationships of superfamily Gammaroidea (Amphipoda) and its allies from Japan. *Crustacean Research* 39: 1–10. [https://doi.org/10.18353/crustacea.39.0\\_1](https://doi.org/10.18353/crustacea.39.0_1)
- Tomikawa K, Kobayashi N, Morino H (2016) Reassessing the taxonomic subdivision of the *Jesogammarus jesoensis* complex (Crustacea: Amphipoda: Anisogammaridae) in northern and central Japan. *Species Diversity* 21: 55–64. <https://doi.org/10.12782/sd.21.1.055>
- Tomikawa K, Morino H, Mawatari SF (2003) A new freshwater species of the genus *Jesogammarus* (Crustacea: Amphipoda: Anisogammaridae) from northern Japan. *Zoological Science* 20: 925–933. <https://doi.org/10.2108/zsj.20.925>
- Tomikawa K, Nakano T, Hanzawa N (2017) Two new species of *Jesogammarus* from Japan (Crustacea, Amphipoda, Anisogammaridae), with comments on the validity of the subgenera *Jesogammarus* and *Annanogammarus*. *Zoosystematics and Evolution* 93: 189–210. <https://doi.org/10.3897/zse.93.12125>
- Tomikawa K, Tashiro S, Kobayashi N (2012) First record of *Gammarus koreanus* (Crustacea, Amphipoda, Gammaroidea) from Japan, based on morphology and 28S rRNA gene sequences. *Species Diversity* 17: 39–48. <https://doi.org/10.12782/sd.17.1.039>
- Tomikawa K, Kobayashi N, Kyono M, Ishimaru S, Grygier MJ (2014) Description of a new species of *Sternomoera* (Crustacea: Amphipoda: Pontogeneiidae) from Japan, with an analysis of the phylogenetic relationships among the Japanese species based on the 28S rRNA gene. *Zoological Science* 31: 475–490. <https://doi.org/10.2108/zs140026>
- Väinölä R, Witt JDS, Grabowski M, Bradbury JH, Jazdzewski K, Sket B (2008) Global diversity of amphipods (Amphipoda; Crustacea) in freshwater. *Hydrobiologia* 595: 241–255. <https://doi.org/10.1007/s10750-007-9020-6>
- Yamamoto S (1994) Volcano slope springs on Mt. Iwaki. *Tokyo Seitoku College Bulletin* 27: 165–170.

# A new species of the genus *Rana sensu lato* Linnaeus, 1758 (Anura, Ranidae) from Wuyi Mountain, Fujian Province, China

Yanqing Wu<sup>1\*</sup>, Shengchao Shi<sup>2\*</sup>, Huiguang Zhang<sup>3</sup>, Weicai Chen<sup>4</sup>,  
Bin Cai<sup>3</sup>, Van Chung Hoang<sup>2,5</sup>, Jun Wu<sup>1</sup>, Bin Wang<sup>2</sup>

**1** Nanjing Institute of Environmental Sciences, Ministry of Ecology and Environment of China, Nanjing 210042, China **2** Chengdu Institute of Biology, Chinese Academy of Sciences, Chengdu 610041, China **3** Research and Monitoring Center, Wuyishan National Park, Wuyishan 354300, China **4** Key Laboratory of Beibu Gulf Environment Change and Resources Utilization of Ministry of Education, Nanning Normal University, Nanning 530001, China **5** Forest Resources and Environment Center, 300 Ngoc Hoi Road, Thanh Tri, Hanoi, Vietnam

Corresponding authors: Jun Wu ([wujun@nies.org](mailto:wujun@nies.org)); Bin Wang ([wangbin@cib.ac.cn](mailto:wangbin@cib.ac.cn))

Academic editor: Annemarie Ohler | Received 6 April 2021 | Accepted 1 September 2021 | Published 26 October 2021

<http://zoobank.org/B991C304-8F01-406E-BB39-ED1993601125>

**Citation:** Wu Y, Shi S, Zhang H, Chen W, Cai B, Hoang VC, Wu J, Wang B (2021) A new species of the genus *Rana sensu lato* Linnaeus, 1758 (Anura, Ranidae) from Wuyi Mountain, Fujian Province, China. ZooKeys 1065: 101–124. <https://doi.org/10.3897/zookeys.1065.67005>

## Abstract

A new species of the frog genus *Rana sensu lato* from Wuyi Mountain, Fujian Province, China is described. Molecular phylogenetic analyses clustered the new species into the *R. johnsi* group and indicated that it was genetically divergent from its closely related species. The new species could be distinguished from its congeners by a combination of the following characters: body size medium, SVL 41.4–45.6 mm ( $42.9 \pm 1.9$  mm,  $n = 4$ ) in adult males and 47.6–50.3 mm ( $n = 2$ ) in adult females; adult male with a pair of internal subgular vocal sacs; lateroventral grooves present on tip of toes; webbing on fourth toes reaching the tip of toe; transverse skin ridges distinctly present on the dorsal surface of thigh and tibia, the number large (mean  $26.5 \pm 2.7$ , range 22–29,  $n = 6$ ); breeding males possess creamy white nuptial pad with tiny velvety spines on the dorsal surface of the first finger, divided into three parts.

## Keywords

Molecular phylogenetic analyses, morphology, *Rana*, taxonomy

\* These authors have contributed equally to this work.

## Introduction

The brown frog genus *Rana* sensu lato Linnaeus, 1758 (Anura, Ranidae Batsch, 1796) is broadly distributed across Eurasia, Indochina, and North America (Frost 2021). The taxonomic arrangements in the group have been controversial for a long time (e.g., Fei et al. 1990; Dubois 1992; Fei et al. 2005, 2009, 2010, 2012; Frost et al. 2006; Che et al. 2007; Pyron and Wiens 2011; Jiang et al. 2020; Wang et al. 2020). A recent phylogenetic framework (Yuan et al. 2016) indicated that *Rana* sensu lato contained nine clades corresponding to eight subgenera and one unresolved species, i.e., *Rana*, *Amerana* Dubois, 1992, *Liuhurana* Fei, Ye, Jiang, Dubois & Ohler, 2010, *Aquarana* Dubois, 1992, *Lithobates* Fitzinger, 1843, *Zweifelia* Dubois, 1992, *Pantherana* Dubois, 1992, *Pseudorana* Fei, Ye & Huang, 1990, and *R. sylvatica* LeConte, 1825. Dubois et al. (2021) upgraded these subgenera to genera (except that the members of *Zweifelia* were placed in *Lithobates*) within *Ranites* Batsch, 1796, and established the new genus *Boreorana* Dubois, Ohler & Pyron, 2021 based on the type species *Rana sylvatica*. In the genus *Rana* sensu lato, 26 species have been recorded in China (Jiang et al. 2020; Wang et al. 2020; Frost 2021), which are *R. amurensis* Boulenger, 1886, *R. arvalis* Nilsson, 1842, *R. asiatica* Bedriaga, 1898, *R. chaochiaoensis* Liu, 1946, *R. chensinensis* David, 1875, *R. chevronta* Hu & Ye, 1978, *R. coreana* Okada, 1928, *R. culaiensis* Li, Lu, & Li, 2008, *R. dabieshanensis* Wang, Qian, Zhang, Guo, Pan, Wu, Wang, & Zhang, 2017, *R. dybowskii* Günther, 1876, *R. hanluica* Shen, Jiang, & Yang, 2007, *R. huanrenensis* Fei, Ye, & Huang, 1990, *R. jiemuxiensis* Yan, Jiang, Chen, Fang, Jin, Li, Wang, Murphy, Che, & Zhang, 2011, *R. jiulingensis* Wan, Lyu, & Wang, 2020, *R. johnsi* Smith, 1921, *R. kukunoris* Nikolskii, 1918, *R. longicrus* Stejneger, 1898, *R. luanchuanensis* Zhao & Yuan, 2017, *R. maoershanensis* Lu, Li, & Jiang, 2007, *R. omeimontis* Ye & Fei, 1993, *R. sangzhiensis* Shen, 1986, *R. sauteri* Boulenger, 1909, *R. shuchinae* Liu, 1950, *R. weiningensis* Liu, Hu, & Yang, 1962, *R. zhengi* Zhao, 1999, and *R. zhenhaiensis* Ye, Fei, & Matsui, 1995. Recent research on this genus discovered several new species from China (Yan et al. 2011; Yuan et al. 2016; Wang et al. 2017; Yang et al. 2017; Zhao et al. 2017), indicating that the diversity of the genus is probably underestimated.

Recently, in Wuyishan National Park, Wuyishan City, Fujian Province, China, we collected several specimens which can be assigned to *Rana* sensu lato based on morphology. Molecular phylogenetic analyses and detailed morphological comparisons indicated the specimens represented an undescribed species of the *R. johnsi* group. Herein we described it as a new species.

## Materials and methods

### Specimens

Twelve unnamed specimens including four adult males, two adult females, and six tadpoles were collected from Wuyishan National Park, Fujian Province, China (Table 1, Fig. 1, Suppl. material 1). For comparisons, 39 specimens of the subgenus *Rana* were

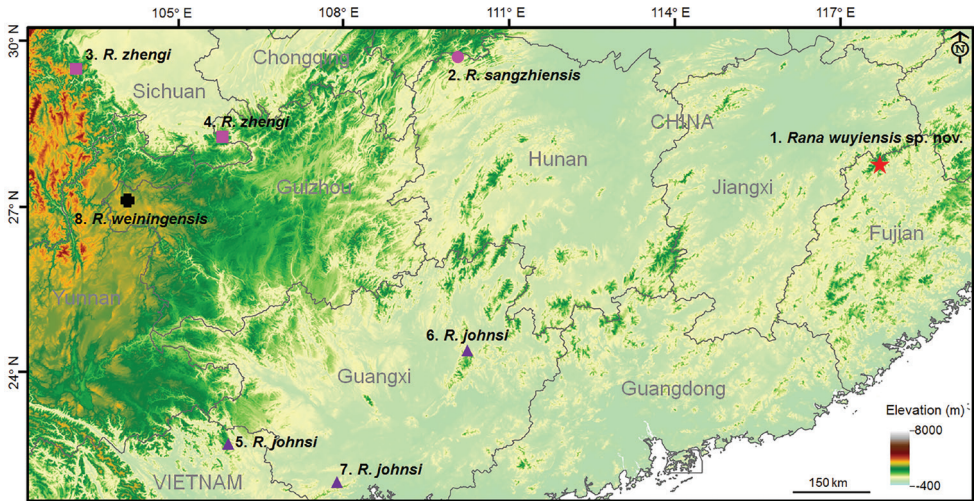


**Figure 1.** Locations for specimens used in this study. **1.** the type locality of *Rana wuyiensis* sp. nov., Wuyi Mountain, Fujian Province, China; **2.** the type locality of *R. sangzhiensis*, Sangzhi County, Hunan Province, China; **3.** the type locality of *R. zhengi*, Hongya County, Sichuan Province, China; **4.** another locality of *R. zhengi*, Gulin County, Sichuan Province, China; **5.** the locality for *R. johnsi* in Caobang Province, Vietnam; **6.** the locality for *R. johnsi* in Jinxiu County, Guangxi Province, China; **7.** the locality for *R. johnsi* in Shiwandashan Mountains, Guangxi Province, China; **8.** the type locality of *R. weiningensis*, Weining County, Guizhou Province, China.

collected, i.e., six *R. zhengi* from Gulin County, Sichuan Province, China; five adult males, two adult females and six tadpoles of *R. sangzhiensis* from its type locality, Sangzhi County, Hunan Province, China; two adult males, one female, and one larval of *R. johnsi* from northern Vietnam; two larval of *R. johnsi* from Jinxiu County, Guangxi Province, China; eight adult males and six tadpoles of *R. johnsi* from Shiwandashan Mountains, Guangxi Province, China; and one adult male of *R. weiningensis* from its type locality, Weining City, Guizhou Province, China (Table 1, Fig. 1, Suppl. material 1). In the field, the frogs and tadpoles were euthanized using isoflurane, and the specimens were fixed in 75% ethanol. Muscle tissue samples were taken and preserved separately in 95% ethanol prior to fixation. The specimens were deposited in Chengdu Institute of Biology (CIB), Chinese Academy of Sciences, Nanning Normal University (NNU), and Institute of Ecology and Biological Resources (IEBR), Vietnam (for voucher numbers see Table 1 and Suppl. material 1).

### Molecular phylogenetic analyses

A total of 40 samples collected in this study was used in molecular analyses, encompassing twelve unnamed specimens from Wuyi Mountain, six *R. sangzhiensis*, six *R. zhengi*, 15 *R. johnsi*, and one *R. weiningensis* (Table 1). Total DNA was extracted using a standard phenol-chloroform extraction protocol (Sambrook et al. 1989). Three mitochondrial genes (16S rRNA, ND2, and Cyt *b*) and three nuclear DNA markers

Table 1. Information for samples used in molecular phylogenetic analyses in this study.

ID	Species	Voucher	Locality	16S	Cyt b	ND2	BDNF	RAG1	Tyrl
1	<i>Rana wuyiensis</i> sp. nov.	CIB WY20201106016	China: Fujiang: Wuyi Mountain	MZ337980	MZ355497	MZ355540	MZ355396	MZ355426	MZ355465
2	<i>Rana wuyiensis</i> sp. nov.	CIB WY20201106018	China: Fujiang: Wuyi Mountain	MZ337981	MZ355498	MZ355541	MZ355397	MZ355427	MZ355466
3	<i>Rana wuyiensis</i> sp. nov.	CIB WY20201106007	China: Fujiang: Wuyi Mountain	MZ337982	MZ355499	MZ355542	MZ355398	MZ355428	MZ355467
4	<i>Rana wuyiensis</i> sp. nov.	CIB WY20201106005	China: Fujiang: Wuyi Mountain	MZ337983	MZ355500	MZ355543	MZ355399	MZ355429	/
5	<i>Rana wuyiensis</i> sp. nov.	CIB WY20200913003	China: Fujiang: Wuyi Mountain	MZ337984	MZ355501	MZ355544	/	MZ355430	MZ355468
6	<i>Rana wuyiensis</i> sp. nov.	CIB WY20200913001	China: Fujiang: Wuyi Mountain	MZ337985	MZ355502	MZ355545	MZ355400	MZ355431	MZ355469
7	<i>Rana wuyiensis</i> sp. nov.	CIB WY20201106017	China: Fujiang: Wuyi Mountain	MZ337986	MZ355503	MZ355546	MZ355401	MZ355432	MZ355470
8	<i>Rana wuyiensis</i> sp. nov.	CIB WY20201106006	China: Fujiang: Wuyi Mountain	MZ337987	MZ355504	MZ355547	MZ355402	MZ355433	MZ355471
9	<i>Rana wuyiensis</i> sp. nov.	CIB WY20200913002	China: Fujiang: Wuyi Mountain	MZ337988	MZ355505	MZ355548	MZ355403	MZ355434	MZ355472
10	<i>Rana wuyiensis</i> sp. nov.	CIB WYS20200829003	China: Fujiang: Wuyi Mountain	MZ337989	MZ355506	MZ355549	MZ355404	MZ355435	MZ355473
11	<i>Rana wuyiensis</i> sp. nov.	CIB WYS20200829002	China: Fujiang: Wuyi Mountain	MZ337990	MZ355507	MZ355550	MZ355405	MZ355436	MZ355474
12	<i>Rana wuyiensis</i> sp. nov.	CIB WYS20200829001	China: Fujiang: Wuyi Mountain	MZ337991	MZ355508	MZ355551	MZ355406	MZ355437	MZ355475
13	<i>Rana zhengi</i>	CIB GL150097	China: Sichuan: Gulin County	MZ337992	MZ355509	MZ355552	MZ355407	MZ355438	MZ355476
14	<i>Rana zhengi</i>	CIB GL150091	China: Sichuan: Gulin County	MZ337993	MZ355510	MZ355553	MZ355408	MZ355439	MZ355477
15	<i>Rana zhengi</i>	CIB GL150088	China: Sichuan: Gulin County	MZ337994	MZ355511	MZ355554	MZ355409	MZ355440	MZ355478
16	<i>Rana zhengi</i>	CIB GL150011	China: Sichuan: Gulin County	MZ337995	MZ355512	MZ355555	MZ355410	MZ355441	MZ355479
17	<i>Rana zhengi</i>	CIB GL150010	China: Sichuan: Gulin County	MZ337996	MZ355513	MZ355556	MZ355411	MZ355442	MZ355480
18	<i>Rana zhengi</i>	CIB GL150068	China: Sichuan: Gulin County	MZ337997	MZ355514	MZ355557	MZ355412	MZ355443	MZ355481
19	<i>Rana sangzhiensis</i>	CIB SZ2012062103	China: Hunan: Sangzhi County: Tiaping Mountain	MZ337998	/	/	/	/	/
20	<i>Rana sangzhiensis</i>	CIB SZ2012062106	China: Hunan: Sangzhi County: Tiaping Mountain	MZ337999	/	/	/	/	/
21	<i>Rana sangzhiensis</i>	CIB SZ2012062104	China: Hunan: Sangzhi County: Tiaping Mountain	MZ338000	MZ355515	/	MZ355413	MZ355444	MZ355482
22	<i>Rana sangzhiensis</i>	CIB TPS20190413-FTY1-5	China: Hunan: Sangzhi County: Tiaping Mountain	MZ338001	MZ355516	MZ355558	MZ355414	MZ355445	MZ355483
23	<i>Rana sangzhiensis</i>	CIB TP20190413-36	China: Hunan: Sangzhi County: Tiaping Mountain	MZ338002	MZ355517	MZ355559	MZ355415	MZ355446	MZ355484
24	<i>Rana sangzhiensis</i>	CIB TPS20190413-FTY1-1	China: Hunan: Sangzhi County: Tiaping Mountain	MZ338003	MZ355518	MZ355560	MZ355416	MZ355447	MZ355485
25	<i>Rana sangzhiensis</i>	CIB TPS20190413-FTY1-2	China: Hunan: Sangzhi County: Tiaping Mountain	MZ338004	MZ355519	MZ355561	MZ355417	MZ355448	MZ355486
26	<i>Rana sangzhiensis</i>	CIB TPS20190413-FTY1-3	China: Hunan: Sangzhi County: Tiaping Mountain	MZ338005	MZ355520	MZ355562	MZ355418	MZ355449	MZ355487
27	<i>Rana sangzhiensis</i>	CIB TPS20190413-FTY1-4	China: Hunan: Sangzhi County: Tiaping Mountain	MZ338006	MZ355521	MZ355563	MZ355419	MZ355450	MZ355488
28	<i>Rana zhengi</i>	SCUM 0405190CJ	China: Sichuan: Hongya County: Zhangsun	KX209206	/	/	/	/	/
29	<i>Rana sangzhiensis</i>	CIB SZ2012062102	China: Hunan: Sangzhi County: Tiaping Mountain	MZ338007	MZ355522	/	MZ355420	MZ355451	MZ355489
30	<i>Rana joubini</i>	NUU 1910030	China: Guangxi: Shiwandashan Mountains	MZ338008	MZ355523	MZ355564	/	MZ355452	/
31	<i>Rana joubini</i>	NUU 1910023	China: Guangxi: Shiwandashan Mountains	MZ338009	MZ355524	MZ355565	/	MZ355453	/
32	<i>Rana joubini</i>	NUU 1910010	China: Guangxi: Shiwandashan Mountains	MZ338010	MZ355525	MZ355566	MZ355421	MZ355454	MZ355490
33	<i>Rana joubini</i>	NUU 1910032	China: Guangxi: Shiwandashan Mountains	MZ338011	MZ355526	MZ355567	/	MZ355455	/
34	<i>Rana joubini</i>	NUU 1910009	China: Guangxi: Shiwandashan Mountains	MZ338012	MZ355527	MZ355568	/	MZ355456	/
35	<i>Rana joubini</i>	NUU 1910001	China: Guangxi: Shiwandashan Mountains	MZ338013	MZ355528	MZ355569	/	MZ355457	MZ355491

ID	Species	Voucher	Locality	16S	Cyt b	ND2	BDNF	RAG1	Tyrl
36	<i>Rana jombhi</i>	NNU 1910035	China: Guangxi: Shiwandashan Mountains	MZ338014	MZ355529	MZ355570	/	MZ355458	/
37	<i>Rana jombhi</i>	NNU 1910021	China: Guangxi: Shiwandashan Mountains	MZ338015	MZ355530	MZ355571	/	MZ355459	/
38	<i>Rana jombhi</i>	NNU 1910017	China: Guangxi: Shiwandashan Mountains	MZ338016	MZ355531	MZ355572	/	MZ355460	/
39	<i>Rana jombhi</i>	NNU 1910002	China: Guangxi: Shiwandashan Mountains	MZ338017	MZ355532	MZ355573	/	MZ355461	MZ355492
40	<i>Rana jombhi</i>	CIB 20070712-1	China: Guangxi: Jinxiu County	MZ338018	MZ355533	MZ355574	/	/	MZ355493
41	<i>Rana jombhi</i>	CIB 20070712	China: Guangxi: Jinxiu County	MZ338019	MZ355534	/	MZ355422	/	/
42	<i>Rana jombhi</i>	IEBR-A 4849	Vietnam: Cao Bang Province	MZ338020	MZ355535	MZ355574	MZ355423	MZ355462	MZ355494
43	<i>Rana jombhi</i>	IEBR-A 4848	Vietnam: Cao Bang Province	MZ338021	MZ355536	MZ355575	MZ355424	MZ355463	MZ355495
44	<i>Rana jombhi</i>	CIB 2012040008	Vietnam: Cao Bang Province	MZ338022	MZ355537	MZ355576	/	/	/
45	<i>Rana uevingensis</i>	CIB 20200806014	China: Guizhou: Weining County	MZ338023	MZ355538	MZ355577	MZ355425	MZ355464	MZ355496
46	<i>Rana amurensis</i>	Tissue ID: MSUZP-SLK-RUS49	Russia: Tomskaya: Teguldekskii district	KX269203	KX269349	KX269418	/	/	/
47	<i>Rana areolata</i>	KU 204370	USA: Kansas: Lyon: just S of Hartsford	AY779229	KX269300	KX269369	/	/	/
48	<i>Rana arvalis</i>	Tissue ID: MSUZP-SLK-MKR21	Russia: Mordovia: Chamzinskii district	KX269197	KX269344	KX269413	/	/	/
49	<i>Rana asiatica</i>	Tissue ID: KIZ-XJ0251	China: Xinjiang: 47 tuan	KX269200	KX269346	KX269415	/	/	/
50	<i>Rana atrovira</i>	MVZ 188961	USA: California: Del Norte Co. Kings Valley	KX269212	/	KX269427	/	/	/
51	<i>Rana berlandieri</i>	JSF 1136	USA: Texas: Hays: San Marcos	AY779235	KX269301	KX269370	/	/	/
52	<i>Rana blairi</i>	JSF 830	USA: Kansas: Douglas: Lawrence	AY779237	/	/	/	/	/
53	<i>Rana boylei</i>	MVZ 148930	USA: California: Lake Co. along Butts Creek	KX269178	KX269299	KX269368	/	/	/
54	<i>Rana buana</i>	QCAZ 13964	Ecuador: Loja: Rio Alamor	AY779212	/	/	/	/	/
55	<i>Rana capito</i>	TNHC 60195	USA: Florida: Marion: Archibald Biological Station	AY779231	/	/	/	/	/
56	<i>Rana cascadae</i>	TNHC-GDC 5297	no data	KX269176	KX269302	KX269371	/	/	/
57	<i>Rana catesbeiana</i>	SCUM 0405176CJ	Per trade	KX269208	KX269354	KX269423	/	/	/
58	<i>Rana chaochiaoensis</i>	SCUM 0405170CJ	China: Sichuan: Zhaojue	KX269192	KX269339	KX269408	/	/	/
59	<i>Rana chensinensis</i>	KIZ RD05SHX01	China: Shaanxi: Huxian	KX269186	KX269333	KX269402	/	/	/
60	<i>Rana chiricahuensis</i>	KU 194442	Mexico: Durango: Rio Chico at Mexico Hwy	AY779225	KX269303	KX269372	/	/	/
61	<i>Rana clamitans</i>	JSF 1118	USA: Missouri: Montgomery: 3 km W Danville	AY779204	KX269304	KX269373	/	/	/
62	<i>Rana coreana</i>	MMS 223	South Korea	KX269202	KX269348	KX269417	/	/	/
63	<i>Rana culdaiensis</i>	KIZ SD080501	China: Shandong: Culaishan shan	KX269190	KX269337	KX269406	/	/	/
64	<i>Rana dabichuanensis</i>	AHU 2016R001	China: Anhui: Dabie Mountains	MF172963	/	/	/	/	/
65	<i>Rana dabmatina</i>	Tissue ID: MSUZP-NFUA-R-21-1	Ukraine: Zakarpatska: Užgorod District: Tschop	AY779222	KX269305	KX269374	/	/	/
66	<i>Rana dhoni</i>	KU 194527	Mexico: Michoacan: Tinzuntzan: Lago Patzcuaro	KX269188	KX269335	KX269404	/	/	/
67	<i>Rana dybowskii</i>	Tissue ID: MSUZP-IVM-1-d	Russia: Primorye region: Khasanskii District	AY779233	GU184219	GU184250	/	/	/
68	<i>Rana forsteri</i>	KU 194581	Mexico: Sinaloa: 37.9 km S	AY779233	GU184219	GU184250	/	/	/
69	<i>Rana graeca</i>	ZMMU A-4293-1	Croatia: Gora (Montenegro): Niksic environs	KX269199	KX269345	KX269414	/	/	/
70	<i>Rana gryllio</i>	MVZ 175945	USA: Florida: Leon: Tall Timbers Research Station	AY779201	/	/	/	/	/
71	<i>Rana hankia</i>	KIZ GX07112915	China: Guangxi: Maershan shan	KX269191	KX269338	KX269407	/	/	/

ID	Species	Voucher	Locality	IGS	Cyt-b	ND2	BDNF	RAG1	Tyr1
72	<i>Rana heckscheri</i>	MVZ 164908	USA: Florida: Gadsden-Leon	AY779205	/	/	/	/	/
73	<i>Rana buanensis</i>	MMS 231	South Korea	KX269183	KX269330	KX269400	/	/	/
74	<i>Rana ibertica</i>	ZMMU A-4292-1	Portugal: Porto: Valongo environs	KX269195	KX269342	KX269411	/	/	/
75	<i>Rana japonica</i>	Tissue ID: KIZ-YPX11775	Japan: Isumi-shi: Chiba Prefecture	KX269220	KX269364	KX269434	/	/	/
76	<i>Rana jiemaensis</i>	KIZ HUN0708013	China: Hunan: Jiemuxi	KX269221	KX269365	/	/	/	/
77	<i>Rana jialingensis</i>	SYS a005519	China: Jiangxi: Mt Guanshan	MT408985	/	/	/	/	/
78	<i>Rana juliani</i>	TNHC 60324	Belize: Cayo District: Little Vaqueros Creek	AY779215	/	KX269375	/	/	/
79	<i>Rana kobai</i>	KUHE: 10051	Japan: Amami	AB685778	/	/	/	/	/
80	<i>Rana koreanis</i>	KIZ CJ06102001	China: Qinghai: Qinghai Lake	KX269185	KX269332	KX269401	/	/	/
81	<i>Rana kuryuensis</i>	KIZ HUI040001	China: Shaandong: Kunyu shan	KX269201	KX269347	KX269416	/	/	/
82	<i>Rana latasiei</i>	Veth 2003	Italy: Campagna: Seveglio 2 km	AY147946	AY147967	/	/	/	/
83	<i>Rana longicrus</i>	NMNS 15022	China: Taiwan: Xiangtianshu: Miaosu	KX269189	KX269336	KX269405	/	/	/
84	<i>Rana lueituentris</i>	MVZ 225749	USA: Washington: Pend Oreille Co. western	KX269213	KX269358	KX269428	/	/	/
85	<i>Rana macromantis</i>	ID: MSUZP-LEM-12	Russia: Dagestan: Agulskiy District	KX269194	KX269341	KX269410	/	/	/
86	<i>Rana macroglossa</i>	UTA A-17185	Guatemala: Solola: Panajachel: Lake Atitlan	AY779243	KX269306	KX269376	/	/	/
87	<i>Rana maculata</i>	KU 195258	Mexico: Oaxaca: Colonia Rodulfo Figueroa	AY779207	KX269307	KX269377	/	/	/
88	<i>Rana magnaocularis</i>	KU 194592	Mexico: Sonora: Arroyo Honda: 15.2 km N	AY779239	KX269308	KX269378	/	/	/
89	<i>Rana montezumae</i>	KU 195251	Mexico: Morelos: Lagunas Zempoala	AY779223	KX269309	KX269379	/	/	/
90	<i>Rana muscosa</i>	MVZ 149006	USA: California: Mono: Meadows western	AY779195	/	/	/	/	/
91	<i>Rana neovolcanica</i>	KU 194536	Mexico: Michoacan: Zurumbueno	AY779236	KX269310	KX269380	/	/	/
92	<i>Rana obolusae</i>	no voucher	USA: Florida: Santa Rosa: 5 km E	AY779203	/	/	/	/	/
93	<i>Rana ometimontis</i>	SCUM 0405196CJ	China: Sichuan: Zhaungcun: Hongya	KX269193	KX269340	KX269409	/	/	/
94	<i>Rana omilemama</i>	KU 195179	Mexico: Guerrero: Agua de Obispo Mexican Plateau	AY779238	KX269311	KX269381	/	/	/
95	<i>Rana onca</i>	LVT 3542	USA: Nevada: Clark: Blue Point-Spring Mexican	AY779249	/	/	/	/	/
96	<i>Rana ornativentris</i>	Tissue ID: KIZ-JP080101	Japan: Kyoto	KX269187	KX269334	KX269403	/	/	/
97	<i>Rana palnipes</i>	AMNH A-118801	Venezuela: Amazonas: Rio Mawarinuma	AY779211	/	/	/	/	/
98	<i>Rana palustris</i>	ROM 21658	USA: New York: Middleburg eastern	KX269207	KX269353	KX269422	/	/	/
99	<i>Rana pipiens</i>	JSF 1119	USA: Ohio: Ottawa: Little Portage State Park	AY779221	/	/	/	/	/
100	<i>Rana pirica</i>	Tissue ID: MSUZP-NPFE-R-08-42	Russia: Sakhalinskaya Province: Makorovskiy District	KX269184	KX269331	/	/	/	/
101	<i>Rana psilonota</i>	KU 195119	Mexico: Jalisco: 2.4 km NW Tapalpa	AY779217	KX269312	KX269382	/	/	/
102	<i>Rana pustulosa</i>	KU 200776	Mexico: Sinaloa: 2.1 km NE Santa Lucia	AY779220	KX269313	KX269383	/	/	/
103	<i>Rana pyrenatica</i>	ZFMK 65447-65448	Spain: Zauriza: Aragón	AY147950	AY147971	/	/	/	/
104	<i>Rana sakuraii</i>	Tissue ID: KIZJP080104	Japan: Tokyo	KX269205	KX269351	KX269420	/	/	/
105	<i>Rana sauteri</i>	SCUM 0405175CJ	China: Taiwan: Kaohsiung	KX269204	KX269350	KX269419	/	/	/
106	<i>Rana septentrionalis</i>	TNHC 72500	Canada: Ontario: Grey	KX269179	KX269314	KX269384	/	/	/
107	<i>Rana serosa</i>	TNHC 60194	USA: Mississippi: Harrison	AY779230	/	/	/	/	/
108	<i>Rana shuchiniae</i>	CIB HUI040009	China: Sichuan: Zhaolue	KX269210	KX269356	KX269425	/	/	/

ID	Species	Voucher	Locality	16S	Cyt b	ND2	BDNF	RAG1	Tyr1
109	<i>Rana sierrae</i>	MVZ 149007	USA: California: Mono Co. Meadows	KX269211	KX269357	KX269426	/	/	/
110	<i>Rana sierramadrensis</i>	KU 195181	Mexico: Guerrero: Agua de Obispo	AV779216	KX269315	KX269385	/	/	/
111	<i>Rana spectabilis</i>	KU 195186	Mexico: Hidalgo: La Estanzuela	AV779227	KX269320	KX269390	/	/	/
112	<i>Rana sphenoccephala</i>	JSF 845	USA: Kansas: Cherokee eastern	AV779251	KX269321	KX269391	/	/	/
113	<i>Rana sylvatica</i>	ID: MSUZP-SUNY-R-4-3	USA: New York: St. Lawrence Co.	KX269209	KX269355	KX269424	/	/	/
114	<i>Rana tagoi</i>	ID: MSUZP-NIJP-R-08-69	Japan: Kyoto	KX269214	KX269359	KX269429	/	/	/
115	<i>Rana tanahumanae</i>	KU 194596	Mexico: Sonora: 14.4 km E Yecora	AV779218	KX269322	KX269392	/	/	/
116	<i>Rana temponaria</i>	ZMMU A-4288-1	Ukraine: Zakarpatska: Uzhgorod district	KX269196	KX269343	KX269412	/	/	/
117	<i>Rana tlalocoi</i>	KU 194436	Mexico: Distrito Federal: Xochimilco	AV779234	KX269323	KX269393	/	/	/
118	<i>Rana tsushimensis</i>	NAP 4191	Japan: Nagasaki: Tsushima	KX269181	KX269329	KX269399	/	/	/
119	<i>Rana uenoi</i>	KIZ YPX36615	Japan: Nagasaki: Tsushima	KX269177	/	/	/	/	/
120	<i>Rana ulina</i>	OKW 135	Japan: Ryukyu Islands	KX269215	KX269360	KX269430	/	/	/
121	<i>Rana villanti</i>	KU 195299	Mexico: Oaxaca: 5.6 mi NE Tapanatepec	AV779214	/	KX269394	/	/	/
122	<i>Rana vibicaria</i>	TNHC GDC2266	Costa Rica: Cartago: El Emplame	KX269180	KX269324	KX269395	/	/	/
123	<i>Rana warszewitschii</i>	JSF 1127	Panama	AV779209	KX269325	KX269396	/	/	/
124	<i>Rana yanagipatensis</i>	KU 194423	USA: Arizona: Greenlee: Apache National Forest	AV779240	KX269319	/	/	/	/
125	<i>Rana zhenhaiensis</i>	KIZ 803271	China: Zhejiang: Zhenhai	KX269218	JF939105	KX269433	/	/	/
126	<i>Odorrana versabilis</i>	HNNU A0019L	China: Hainan: Limu shan	KX269223	KX269367	KX269436	/	/	/
127	<i>Pelophylax nigromaculatus</i>	SCUM 045199CJ	China: Sichuan: Hongya	KX269216	KX269361	KX269431	/	/	/
128	<i>Rogosa tiantaiensis</i>	SCUM 0405192CJ	China: Anhui: Huang shan region	KX269222	KX269366	KX269435	/	/	/
129	<i>Hylarana guentheri</i>	SCUM H002CJ	China: Hainan: Sanya	KX269219	KX269363	/	/	/	/

Table 2. Primers used for PCR and sequencing.

Locus	Primer name	Sequences (5' end, 3' end)	Temperature (°C)	Source
16S	16SAR	AAGGCTAAGATGAACCCATAAAAGTTCT	55	Kocher et al. (1989)
	R16	ATAGTGGGTATCTAATCCCAGTTTGTGTTT	55	Sumida et al. (2000)
ND2	HERP322	TYCGARGACAGAGGTTTRAG	50	Yuan et al. (2016)
	HERP323	CAYCCACGRGCVATYGAA	51	Yuan et al. (2016)
Cyt b	HERP328	GAAAARCTTCGTTGTWATTCAACTA	52	Yuan et al. (2016)
	HERP329	CTACKGGTTTCCYCCRAITTCATGT	53	Yuan et al. (2016)
Tyr	Tyr1G	TGCTGGCRCTCTCCARTCCCA	57	Bossuyt and Milinkovitch (2000)
	Tyr1B	AGGTCCTCYTRAGGAAGGAATG	57	Bossuyt and Milinkovitch (2000)
RAG1	AmpF2	ACNGNMGICARATCTTYCARCC	50	Hoegg et al. (2004)
	AmpR2	GGTGTTTAAACACAATCTTCCATYTCRTA	50	Hoegg et al. (2004)
BDNF	BDNF 2F	GAGTGGGTCAAGAGGAGG	55	Zhou et al. (2012)
	BDNF_2R	ACTGGGTAGTTCGGGCATT	55	Zhou et al. (2012)

(Tyr, BDNF, and RAG1) were amplified and sequenced for the samples. Primer sequences used for PCR are presented in Table 2. Gene fragments were amplified under the following conditions: an initial denaturing step at 95 °C for 4 min; 36 cycles of denaturing at 95 °C for 30 s, 40 s at appropriate annealing temperature (Table 2); and extending at 72 °C for 70 s. PCR products were sequenced with primers same as used in PCR. Sequencing was conducted using an ABI3730 automated DNA sequencer. New sequences were deposited in GenBank (Table 1).

For phylogenetic analyses, the corresponding sequences for congeners especially for the topotypes of species in the subgenus *Rana* were downloaded from GenBank (Table 1), mainly derived from previous studies (Yuan et al. 2016; Wang et al. 2017; Wan et al. 2020). For phylogenetic analyses, corresponding sequences of one *Odorrana versabilis* (Liu & Hu, 1962) and one *Pelophylax nigromaculatus* (Hallowell, 1861) were also downloaded (Table 1), and used as outgroups according to Yuan et al. (2016).

Sequences were assembled and aligned using the ClustalW module in BioEdit v.7.0.9.0 (Hall 1999) with default settings. The protein-coding gene (Cytb, ND2, BDNF, RAG1, and Tyr1) sequences were translated to amino acid sequences in MEGA v. 6.0 (Tamura et al. 2013), adjusted for open reading frames, and checked to ensure absence of premature stop codons. No-sequenced fragments were treated as missing data. For phylogenetic analyses based on mitochondrial DNA, the dataset was concatenated with mitochondrial gene sequences. The best partition scheme and the best evolutionary model for each partition were chosen for the phylogenetic analyses using PARTITION-FINDER v. 1.1.1 (Robert et al. 2012). In this analysis, 16S gene and each codon position of protein-coding mitochondrial gene were defined, and Bayesian Inference Criteria was used. As a result, the analysis suggested that the best partition scheme is 16S gene/each codon position of protein-coding gene, and selected GTR + G + I model as the best model for each partition. Phylogenetic analyses were conducted using maximum likelihood (ML) and Bayesian Inference (BI) methods, implemented in PhyML v. 3.0 (Guindon et al. 2010) and MrBayes v. 3.2 (Ronquist et al. 2012), respectively. For the ML tree, branch supports (bs) were drawn from 10,000 nonparametric bootstrap replicates. In BI, two runs each with four Markov chains were simultaneously run for 50 million generations with sampling every 1,000 generations. The first 25% trees were removed as the “burn-in” stage followed by calculations of Bayesian posterior probabilities (bpp), and the 50% majority-rule consensus of the post burn-in trees were sampled at stationarity. In addition, to access the genetic isolation between the undescribed species and its closely related species on nuclear DNA, one haplotype network for each nuclear gene dataset was constructed, using the maximum parsimony method in TCS v. 1.21 (Clement et al. 2000). Genetic distance of uncorrected-*p*-distance model on 16S gene sequences between the new species and its closely related species were estimated using MEGA.

## Morphological comparisons

All six adult specimens of the undescribed species were measured (Suppl. material 1). For comparisons, five adult male specimens of *R. sangzhiensis*, eleven adult male

specimens of *R. jobnsi*, and 22 adult male specimens of *R. zhengi* used in Jiang et al. (1997) were also measured (Suppl. material 1). The terminology and methods followed Fei et al. (2009). Measurements were taken with a dial caliper to 0.1 mm. Twenty-two morphometric characters of adult specimens were measured:

- ED** eye diameter (distance from the anterior corner to the posterior corner of the eye);  
**FIIL** third finger length (distance from base to tip of finger III);  
**FII** second finger length (distance from base to tip of finger II);  
**FIL** first finger length (distance from base to tip of finger I);  
**FIVL** fourth finger length (distance from base to tip of finger IV);  
**FL** foot length (distance from tarsus to the tip of fourth toe);  
**HAL** hand length (distance from tip of third digit to proximal edge of inner palmar tubercle);  
**HDL** head length (distance from the tip of the snout to the articulation of jaw);  
**HDW** maximum head width (greatest width between the left and right articulations of jaw);  
**IND** internasal distance (minimum distance between the inner margins of the external nares);  
**IOD** interorbital distance (minimum distance between the inner edges of the upper eyelids);  
**LAL** length of lower arm and hand (distance from the elbow to the distal end of the Finger IV);  
**LW** lower arm width (maximum width of the lower arm);  
**SL** snout length (distance from the tip of the snout to the anterior corner of the eye);  
**SNT** distance between the nasal the posterior edge of the vent;  
**SVL** snout-vent length (distance from the tip of the snout to the posterior edge of the vent);  
**TFL** length of foot and tarsus (distance from the tibiotarsal articulation to the distal end of the Toe IV);  
**THL** thigh length (distance from vent to knee);  
**TL** tibia length (distance from knee to tarsus);  
**TW** maximal tibia width;  
**TYD** maximal tympanum diameter;  
**UEW** upper eyelid width (greatest width of the upper eyelid margins measured perpendicular to the anterior-posterior axis).

To reduce the impact of allometry in adults, the correct value from the ratio of each character to SVL was calculated, and then was log-transformed for the following morphometric analyses. One-way ANOVA tests were conducted to test the significance of differences on morphometric characters between the undescribed species and its closely related species. The significance level was set at 0.05.

The morphological description follows the definition in Fei et al. (2009). Sex was determined by examining the gonads. The description of toe webbing followed Savage

(1975). The description of digital pad followed Ohler (1995). Comparison characters of known congeners were obtained from the literature (Stejneger 1898; Liu 1946; Fei et al. 1990, 2005, 2009, 2012; Liu et al. 1993; Ye et al. 1993, 1995; Lu et al. 2007; Shen et al. 2007; Li et al. 2008; Yan et al. 2011; Wang et al. 2017; Zhao et al. 2017; Wan et al. 2020). We also examined a series of specimens of *Rana* (Suppl. material 1).

## Results

### Phylogenetic analyses

ML and BI trees of the mitochondrial DNA dataset presented almost consistent topology (Fig. 2A, B). In mitochondrial DNA trees, all samples of the undescribed species were strongly nested into one clade (all supports = 100; Fig. 2B). The *R. johnsi* group was strongly supported as a monophyletic group containing all samples of *R. johnsi*, *R. sangzhiensis*, *R. zhengi*, and the undescribed species (all supports = 100; Fig. 2B). The *R. johnsi* group was clustered into the clade corresponding to the subgenus *Rana* (Fig. 2A). The *R. johnsi* group contained two clades. In the first clade, samples of *R. sangzhiensis* and *R. zhengi* were nested into a clade (all supports = 100), which was weakly clustered as the sister of the undescribed species clade (bs = 52; bpp = 0.80; Fig. 2B). In the second clade, three *R. johnsi* samples from Vietnam were clustered into one clade, which was sister to the clade containing samples of *R. johnsi* from two localities of Guangxi Province, China (Figs 1, 2B; Table 1). In addition, the topotype specimen of *R. weiningensis* was phylogenetically far from the *R. johnsi* group, and clustered as the basal clade of the genus *Rana* (Fig. 2A). Haplotype networks based on three nuclear genes all indicated that the undescribed species did not share haplotype with its closely related species *R. johnsi*, *R. sangzhiensis*, and *R. zhengi* (Fig. 2C–E), further indicating the genetic divergence between the undescribed species and its closely related species. As note, on each gene, samples of *R. sangzhiensis* and *R. zhengi* massively shared common haplotypes (Fig. 2C–E), indicating their very shallow genetic divergence. The genetic distance on 16S between all samples of undescribed species is less than 0.2% (range 0.0%–0.2%). The genetic distance between the species and its closely related species were as following: vs. *R. johnsi* from Vietnam 1.3% (range 1.1%–1.7%), vs. *R. johnsi* from Guangxi, China 0.8% (range 0.8%–0.9%), vs. *R. zhengi* 1.0% (range 0.9%–1.1%), and vs. *R. sangzhiensis* 0.9% (range 0.8%–1.1%), being similar to that between the latter four groups (range 0.8%–1.4%). As note, the genetic distance between *R. zhengi* and *R. sangzhiensis* was 0.2% (range 0.0%–0.4%), and that between *R. johnsi* from Vietnam and *R. johnsi* from Guangxi, China was 0.5% (range 0.4%–1.1%).

### Morphological comparisons

The *R. johnsi* group is phylogenetically clustered into the subgenus *Rana*, but this group could be identified from other species of the subgenus *Rana* by the tip of toes with lateroventral grooves (vs. absent in other species of subgenus *Rana*). The undescribed



species could be assigned to this species group by a series of morphological characters: tip of toes flat with lateroventral grooves; body size medium, SVL 41.4–45.6 mm ( $42.9 \pm 1.9$  mm,  $n = 4$ ) in adult males and 47.6–50.3 mm ( $n = 2$ ) mm in adult females; dorsolateral fold distinct and thin, extending straight from posterior margin of upper eyelid to above groin; tympanum distinct, oval; tibio-tarsal articulation reaching forward beyond tip of snout when leg starched forward; skin ridges distinctly arranged on the dorsal surface of thighs and tibiae; adult males with a pair of internal subgular vocal sacs; breeding males possess creamy white nuptial pad with tiny hoar velvety spines on the dorsal surface of the first finger, divided into three parts.

Although the *R. johnsi* group and *R. weiningensis* both have lateroventral grooves on the tip of toes, the undescribed species in the *R. johnsi* group could be easily distinguished from *R. weiningensis* by the following characters: males with internal subgular vocal sacs (vs. absent in the latter); males with larger body size (41.4–45.6 mm,  $n = 4$  vs. 32.8–37.4 mm,  $n = 3$  in the latter); and more developed webbing between toes (webbing on fourth toes reaching tip of toe vs. reaching distal subarticular tubercle in the latter).

In the *R. johnsi* group, the undescribed species could be identified from its closely related species on morphology. ANOVA tests indicated that on the number of transverse skin ridges on the dorsal surface of thighs and tibiae, the undescribed species significantly differs from its closely related species (all  $p$ -values  $< 0.01$ ; Table 3; Fig. 3). The undescribed species has larger number of transverse skin ridges either on thighs (mean  $14.0 \pm 1.7$ , range 12–16,  $n = 6$ ), on tibiae (mean  $12.5 \pm 2.0$ , range 9–15,  $n = 6$ ), and totally on the two body parts (mean  $26.5 \pm 2.7$ , range 22–29,  $n = 6$ ) than *R. sangzhiensis* (on thighs mean  $9.7 \pm 1.3$ , range 7–11,  $n = 7$ ; on tibiae mean  $10.1 \pm 1.1$ , range 8–11,  $n = 7$ ; and totally on the two parts mean  $19.9 \pm 1.8$ , range 17–22,  $n = 7$ ), *R. zhengi* (on thighs mean  $10.0 \pm 1.8$ , range 7–15,  $n = 22$ ; on tibiae mean  $8.1 \pm 1.3$ , range 6–12,  $n = 22$ ; and totally on the two parts mean  $18.1 \pm 2.7$ , range 15–22,  $n = 22$ ), *R. johnsi* from Vietnam (on thighs mean  $9.3 \pm 2.3$ , range 8–12,  $n = 3$ ; on tibiae mean  $9.0 \pm 1.0$ , range 8–10,  $n = 3$ ; and totally on the two parts mean  $18.3 \pm 3.2$ , range 16–22,  $n = 3$ ), and *R. johnsi* from Guangxi, China (on thighs mean  $10.3 \pm 0.9$ , range 9–12,  $n = 9$ ; on tibiae mean  $8.8 \pm 1.8$ , range 6–12,  $n = 9$ ; and totally on the two parts mean  $19.1 \pm 2.0$ , range 16–22,  $n = 9$ ).

On morphometric characters, the results of One-way ANOVA showed that in male, the undescribed species was significantly different from *R. sangzhiensis* on SVL, HDL, SNT, IOD, UEW, ED, TYD, LAL, HAL, LW, THL, TL, TW, TFL, and FL (all  $p$ -values  $< 0.05$ ), significantly different from *R. zhengi* on HDL, HDW, SL, IND, IOD, UEW, TYD, LAL, LW, THL, TL, TW, and FL (all  $p$ -values  $< 0.05$ ), significantly different from *R. johnsi* from Vietnam on SVL, SNT, IND, ED, TYD, and LAL (all  $p$ -values  $< 0.05$ ), and significantly different from *R. johnsi* from Guangxi, China on HDL, HDW, SNT, IND, UEW, ED, LAL, LW, FIL, FIIL, and TW (all  $p$ -values  $< 0.05$ ; Table 4).

In total, molecular phylogenetic analyses and morphological comparisons indicated that our specimens from Wuyi Mountain, Fujian Province, China should be classified into the *R. johnsi* group, and are significantly divergent from its closely related species. The specimens should represent a new species which is described as following section.



## Taxonomic account

### *Rana wuyiensis* sp. nov.

<http://zoobank.org/66BA9380-4998-4EAF-9B58-7E0AEAB2C58C>

Figs 3–6; Tables 1–4, Suppl. material 1

**Material examined.** *Holotype* (Figs 4, 5). CIB WY20200913003, adult male, collected by Yanqing Wu on 13 September 2020 from Wuyishan National Park (27.760°N, 117.743°E, ca. 1341 m a.s.l.), Wuyishan City, Fujiang Province, China. **Paratypes.** Five adult specimens from the same place as holotype collected by Yanqing Wu. One female CIB WYS20200829001 and two males CIB WYS20200829002 and CIB WY20200829003 were collected on 29 August 2020. One female CIB WY20200913002 and one male CIB WY20200913001 were collected on 13 September 2020.

**Other material examined.** Six tadpoles collected from the same place as holotype (Table 1) by Yanqing Wu on 01 November 2020.

**Diagnosis.** *Rana wuyiensis* sp. nov. is distinguished by a combination of the following morphological characters: body size medium, SVL 41.4–45.6 mm ( $42.9 \pm 1.9$  mm,  $n = 4$ ) in adult males, and 47.6–50.3 mm ( $n = 2$ ) in adult females; lateroventral

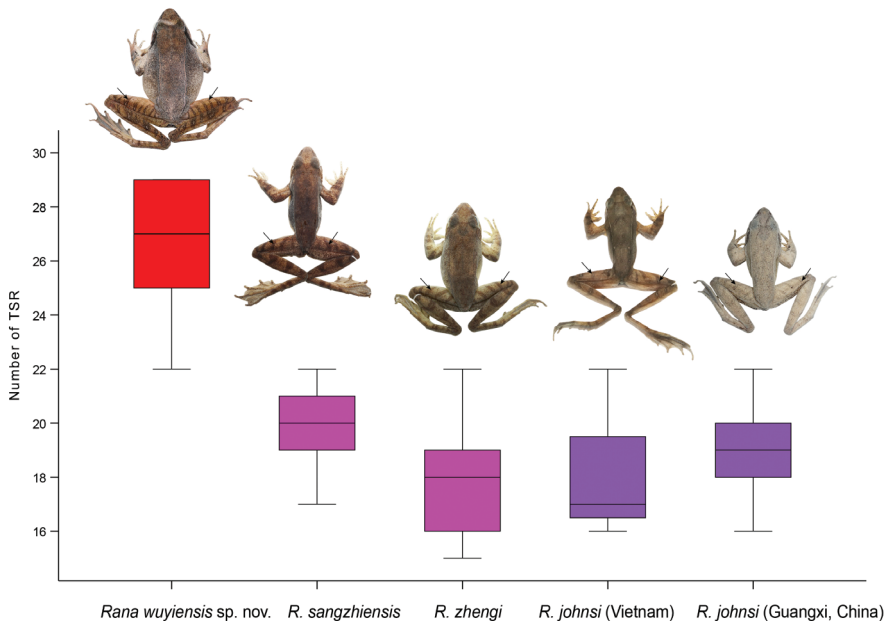


**Figure 3.** Box-plot showing the difference on the number of transverse skin ridges on the dorsal surface of thighs and tibiae between different species. Specimens of different species: the holotype CIB WY20200913003 of *Rana wuyiensis* sp. nov., the topotype specimen CIB SZ2012061203 of *R. sangzhiensis*, the topotype specimen CIB 950300 of *R. zhengi*, the specimen NNU 1910009 of *R. johnsi* from Shiwandashan, Guangxi Province, China, and the specimen IEBR.A 4848 of *R. johnsi* from Vietnam. Abbreviation: TSR, transverse skin ridges.

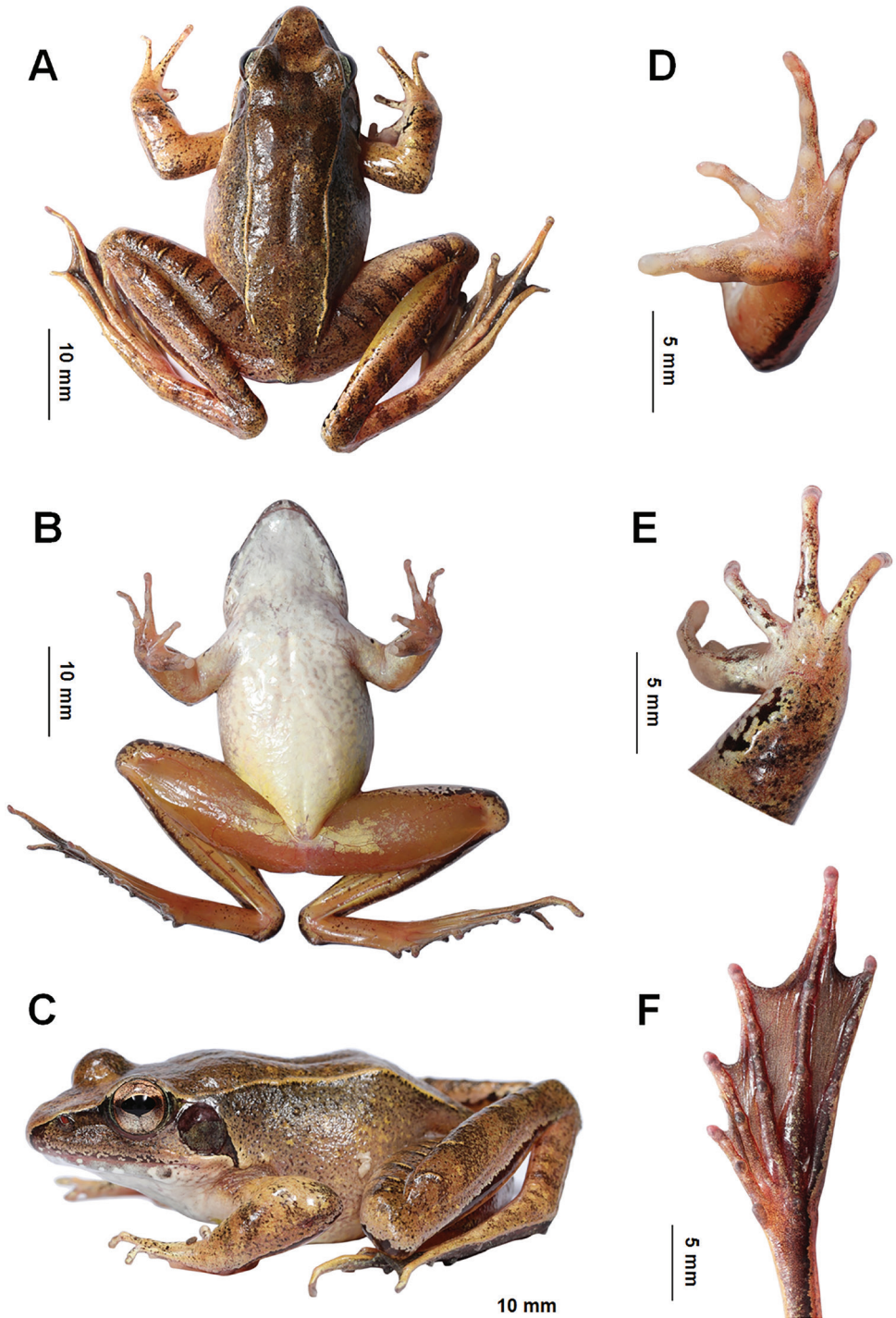


**Figure 4.** Photos of the holotype CIB WY20200913003 of *Rana wuyiensis* sp. nov. in life **A** dorsal view. **B** ventral view **C** lateral view **D** ventral view of hand **E** dorsal view of hand **F** ventral view of foot.

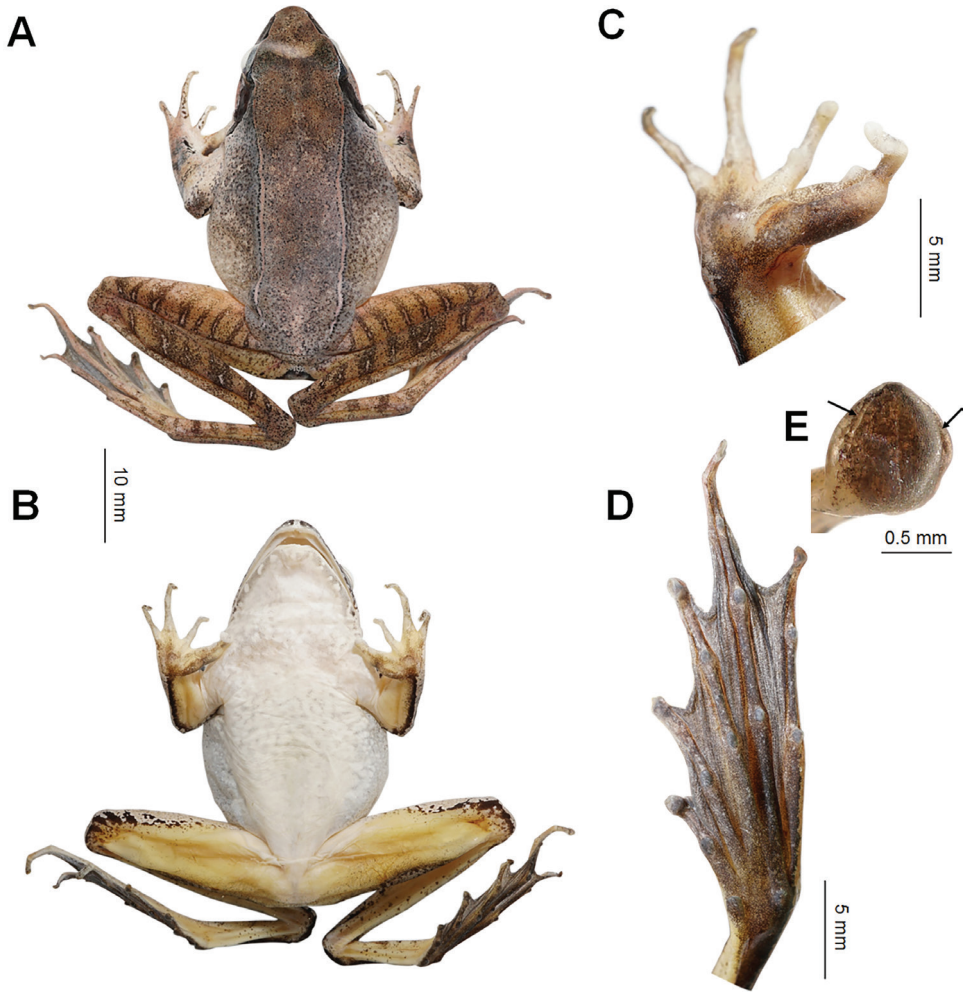


**Figure 5.** Photos of the holotype specimen CIB WY20200913003 of *Rana wuyiensis* sp. nov. **A** dorsal view **B** ventral view **C** ventral view of hand **D** ventral view of foot **E** ventral view of the toe highlighting the lateroventral grooves (arrows).

grooves present on tip of toes; transverse skin ridges distinctly present on the dorsal surface of thighs and tibiae, the number large (mean  $26.5 \pm 2.7$ , range 22–29,  $n = 6$ ); adult male with a pair of internal subgular vocal sacs; webbing on fourth toes reaching the tip of toe; breeding males possess creamy white nuptial pad with tiny hoar velvety spines on the dorsal surface of the first finger, divided into three parts.

**Etymology.** The specific name *wuyiensis* is in reference to the type locality, Wuyi Mountain, Fujian Province, China.

**Suggested common name.** Wuyi Brown Frog (in English), Wuyi Lin Wa (in Chinese; 武夷林蛙).

**Description of holotype (Figs 4, 5). Adult male;** SVL 41.4 mm. Head significantly longer than wide (HDW/HDL ratio = 0.85); snout pointed and projecting over lower lip; nostril closer to tip of snout than eye; canthus rostralis distinct; internasal distance distinctly wider than interorbital distance (IOD/IND ratio = 0.81); loreal region slightly oblique and concave; upper eyelids narrower than interorbital distance; tympanum rounded, diameter three quarters of eye (TD/ED ratio = 0.75), and separated from eye by a short distance about one quarter of tympanum diameter; tympanic rim feebly elevated; pupil oval and horizontal, notched at middle lower margin; a skin fold present posterior to tympanum, disconnected with dorsolateral fold, swollen near shoulder; vomerine teeth in two short row, four or five for each, oblique and separated by a distance about one row of teeth; tongue deeply notched posteriorly, depth about one sixth of entire tongue length; a pair of internal subgular vocal sacs present, openings slit like, small, length as wide as finger tips, positioned at on inner mandible near the corners of mouth.

Forearms moderate, width 0.09 ratio of SVL; hand 0.27 ratio of SVL; fingers elongated, with narrow lateral fringes, rudimentary webbed, webbing formula I  $3\frac{2}{3}$  –  $2\frac{2}{3}$  II  $2\frac{1}{2}$  –  $3\frac{1}{2}$  III  $3\frac{1}{2}$  – 3 IV; tips of fingers rounded, not swollen, without lateroventral groove; finger II distinctly shorter than I, relative finger lengths II < I < IV < III; subarticular tubercles prominent, rounded; supernumerary tubercles indistinct, oval, present on bases of all fingers; inner metacarpal tubercle distinct, near oval, positioned near inner surface of base of finger I, inner side partially covered with nuptial pad; two outer metacarpal tubercles partially separated near the joint of metacarpals of fingers III and IV, the inner oval and larger, the outer elongated and smaller; nuptial pad present on inner and dorsal surface of finger I, covered with velvety spines, partially divided into three parts, the basal part on inner side of inner metacarpal tubercle, the middle part largest, on third phalanx, the distal part smallest, on first and second phalanxes.

Hindlimbs long, tibia 0.64 ratio of SVL and length of foot and tarsus 0.84 ratio of SVL; thigh shorter than tibia, heels overlap when hindlimbs flexed at right angles to axis of body; tibio-tarsal articulation reaching far beyond snout when hindlimb stretched forward along body; toes entirely webbed, inner edge of toe I and outer edge of toe V with narrow lateral fringe, relative toe lengths I < II < III < V < IV, toes webbing formula:  $1\frac{1}{3}$  – 2 II  $1\frac{1}{3}$  –  $2\frac{1}{3}$  III  $1\frac{1}{2}$  –  $2\frac{2}{3}$  IV 3 –  $1\frac{1}{3}$  V; tip of toes somewhat flat, lateroventral grooves present on all tip of toes and disconnected at middle of front edge; subarticular tubercles prominent and oval; supernumerary tubercles absent; inner metatarsal tubercle oval and prominent, outer metatarsal tubercle rounded, indistinct.

Dorsal skin smooth, supratympanic fold absent; dorsolateral folds distinct, narrow, extending from edge of upper eyelid to hip, not curve above tympanum. Ventral skin smooth, skins around cloaca with numerous flat tubercles. Skin on hindlimbs with transverse paralleled ridges, eight on both thighs, six and seven on left and right tibias, four and two on left and right tarsal. Tarsal fold present.

**Coloration in life (Fig. 4).** Dorsal surface basically medium brown, scattered with dense dark brown pigments all over; dorsolateral skin folds and skin ridges on dorsal

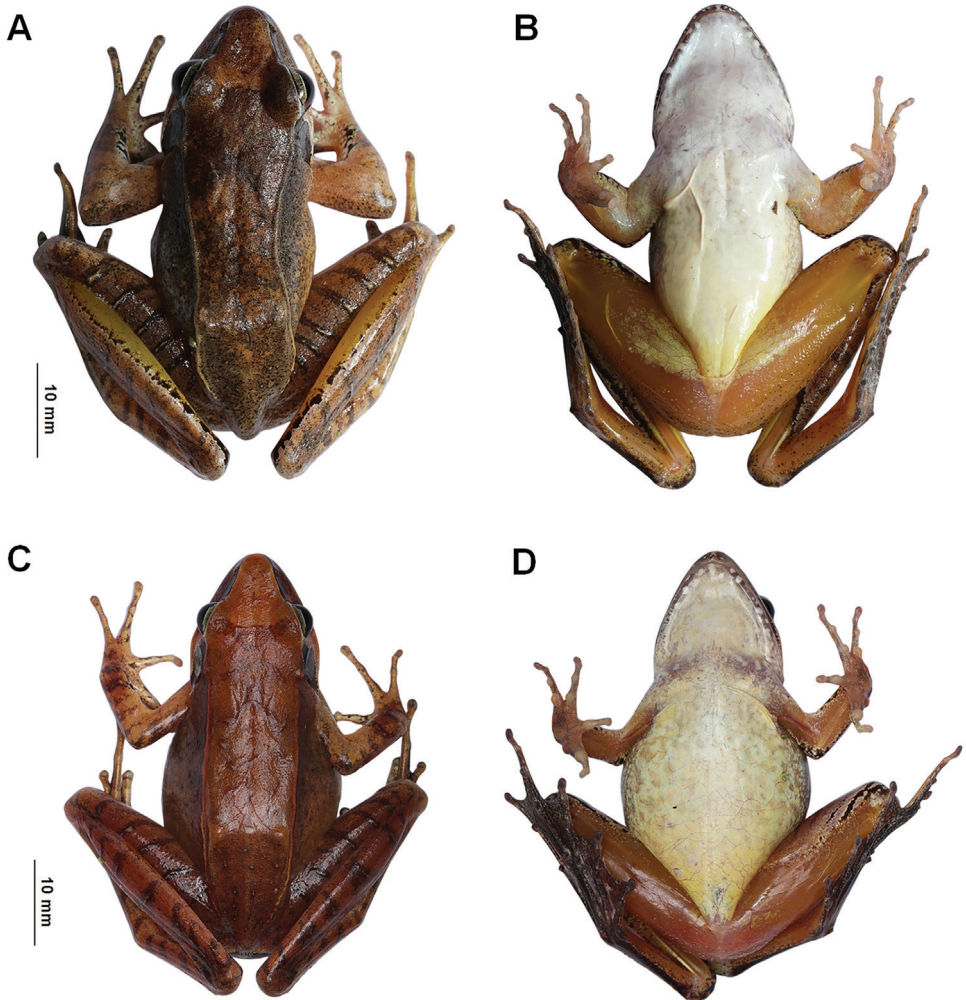


**Figure 6.** Color variation in *Rana wuyiensis* sp. nov. **A** dorsal view of the adult male specimen CIB WY20200913001 **B** ventral view of CIB WY20200913001 **C** dorsal view of the adult female CIB WY20200913002 **D** ventral view of CIB WY20200913002.

limbs yellow brown with deep brown fringes; five ambiguous deep brown cross bands present on dorsal forelimbs; irregular black patches present on inner surface of forearm near wrist, anterior knee and lateral tibia; lower edge of canthus rostralis dark brown; skins on tympanum and anterior to the fold behind tympanum deep brown; ventral skin basically cream white on body and arm; lips light brown with cream white patches; throat, chest, and upper abdomen with irregular light orangish short bars; ventral hindlimbs mostly flesh colored, with a small region near base of tinged yellowish white; ventral hand flesh-colored with brown pigments; ventral feet covered with dense brown pigments. Nuptial pad hoar. Iris mostly copper with dark cracks, regions anterior and posterior to pupil deeper.

**Coloration in preserve (Fig. 5).** Body coloration lighter than in life, dark brown pigments more prominent. Skins between upper eyelids with an ambiguous brown pattern. Ventral body mostly white, with brown pattern; ventral limbs yellowish. Ventral hand and feet greyish. Skins on temporal region with prominent dark patches. Lateral head before eyes blackish. Iris dark with metal luster.

**Secondary sexual characters.** Breeding males with nuptial pad on dorsal surface of finger I, covered with velvety spines, divided into three parts. Male with a pair of internal subgular vocal sacs.

**Variations.** For measurements of type series specimens see Tables 4, Suppl. material 1. Coloration of the two females lighter (Fig. 6A), basically yellowish brown. Black edges of dorsolateral fold absent on CIB WY20200913002 (Fig. 6C) and indistinct on CIB WYS20200829001. The number of skin ridges on dorsal thigh range from five to eight. The skin ridges on tibia range from four to eight.

**Distribution and ecology.** Currently, *Rana wuyiensis* sp. nov. is known from Wuyishan National Park, Wuyishan City, Fujian Province, China. In our surveys from 2017 to 2021, the species was found only at one site. All individuals of the new species used in this work were collected from a stream and nearby grassland under the evergreen broad-leaf forest (Fig. 7). Six adult individuals and some very small tadpoles at early stages of development were found in the late August and early September. Only relative larger and middle-staged tadpoles were collected in the early November. This suggests that the breeding season of this species may begin in July or early August.

## Discussion

Our results based on mitochondrial DNA and nuclear DNA of several populations of *R. zhengi* and *R. sangzhiensis* indicated that the two groups have very low genetic divergence. This is identical to the results of previous molecular phylogenetic analyses in Wan et al. (2020). In addition, we did not find morphological characters for separating the two groups, being consistent with the results of Jiang et al. (1997) and Fei et al. (2009). Based on this evidence, we support the proposal that *R. zhengi* should be synonymized with *R. sangzhiensis*. Accordingly, *R. sangzhiensis* is at least distributed from southwestern part of Sichuan to western Hunan provinces, China. On the contrary, *Rana wuyiensis* sp. nov. differs from its closely related species not only on morphology but also on molecular data, supporting the separation of the new species.

Moreover, the divergence between *Rana wuyiensis* sp. nov. and its closely related species in the *R. johnsi* group is likely corresponding to their separated distributional ranges (Fig. 1). Wuyi Mountain is located at the southeastern edge of the mainland China, far from the “west” distributional ranges of *R. johnsi* and *R. sangzhiensis* in southwestern China (at least > 400 km in a straight line between them; Fig. 1), and the distribution ranges belong to different biota (e.g., Zhang 2009; Fei et al. 2010). This indicates that vicariance might be the primary factor for the speciation of the species. Whatever, the discovery of the new species greatly expanded the distributional range of the *R. johnsi* group to the southeastern China and would promote exploring the biogeographical patterns in the frog group.



**Figure 7.** Habitats of *Rana wuyiensis* sp. nov. in the type locality, Wuyi Mountain, Fujian Province, China **A** landscape of montane forests in the type locality **B** a mountain stream in the type locality.

However, to date, *Rana wuyiensis* sp. nov. was found only at one site in Wuyi Mountain, and it probably has a low population size according to our eleven-times surveys which included forty sites every time in April, June, and August from 2018 to 2021. Although this site is in the central part of the Wuyishan National Park, the breeding

habitat is vulnerable due to local human activities especially tea plantation (Fig. 7A) and/or local nature disaster (for example, the novel rainstorm in 2020 in Wuyi Mountain; our unpublished data). Therefore, we need to understand its population status and major threats, and then take appropriate actions to prepare strategies for its conservation.

## Acknowledgements

We thank the editor and reviewers for their helpful suggestions on our work. This work was supported by Project of Biological Resources Survey in Wuyishan National Park. We thank Zhonghao Luo, Binqing Zhu, and Ningning Lu for their help with field work.

## References

- Batsch AJGK (1796) Umriß der gesammten Naturgeschichte: ein Auszug aus den frühern Handbüchern des Verfassers für seine Vorlesungen. Christian Ernst Gabler, Jena & Leipzig, 287 pp.
- Bedriaga JV (1898) Amphibien und Reptilien. Wissenschaftliche Resultate der von N. M. Przhevalski nach Central-Asien unternommenen Reisen, & c.-Nauchnuie Rezul'tatui puteshestvii N. M. Przheval'skagho po tzentral'noi Azii, & c. Volume 3, Zoologischer Theil, Part 1. Akadamie der Wissenschaften, St. Petersburg, 71–278.
- Boulenger GA (1886) Notes sur les grenouilles rousses d'Asie. Bulletin de la Société Zoologique de France 11: 595–600. <https://doi.org/10.5962/bhl.part.24010>
- Boulenger GA (1909) Descriptions of four new frogs and a new snake discovered by Mr. H. Sauter in Formosa. Annals and Magazine of Natural History Series 8(4): 492–495. <https://doi.org/10.1080/00222930908692704>
- Che J, Pang JF, Zhao EM, Matsui M, Zhang YP (2007) Phylogenetic relationships of the Chinese Brown Frogs (genus *Rana*) inferred from partial mitochondrial 12S and 16S rRNA gene sequences. Zoological Science 24: 71–80. <https://doi.org/10.2108/zsj.24.71>
- Clement M, Posada D, Crandall KA (2000) TCS: a computer program to estimate gene genealogies. Molecular Ecology 9(10): 1657–1659. <https://doi.org/10.1046/j.1365-294x.2000.01020.x>
- David A (1875) Journal de mon Troisième Voyage d'Exploration dans l'Empire Chinoise. Vol. 1. Hachette, Paris, 383 pp. <https://doi.org/10.5962/bhl.title.118647>
- Dubois A (1992) Notes sur la classification des Ranidae (Amphibiens anoures). Bulletin Mensuel de la Société Linnéenne de Lyon 61: 305–352. <https://doi.org/10.3406/linly.1992.11011>
- Dubois A, Ohler A, Pyron RA (2021) New concepts and methods for phylogenetic taxonomy and nomenclature in zoology, exemplified by a new ranked cladonomy of recent amphibians (Lissamphibia). Megataxa 5: 1–738. <https://doi.org/10.11646/megataxa.5.1.1>
- Fei L, Hu SQ, Ye CY, Huang YZ (2009) Fauna Sinica. Amphibia Vol. 2 Anura. Science Press, Beijing, 969–1121.
- Fei L, Ye CY (2005) The key and illustration of Chinese. Sichuan Publishing House of Science and Technology. Chongqing, China, 102–116.

- Fei L, Ye CY, Huang YZ (1990) Key to Chinese Amphibians. Publishing House for Scientific and Technological Literature. Chongqing, China, 364 pp.
- Fei L, Ye CY, Jiang JP (2010) Phylogenetic systematics of Ranidae. *Herpetologica Sinica/Liang qi pa xing dong wu xue yan jiu* 12: 1–43.
- Fei L, Ye CY, Jiang JP (2012) Colored Atlas of Chinese Amphibians and their Distributions. Sichuan Publishing House of Science and Technology, Chengdu, 293–341.
- Fitzinger LJFJ (1843) *Systema Reptilium. Fasciculus Primus*. Braumüller et Seidel, Wien, 106 pp.
- Frost DR (2021) Amphibian Species of the World: an Online Reference. Version 6.0. American Museum of Natural History, New York. <http://research.amnh.org/herpetology/amphibia/index.html> [Accessed on: 2021-4-02]
- Frost DR, Grant T, Faivovich J, Bain RH, Haas A, Haddad CFB, de Sá RO, Channing A, Wilkinson M, Donnellan SC, Raxworthy CJ, Campbell JA, Blotto BL, Moler PE, Drewes RC, Nussbaum RA, Lynch JD, Green DM, Wheeler WC (2006) The amphibian tree of life. *Bulletin of the American Museum of Natural History* 297: 1–370. [https://doi.org/10.1206/0003-0090\(2006\)297\[0001:TATOL\]2.0.CO;2](https://doi.org/10.1206/0003-0090(2006)297[0001:TATOL]2.0.CO;2)
- Guindon S, Dufayard JF, Lefort V, Anisimova M, Hordijk W, Gascuel O (2010) New algorithms and methods to estimate maximum-likelihood phylogenies: assessing the performance of PhyML 3.0. *Systematic Biology* 59(3): 307–321. <https://doi.org/10.1093/sysbio/syq010>
- Günther ACLG (1876) Description of a new frog from north-eastern Asia. *Annals and Magazine of Natural History, Series 4*, 17(101):387–387. <https://doi.org/10.1080/00222937608681973>
- Hall TA (1999) BIOEDIT: a user-friendly biological sequence alignment editor and analysis program for Windows 95/98/NT. *Nucleic Acids Symposium Series* 41(41): 95–98.
- Hallowell E (1861 “1860”) Report upon the Reptilia of the North Pacific Exploring Expedition, under command of Capt. John Rogers, U.S. N. *Proceedings of the Academy of Natural Sciences of Philadelphia* 12: 480–510.
- Hu SQ, Fei L, Ye CY (1978) Three new amphibian species in China. *Materials for Herpetological Research*, Chengdu 4: 20.
- Jiang JP, Fei L, Ye CY, Zeng XM, Zhen MQ, Xie F, Chen YY (1997) Studies on the taxonomics of species of *Pseudorana* and discussions of the phelogenetical relationships with its relative genera. *Cultum Herpetologica Sinica/Liang qi pa xing dong wu xue yan jiu* 6–7: 67–74.
- Jiang JP, Xie F, Li C, Wang B (2020) Species Catalogue of China. Vol. 2. Animals, Vertebrates (IV), Amphibians. Science Press, Beijing, 129 pp.
- LeConte JE (1825) Remarks on the American species of the genera *Hyla* and *Rana*. *Annals of the Lyceum of Natural History of New York* 1: 278–282. <https://doi.org/10.1111/j.1749-6632.1825.tb00012.x>
- Li PP, Lu YY, Li A (2008) A new species of brown frog from Bohai, China. *Asiatic Herpetological Research* 11: 62–70.
- Linnaeus C (1758) *Systema Naturae per Regna Tria Naturae, Secundum Classes, Ordines, Genera, Species, cum Characteribus, Differentiis, Synonymis, Locis*. 10<sup>th</sup> edn. Vol. 1. L. Salvii, Stockholm. <https://doi.org/10.5962/bhl.title.37256>
- Liu CC (1946) A new woodfrog *Rana chaochiaensis* with a discussion of its allied species, from West China. *Journal of the West China Border Research Society, Series B* 16: 7–14.
- Liu CC (1950) Amphibians of western China. *Fieldiana. Zoology Memoires* 2: 1–397. [+ 10 pls.] <https://doi.org/10.5962/bhl.part.4737>

- Liu CC, Hu SQ (1962) A herpetological report of Kwangsi. *Acta Zoologica Sinica/ Dong wu xue bao*, Beijing 14(Supplement): 73–104.
- Liu CC, Hu SQ, Yang FH (1962) Preliminary report of Amphibia from western Kweichow. *Acta Zoologica Sinica/ Dong wu xue bao*, Beijing 14: 381–392.
- Liu MY, Zhang SQ, Liu M (1993) A new species of Ranidae from Liaoning, China (Anura). *Acta Zootaxonomica Sinica* 18: 493–497.
- Lu YY, Li PP, Jiang DB (2007) A new species of *Rana* (Anura, Ranidae) from China. *Acta Zootaxonomica Sinica/ Dong wu fen lei xue bao*, Beijing 32: 792–801.
- Nikolskii AM (1918) Fauna rossii i sopedel'nykh stran. *Zemnovodnye*. Russian Academy of Sciences, Petrograd, 284 pp.
- Nilsson S (1842) Skandinavisk Herpetologi eller Beskrifning öfver de Sköldpaddor, Odlor, Ormar och Grodor, som Förekomma I Sverige Och Norrige, Hemte Deras Lefnadssätt, Födöamnen, Nyttä och Skada MM. Gleerups, Lund, 347 pp. <https://doi.org/10.5962/bhl.title.43795>
- Ohler A (1995) Digital pad morphology in torrent-living Ranid frogs. *Asiatic Herpetological Research* 6: 85–96.
- Okada Y (1928) Frogs in Korea. *Chosen Natural History Society Journal/ Chosen Hakubutsu Gakkai zasshi* 6: 15–46.
- Pyron RA, Wiens JJ (2011) A large-scale phylogeny of Amphibia including over 2800 species, and a revised classification of advanced frogs, salamanders, and caecilians. *Molecular Phylogenetics and Evolution* 61: 543–583. <https://doi.org/10.1016/j.ympev.2011.06.012>
- Ronquist F, Teslenko M, Van Der Mark P, Ayres DL, Darling A, Höhna S, Larget B, Liu L, Suchard MA, Huelsenbeck JP (2012) MrBayes 3.2: efficient Bayesian phylogenetic inference and model choice across a large model space. *Systematic Biology* 61: 539–542. <https://doi.org/10.1093/sysbio/sys029>
- Sambrook J, Fritsch EF, Maniatis T (1989) *Molecular cloning: a laboratory manual*. Cold Spring Harbor Laboratory Press, New York, 1659 pp.
- Savage JM (1975) Systematics and distribution of the Mexican and Central American stream frogs related to *Eleutherodactylus rugulosus*. *Copeia* 2: 254–306. <https://doi.org/10.2307/1442883>
- Shen Y, Jiang J, Yang D (2007) A new species of the genus *Rana*—*Rana hanluica* sp. nov. from Hunan Province, China (Anura: Ranidae). *Acta Zoologica Sinica* 53: 481–488.
- Shen YH (1986) A new ranid species (*Rana sangzhiensis*) from Hunan. *Acta Herpetologica Sinica/ Liangqi boxing dongwu yanjiu*, New Series, Chengdu 5(4): 290–294.
- Smith MA (1921) New or little-known reptiles and batrachians from southern Annam (Indo-China). *Proceedings of the Zoological Society of London* 1921: 423–440. <https://doi.org/10.1111/j.1096-3642.1921.tb03271.x>
- Stejneger L (1898) On a collection of batrachians and reptiles from Formosa & adjacent islands. *Journal of the College of Science, Imperial University, Japan* 12: 215–225.
- Tamura K, Stecher G, Peterson D, Filipowski A, Kumar S (2013) MEGA6: molecular evolutionary genetics analysis, version 6.0. *Molecular Biology and Evolution* 30: 2725–2729. <https://doi.org/10.1093/molbev/mst197>
- Wan H, Lyu ZT, Qi S, Zhao J, Li PP, Wang YY (2020) A new species of the *Rana japonica* group (Anura, Ranidae, Rana) from China, with a taxonomic proposal for the *R. johnsi* group. *ZooKeys* 942: 141–158. <https://doi.org/10.3897/zookeys.942.46928>

- Wang C, Qian L, Zhang C, Guo W, Pan T, Wu J, Wang H, Zhang B (2017) A new species of *Rana* from the Dabie Mountains in eastern China (Anura, Ranidae). *ZooKeys* 724: 135–153. <https://doi.org/10.3897/zookeys.724.19383>
- Wang K, Ren JL, Chen HM, Lyu ZT, Guo XG, Jiang K, Chen JM, Li JT, Guo P, Wang YY, Che J (2020) The updated checklists of amphibians and reptiles of China. *Biodiversity Science* 28(2): 189–218. <https://doi.org/10.17520/biods.2019238>
- Yan F, Jiang K, Chen H, Fang P, Jin J, Li Y, Wang S, Murphy RW, Che J, Zhang Y (2011) Matrilineal history of the *Rana longicrus* species group (*Rana*, Ranidae, Anura) and the description of a new species from Hunan, southern China. *Asian Herpetological Research* 2(2): 61–71. <https://doi.org/10.3724/SPJ.1245.2011.00061>
- Yang BT, Zhou Y, Min MS, Matsui M, Dong BJ, Li PP, Fong JJ (2017) Diversity and phylogeography of Northeast Asian brown frogs allied to *Rana dybowskii* (Anura, Ranidae). *Molecular Phylogenetics and Evolution* 112: 148–157. <https://doi.org/10.1016/j.ympev.2017.04.026>
- Ye CY, Fei L, Hu SQ (1993) Rare and economic amphibians of China. Sichuan Publishing House of Science and Technology, Chengdu, 412 pp.
- Ye CY, Fei L, Matsui M (1995) Taxonomic studies of Chinese *Rana japonica* Guenther. *Acta Herpetologica Sinica* 4: 82–87.
- Yuan ZY, Zhou WW, Chen X, Poyarkov Jr NA, Chen H-M, Jang-Liaw N-H, Chou WH, Matzke NJ, Iizuka K, Min M-S, Kuzmin SL, Zhang YP, Cannatella DC, Hillis DM, Che J (2016) Spatiotemporal diversification of the true frogs (genus *Rana*): a historical framework for a widely studied group of model organisms. *Systematic Biology* 65: 824–842. <https://doi.org/10.1093/sysbio/syw055>
- Zhao EM (1999) Diagnoses of a new frog and a new snake from China. *Sichuan Journal of Zoology/Sichuan dong wu* 18(3): 1.
- Zhao HP, Yang JX, Wang CP, Li PP, Murphy RW, Che J, Yuan ZY (2017) A new species of the genus *Rana* from Henan, central China (Anura, Ranidae). *ZooKeys* 694: 95–108. <https://doi.org/10.3897/zookeys.694.12513>

## Supplementary material I

### Table S1

Authors: Bin Wang

Data type: morphological measurements of adults

Explanation note: Measurements of adult specimens of *Rana wuyiensis* sp. nov. and its closely related species. Units given in mm. See abbreviations for the morphological characters in Materials and methods section.

Copyright notice: This dataset is made available under the Open Database License (<http://opendatacommons.org/licenses/odbl/1.0/>). The Open Database License (ODbL) is a license agreement intended to allow users to freely share, modify, and use this Dataset while maintaining this same freedom for others, provided that the original source and author(s) are credited.

Link: <https://doi.org/10.3897/zookeys.1065.67005.suppl1>

# New archidermapteran earwigs (Dermaptera) from the Middle Jurassic of Inner Mongolia, China

Shurong Xiong<sup>1</sup>, Michael S. Engel<sup>2,3</sup>, Lifang Xiao<sup>1</sup>, Dong Ren<sup>1</sup>

**1** College of Life Sciences and Academy for Multidisciplinary Studies, Capital Normal University, 105 Xisanhuanbeilu, Haidian District, Beijing 100048, China **2** Division of Entomology, Natural History Museum, and Department of Ecology & Evolutionary Biology, University of Kansas, 1501 Crestline Drive – Suite 140, Lawrence, Kansas 66045-4415, USA **3** Division of Invertebrate Zoology, American Museum of Natural History, Central Park West at 79<sup>th</sup> Street, New York, New York 10024-5192, USA

Corresponding author: Dong Ren ([rendong@mail.cnu.edu.cn](mailto:rendong@mail.cnu.edu.cn))

Academic editor: Fabian Haas | Received 8 August 2021 | Accepted 13 September 2021 | Published 26 October 2021

<http://zoobank.org/DC70097D-1B70-42E4-BA6F-9C15F0213EA2>

**Citation:** Xiong S, Engel MS, Xiao L, Ren D (2021) New archidermapteran earwigs (Dermaptera) from the Middle Jurassic of Inner Mongolia, China. ZooKeys 1065: 125–139. <https://doi.org/10.3897/zookeys.1065.72720>

## Abstract

Two new species of Archidermaptera are described and figured from the Middle Jurassic Jiulonghsan Formation of Daohugou, Inner Mongolia, China. *Aneuroderma oiodes* **gen. & sp. nov.** is described in the family Protodiplatyidae and *Sinopalaeodermata concavum* **sp. nov.** is established in the family Dermapteridae. Both new species share the typical characters of the extinct suborder Archidermaptera (e.g., pentamerous metatarsi, filiform and multimerous cerci, externalized ovipositor). *Aneuroderma* **gen. nov.** is compared with other genera of the Protodiplatyidae, while *S. concavum* **sp. nov.** allows us to emend the diagnosis of the genus *Sinopalaeodermata*. We briefly discuss the diversity of Archidermaptera and challenges to understanding relationships among this mid-Mesozoic diversity.

## Keywords

Dermapteridae, earwigs, new genus, new species, Protodiplatyidae, systematic palaeontology

## Introduction

The Dermaptera (earwigs) are, like all organisms, an interesting mosaic of primitive and derived traits – on the one hand they have a typical ‘orthopteroid’ habitus with chewing mouthparts, while on the other extant species have specialized cerci

modified as forceps; a vestigial ovipositor; reduced tarsal count; a shortened and tegminized forewing; a unique hind wing composed of a greatly enlarged anal fan, reduced remigium, and distinctive folding pattern; and have lost ocelli (Haas 1995; Grimaldi and Engel 2005). Dermaptera also have specialized maternal care widespread through the order, and date to at least the Early Cretaceous, and perhaps the latest Jurassic (Engel 2009). While the order is of unexceptional diversity in terms of species numbers, with only about 2000 extant species, there is considerable morphological variety, particularly in the form of the thoraces, tegmina, abdomens, and cerci (Haas 1995; Sakai 1996; Grimaldi and Engel 2005). The order is of modest age, with crown-group representatives extending to the Early Cretaceous, and the clade as a whole extending to the Triassic when considering stem groups (Bey-Bienko 1936; Vishniakova 1980; Carpenter 1992). It is possible that the extinct order Protelytroptera are further stem-Dermaptera, extending the combined lineage into the Early Permian (Haas and Kukalová-Peck 2001; Grimaldi and Engel 2005).

Excluding the Protelytroptera, the earliest definitive earwigs are classified in the suborder Archidermaptera, distinguished from other suborders by the pentamerous metatarsi, frequent presence of venation in the forewing tegmina, which are often longer, and a prominent externalized ovipositor (Engel 2003). In addition, species plesiomorphically retain ocelli and usually long, multiarticulated cerci that are, of course, not forcipate. In addition, the pro- and mesotarsi are more developed than their counterparts of the Eodermaptera and Neodermaptera, with 4 or 5 tarsomeres rather than the trimerous condition of more derived clades. Presently, there are three families recognized within the family: Protodiplatyidae, Turanoviidae, and Dermapteridae (Engel 2003; Engel and Haas 2007). Hitherto, there have been 31 species classified in 19 genera, with specimens being comparatively rare (Xing et al. 2016a; Xing et al. 2016b; Tihelka 2019). Current records are from the Late Triassic of England, Australia, and Kyrgyzstan; the Middle Jurassic of China; the Late Jurassic of Kazakhstan; and the Early Cretaceous of China (Martynov 1925; Bey-Bienko 1936; Vishniakova 1980; Zhang 1994, 2002; Jarzembowski 1999; Wappler et al. 2005; Shcherbakov 2008; Zhao et al. 2011) (Table 1).

Herein we describe a new genus and species of Protodiplatyidae and a new species of Dermapteridae, both preserved in the Middle Jurassic Jiulongshan Formation of Inner Mongolia Province, China. This discovery increases the diversity of Archidermaptera and complements our limited understanding of this suborder.

## Materials and methods

Three specimens were collected from the Middle Jurassic Jiulongshan Formation at Daohugou Village, Ningcheng County, Inner Mongolia, northeastern China. The age of the fossil deposit is approximately 164–165 Ma (Chen et al. 2004; Ren et al. 2010; Gao et al. 2021; Yang et al. 2021), within the Callovian stage of the later Middle Jurassic. The material is housed in the Key Lab of Insect Evolution and Environmental Changes, the College of Life Sciences, Capital Normal University, Beijing

**Table I.** Hierarchical classification of Archidermaptera and summary of tarsal formulae, where known. Interrogative marks (?) indicate missing data.

		Genus	Species	Data	
Suborder Archidermaptera Bey-Bienko, 1936	Superfamily Protodiplatyoidae Martynov, 1925	Family Dermapteridae Vishniakova, 1980	Genus <i>Brevicula</i> Whalley, 1985	<i>B. gradus</i> Whalley, 1985	4/5-4/5-5*
				<i>B. maculata</i> Kelly et al., 2018	?-?-?
			Genus <i>Dacryoderma</i> Engel, 2021	<i>D. teres</i> (Tihelka, 2019)	?-?-?
			Genus <i>Dermapteron</i> Martynov, 1925	<i>D. incerta</i> Martynov, 1925	?-?-?
			Genus <i>Dimapteron</i> Kelly et al., 2018	<i>D. corami</i> Kelly et al., 2018	?-?-?
			Genus <i>Jurassimedeola</i> Zhang, 2002	<i>J. orientalis</i> Zhang, 2002	?-?-?
			Genus <i>Palaeodermapteron</i> Zhao et al., 2011	<i>P. dicranum</i> Zhao et al., 2011	5-5-5
			Genus <i>Phanerogramma</i> Cockerell, 1915	<i>P. australis</i> Kelly et al., 2018	?-?-?
				<i>P. dunstani</i> Kelly et al., 2018	?-?-?
				<i>P. gouldsbroughi</i> Kelly et al., 2018	?-?-?
				<i>P. heeri</i> (Giebel, 1856)	?-?-?
				<i>P. kellyi</i> Tihelka, 2019	?-?-?
			Genus <i>Sinopalaeodermata</i> Zhang, 2002	<i>S. concavum</i> sp. nov.	5-5-5
				<i>S. neimongolense</i> Zhang, 2002, nom. emend.	5-5-5
	Genus <i>Trivenapteron</i> Kelly et al., 2018	<i>T. moorei</i> Kelly et al., 2018	?-?-?		
	Genus <i>Valdopterion</i> Kelly et al., 2018	<i>V. woodi</i> Kelly et al., 2018	?-?-?		
	Family Protodiplatyidae Martynov, 1925	Genus <i>Abrderma</i> Xing et al., 2016b	<i>A. gracilentum</i> Xing et al., 2016b	?-?-5	
		Genus <i>Aneuroderma</i> gen. nov.	<i>A. oiodes</i> sp. nov.	5-5-5	
		Genus <i>Archidermapteron</i> Vishniakova, 1980	<i>A. martynovi</i> Vishniakova, 1980	4-4-5	
		Genus <i>Asiodiplatys</i> Vishniakova, 1980	<i>A. speciosus</i> Vishniakova, 1980	4-4-5	
		Genus <i>Barbderma</i> Xing et al., 2016a	<i>B. oblonguatum</i> Xing et al., 2016a	?-?-?	
		Genus <i>Longicerciata</i> Zhang, 1994	<i>L. mesozoica</i> Zhang, 1994	5-5-5	
			<i>L. rumpens</i> Zhang, 1994	5-5-5	
		Genus <i>Microdiplatys</i> Vishniakova, 1980	<i>M. campodeiformis</i> Vishniakova, 1980	4-4-5	
			<i>M. oculatus</i> Vishniakova, 1980	4-4-5	
			<i>M. perfectus</i> Vishniakova, 1985	4-4-5	
		Genus <i>Perissoderma</i> Xing et al., 2016b	<i>P. triangulum</i> Xing et al., 2016b	5-5-5	
		Genus <i>Protodiplatys</i> Martynov, 1925	<i>P. fortis</i> Martynov, 1925	4-4-5	
			<i>P. gracilis</i> Vishniakova, 1980	4-4-5	
			<i>P. mongoliensis</i> Vishniakova, 1986	4-4-5	
		Genus <i>Sinoprotodiplatys</i> Nel et al., 2012	<i>S. ellipsoideuata</i> Xing et al., 2016a	5-5-5	
<i>S. zhangii</i> Nel et al., 2012			5-5-5		
Family Turanoviidae Engel, 2003 (Turanodermaptera Engel, 2019)		Genus <i>Turanovia</i> Vishniakova, 1980	<i>T. incompleta</i> Vishniakova, 1980	?-?-?	

\*Note that Whalley (1985) indicated that he could not determine the number of tarsomeres, stating that, "It is not possible to count the exact number of tarsal segments, of which there are certainly four and may well be five." Thus, we can only state that there are at least four tarsomeres, but it could be fully pentamerous.

(CNU; Dong Ren, Curator). Specimens were examined using a Leica M205C dissecting microscope, with ethanol added to help improve clarity and contrast with the surrounding matrix, thereby aiding the identification of fine details and the preparation of photographs. The detailed and enlarged photos were taken using a Nikon SMZ 25 microscope with a Nikon DS-Ri 2 digital camera. Line drawings were prepared using Adobe Illustrator CC and Adobe Photoshop CS5 graphics software. The higher classification followed herein is that of Engel and Haas (2007), and the morphological terminology employed in this paper is based on that of Giles (1963), Günther and Herter (1974).

## Systematic palaeontology

Order Dermaptera de Geer, 1773

Suborder Archidermaptera Bey-Bienko, 1936

Family Protodiplatyidae Martynov, 1925

Genus *Aneuroderma* Xiong, Engel & Ren, gen. nov.

<http://zoobank.org/1A4122EC-F912-4D76-9D89-A581796CF071>

**Diagnosis.** Moderate-sized earwigs, with numerous setose and distinctively sculptured (densely punctate-granulose throughout, particularly on head and thorax). Head broad, nearly as wide as anterior border of pronotum, posterior margin nearly straight. Antenna with 20 antennomeres; scape robust and slightly broader than remaining antennomeres; pedicel slightly longer than wide; all flagellomeres longer than wide. Compound eyes large and situated at posterior temples; ocelli absent. Dorsal surface without Y-shaped ecdysial cleavage scar. Pronotum approximately oval, anterior and posterior margins subequal in width, lateral margin convex and rounded. Tegmina without longitudinal veins; tegmina and squamata covering abdominal segment II. Legs with abundant short setae; femora carinulate; all tarsi pentamerous (i.e., tarsal formula 5-5-5 rather than the 4-4-5 of some genera); pretarsal claws simple. Female with exposed ovipositor. Pygidium small. Cerci filiform and long, with about 30 cercomeres.

**Etymology.** The generic name is a combination of the Greek prefix *a-* (*ἄ-*, alpha privativum designating negation), *neûron* (*νεῦρον*, meaning, “nerve”), and *dérma* (*δέρμα*, genitive *dérmatos*, meaning, “skin” – an allusion to the leathery tegmina and from which the ordinal name is derived, Dermaptera literally meaning, “skin wings”), referencing the absence of tegminal venation, a rare feature among Archidermaptera. The gender of the name is neuter.

*Aneuroderma oiodes* Xiong, Engel & Ren, gen. et sp. nov.

<http://zoobank.org/3AE3DBE5-7926-461C-866C-EE41EBDB272A>

Figs 1–3

**Diagnosis.** As for the genus (*vide supra*).

**Type material.** **Holotype**, a completely preserved female, CNU-DER-NN2021003C/P; **paratype**, CNU-DER-NN2021004C/P. All type material deposited in the College of Life Sciences, Capital Normal University, Beijing, China.

**Locality and horizon.** Jiulongshan Formation (Middle Jurassic); Daohugou Village, Wuhua Township, Ningcheng County, Inner Mongolia, China.

**Description.** Adult female, preserved in both dorsal and ventral aspects. Body with numerous setae and distinctively sculptured (densely punctate-granulose throughout, particularly on head and thorax). Total length as preserved (excluding antennae, ovipositor, and cerci) about 10.75 mm. Head medial length from clypeal apex to pos-

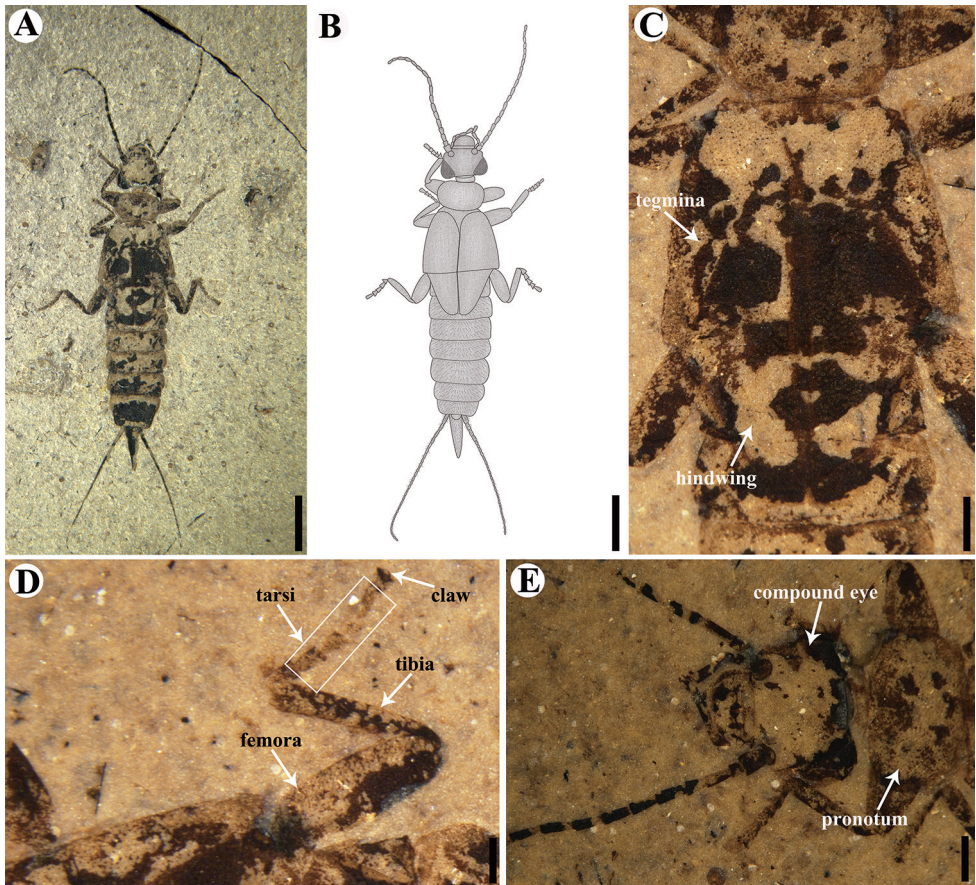


**Figure 1.** Holotype of *Aneuroderma oiodes* gen. et sp. nov. CNU-DER-NN2021003C. **A** Photograph of dorsal aspect **B** line drawing of dorsal aspect **C** dorsal view of tegmina and squamata of hind wings **D** anterior lateral (prolateral) view of right midleg **E** dorsal aspect of head. Scale bars: 2.0 mm (**A**, **B**); 0.5 mm (**C**, **D**, **E**). The tegmina and squamata of the hind wings in **C**, the right midleg in **D**, and the head in **E** are photographed under ethanol.

terior border 1.57 mm, maximum width (across level of compound eyes) 1.56 mm, prognathous; maxillary palpus pentamerous, ca 1.33 mm long (Fig. 1E). Antennal length 5.2 mm, with 20 elongate antennomeres; scape thick, broader than remaining antennomeres, longer than wide, length 0.31 mm, apical width 0.22 mm; pedicel shortest, length 0.17 mm; flagellomeres longer than wide and distally becoming tapered. Compound eyes large and prominent, located near posterior margin of head, compound eye length 0.72 mm; distance between compound eyes distinctly longer than compound eye length (Fig. 1E). Ocelli absent. Pronotum approximately oval and almost as broad as posterior margin of head, medial length 1.12 mm, maximum width 1.71 mm; anterior margin 1.56 mm wide, posterior margin 1.53 mm wide, anterior margin nearly straight, posterior margin slightly convex and lateral margins convex-

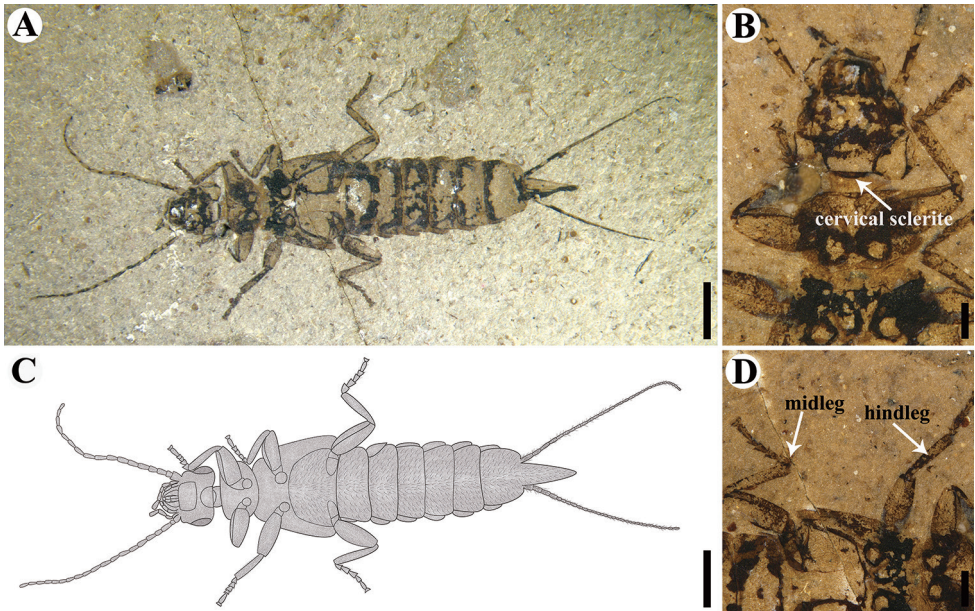


**Figure 2.** Holotype of *Aneuroderma oiodes* gen. et sp. nov. CNU-DER-NN2021003P. **A** Photograph of ventral aspect **B** ventral view of head **C** line drawing of ventral aspect **D** ventral view of midleg and hindleg. Scale bars: 2.0 mm (**A**, **C**); 0.5 mm (**B**, **D**). The head in **C** and the right midleg and hindleg in **D** are photographed under ethanol.

ly rounded. Tegmina well developed, without venation, length 2.41 mm, maximum width 1.39 mm, lateral margins arc-shaped, posterior margins truncate, squamata extending well beyond tegminal apex, tegmina and squamata covering abdominal terga I and II (Fig. 1C). Femora compressed and ventrally carinulate; tibiae elongate, slender, almost as long as femora; all tarsi pentamerous (Fig. 2D). Pretarsal claws present and simple; arolium absent (Fig. 1D). Abdomen cylindrical, with dense, soft, short setae, lateral margins relatively convex, almost all segments wider than long with apical margins straight, abdominal length as preserved (excluding cerci) 5.38 mm, maximum width 2.41 mm. Abdomen distally with external ovipositor, length 1.64 mm. Pygidium small. Cerci 5.33 mm long, longer than one-half abdominal length, with ca 30 elongate cercomeres, margins with abundant short setae.

**Etymology.** The specific epithet is the Greek neuter adjective *oïodes* (ὀϊόδες, meaning, “oval” or “egg-like”), as a reference to the ovoid pronotum.

**Remarks.** The new genus is placed within Protodiplatyidae on the basis of the characteristic filiform antenna with 17–23 antennomeres; pedicel and flagellomere I subequal in size; pentamerous metatarsus; cerci elongate, slender, and multimerous; and externalized ovipositor in females.

Key diagnostic characters of *Aneuroderma* gen. nov. are summarized in Table 2 and compared with those of nine genera of Protodiplatyidae. *Aneuroderma* gen. nov. can be distinguished from *Archidermapteron* Vishniakova, 1980 by the posterior margin of head as wide as anterior border of pronotum, 20 antennomeres, tegmina without lon-

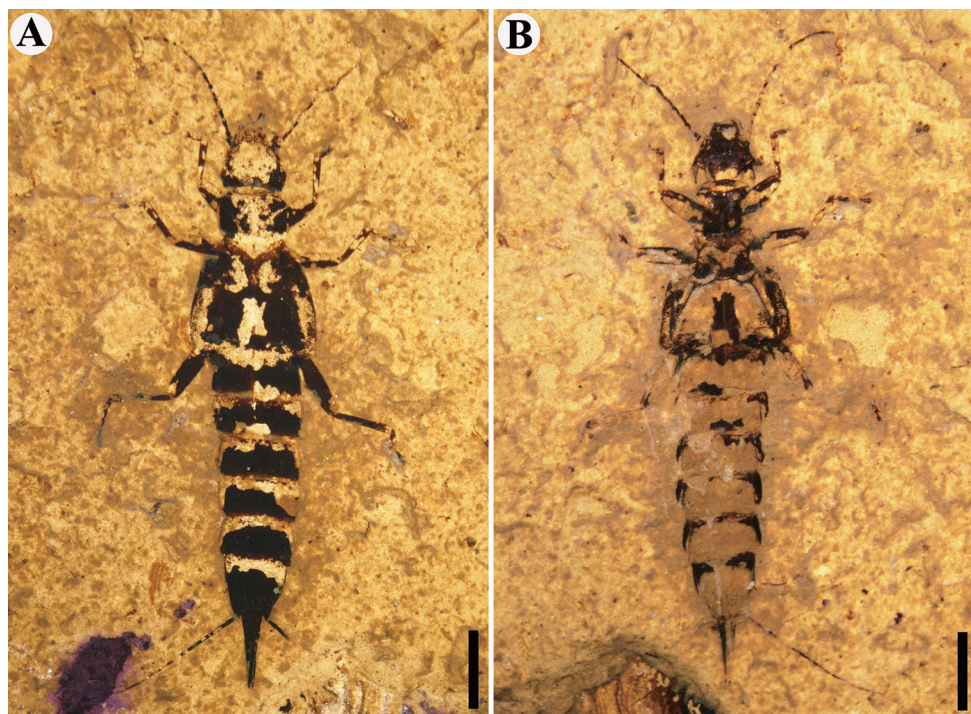


**Figure 3.** Paratype of *Aneuroderma oiodes* gen. et sp. nov. CNU-DER-NN2021004C/P. **A** Photograph of dorsal aspect **B** photograph of ventral aspect. Scale bars, 2.0 mm (**A**, **B**). The body in **A** and **B** are photographed under ethanol.

gitudinal veins, and hind wings extending to apex of abdominal segment II, pygidium small, 30 cercomeres, and a cercus/body ratio of 0.5. By contrast, *Archidermapteron* has the head narrower than the pronotum, the tegmina with longitudinal veins, hind wings extending beyond abdominal segment IV, pygidium transverse and trapeziform, and 40 cercomeres that together are slightly shorter than the body. *Aneuroderma* gen. nov. differs from *Longicerciata* Zhang, 1994 by the latter with the head broader than the pronotum, 26 antennomeres, at least 36 cercomeres, and a cercus/body ratio of 1. *Aneuroderma* gen. nov. differs from *Barbderma* Xing et al., 2016a in the number of antennomeres (20 instead of 19), and the hind wings extending to the apex of abdominal segment II, instead of segment I. *Aneuroderma* gen. nov. is similar to *Asiodiplatys* Vishniakova, 1980 in that the tegmina lack longitudinal veins and the hind wings extend to the apex of abdominal segment II, but the former differs from the latter in only 20 antennomeres (vs. 22 antennomeres), the posterior margin of the pronotum straight (vs. pronotum with shallow, broad notch anteriorly), and 30 cercomeres (vs. 40 cercomeres). *Aneuroderma* gen. nov. can be separated from *Abrderma* Xing et al., 2016b, *Microdiplatys* Vishniakova, 1980, *Perissoderma* Xing et al., 2016b, and *Protodiplatys* Martynov, 1925, by the following traits: (1) absence of longitudinal veins in tegmina (present in the aforementioned genera), and (2) 20 antennomeres (vs. 17 to 19 in the other genera). The new genus is readily differentiated from *Sinoprotodiplatys* Nel et al.,

**Table 2.** Summary and comparisons of key characters for several described genera of Protodiplatyidae. Interrogative marks (?) indicate data unavailable.

Genus	Head	Number of antennomeres	Pronotum	Tegmina	Pygidium	Cerci (ratio lengths cercus/body, cercomeres)
<i>Abrderma</i>	Broader than pronotum	17–19	Elliptical, anterior and posterior margins subequal in width	With venation, reaching second abdominal segment	Small	0.2, ?
<i>Archidermapteron</i>	Narrower than pronotum	17–19	Reniform, broad notch anteriorly	With venation, reaching fourth abdominal segment	Transverse, trapeziform	1.0, at least 40
<i>Asiodiplatys</i>	Narrower than pronotum	22	With shallow, broad notch anteriorly	Without venation, not reaching second abdominal segment	?	0.5, 40
<i>Barbderma</i>	?	19	Oblong or trapezoidal, anterior and posterior margins subequal in width	With venation, reaching first abdominal segment	Small	0.42, ?
<i>Longicerciata</i>	Broader than pronotum	26	Transverse, anterior margin wider than posterior margin	Without venation, reaching fourth abdominal segment	?	1.0, at least 36
<i>Microdiplatys</i>	Broader than pronotum	19	Transverse	With venation, reaching fourth abdominal segment	Not protruding	1.0, at least 36
<i>Perissoderma</i>	Narrower than pronotum	17	Elliptical, anterior margin wider than posterior margin	With venation, reaching third abdominal segment	Small	0.5, ?
<i>Protodiplatys</i>	Narrower than pronotum	17–18	Transverse, notch in front, broadly rounded posteriorly	With venation, reaching fourth abdominal segment	Transverse, trapeziform	0.5, no more than 40
<i>Sinoprotodiplatys</i>	Narrower than pronotum	18	Anterior and posterior margins subequal in width	Without venation, reaching fourth abdominal segment	?	0.8, 20
<i>Aneuroderma</i> gen. nov.	As wide as pronotum	20	Oval, anterior and posterior margins subequal in width	Without venation, reaching second abdominal segment	Small	0.5, 30

2012 by the posterior margin of the head and anterior border of the pronotum equal in width (head narrower than pronotum in the latter), 20 antennomeres, and 30 cercomeres (18 antennomeres and 20 cercomeres in the latter). Lastly, the distinctive punctate sculpture of the new genus is quite distinctive among several Archidermaptera.

## Family Dermapteridae Vishniakova, 1980

### Genus *Sinopalaeodermata* Zhang, 2002

*Sinopalaeodermata* Zhang, 2002: 351. Type species: *Sinopalaeodermata neimonggolensis* Zhang, 2002, *nomen imperfectum* [*recte neimonggolense*], by original designation.

**Emended diagnosis** [modified from Zhang (2002)]. Moderate-sized earwigs, with short and fine pubescence; head triangular, length subequal to width, mandibles denticulate; antenna filiform, with at least 19 antennomeres (as noted by Zhang

(2002)), scape stout and enlarged, pedicel rather small, clearly shorter than scape and flagellomere I; ocelli present; neck prominent, divided into anterior and posterior cervical sclerites ('blattoid' neck arrangement). Pronotum transverse, broader than long and about as broad as head. Femora compressed and ventrally carinate; all tarsi pentamerous, shorter than tibiae; pretarsal claws well developed and bearing broom-shaped arolia. Procoxal cavities positioned close to each other; mesocoxal cavities remote, metacoxal cavities elongate transversely and moderately separated. Tegmina with longitudinal veins strongly developed, main veins of Sc, R, M, and Cu present. Female with a pair of elongate valvulae entirely exposed. Cerci flexible, long, filiform, and multimerous.

**Included species.** Aside from the type species, the genus currently includes *S. concavum* Xiong, Engel & Ren, sp. nov. (*infra*).

***Sinopalaeodermata concavum* Xiong, Engel & Ren, sp. nov.**

<http://zoobank.org/9759E27B-8954-48A1-B220-57514C01F07F>

Figures 4, 5

**Diagnosis.** The new species can be distinguished from the type species, *Sinopalaeodermata neimonggolense* (note that the name *Sinopalaeodermata* is neuter, not feminine, as *dérmat*a is the neuter nominative plural of *dérma*; and given that the specific epithet is adjectival it must still agree in gender with the generic name) by the relatively straight apical margin of the penultimate sternum (in *S. neimonggolense* the penultimate sternum has a concave margin); the roughly reniform pronotum, with the anterior margin concave medially the posterior margin weakly convex, and lateral margins rounded (in *S. neimonggolense* the pronotum is approximately rectangular, with the anterior margin almost as wide as the posterior margin, and the lateral margins relatively straight and parallel to each other); the tegmina with a more pronounced concave arc marginally at the apex of Rs (in *S. neimonggolense* the margin is more sloping rather than deeply concave); and M does not extend to near the apex of CuA, with CuP terminating more proximal to CuA (even before the tangent with M) (in *S. neimonggolense* M terminates more proximally and CuP extends to the apex of CuA).

**Holotype.** A completely preserved female, CNU-DER-NN2021005C/P, deposited in the College of Life Sciences, Capital Normal University, Beijing, China.

**Locality and horizon.** Jiulongshan Formation (Middle Jurassic); Daohugou Village, Wuhua Township, Ningcheng County, Inner Mongolia, China.

**Description.** Adult female, preserved in both dorsal and ventral aspects. Total length as preserved (excluding antennae, cerci, and valvulae) about 18.02 mm. Body with sparse pubescence and punctate. Head medial length from clypeal apex to posterior border 2.08 mm, maximum width (across level of compound eyes) 2.27 mm, triangular. Compound eye large, ovate, located near posterior margin of head; compound eye length 0.91 mm; width between compound eyes 2.58 mm. Ocelli comparatively small. Cervix with large anterior and posterior cervical sclerites, anterior sclerite slightly larger than posterior sclerite. Pronotum approximately reniform, medial length 1.46

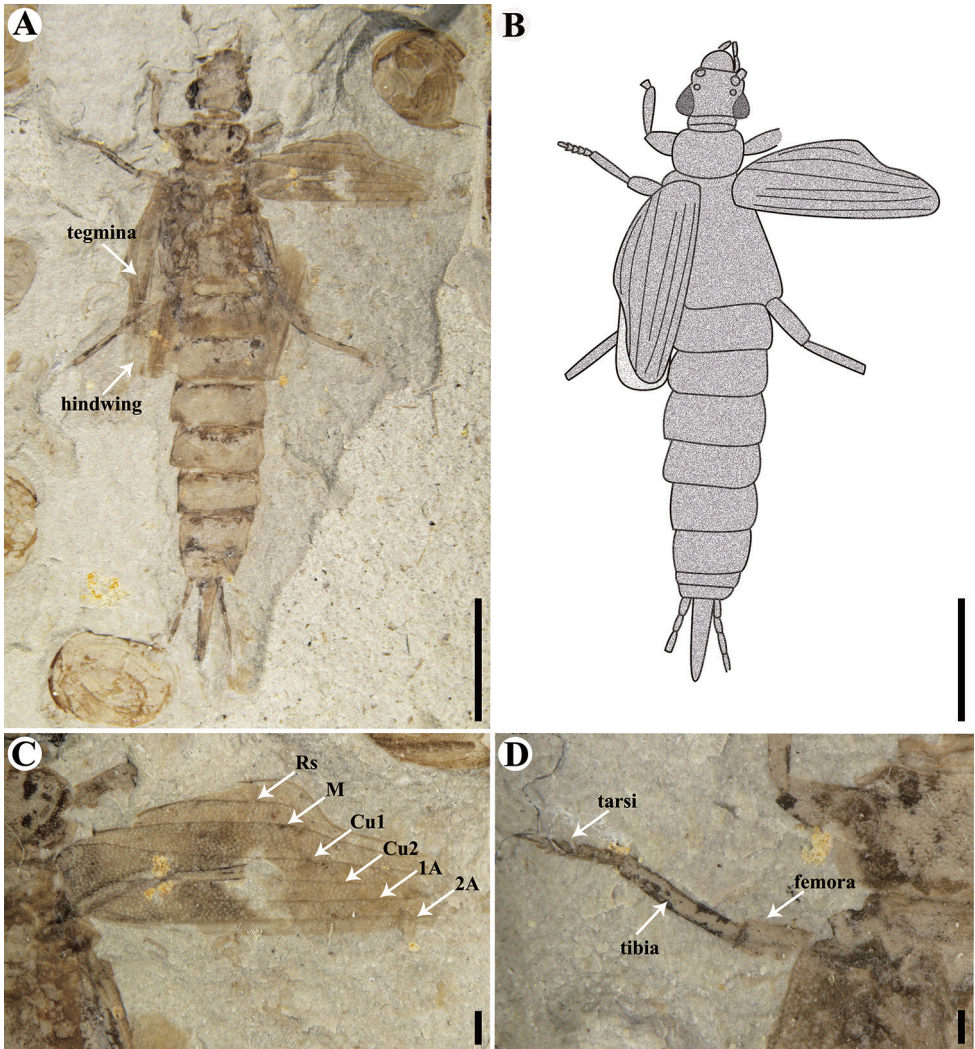


**Figure 4.** Holotype of *Sinopalaeodermata concavum* sp. nov. CNU-DER-NN2021005C. **A** Photograph of dorsal aspect **B** line drawing of dorsal aspect **C** dorsal view of right tegmen **D** anterior lateral (pro-lateral) view of left midleg. Scale bars: 4.0 mm (**A**, **B**); 0.5 mm (**C**, **D**).

mm, maximum width 2.58 mm, anterior width 1.64 mm, posterior width 2.07 mm, anterior margin concave and posterior margin arched, lateral margins convexly rounded. Mesoscutellum large, elliptical, entirely exposed. Tegmina present, not truncated, length 6.73 mm, maximum width 2.55 mm, with medially sinuate anterior (lateral) margin and straight posterior (mesal) margin. Veins simple, Rs curved anterior margin, fading out just before margin; M simple, basally and apically straight, gently curved medially; Cu with two branches (CuA and CuP), CuP terminates proximal to CuA; A1 and A2 simple and straight, running parallel to each other and posterior margin,

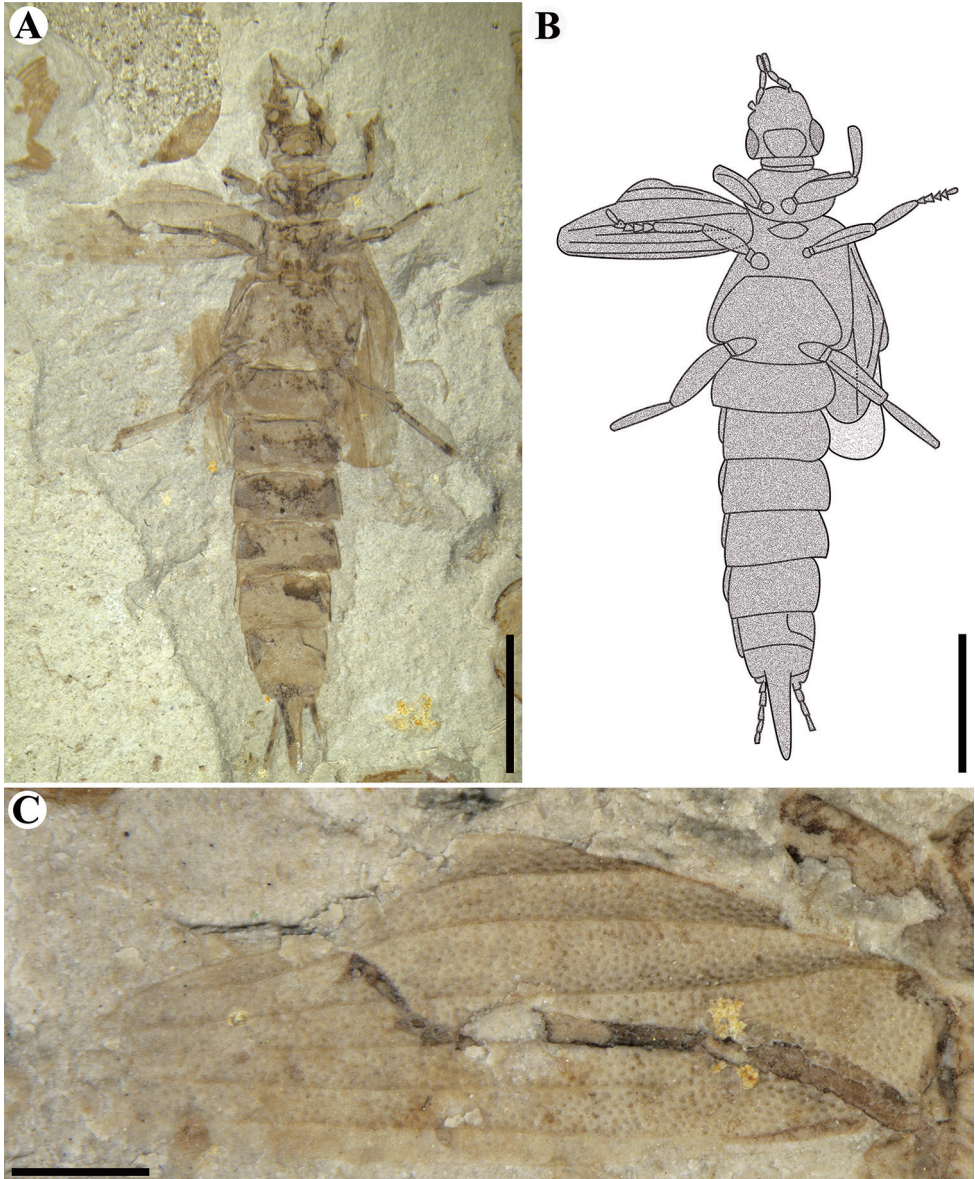


**Figure 5.** Holotype of *Sinopalaeodermata concavum* sp. nov. CNU-DER-NN2021005P. **A** Photograph of ventral aspect **B** line drawing of ventral aspect **C** ventral view of right midleg and tegmen. Scale bars: 4.0 mm (**A, B**); 1 mm (**C**).

terminating apically (Fig. 4C). Femora compressed and ventrally carinate (Fig. 4D); tibiae elongate, slender, and almost as long as femora; tarsi pentamerous, tarsomere IV slightly extending under base of tarsomere V (Fig. 5C). Pretarsal claws present but not well preserved. Abdominal length as preserved (excluding cerci) 9.75 mm, maximum width 3.52 mm; all segments distinctly wider than long, lateral abdominal margins

gently convex. Pygidium not evident. Ovipositor exposed, 2.84 mm long. Cerci as preserved only 2.9 mm long, with segments but not clearly preserved.

**Etymology.** The specific epithet is taken from the Latin adjective *concauus* (meaning, “concave”), in reference to the more pronounced concave margin to the tegmina relative to the type species.

## Discussion

Both of the new species described herein are easily recognized as archidermapterans owing to the pentamerous metatarsi (and more than three pro- and mesotarsomeres); elongate, flexible, and multimerous cerci; and the externalized ovipositor. Jurassic earwigs are known mostly from four assemblages: the Jiulongshan flora of the Middle Jurassic, the England flora of the Early and Late Jurassic, and the Karatau flora of the Late Jurassic (Vishniakova 1980; Zhang 1994, 2002; Zhao et al. 2011; Kelly et al. 2018; Tihelka 2019). Archidermaptera were seemingly the most abundant form of earwigs during these epochs, with 28 species in 21 genera (Table 1), compared to only seven species in five genera of Eodermaptera. Numerous fossil insects and plants have been described from the Jiulongshan Formation (e.g., Ren et al. 2010; Gao et al. 2021), yet earwigs are comparatively rare, with only eight species reported from the locality.

Tarsal formulae have been used to distinguished significant groups of fossil Dermaptera. All Neodermaptera and Eodermaptera have three tarsomeres (3-3-3), while the number of tarsomeres is greater, where known, among Archidermaptera (Table 1) (Engel 2003). Unfortunately, tarsi are unknown for many fossil genera, particularly among the Dermapteridae, and so general patterns are difficult to determine. Nonetheless, historically the Dermapteridae have been considered to have a 5-5-5 formula, while Protodiplatyidae include genera with 5-5-5 and 4-4-5 formulae (Engel 2003; Zhao et al. 2011). What remains to be ascertained from a detailed phylogenetic study is whether the variable tarsal formulae among Protodiplatyidae is reflective of paraphyly on the part of this family, or whether it renders Dermapteridae paraphyletic. Unfortunately, currently available specimens and data do not allow for a robust resolution of this difficulty, thus emphasizing the need for further exploration of Jurassic and Late Triassic deposits throughout the world in the hope of recovering more completely preserved material of these lineages and allowing a comprehensive comparison among living and fossil Dermaptera.

## Conclusion

Based on three well-preserved fossil specimens from the Middle Jurassic, we describe a new genus and two new species, *Aneuroderma oiodes* gen. et sp. nov. (Protodiplatyidae) and *Sinopalaeodermata concavum* sp. nov. (Dermapteridae). We make extensive comparisons with other Archidermaptera and discuss challenges in understanding relationships among these Triassic and Jurassic lineages.

## Acknowledgments

We express our gratitude to the Editorial Board of *Zookeys*, and in particular Dr Fabian Haas. We thank Dr Petr Kocarek and another anonymous reviewer for their valuable comments on this manuscript. We are grateful to Yue Mao (Capital Normal University) for helpful discussions and advice with the project. D.R. was supported by grants from the National Natural Science Foundation of China (grant nos. 31730087, 32020103006 and 41688103). The authors declare no competing interests.

## References

- Bey-Bienko GYa (1936) Insectes dermaptères, Faune de l'URSS. Akadem iya Nauk SSSR, Zoologicheskij Instiute, Moscow, 239 pp.
- Carpenter FM (1992) Treatise on Invertebrate Paleontology, Part R Arthropoda 4, Vol. 3: Superclass Hexapoda. The Geological Society of America, Inc. & The University of Kansas, Kansas. 655 pp.
- Chen W, Ji Q, Liu DY, Zhang Y, Song B, Liu XY (2004) Isotope geochronology of the fossil-bearing beds in the Daohugou area, Ningcheng, Inner Mongolia. *Geological Bulletin of China* 23(12): 1165–1169.
- Cockerell TDA (1915) British fossil insects. *Proceedings of the United States National Museum* 49: 469–499. <https://doi.org/10.5479/si.00963801.49-2119.469>
- Engel MS (2003) The earwigs of Kansas, with a key to genera north of Mexico (Insecta: Dermaptera). *Transactions of the Kansas Academy of Science* 106: 115–123. [https://doi.org/10.1660/0022-8443\(2003\)106\[0115:TEOKWA\]2.0.CO;2](https://doi.org/10.1660/0022-8443(2003)106[0115:TEOKWA]2.0.CO;2)
- Engel MS (2009) Gregarious behaviour in Cretaceous earwig nymphs (Insecta, Dermaptera) from southwestern France. *Geodiversitas* 31: 129–135. <https://doi.org/10.5252/g2009n1a11>
- Engel MS (2019) A new species of spongiphorine earwig in Miocene amber from the Dominican Republic (Dermaptera: Spongiphoridae). *Novitates Paleontologicae* 2(6): 560–565. <https://doi.org/10.11646/palaeontology.2.6.3>
- Engel MS (2021) A new genus of Early Jurassic earwigs from England (Dermaptera). *Novitates Paleontologicae* 22: 1–3. <https://doi.org/10.17161/np.22.15759>
- Engel MS, Haas F (2007) Family-group names for earwigs (Dermaptera). *American Museum Novitates* 3567: 1–20. [https://doi.org/10.1206/0003-0082\(2007\)539\[1:FNFED\]2.0.CO;2](https://doi.org/10.1206/0003-0082(2007)539[1:FNFED]2.0.CO;2)
- Gao TP, Shih CK, Ren D (2021) Behaviors and interactions of insects in mid-Mesozoic ecosystems of northeastern China. *Annual Review of Entomology* 66: 337–354. <https://doi.org/10.1146/annurev-ento-072720-095043>
- Geer CDE (1773) *Mémoires pour servir à l'histoire des insectes* (tome troisième). Hesselberg, Stockholm, 696 pp.
- Giebel GC (1856) Die Insecten und Spinnen der Vorwelt mit steter Berücksichtigung der lebenden Insekten und Spinnen. *Die Fauna der Vorwelt* 2: 1–511.
- Giles ET (1963) The comparative external morphology and affinities of the Dermaptera. *Transactions of the Royal Entomological Society of London* 115: 95–164. <https://doi.org/10.1111/j.1365-2311.1963.tb00816.x>

- Grimaldi D, Engel MS (2005) *Evolution of the Insects*. Cambridge University Press, New York, 755 pp.
- Günther K, Herter K (1974) *Dermaptera (Ohrwürmer)*. Handbuch der Zoologie: Eine Naturgeschichte der Stämme des Tierreiches. IV Band: Arthropoda – 2 Hälfte: Insecta, Zweite Auflage, 2 Teil: Spezielles 11: 1–158.
- Haas F (1995) The phylogeny of the Forficulina, a suborder of the Dermaptera. *Systematic Entomology* 20(2): 85–98. <https://doi.org/10.1111/j.1365-3113.1995.tb00085.x>
- Haas F, Kukulová-Peck J (2001) Dermaptera hindwing structure and folding: new evidence for familial, ordinal and superordinal relationships within Neoptera (Insecta). *European Journal of Entomology* 98: 445–509. <https://doi.org/10.14411/eje.2001.065>
- Jarzemowski EA (1999) *Arthropods–2: Insects*. In Swift A, Martill DM. (eds) *Fossil of the Rhaetian Penarth Group*. Palaeontological Association Field Guides to Fossils 9: 149–60. London: The Palaeontological Association, 312 pp.
- Kelly RS, Ross AJ, Jarzemowski EA (2018) Earwigs (Dermaptera) from the Mesozoic of England and Australia, described from isolated tegmina, including the first species to be named from the Triassic. *Earth and Environmental Science Transactions of the Royal Society of Edinburgh* 107: 129–143. <https://doi.org/10.1017/S1755691017000329>
- Martynov AV (1925) To the knowledge of fossil insects from Jurassic beds in Turkestan. 2. Raphidioptera (continued), Orthoptera (s.l.), Odonata, Neuroptera. *Bulletin de l'Academie des sciences de Russie*. VI serie 19: 569–598.
- Nel A, Garrouste C, Waller A, (2012) Evolution and palaeosynecology of the Mesozoic earwigs (Insecta: Dermaptera). *Cretaceous Research* 33(1): 189–195. <https://doi.org/10.1016/j.cretres.2011.10.002>
- Ren D, Shih CK, Gao TP, Yao YZ, Zhao YY (2010) *Silent Stories — Insect Fossil Treasures from Dinosaur Era of the Northeastern China*. Science Press, Beijing, 322 pp.
- Sakai S (1996) Notes on the contemporary classification of Dermaptera and recent references on Dermaptera. In: Sakai S (Ed.) *Taxonomy of the Dermaptera: Proceedings of 20<sup>th</sup> International Congress of Entomology*. Firenze, Italy, 25–31 August 1996, 1–10.
- Shcherbakov DE (2008) Madygen, Triassic Lagerstätte number one, before and after Sharov. *Alavesia* 2: 113–124.
- Tihelka E (2019) New Mesozoic earwigs from England, with a catalogue of fossil Dermaptera. *Proceedings of the Geologists' Association* 130(5): 609–611. <https://doi.org/10.1016/j.pgeola.2019.06.003>
- Vishniakova VN (1980) Earwig (Insecta: Forficulida) from the Upper Jurassic of the Karatau range. *Paleontological Journal* 14: 63–79.
- Vishniakova VN (1985) Novaya ukhovertka iz Yury Sibiri. *Yurskie Nasekomye Sibiri i Mongolii* 146–147.
- Vishniakova VN (1986) Earwigs. Forficulida (=Dermaptera), in *Nasekomye v rannemelovykh ekosistemakh zapadnoy Mongolii*. The Joint Soviet-Mongolian Palaeontological Expedition 28:171.
- Wappler T, Engel MS, Haas F (2005) The earwigs (Dermaptera: Forficulidae) from the middle Eocene Eckfeld Maar, Germany. *Polskie Pismo Entomologiczne* 74: 227–250.

- Whalley PES (1985) The Systematics and palaeogeography of the Lower Jurassic insects of Dorset, England. *Bulletin of the British Museum (Natural History), Geology Series* 39(3): 107–189.
- Xing CY, Shih CK, Zhao YY, Ren D (2016a) New protodiplatyids (Insecta: Dermaptera) from the Lower Cretaceous Yixian Formation of northeastern China. *Cretaceous Research* 64: 59–66. <https://doi.org/10.1016/j.cretres.2016.03.016>
- Xing CY, Shih CK, Zhao YY, Ren D (2016b) New earwigs in Protodiplatyidae (Insecta: Dermaptera) from the Middle Jurassic Jiulongshan Formation of northeastern China. *Zootaxa* 4205(2): 180–188. <https://doi.org/10.11646/zootaxa.4205.2.7>
- Yang HR, Shi CF, Engel MS, Zhao ZP, Ren D, Gao TP (2021) Early specializations for mimicry and defense in a Jurassic stick insect. *National Science Review* 8: nwaa056. <https://doi.org/10.1093/nsr/nwaa056>
- Zhang JF (1994) Discovery of primitive fossil earwigs (Insecta) from Late Jurassic of Laiyang, Shangdong and its significance. *Acta Palaeontologica Sinica* 33(2): 229–245.
- Zhang JF (2002) The most primitive earwigs (Archidermaptera, Dermaptera insect) from the Upper Jurassic of Nei Monggol Autonomous Region, northeastern China. *Acta Micropalaeontologica Sinica* 17: 459–464.
- Zhao JX, Shih CK, Ren D, Zhao YY (2011) New primitive fossil earwig from Daohugou, Inner Mongolia, China (Insecta: Dermaptera: Archidermaptera). *Acta Geologica Sinica (English Edition)* 85(1): 75–80. <https://doi.org/10.1111/j.1755-6724.2011.00380.x>



# Taxonomic and identification review of adventive *Fiorinia* Targioni Tozzetti (Hemiptera, Coccoomorpha, Diaspididae) of the United States

Muhammad Z. Ahmed<sup>1,2</sup>, Matthew R. Moore<sup>3</sup>, Eric A. Rohrig<sup>2</sup>,  
Cindy L. McKenzie<sup>1</sup>, Di Liu<sup>4</sup>, Jinian Feng<sup>4</sup>,  
Benjamin B. Normark<sup>5</sup>, Douglass R. Miller<sup>2,6</sup>

**1** Subtropical Insects and Horticulture Research, Agricultural Research Service, United States Department of Agriculture, 2001 South Rock Road, Fort Pierce, Florida, USA **2** Florida State Collection of Arthropods, Division of Plant Industry, Florida Department of Agriculture and Consumer Services, Gainesville, Florida, USA **3** Molecular Diagnostics Laboratory, Division of Plant Industry, Florida Department of Agriculture and Consumer Services, Gainesville, Florida, USA **4** Key Laboratory of Plant Resources and Pest Management, Ministry of Education, Entomological Museum, College of Plant Protection, Northwest A & F University, Yangling, Shaanxi Province, China **5** Department of Biology and Graduate Program in Organismic and Evolutionary Biology, University of Massachusetts, Amherst, Massachusetts, USA **6** Retired Research Entomologist, Systematic Entomology Lab, Agricultural Research Service, United States Department of Entomology, Beltsville, Maryland, USA

Corresponding author: Muhammad Z. Ahmed ([muhammad.ahmed@usda.gov](mailto:muhammad.ahmed@usda.gov))

---

Academic editor: Roger Blackman | Received 27 May 2021 | Accepted 19 August 2021 | Published 27 October 2021

---

<http://zoobank.org/D3943238-0B1B-48B0-8FA8-C8E5EED83736>

---

**Citation:** Ahmed MZ, Moore MR, Rohrig EA, McKenzie CL, Liu D, Feng J, Normark BB, Miller DR (2021) Taxonomic and identification review of adventive *Fiorinia* Targioni Tozzetti (Hemiptera, Coccoomorpha, Diaspididae) of the United States. ZooKeys 1065: 141–203. <https://doi.org/10.3897/zookeys.1065.69171>

---

## Abstract

This work provides general descriptions, illustrations, molecular diagnostic data, taxonomic keys, slide mounting recommendations, and Florida distribution records for *Fiorinia* Targioni Tozzetti species occurring in the USA. Species treated are *F. externa* Ferris, *F. fioriniae* (Targioni Tozzetti), *F. japonica* Kuwana, *F. pinicola* Maskell, *F. phantasma* Cockerell & Robinson, *F. proboscitaria* Green, and *F. theae* Green. New descriptions of second-instar males and females of all seven species in addition to first-instar nymphs and adult females of *F. phantasma* and *F. proboscitaria* are presented. Taxonomic keys to second-instar males and females are developed for the first time and previously available taxonomic keys to first-instar nymphs and adult females are improved. DNA sequences were used to further evaluate the monophyly of *Fiorinia* and provide additional diagnostic tools for *Fiorinia* species. Multigene phylogenetic analyses, COI barcoding methods, and examination of type material indicate that *F. yongxingensis* Liu, Cai & Feng,

2020, **syn. nov.** is a junior synonym of *F. phantasma*. A morphological survey of the genus demonstrates, for the first time, the utility of second-instar males for diagnostics. This study will help inform regulatory and pest management decisions by facilitating morphological and molecular identification of adventive *Fiorinia* species occurring in the USA.

### Keywords

Armored scale insects, DNA barcodes, Florida, palms, phantasma scale, slide mounting

## Introduction

The genus *Fiorinia* (Hemiptera, Diaspididae) comprises 70 species (García Morales et al. 2016) apparently native to Asia (Williams and Watson 1988). The genus, as presently defined, appears to represent a monophyletic group, according to a recent molecular phylogenetic analysis (Normark et al. 2019). Species in the genus are pupillarial; i.e., the adult female remains inside the exuviae of the second-instar female and does not form a scale cover. Seven species have been reported to cause economic damage, including *F. externa* Ferris, 1942 (McClure 1977), *F. fioriniae* (Targioni Tozzetti, 1867) (Beardsley and González 1975), *F. japonica* Kuwana, 1902 (Tang 1984), *F. phantasma* Cockerell & Robinson, 1915 (Ahmed 2018; Liu et al. 2020), *F. pinicola* Maskell, 1897 (Miller and Davidson 1990), *F. proboscitaria* Green, 1900 (Ahmed and Stocks 2020), and *F. theae* Green, 1900 (Gill 1997). Unfortunately, all seven species have been introduced into the USA during successive waves of invasion. *Fiorinia fioriniae*, *F. phantasma*, *F. proboscitaria*, and *F. theae* are established in Florida; *F. externa* is commonly intercepted in Florida but has not become established (Suppl. material 1: Fig. S1).

*Fiorinia phantasma*, commonly known as phantasma scale, was described from the Philippine Islands in 1915. Subsequently, a major global expansion of *F. phantasma* occurred over the last decade through movement of nursery stock (Watson et al. 2015). *Fiorinia phantasma* is now documented from 19 countries (China (Hong Kong, Mainland China, Taiwan), France, French Polynesia, Grenada, Indonesia, Malaysia, Maldives, Nauru, Netherlands, New Caledonia, Papua New Guinea, Philippines, Reunion, Saint Barthelemy and Saint Martin, Singapore, Solomon Islands, Thailand, United States (American Samoa, Florida, Hawaii, Guam), and Vietnam). In some areas, *F. phantasma* may reach heavy infestations causing serious plant damage (Watson et al. 2015; García Morales et al. 2016). In one particularly impactful infestation of *F. phantasma*, approximately 6,000 palms were severely infested and declining at a resort in the Maldives (Watson et al. 2015). A polyphagous pest, *F. phantasma* has been reported on 25 families and 56 genera of hosts, including many nursery and ornamental plants, particularly palms, as well as several fruit crops (Watson et al. 2015; García Morales et al. 2016; Ahmed et al. 2021). For the nursery and greenhouse sector, palms account for sales of approximately \$400 million annually in Florida and well over \$1 billion annually in the USA (Khachatryan and Hodges 2012). Scale insects feed on all

parts of their host plants, but *F. phantasma* is common on leaves, causing chlorosis, leaf drop, and ultimately plant death. This pest has the potential to cause economic harm in the USA to nurseries, landscape industries, and homeowners.

The first North American continental report of *F. phantasma* was in Florida and included more than twenty heavily infested Canary Island date palms (*Phoenix canariensis* Chabaud) along both sides of a road in Miami-Dade County (Ahmed 2018). The population was likely there for some time, considering the density of the scales and the presence of specimens on many trees. It is not surprising that the Florida infestation was not detected earlier because the scale is identical in field appearance to other *Fiorinia* species that occur in Florida (Ahmed 2018). *Fiorinia* species infestations start with the arrival of crawlers (first-instar nymphs), either by wind, or via infested plant material or garden tools because crawlers constitute the only mobile stage besides adult males, which do not feed. Crawlers settle on plant parts and molt into second-instar males and females within a few days.

The main pest management challenge is detection of new *F. phantasma* infestations. *Fiorinia phantasma* occurs in two Florida counties, Miami-Dade and Palm Beach, and is usually found on palms (FDACS-DPI Entomology Database 2021). Detection is complicated by the presence of *F. fioriniae*, which is commonly found on palms throughout most of Florida (FDACS-DPI Entomology Database 2021). *Fiorinia japonica*, another morphologically and behaviorally similar species, also infests palms, but is only found in California and several east coast states in the USA. Should *F. japonica* become established in Florida, it would be difficult to detect because the species looks identical in the field to the other *Fiorinia* species infesting palms. Heavy infestations of another *Fiorinia* species, *F. proboscidaria*, were recently recorded on citrus from residential areas in Florida. Regulatory efforts aimed at preventing its introduction to and establishment in commercial citrus growing areas in Florida are being implemented (Ahmed and Stocks 2020). To date, the only way to identify these species has been to mount adult females on a microscopic slide and examine them with a compound microscope. The regulatory and pest management situation surrounding *Fiorinia* species in the USA, and especially Florida, is dynamic and subject to identification challenges. Thus, it is important to develop identification tools for *Fiorinia* adult females and other commonly collected life stages using diagnostic molecular and morphological data. Without reliable and correct identification, one cannot properly make regulatory and control decisions.

The purpose of this study is to provide taxonomic keys for immatures of seven *Fiorinia* species occurring in the USA. We also provide line drawings and diagnoses of slide-mounted second-instar males and females, DNA sequence data for multiple loci for molecular diagnostics, and extensive records of the species' distributions in Florida. We newly describe and illustrate first-instar nymphs and adult females of two species, *F. phantasma* and *F. proboscidaria*. In addition, we provide updated taxonomic keys for first-instar nymphs (adapted from Howell 1977) and adult females (Watson et al. 2015).

## Materials and methods

### Taxon sampling

Four species of *Fiorinia* (*F. fioriniae*, *F. phantasma*, *F. proboscidea*, *F. theae*) were collected from Florida (Suppl. material 2: Table S1). *Fiorinia externa* samples were collected from Christmas trees imported from outside of Florida. First- and second-instar nymphs and adult females from infested plant materials were preserved in 100% ethanol for slide mounting and molecular analysis. *Fiorinia japonica* and *F. pinicola* specimens were borrowed from the United States National Museum of Natural History, scale insect collection, Beltsville, Maryland (USNM). *Fiorinia pinicola* specimens were provided to us by Natalia von Ellenrieder (California Department of Food and Agriculture) (Suppl. material 2: Table S1). The details for specimens examined for description and diagnosis is provided in the figure captions of each species. Due to regulatory issues surrounding *F. yongxingensis* Liu, Cai & Feng, 2020 from Hainan, China, its DNA sequences were obtained in China by one of us (DL). All samples were initially mounted in Hoyer's medium for visibility during illustration and were transferred to balsam medium for permanent preservation. This was done by placing the Hoyer's slide in a petri dish filled with water, just enough that the slide is slightly submerged, for a few hours depending on the age of the Hoyer's slide. Once the slide cover is detached and loosened, it can easily be removed. The specimen can then be removed from the slide without being damaged. Specimens were soaked in a watch glass filled with water overnight to rinse Hoyer's media out of the specimen. After soaking, specimens were placed on a new slide with a drop of balsam and covered with a new coverslip. Illustrations were made using a Leica DMRB compound microscope and a camera lucida. Morphological terminology follows that of Miller and Davidson (2005). Numerical values were taken from a minimum of five specimens, if available, from as many Florida localities as possible. All specimens were deposited in the Florida State Collection of Arthropods, Gainesville (FSCA) unless otherwise indicated. Other depositories included USNM (United States National Museum of Natural History, scale insect collection, Beltsville, Maryland), UMEC (University of Massachusetts Entomology Collection, Amherst, Massachusetts), and Entomology Museum, Northwest Agricultural and Forestry University, Shaanxi, China.

In addition to the freshly collected *Fiorinia* specimens described above, additional specimens and sequences were included in analyses of DNA sequences (Suppl. material 2: Table S1): fresh specimens of the outgroups *Thysanoflorinia leei* Williams and *T. nephilii* (Maskell) collected in Florida; ethanol-preserved specimens of *Fiorinia* sp. collected in Lambir Hills National Park, Malaysia, in 2013; cytochrome oxidase I (COI) sequences of Diaspididae from the BOLD database (Ratnasingham and Hebert 2007), along with one sequence of *Pseudococcus* sp. (BOLD record AMSMB002-15; BIN BOLD:ACZ2386) as an outgroup; and cytochrome oxidase I and II (COI-II), elongation factor 1a (EF1a), and large ribosomal subunit (28S) sequences of the genus *Fiorinia* reported in Normark et al. (2019), along with exemplars of other species of Fioriniina and one sequence of *Unaspis yanonensis* (Kuwana) as an outgroup.

## Slide mounting of immature stages

Slide mounting is considered mandatory for morphological identification of armored scale insects because it is nearly impossible to identify taxonomic features without doing so. Moreover, for museum curation purposes, slide mounting is the best way to archive scale insects in a reference collection. There are studies available on methods for mounting hemipterans (Hodges and Evans 2005), but many are not specific to scale insects or armored scales (Wirth and Marston 1968). Previously published mounting methods for scale insects (McKenzie 1957; Wilkey 1990; Watson 2002) need to be reevaluated to meet the need for rapid identification as pest species are spreading swiftly through national and international trade. Recently published methods have focused on modifying slide mounting to enhance safety since the reagents can be corrosive, flammable, or carcinogenic, or can produce toxic fumes (Sirisena et al. 2013). Another recent study modified the watch glass with a sieve to process specimens in a shorter period (Barbecho and Lit 2015). Nevertheless, a reliable protocol for slide mounting of immature armored scale insects still needs to be established. Mounting methods are also biased towards adult scales, despite the importance of first and second-instar nymphs to armored scale biology. These immature life stages are commonly found in the field, but are taxonomically studied to a much lesser degree than adults. We evaluated several methods to enhance safety and reduce the time required to mount fresh and absolute ethanol-preserved specimens of first- and second-instar nymphs of *Fiorinia* species.

### (i) Standard slide mounting method (6 steps)

Initially, a 67 mm beveled-edge watch glass (Prolab Scientific) and micro spatula were used. Fisher 10% potassium hydroxide (KOH) was used in step 1 for heating and maceration. Following this step, specimens were placed into a Humboldt mesh (Replacement Mesh Disk 5 cm dia. No. 325H-3807.325) container that was then placed inside the watch glass, eliminating the need for the micro spatula in the following steps until the final mount. Forceps (Bioquip Swiss style #4) were used to remove the mesh from the 4.8 cm watch glass (Item#742300, Carolina) while switching between steps. Glacial acetic acid (Fisher) was used in step 2 for removal of the remaining 10% KOH from step 1. Acid fuchsin stain (Bioquip) was used with a 3:7 dye to acetic acid ratio in step 3 to stain the specimens. For dehydration of the cuticle in the 4<sup>th</sup> step, 75% and 95% EtOH were used. Clove oil (Spectrum Chemical) was used in step 5 to remove any remaining wax from the specimens. A disposable transfer pipette (13-711-9D, Fisher) which holds 3.2 ml, was used in steps 2–5. In the final step 6 filtered Canada balsam (CAS 8007-47-4, Fisher) was used as the medium and placed on a glass slide (22-038-103, Fisher). A glass coverslip (12-545-80P, Fisher) was placed on the specimen in balsam to complete the mount. The 6 steps required for the standard slide mounting method are as follows:

1. Heating: specimens were set in a watch glass filled with 10% KOH and heated at 85 °C for 5–10 mins. After heating, gut contents were teased out using a micro-spatula to gently tap the dorsum.

2. KOH removal: specimens were moved to a watch glass of 95% glacial acetic acid for 10 mins to remove any remaining KOH.

3. Staining: Acid fuchsin stain was added and let sit for 5 mins.

4. Stain correcting: specimens were moved to a watch glass of 75% EtOH for 10 mins. Specimens were then placed in 95% EtOH for another 10 mins to dehydrate.

5. Wax removal: specimens were soaked in clove oil for 5 to 10 mins. This helps to remove any remaining wax or lipids and makes specimen bodies flexible to be easily spread on a slide.

6. Mounting: on a labeled slide, a drop of balsam was placed in a center and spread to avoid specimen drift. The specimen was then placed in the balsam dorsoventrally (i.e. ventral side up) and legs and antennae were positioned properly. A coverslip was placed on the balsam, and the slide was placed on a hot plate at 30 °C for 10 mins to remove any bubbles.

Due to the multiple steps in this method, which require each specimen to be moved from 5 different watch glasses before mounting, many first-instar nymphs were lost or damaged. Additionally, this method was time consuming. In an attempt to reduce the loss of first-instar nymphs, minimize damage, reduce the amount of chemical usage, and save time, we subsequently developed alternative methods – see below.

### **(ii) Modified slide mounting method A (1 step)**

For fresh specimens (not preserved in ethanol).

1. Mounting: on a labeled slide, a drop of Hoyer's medium was placed in the center and spread to avoid specimen drift. Fresh specimens picked from plant material were placed in a Hoyer's medium dorsoventrally and legs and antennae were positioned properly. In this protocol, we omitted steps 1–5 of the standard method and mounted specimens directly into Hoyer's medium. This was effective in preventing loss of specimens and reducing the amount of chemical usage.

### **(iii) Modified slide mounting method B (4 steps)**

For ethanol-preserved specimens.

1. Heating: specimens were placed in a watch glass filled with 10% KOH and heated for 5 mins at 85 °C.

2. Rehydrating: specimens were placed in water and left to soak for 5–10 mins. We found that heating the specimens prior to submerging them in water aided in the rehydration process.

3. Cleaning: specimens were moved to a watch glass filled with Hoyer's medium. Because Hoyer's medium is a self-cleaning fluid (Anderson 1954), specimens were placed in the dish to accelerate the cleaning.

4. Mounting: on a labeled slide, a drop of Hoyer's medium was placed in the center and spread to avoid specimen drift. The specimen was placed in the Hoyer's medium dorsoventrally and legs and antennae were positioned properly.

**(iv) Modified slide mounting method C – balsam method with mesh container (7 steps)**

For fresh specimens and ethanol-preserved specimens.

1. Heating and cleaning: specimens were placed in a watch glass filled with 10% KOH and heated at 85 °C for 5–10 mins. After heating, cavity contents were teased out using a micro-spatula. Once this step was completed, specimens were moved to a container modified using mesh placed in a watch glass (Fig. 1). The modified mesh container was made using a plastic 5 ml screw-top tube and fine wire mesh (Humboldt, Elgin, IL United States). The top was cut out of the screw-top tube and the mesh was put in its place, allowing liquid to move through the mesh while keeping the specimens inside.

2. Rehydration: specimens were placed in water and left to soak for 5 to 10 mins.

3. KOH removal: specimens were moved to a watch glass of 95% acetic EtOH (a few drops of glacial acetic acid with 95% ethanol) for 10 mins.

4. Staining: after removing 95% acetic EtOH, acid fuchsin stain was added and let sit for 5 mins.

5. Stain correction and dehydration: specimens were moved to a watch glass of 75% EtOH for 10 mins. Specimens were then placed in 95% EtOH for another 10 mins to dehydrate the cuticles.

6. Wax removal: specimens were soaked in clove oil for 5 to 10 mins.

7. Mounting: on a labeled slide, a drop of balsam was placed in a center and spread to avoid specimen drift. The specimen was placed in the balsam and legs and antennae were positioned properly. A coverslip was placed on the balsam and the slide was placed on a hot plate at 30 °C to remove any bubbles.

Although the mesh is effective in keeping first- and second-instar nymphs in the container without damage, a few problems were noted. The mesh does not sit flat against the glass bottom of the watch glass, so the cleaning step cannot be done in the mesh. Cleaning must be done in a watch glass and then specimens must be moved back into the mesh for the remaining steps. Due to the smaller size of the mesh container, range of motion using microtools throughout this process can be limited. Similar to processing in a watch glass without mesh, specimens can get stuck on the upper sides of the modified dish. Visibility of first-instar nymphs can be hampered by the reflective coloration of the mesh.

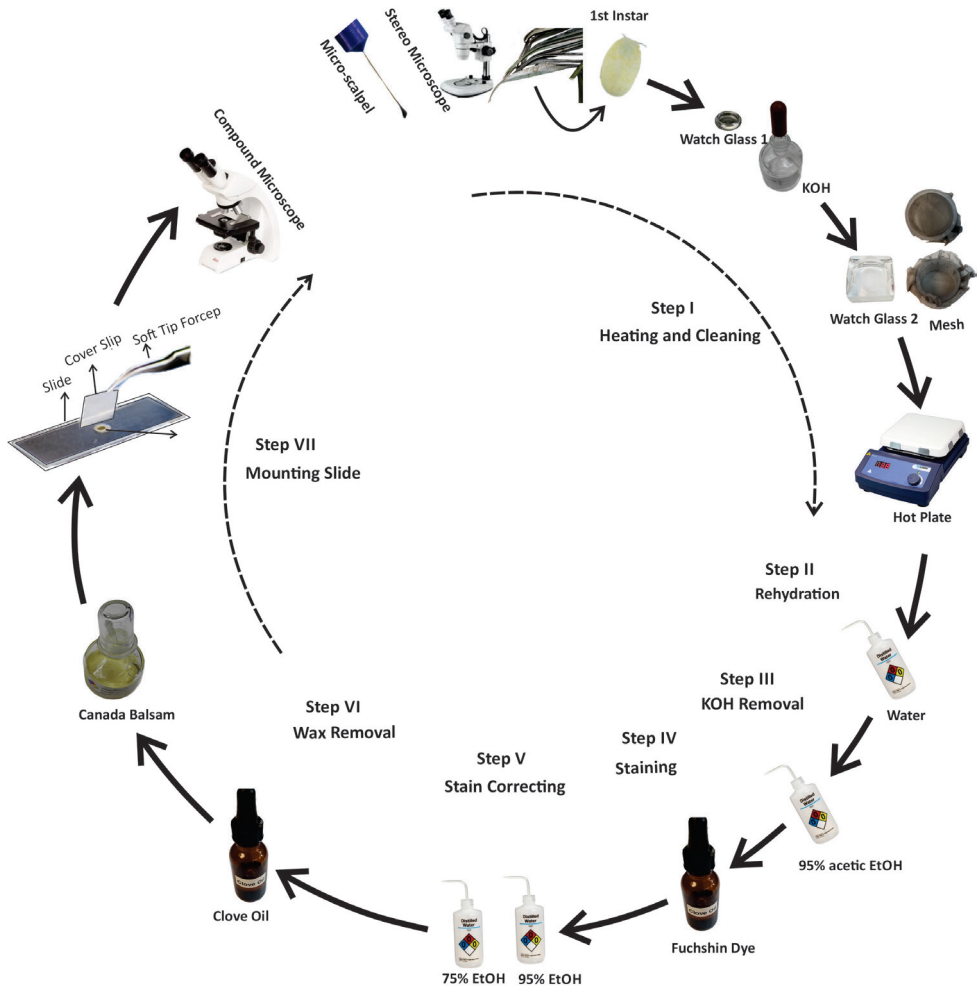


**Figure 1.** Illustration of modified slide mounting method C (balsam method with mesh container).

There are several steps involved in traditional slide-mounting protocols (method i) that require each specimen to be moved to and from at least five different watch glasses before eventually being slide mounted. Many first-instar nymphs can be lost or damaged during these steps. We recommend using the mesh container during the slide-mounting protocol (method iv). Use of this container will decrease mounting time, reduce specimen loss, decrease the quantity of chemical reagents, and generate quality slides. All steps can easily be performed using the mesh container except for the cleaning step. Unfortunately, the cleaning step must be done in a watch glass and then the specimens should be moved back into the mesh container to finish the mounting process. Although this procedure is laborious, we recommend it when the aim is to make permanent mounts for deposit in archival collections. The other mounting procedure is to place first-instar specimens directly into Hoyer's mounting medium on a slide (method ii, iii). This

protocol has fewer steps and less chance of specimen loss, and yields specimens with superior visibility. We recommend this protocol for rapid species diagnosis. Unfortunately, the mounts are only temporary unless slides are ringed to prevent deterioration.

## DNA extractions, polymerase chain reaction (PCR), and sequencing

DNA was extracted from individual *Fiorinia* and *Thysanofiorinia* specimens using the Qiagen Blood and Tissue Kit per the manufacturer's protocol. Extractions were non-destructive, and recovery of individual scale vouchers was attempted. DNA was quantified on a Nanodrop 2000 and PCRs had a target input of at least 5 ng of genomic DNA. PCRs were performed using the Kapa HiFi HotStart PCR Kit, in a total volume of 25  $\mu$ L.

The standard cytochrome oxidase I (COI) barcode region was targeted for each species using the primer pair PCOF1 (Park et al. 2010) and HCO2198/LEPR1 (Folmer et al. 1994; Hebert et al. 2004). Park et al. (2010) suggested PCOF1/LEPR1 for COI barcoding of scale insects. Some species failed to amplify with this primer combination, necessitating the alternative reverse primer HCO2198. Thermocycles were as follows: 1) initial denaturing at 95 °C for two mins, 2) 98 °C for 30 secs, 3) 50 °C for 30 secs, 4) 72 °C for 40 secs [32 cycles of steps 2–5], 5) final extension at 72 °C for seven mins, and 6) a final hold of 4 °C.

Two other loci, the large ribosomal subunit (28S D2/D3 expansion region) and elongation factor 1 $\alpha$  (EF1 $\alpha$ ) were also targeted, for comparison with the results of Normark et al. (2019). The primer pair for EF1 $\alpha$  was EF-1 $\alpha$  (a) (Morse and Normark 2006) and EF2 (Palumbi 1996). The primer pair for 28S was s3660 (Dowton and Austin 1998; Morse and Normark 2006) and a335 (Whiting et al. 1997; Normark et al. 2019). Thermocycles for s3660/a335 were as follows: 1) initial denaturing at 95 °C for two mins, 2) 98 °C for 30 secs, 3) 62 °C for 30 secs, 4) 72 °C for one minute [32 cycles of steps 2–5], 5) final extension at 72 °C for seven mins, and 6) a final hold of 4 °C. Thermocycles for EF-1 $\alpha$ (a)/EF2 were as follows: 1) initial denaturing at 95 °C for two mins, 2) 98 °C for 30 secs, 3) 64 °C for 30 secs, 4) 72 °C for 45 secs [35 cycles of steps 2–5], 5) final extension at 72 °C for seven mins, and 6) a final hold of 4 °C.

PCRs were visualized on 1.5% agarose gels. Positive PCRs were purified and prepared for sequencing using BigDye Terminator v3.1 chemistry. Amplicons were sequenced bidirectionally on the ABI SeqStudio platform at FDACS-DPI. Sequence chromatograms were trimmed and assembled in Sequencher 5.4.6. Newly generated sequences were deposited in GenBank (Suppl. material 2: Table S1) (COI: MW883907–MW883949; 28S: MW883848–MW883886; EF1 $\alpha$ : MW893442–MW893456).

## Data analysis

Cytochrome oxidase I barcode sequences (5'-COI) were initially aligned using an on-line version of MAFFT 7 (Katoh and Standley 2013) with the FFT-NS-2 strategy for relatively short, similar sequences. A few sequences with excessive ambiguities or large

insertions were excluded from further analysis. The resulting barcode matrix included 1177 terminal taxa and was 649 bp in length.

Sequences were aligned using the default settings of MUSCLE (Edgar 2004) and Clustal W (Larkin et al. 2007) as implemented in MEGA X (Kumar et al. 2018). The lengths of the alignments were 645bp (5'-COI), 226 bp (3'-COI), 504 bp (COII), 708 bp (EF1 $\alpha$ , introns omitted), and 425 bp (28S, regions of uncertain homology omitted). Alignments were concatenated as a single nexus file in Mesquite 3.51 (Maddison and Maddison 2018). PCR amplifications with 3'COI/COII primers failed to produce clear bands or clean sequence data on each attempt in this study. All of 3'COI/COII sequences used in this study were from Normark et al. (2019).

Neighbor-joining and distance analyses of the 5'-COI matrix were conducted in MEGA X (Kumar et al. 2018). Neighbor-joining trees were constructed using the K2P model (Kimura 1980) with partial deletion of missing data and a site coverage cutoff of 95%. Node support was assessed using 10,000 bootstrap replicates. The resulting tree topology was adjusted in FigTree v1.4.3 (Rambaut 2012) to arrange nodes and collapse large clusters. Intra- and interspecific K2P distances among *Fiorinia* species were calculated with the same parameters as above using a separate alignment that only included *Fiorinia* barcodes.

Phylogenetic analyses were conducted using 3 sequence regions reported in Normark et al. (2019): portions of cytochrome oxidase I and II (using a 3' portion of COI nonoverlapping with the 5'-COI barcoding matrix: 3'-COI & COII), elongation factor 1a (EF1 $\alpha$ ), and the large ribosomal subunit (28S), as well as the 5'-COI region. The aim was to assess the monophyly of *Fiorinia* and the relationship of *Fiorinia* species to other species of Fioriniina.

Maximum Likelihood (ML) phylogenetic analyses were conducted on the XSEDE computing cluster as part of the CIPRES Science Gateway (Miller et al. 2010). ML analyses were conducted using IQ-TREE version 2.0 (Minh et al. 2020). The concatenated matrix (111 terminal taxa; 2508 bp long) was partitioned by gene [27% (30/111 taxa) coverage for COI-5P: 1–645 (645 bp) + 55% (61/111) for EF1a: 646–1353 (708 bp) + 38% (42/111) for COII: 1354–1857 (504 bp) and COI-3P: 1858–2083 (226 bp) + 100% (111/111) for 28S: 2084–2508 (425 bp)] and by codon position for EF1 $\alpha$  (2 partitions: positions 1 & 2 vs. position 3). Best fit models of sequence evolution were assessed using Bayesian Information Criteria by ModelFinder (Kalyaanamoorthy et al. 2017) in the following partition order: 5'-COI & 3'-COI (TIM+F+I+G4), EF1 $\alpha$  positions 1 & 2 (TIM3e+I+G4), EF1 $\alpha$  position 3 (TPM3+F+G4), COII (TN+F+I+G4) and 28S (TVM+F+I+G4). Maximum parsimony tree searches were conducted in MP-Boot (Hoang et al. 2018b) with default parsimony ratchet settings.

Node support was assessed by 10,000 ultrafast ML bootstrap replicates (Hoang et al. 2018a), 10,000 SH-aLRT replicates (Guindon et al. 2010), and 1000 standard ML bootstrap replicates. Maximum parsimony (MP) support for nodes was assessed using 10,000 ultrafast bootstraps in MPBoot (Hoang et al. 2018b). Strong node support values are provided on the tree from left to right as ML standard BS (> 75), ML ultrafast BS (> 95), SH-aLRT (> 80), and MP ultrafast BS (> 95) (Guindon et al. 2010; Hoang et al. 2018a, b).

## Results

### Phylogenetic analyses

Maximum Likelihood analyses estimated a consensus bootstrap tree with a log-likelihood of -20,889.543 for the multigene tree (Fig. 2, Suppl. material 1: Fig. S2) and -3006.382 for the 28S tree (Suppl. material 1: Fig. S3). Parsimony ratchet analyses found five equally parsimonious trees with 4123 steps. A clade of grass-feeding Fioriniina (*Unachionaspis* MacGillivray + [*Kuwanaspis* MacGillivray + *Nikkoaspis* Kuwana]) was recovered, but the node was only weakly supported (Fig. 2). As in Normark et al. (2019), the Australasian Fioriniina (*Pseudaulacaspis* MacGillivray in part; *Poliaspis* Maskell; *Anzaspis* Henderson) were recovered as a clade by likelihood and parsimony methods, but with relatively higher support in some analyses (BS 80; SH-aLRT 92). These Australasian Fioriniina were sister to a clade of *Fiorinia* + *Lineaspis* MacGillivray + *Pseudaulacaspis* in part, with weak support except for SH-aLRT (92). The clade of *Fiorinia* + *Lineaspis* + *Pseudaulacaspis* was found by likelihood and parsimony, with some strong support (ML UF BS 95; SH-aLRT 93) (Fig. 2). Relationships within this clade were not entirely resolved, resulting in a polytomy. *Fiorinia* is monophyletic in our tree, with the exception of two isolates (*Fiorinia* sp., D4815B and D4815C) which were represented only by 28S data. These two isolates belong to an undescribed *Fiorinia* species from Malaysia. The remaining *Fiorinia* isolates formed a clade in likelihood analyses (SH-aLRT 99). Relationships among *Fiorinia* species were generally weakly supported. A terminal group of *Fiorinia phantasma* + *F. yongxingensis* was present in every analysis with strong support suggesting synonymy (Fig. 2).

The slide-mounted cuticle of D4815B and other specimens in the same lot have been re-examined by BBN and they clearly belong to a pupillarial species whose morphology is completely consistent with the genus *Fiorinia*. These results might imply that the lineage leading to D4815B and D4815C represents a second origin of the pupillarial habit in Fioriniina. These two isolates were placed within a section of a *Fiorinia* + *Rolaspis* + *Pseudaulacaspis* (in part) clade in the ML phylogenetic tree using only 28S data (Suppl. material 1: Fig. S3). They were placed with five species of *Pseudaulacaspis*

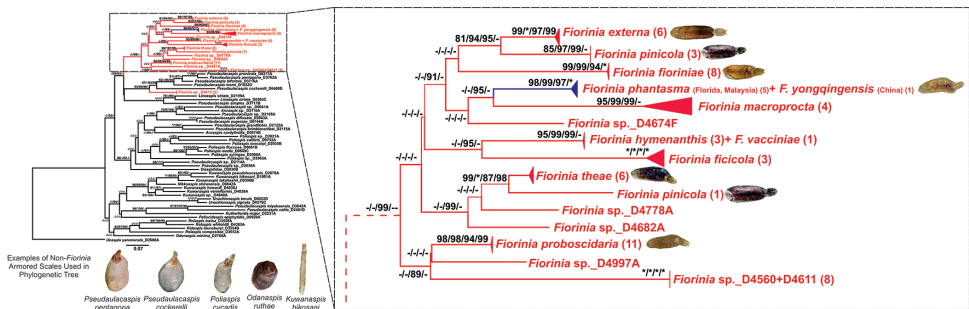


**Figure 2.** Maximum Likelihood bootstrap consensus tree of the subtribe Fioriniina based on 28S, EF1- $\alpha$ , 5'-COI, 3'-COI, and COII. The clade highlighted in red indicates a monophyletic *Fiorinia*. The close-up of *Fiorinia* clade is presented on right side. High-resolution figure of the main tree is in Suppl. material 1: Fig. S2.

(including *P. biformis*, *P. cockerelli*, *P. momi*, *P. pentagona*, and *P. prunicola*) with strong support (Suppl. material 1: Fig. S3). In addition to these five species of *Pseudaulacaspis*, three species of *Rolaspis* (including *R. incisa*, *R. lounsburyi*, and *R. whitehilli*), and one species of *Pellucidaspis* (*P. epiphytidis*) were also placed within this *Fiorinia* clade.

## COI barcoding

This study produced 43 new sequences of the COI barcode region, 37 of which represent nine *Fiorinia* species (Fig. 3, Suppl. material 1: Fig. S4). The remaining 6 COI barcode sequences represent two species of *Thysanofiorinia*. These new barcode sequences range in length 562 bp–645 bp. In the neighbor-joining analyses of Diaspididae COI barcodes, *Fiorinia* species cluster near the species of *Kuwanaspis*, *Unachionaspis*, and *Pseudaulacaspis* (all members of Fioriniina), along with a sequence assigned to the genus *Aulacaspis* (subtribe Chionaspidina). (Fig. 3). *Fiorinia* species represented by multiple barcode sequences each formed well-supported clusters (100 BS) in the neighbor-joining tree, with one exception: *F. theae*. *Fiorinia theae* forms two well supported clusters whose relationship to each other is not resolved in this analysis (Fig. 3).

The alignment for calculating K2P distances among *Fiorinia* species included 37 terminal taxa and was 645 bp long. Based on the 95% site cutoff, calculations involved 560 total positions. Intraspecific K2P distances were low, except for specimens identified as *F. theae* (Table 1). Interspecific K2P distances between *Fiorinia* species ranged from 9.1% to 15.2% (Table 1). Sequences of *F. phantasma* from the population from Florida and Malaysia and sequences of *F. yongxingensis* were identical and were placed together in the tree with strong support (Fig. 3).

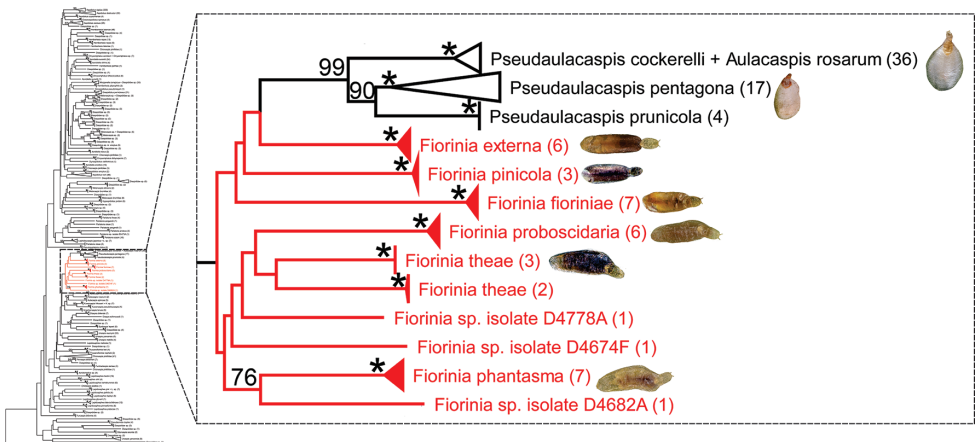


**Figure 3.** Neighbor-joining tree of Diaspididae 5'-COI barcodes. Terminal taxa are labeled to their narrowest identification-level. Numbers in parentheses after terminal taxa indicate how many sequences are represented in each cluster. The cluster of *Fiorinia* species is highlighted in red. Bootstrap support values greater than 75 are indicated on the tree. Nodes with 100 percent bootstrap support are indicated by a “\*”. The close-up of the *Fiorinia* clade is presented on the right side. High-resolution figure of the main tree is in Suppl. material 1: Fig. S4.

**Table 1.** Summary of *Fiorinia* COI barcode intra- and interspecific K2P distances.

Species	Intra. K2P Dist.	Inter. K2P Dist.
<i>Fiorinia externa</i> (n = 6)	0.00%	9.1%–12.4%
<i>Fiorinia fioriniae</i> (n = 7)	0.00%–0.02%	11.8%–14.8%
<i>Fiorinia phantasma</i> (n = 7)	0.00%–0.09%	9.1%–13.7%
<i>Fiorinia pinicola</i> (n = 3)	0.00%	9.1%–15.2%
<i>Fiorinia proboscitaria</i> (n = 6)	0.00%–0.02%	9.9%–14.2%
<i>Fiorinia theae</i> (n = 5)	0.00%–8.00%	9.5%–14.8%
<i>Fiorinia</i> sp. isolate D4778A (n = 1)	N/A	9.5%–13.9%
<i>Fiorinia</i> sp. isolate D4674F (n = 1)	N/A	9.5%–12.7%
<i>Fiorinia</i> sp. isolate D4682A (n = 1)	N/A	9.1%–15.2%

## General descriptions of second-instar nymphs of *Fiorinia* species occurring in the USA

### Second-instar females

With two definite pairs of lobes; third lobes and sometimes fourth lobes represented by series of points. Median lobes yoked, medial margins divergent or nearly parallel, longer than lateral margin, with series of notches. Second lobes bilobed, usually smaller than median lobes, sometimes wider, medial lobule largest, sometimes with small notches, lateral lobule sometimes with one or two small notches. Third lobes usually represented by raised sclerotized area with small series of notches, often divided into two lobules by seta marking segment VI. Fourth lobes sometimes represented by series of sclerotized points. Gland spine arrangement of two types: *F. proboscitaria* and *F. theae* with single gland spine on each side of each of segments II–VIII, gland spines on each side of segments II–IV larger than those on segments V–VIII, without gland spines on segment I; remaining species with single gland spine on each side of segments II–V, absent from segment VI, present on each side of segments VII and VIII, gland spines on each side of segments II–V larger than those on segments VI–VIII, with two or three smaller gland spines on each side of segment I; gland spines with barely perceptible sclerotization posterolaterad of each spiracle. Macroducts barrel shaped, marginal, with four or five on each side of pygidium from segments III or IV–VII. Microducts restricted to venter, three different patterns on abdomen; in *F. proboscitaria* and *F. theae* longitudinal lines on each side of abdomen from II–VI, each line composed of one or more ducts on each segment, mediolateral line on segments III or IV, V or VI, submarginal line on segments II–VI; in *F. externa*, *F. fioriniae*, *F. japonica*, and *F. pinicola* longitudinal lines on each side of abdomen from II–VI, each line composed of one or rarely two ducts on each side of each segment, mediolateral line on segments II–V or VI, submarginal line on segments II–VI; in *F. phantasma* longitudinal lines restricted to mediolateral areas of segments II–IV or V, other lines absent; microducts on head and thorax usually anterior of clypeus, laterad of labium, and posterior of each spiracle. Perispiracular pores associated with anterior spiracles only, with three loculi, one or two pores associated with each spiracle. Anal opening normally located in center of pygidium mesad of fourth marginal macroduct counting

forward from posterior macroduct. Dorsal setae present near body margin on head and thorax, with one seta submarginally on each side of each abdominal segment; also present in mediolateral area on each side of body on any or all of abdominal segments I–VI; usually with one mediolateral seta on each side of head. Ventral setae in small numbers in marginal areas of head and thorax, with one seta usually present laterad of each spiracle; abdominal segments with one marginal and one submarginal seta on each side of each segment and with one mediolateral seta on each side of segments IV–VI. Antennae each normally with one long seta and two small sensillae. Cicatrices present or absent on each side of abdominal segment I. Two inconspicuous lobes present submarginally on head of *F. proboscitaria* and *F. theae*.

## Notes

Characters most useful in distinguishing among species are: a) number of marginal macroducts; b) arrangement of gland spines; c) arrangement of microducts; d) presence or absence of cicatrices; e) presence or absence of lobes on head; f) relative size of median lobes compared to medial lobule of second lobe; g) shape of median lobes.

Second-instar females of *Fiorinia* species can be distinguished from most similar genera by having the following: median lobes yoked, usually divergent, medial margin longer than lateral, with one pair of setae between; dorsal macroducts confined to body margin, with four or five on each side of pygidium; with two pairs of definite lobes, second pair bilobular. However, we have been unable to distinguish between second-instar females of the *Fiorinia* species treated here and *Pseudaulacaspis cockerelli* (Comstock) and *P. pentagona* (Targioni Tozzetti). There are consistent differences in the distribution of the gland spines in most species of *Fiorinia*, but *F. proboscitaria* and *F. theae* are identical to *P. cockerelli* and *P. pentagona*. It is remarkable that the second-instars are so similar, but the adult females are quite different.

## Second-instar males

With two definite pairs of lobes; remaining body margin often with numerous projections, not organized into clear lobes. Median lobes spaced apart, without zygosis, usually with small medial lobule and large, conspicuous lateral lobule, medial lobule with one or two projections, lateral margin with several notches and projections. Second lobes usually associated with a dense cluster of marginal ducts, with series of projections, rarely bilobed, smaller than median lobes. Gland spines of three sizes: largest in clusters posterolaterad of each anterior spiracle, posterolaterad of posterior spiracle, and submarginal on abdominal segment I and sometimes II; medium-sized gland spines on body margin of anterior abdominal segments; small gland spines laterad of anterior spiracle on *F. externa* and *F. theae*. Macroducts barrel shaped, of two sizes: larger ducts grouped into communal ducts (= glanduliferous craters; Takagi 1999) that exit through single orifice with numerous fine filaments or series of short projections on margin; communal ducts either separate or associated with clusters of smaller

macroducts; smaller macroducts ca. half as large as larger ducts, arranged singly or in clusters on prepygidial and pygidial margin. Microducts present on dorsum and venter, arranged in longitudinal lines, of two sizes: smaller size relatively slender, longer than wide, present on venter of most abdominal segments, on venter of head, in ventromedial areas of thorax, and on dorsum of posterior two or three segments; larger ducts ca. as long as wide present on venter in submarginal areas of thorax, on dorsum in submarginal areas of prothorax to anterior abdominal segments and submedially on anterior abdominal segments. Perispiracular pores associated with anterior spiracles only, with three loculi, 1–3 pores associated with each spiracle. Anal opening normally located in center of pygidium mesad of anterior edge of posterior cluster of macroducts. Dorsal setae present near body margin on head and thorax, setae associated with duct clusters long and conspicuous; also present in mediolateral area on each side of body on any or all of abdominal segments I–VI, usually with several mediolateral seta on each side of head. Ventral setae in small numbers in marginal areas of head and thorax, with one seta usually present laterad of each spiracle; abdominal segments with one marginal and one submarginal seta on each side of each segment and with one mediolateral seta on each side of segments IV–VII. Antennae each normally with one long seta and two small sensillae. Cicatrices absent.

## Notes

Characters most useful in distinguishing among species are: a) arrangement and number of communal ducts b) organization of duct clusters c) arrangement of microducts; d) arrangement of gland spines. Second-instar males of *Fiorinia* are remarkably similar to the same instar of *Pseudaulacaspis* species by each having unusual lobes, duct clusters, and communal ducts (Takagi and Kawai 1967). *Pseudaulacaspis* species differ primarily by the presence of many ventral microducts on the head and barrel-shaped microducts in the medial and submedial areas of the abdominal venter, whereas *Fiorinia* species possess no more than two ventral microducts on the head, and slender microducts on the submedial areas of the abdominal venter. In Normark et al. (2019), the subtribe Fioriniina comprises many genera and species with second-instar males that are similar in appearance to the species treated here.

## First-instar nymphs

Howell (1977) gave a general description of the first-instar nymphs of the species that he examined. We will not repeat that here. Below, we present diagnoses of the two species that were not included in the Howell (1977), i.e., *F. phantasma* and *F. proboscidaria*.

First-instar nymphs of *Fiorinia* species can be recognized by having the following combination of characters: antennae five segmented; apical segment annulate; large duct on each side of dorsum of head; submedial longitudinal line of microducts on each side of thorax; second lobes bilobulate. First-instar nymphs of *Fiorinia* species are similar to some species of *Pseudaulacaspis* (*P. cockerelli* and *P. pentagona*) but differ by normally

having a submedial longitudinal line of microducts on each side of thorax, whereas these ducts are absent from *P. cockerelli* and *P. pentagona* (Tippins and Howell 1983).

## Keys to *Fiorinia* species occurring in the USA using immature instars

### First-instar nymphs (adapted from Howell 1977).

- 1 Lobules of pygidial lobe 2 rounded ..... 2
- Lobules of pygidial lobe 2 truncate ..... *F. externa*
- 2 Gland spines on segment VI more than ½ length of gland spine on segment VII..... 3
- Gland spines on segment VI less than ½ length of gland spine on segment VII..... 5
- 3 Sclerotized pattern outside of oval surrounding large duct on dorsum of head mostly thin and serpentine like; large duct short, broad, with inner apex nearly flat ..... 4
- Sclerotized pattern outside of oval surrounding large duct on dorsum of head mostly in clumps; large duct elongate, narrow, with inner apex mushroom shaped ..... *F. phantasma* (Fig. 10)
- 4 Gland spine on segment VI ca. ½ length of gland spine on segment VII..... *F. fioriniae*
- Gland spine on segment VI nearly equal to length of gland spine of segment VII..... *F. proboscitaria* (Fig. 16)
- 5 Dorsal submedian thoracic ducts present; inner apex of large duct on dorsum of head flat..... 6
- Dorsal submedian thoracic ducts absent (occasionally orifices present); inner apex of large duct on dorsum of head mushroom shaped..... *F. japonica*
- 6 Gland spine on segment VI noticeably longer than those on segments I–V; pattern of dorsal derm on abdomen fine ..... *F. pinicola*
- Gland spine on segment VI equal to those on segments I–V; pattern of dorsal derm on abdomen coarse ..... *F. theae*

### Second-instar females

- 1 With 5 pairs of marginal macroducts ..... 2
- With 4 pairs of marginal macroducts ..... *F. theae* (Fig. 20), *F. proboscitaria* (Fig. 18)
- 2 With submarginal longitudinal line of microducts on venter; with 4 large-sized gland spines on each side of body; without deep incision anterior of 5<sup>th</sup> macroduct (segment III) on older specimens..... 3
- Without submarginal longitudinal line of microducts on venter; with 3 large-sized gland spines on each side of body; with deep incision anterior of 5<sup>th</sup> macroduct (segment III) on older specimens..... *F. phantasma* (Fig. 12)

- 3 Median lobes broad, as wide as or wider than medial lobule of second lobe 4
- Median lobes narrow, narrower than medial lobule of second lobe.....  
..... *F. externa* (Fig. 4)
- 4 With 3 pairs of microducts on head; space between bases of median lobes  
wider than medial lobule of second lobes ..... *F. fioriniae* (Fig. 6)
- With 1 pair of microducts on head; space between bases of median lobes  
equal to or narrower than medial lobule of second lobes .....  
..... *F. japonica* (Fig. 8), *F. pinicola* (Fig. 14)

**Second-instar males**

- 1 One or 2 duct clusters on each side of body, or definitive clusters absent ....2
- Three duct clusters on each side of body ..... *F. externa* (Fig. 5)
- 2 Communal ducts present; small macroducts on pygidial margin in at least 1  
cluster ..... 3
- Communal ducts absent; small macroducts on pygidial margin not in tight  
cluster ..... *F. fioriniae* (Fig. 7)
- 3 Communal ducts incorporated in cluster of small macroducts ..... 5
- Communal ducts separate, not in cluster with small macroducts ..... 4
- 4 With 1 communal duct on each side of pygidium.... *F. proboscitaria* (Fig. 19)
- With 2 communal ducts on each side of pygidium ..... *F. theae* (Fig. 21)
- 5 With 1 communal duct on each side of body..... *F. phantasma* (Fig. 13)
- With 2 communal ducts on each side of body ..... 6
- 6 With 5 or more gland spines on each side of body between anterior and pos-  
terior spiracles..... *F. pinicola* (Fig. 15)
- With fewer than 5 gland spines on each side of body between anterior and  
posterior spiracles..... *F. japonica* (Fig. 9)

**Adult Females (adapted from Watson et al. (2015))**

- 1 Interantennal process absent .....2
- Interantennal process present..... 5
- 2 Antennae each with a long spur making them longer than wide..... 3
- Antennae each with a short spur making them more or less as long as wide..  
..... *F. externa*
- 3 Fewer than 7 marginal macroducts on each side of pygidium.....4
- Seven or 8 marginal macroducts on each side of pygidium..... *F. pinicola*
- 4 Four to 6 (normally 5) marginal macroducts on each side of pygidium; clus-  
ters of ventral microducts near body margins of abdominal segments III and  
IV ..... *F. japonica*
- Three or 4 (normally 3) marginal macroducts on each side of pygidium; clus-  
ters of ventral microducts absent near body margins of abdominal segments  
III and IV ..... *F. fioriniae*

- 5 Interantennal process without spicules; body narrow, with almost parallel sides..... **6**
- Interantennal process with spicules; body wide, narrowing abruptly to triangular pygidium ..... *F. phantasma* (Fig. 11)
- 6 Seven or 8 marginal macroducts on each side of body; head rounded.... *F. theae*
- Three to 5 marginal macroducts on each side of body; head conical.....  
..... *F. proboscitaria* (Fig. 17)

## Species accounts

### *Fiorinia externa* Ferris, 1942

**Field characteristics.** First-instar exuviae barely touching second-instar exuviae. Distinct indentation formed between attachment of first- and second-instar exuviae. Second-instar exuviae narrow, parallel sided, and elongate; longitudinal ridge absent or weakly developed. Second-instar exuviae reddish brown anteriorly and light brown to yellow posteriorly. Posterior end of adult female within second-instar exuviae rounded (Suppl. material 1: Fig. S1).

**First-instar nymph.** Described in Howell (1977).

**Second-instar female.** Median lobes slender, narrower than medial lobule of second lobe, not projecting beyond medial lobule of second lobes. With five pairs of marginal macroducts. Swelling of body margin adjacent to macroduct usually pointed. With four large gland spines on margin of each side of body from abdominal segments II–V; usually without small gland spine on each side of abdominal segment VI; with small gland spines on margin or submargin of abdominal segment I. With one microduct on each side of head. Longitudinal line of microducts present submarginally on venter of II–V, normally with one microduct on each side of each segment. Cicatrices absent.

**Second-instar male.** Three duct clusters on each side of body; posterior cluster composed of several small ducts and two communal ducts. Five longitudinal lines of microducts on venter of abdomen (one medial, two mediolateral, two submarginal). Cluster of small microducts with sclerotized orifice laterad of anterior spiracle. Fewer than five large-sized gland spines on each side of body between anterior and posterior spiracles. Antennae each with one enlarged seta.

**Florida collection records.** All records are on Christmas trees imported from states outside of Florida. This species is not established in Florida, and its common host, *Abies fraseri*, also does not occur naturally in Florida. It has been found on imported Christmas trees in the following localities in Florida: Broward Co., Miramar, November 20, 2013, on *Abies fraseri*, S. Alspach (2013-8494); Broward Co., Davie, December 10, 2013, on *Abies fraseri*, S. Beidler (2013-8906); Citrus Co., Inverness, December 4, 2013, on *Abies fraseri*, S. Jenner (2013-9766); Hamilton Co., White Springs, December 11, 2012, on *Abies fraseri*, H. Randolphs (2012-9239); Hillsborough Co., Tampa, November 20, 2012, on *Abies fraseri*, T. Streeter (2012-8844); Marion Co., Ocala, December 2, 2013, on *Abies fraseri*, S. Wayte (2013-8755); Monroe

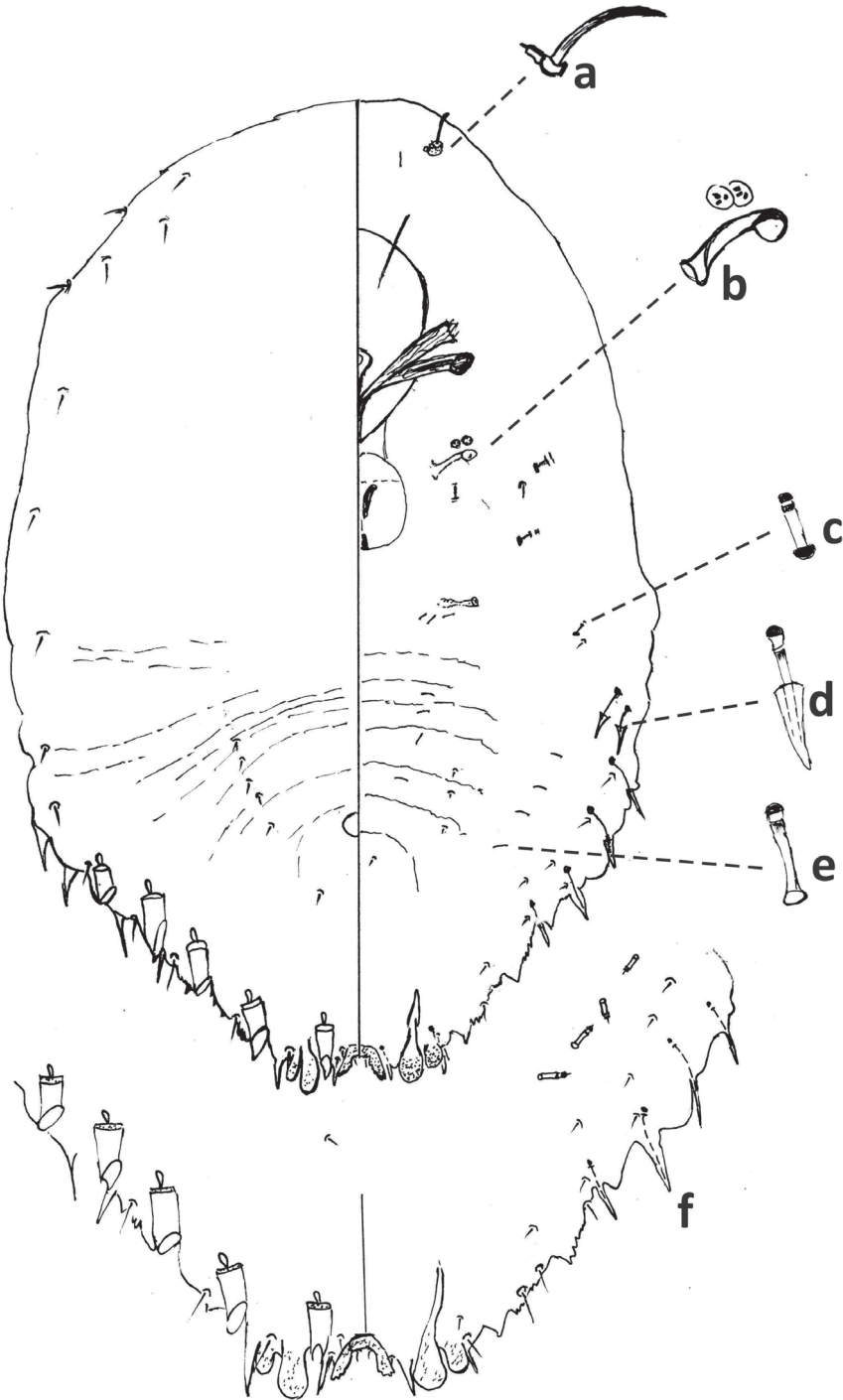


**Figure 4.** *Fiorinia externa*, second-instar female, Alleghany Co., Glade Creek, North Carolina, November 22, 2019, on *Abies fraseri*, A. Bartlett, (2019-6449). Abbreviations: a) antenna; b) anterior spiracle; c) microduct with sclerotized orifice; d) large gland spine; e) small microduct; f) enlargement of pygidium.

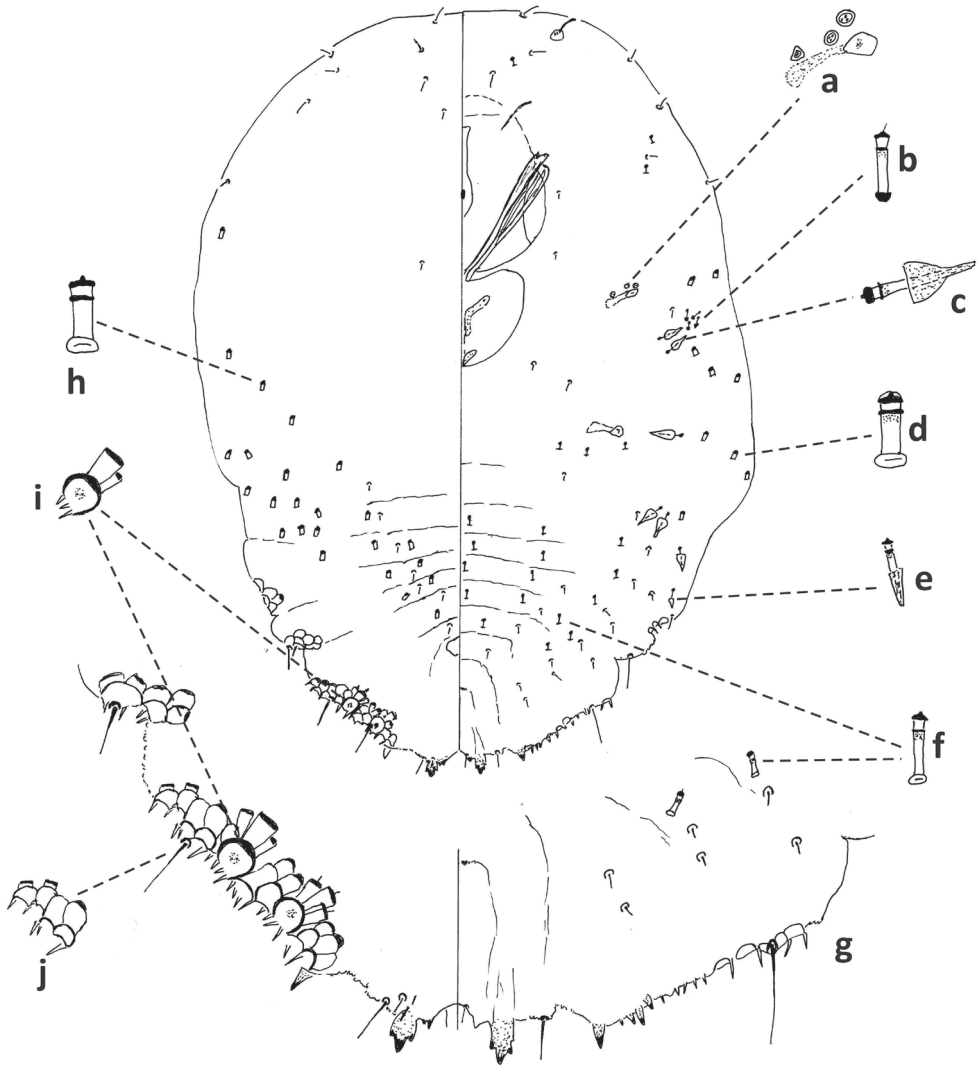


**Figure 5.** *Fiorinia externa*, second-instar male, Alleghany Co., Glade Creek, North Carolina, November 22, 2019 on *Abies fraseri*, A. Bartlett, (2019-6449). Abbreviations: a) anterior spiracle; b) microduct with sclerotized orifice; c) large microduct; d) large gland spine; e) small gland spine; f) small microduct; g) enlargement of pygidium; h) large microduct; i) enlargement of communal duct; j) enlargement of portion of duct cluster.

Co., Tavernier, November 28, 2012, on *Abies fraseri*, J. Farnum (2012-8924); Volusia Co., Port Orange, November 27, 2017, on *Abies fraseri*, K. Coffey (2017-4496).

**Specimens examined for description and diagnosis.** Alleghany Co., Glade Creek, North Carolina, November 22, 2019 on *Abies fraseri*, A. Bartlett, 5 2<sup>nd</sup> ♀, 5 2<sup>nd</sup> ♂, 10 ad ♀ (2019-6449), Alleghany Co., Laurel Springs, North Carolina, December 8, 2020 on *Abies fraseri*, L. Milton, 10 ad ♀ (2020-4778).

**Other specimens examined from USNM.** Japan, Kobe, Arboretum, May 8, 2006, on *Tsuga? sieboldii*, S. Lyon 7 2<sup>nd</sup> ♀ (0606537). United States, Connecticut, Danbury, September 7, 1944, on hemlock, S.W. Bromley 3 1<sup>st</sup> ♀ (JOH 07-77); Connecticut, Fairfield Co., New Canaan, November 3, 1950, on Nordman fir, S.W. Bromley 1 1<sup>st</sup> ♀, 18 2<sup>nd</sup> ♀, 20 ad ♀. New York, Nassau Co., Oyster Bay, May 17, 1947, on hemlock, B.F. Maker 2 1<sup>st</sup> ♂ (JOH 10-77); New York, Suffolk Co., Brookhaven, November 25, 1985, on leaves of hemlock, T. Kowalsick (ek-01-86); Pennsylvania, Radnor, July 26, 1946, on hemlock, S.W. Bromley 1 1<sup>st</sup> ♀ (JOH 08-77).

### *Fiorinia fioriniae* Targioni Tozzetti, 1867

**Field characteristics.** First-instar exuviae overlapping second-instar exuviae. Without indentation formed between attachment of first- and second-instar exuviae. Second-instar exuviae oval, convex marginally; yellow to light brown; longitudinal ridge conspicuous. Posterior end of adult female within second-instar exuviae rounded. Heavily infested leaves with slight white secretion.

**First-instar nymph.** Described in Howell (1977).

**Second-instar female.** Median lobes broad, equal to or wider than medial lobule of second lobe, projecting ca. same or slightly less than medial lobule of second lobes. With five pairs of marginal macroducts. Swelling of body margin adjacent to macroduct usually rounded. With four large gland spines on margin of each side of body from abdominal segments II–V; usually without small gland spine on each side of abdominal segment VI; with small gland spines on margin or submargin of abdominal segment I. With three microducts on each side of head. Longitudinal line of microducts present submarginally on venter of abdominal segments II–VI, normally with one microduct on each side of each segment. Cicatrices absent.

**Second-instar male.** Submargin of abdominal segments II–VI with scattered small-sized macroducts, not in clusters; communal ducts absent. Medial longitudinal line of microducts absent. Cluster of small microducts with sclerotized orifice laterad of anterior spiracle absent. Fewer than five gland spines on each side of body between anterior and posterior spiracles. Antennae each with several enlarged setae.

**Notes.** The single specimen collected with identified adult females of this species is unusual and may not be the second-instar male of this species. U.S. populations of *Fiorinia fioriniae* have been reported to be parthenogenetic (Tippins 1970), so it is surprising to find a male, although many scale insect species with parthenogenetic populations also have sexual populations (Nur 1990). The specimen is unusual among second-instar males of *Fiorinia* in lacking tight clusters of marginal ducts. There exist a few other species of *Fiorinia* with males that similarly lack these ducts, for instance *F. nachiensis* Takahashi of Japan; thus it is plausible that this really is the male of *F. fioriniae*.

**Florida collection records.** Brevard Co., Melbourne, February 22, 1984, on *Phoradendron* sp., F.A. Smith (1984-2933, 3014) (2 slides); Brevard Co., Sharpes, January 19, 1972, on *Callistemon* sp., H.C. Levan (1972-005–008) (4 slides); Broward Co.,

Dania, January 4, 1966, on *Howea* sp., J.W. Shirah (1966-7369); Broward Co., Dania, June 26, 1981, on *Mangifera indica*, M. McDonald (1981-1606) (2 slides); Broward Co., Dania, August 24, 2011, on *Persea* sp., G. Azone (2011-5990); Broward Co., Davie, April 3, 1962, on *Ilex* sp., D.P. McLean (1962-2896) (2 slides); Broward Co., Davie, October 12, 1978, on *Camellia* sp., R. Gaskalla (1978-2879) (2 slides); Broward Co., Coral Springs, October 5, 2011, on *Persea americana*, L. Charlton (2011-7789) (2 slides); Broward Co., Fort Lauderdale, February 5, 1968, on *Callistemon* sp., D.C. Clinton (1968-2883) (2 slides); Broward Co., Fort Lauderdale, February 6, 1970, on *Callistemon* sp., D.C. Clinton (1970-2878) (2 slides); Broward Co., Fort Lauderdale, May 2, 1974, on *Sabal* sp., J.A. Reinert (1974-2915) (2 slides); Broward Co., Fort Lauderdale, November 13, 1979, on *Callistemon citernus*, K. Tyson (1979-7500) (2 slides); Broward Co., Fort Lauderdale, February 25, 1988, on *Howea forsteriana*, J. McCluskie (1985-2925) (2 slides); Broward Co., Fort Lauderdale, February 25, 1988, on *Manilkara roxburghiana*, J. Hickey (1988-005); Broward Co., Fort Lauderdale, January 8, 1984, on *Manilkara roxburghiana*, J. Hickey (1984-3287) (3 slides); Broward Co., Fort Lauderdale, December 26, 2003, on *Leucospermum* sp., G. Farina (2003-6693); Broward Co., Fort Lauderdale, June 4, 2004, on *Laurus nobilis*, F.W. Howard (2004-4142) (3 slides); Broward Co., Hollywood, February 19, 1979, on *Persea americana*, R. Gaskalla (1978-3264) (2 slides); Broward Co., Hollywood, June 1986, on *Howea forsteriana*, D. Fenster (1986-008) (3 slides); Broward Co., Hollywood, December 5, 1997, on *Ravenia rivularis*, M.S. Quintanilla (1997-2912) (3 slides); Broward Co., North Lauderdale, May 28, 1981, on *Dicytosperma album*, D. Clinton and J. Aubry (1981-2895, 2904) (2 slides); Broward Co., Tamarac, March 21, 2012, on *Persea americana*, C. Millan (2012-1986); Broward Co., on unknown host, June 4, 2004, on *Laurus nobilis*, F.W. Howard (2004-4142-301); Charlotte Co., Punta Gorda, August 9, 2007, on *Camellia japonica*, D. Renz (2007-5759); Collier Co., Naples, August 28, 2013, on *Palmae*, R. Nanneman (2013-6323); Duval Co., Nocatee, April 4, 1978, on *Persea americana*, L.J. Chambliss (1978-3288) (2 slides); Escambia Co., Pensacola, November 3, 1988, on *Prunus angustifolia*, G. Corbitt and R. Burns (1988-2899); Glades Co., Moore Haven, October 4, 2006, on *Celtis laevigata*, L. Richards (2006-7213); Hendry Co., Devils Garden, November 20, 2014, on *Persea palustris*, M. Terrell (2014-788) (2 slides); Highlands Co., April 28, 1975, on *Camellia* sp., R.F. Denno, J.A. Davidson, D.R. Miller (1975-2886); Highlands Co., on unknown host, July 24, 1987 on *Persea borbonia*, R. Payne (1987-2988) (2 slides); Highlands Co., Lake Placid, November 1970, on *Camellia* sp. J.A. Weidhaas (1970-3265, 3854) (2 slides); Hillsborough Co., Sun City, November 14, 1994, on *Phoradendron leucarpum*, M. Runnals (1994-2918, 3924) (2 slides); Hillsborough Co., Tampa, April 10, 1964, on *Sabal* sp., S.A. Fuller (1964-2901); Hillsborough Co., Tampa, March 25, 1983, on *Hedera* sp., E.R. Simmons (1983-2998, 3943) (2 slides); Miami-Dade Co., Homestead, June 9, 1979, on *Manilkara roxburghiana*, P. Choborda (1979-011); Indian River Co., Vero Beach, December 16, 1970, on *Callistemon* sp., R.H. Kendrick (1970-012–016) (5 slides); Lake Co., Tavares, September 9, 2012, on *Hedera* sp., M. Sellers (2012-6901); Lee Co., Sanibel Island, April 4, 1978, on *Zamia* sp., R. Driggers (1978-2936); Leon Co., Tallahassee, February 3, 1916, on *Camellia* sp. A.C.M. (1916-017); Leon Co., Tallahassee,

February 3, 1916, on *Camellia* sp., A.C.M. (1916-2850) (4 slides); Leon Co., Tallahassee, October 31, 1919, on *Camellia* sp., P.F. Robertson (1919-021); Levy Co., Bronson, January 4, 2011, on *Camellia* sp., W. Bailey (2011-29); Lucie Co., Fort Pierce, January 16, 1980, on *Dracaena* sp., E.W. Campbell (1980-2944); Lucie Co., Lakewood Park, July 16, 1980, on *Acoelorrhaphe wrightii*, E.W. Campbell (1980-483, 2937) (2 slides); Madison Co., Greenville, March 12, 1993, *Ilex* sp., F. Bennett (1993-2903); Manatee Co., Oneco, December 17, 1987, on *Callistemon* sp., A. Waters (1987-014); Manatee Co., Snead Island, April 3, 1991, on *Schinus* sp., Runnals M. (1991-2922); Manatee Co., Snead Island, April 3, 1991, on *Schinus* sp. Runnals M. (1991-006–007) (2 slides); Marion Co., Weirsdale, December 22, 1985, on *Hedera canarensis*, F.J. McHenry (1985-2832, 2894) (2 slides); Martin Co., Hobe Sound, April 21, 1980, on *Persea americana*, E.W. Campbell (1980-2959); Martin Co., Hobe Sound, June 9, 1981, on *Callistemon viminalis*, S. Hakala (1981-418); Martin Co., Jensen Beach, September 27, 1978, on *Dictyosperma* sp., E.W. Campbell (1978-7502) (2 slides); Martin Co., Palm City, February 8, 2012, on *Magnolia virginiana*, L. West (2012-833) (2 slides); Martin Co., Palm City, October 17, 2012, on *Persea palustris*, L. West (2012-7964) (2 slides); Martin Co., Palm City, September 1, 1977, on *Magnolia* sp., E.W. Campbell (1977-2890, 2884) (2 slides); Martin Co., Stuart, January 31, 1978, on *Eugenia* sp., E.W. Campbell (1978-0955, 3283) (2 slides); Martin Co., Stuart, November 17, 1978, on *Myrica* sp., E.W. Campbell (1978-021); Miami-Dade Co., Big Cypress National Preserve, February 16, 1978, on *Magnolia* sp., A. Harmon and D. Martinelli (1978-2910); Miami-Dade Co., Big Cypress National Preserve, February 16, 1978, on *Magnolia virginiana*, A. Hamon and D. Martinelli (1978-006–007) (2 slides); Miami-Dade Co., Coral Gables, August 13, 2010, on *Gymnanthes lucida*, K. Griffiths (2010-4926); Miami-Dade Co., Florida City, November 19, 1986, on *Mimusops roxburghiana*, L.D. Howerton (1986-962); Miami-Dade Co., Florida City, November 19, 1986, on *Mimusops roxburghiana*, L.D. Howerton (1986-2914, 2980) (2 slides); Miami-Dade Co., Hialeah, March 28, 1979, on *Callistemon viminalis*, D. Stocks (1979-3382, 3869) (2 slides); Miami-Dade Co., Hialeah, January 1, 1980, on *Callistemon* sp., D. Stocks and W. James (1980-2952); Miami-Dade Co., Homestead, January 24, 1962, on *Macadamia* sp., R.J. McMillan (1962-3276) (2 slides); Miami-Dade Co., Homestead, October 16, 1962, on *Melaleuca* sp., J.H. Knowles (1962-2897) (2 slides); Miami-Dade Co., Homestead, February 2, 1969, on *Persea* sp., D.O. Wolfenbarger (1969-491) (2 slides); Miami-Dade Co., Homestead, March 28, 1969, on *Persea* sp. D.O. Wolfenbarger (1969-026–031) (4 slides); Miami-Dade Co., Homestead, February 2, 1978, on *Hedera* sp., W.E. Wyles (1978-488); Miami-Dade Co., Homestead, February 27, 1978, on *Hedera* sp., W.E. Wyles (1978-7522) (5 slides); Miami-Dade Co., Homestead, June 8, 1979, on *Manilkara roxburghiana*, P. Chobrdá (1979-0146) (4 slides); Miami-Dade Co., Homestead October 3, 1979, on *Persea americana*, W.E. Wyles (1979-2928); Miami-Dade Co., Homestead, September 11, 2007, on *Persea americana*, B. Saunders (2007-6958); Miami-Dade Co., Homestead, July 31, 2018, on *Gymnanthes lucida*, W. Mazuk (2018-4092) (2 slides); Miami-Dade Co., Kendall, February 24, 1989, on *Camellia* sp., W. Francillon (1989-2855) (2 slides); Miami-Dade Co., Miami, April 22, 1966, on *Chamaedora* sp., C.F. Dowling (1966-2876) (2 slides); Miami-Dade Co.,

Miami, June 6, 1967, on *Chamaerops* sp., J.S. Sloan (1967-2907) (2 slides); Miami-Dade Co., Miami, October 26, 1967 on *Callistemon viminalis*, J.F. Dillon (1967-3305) (2 slides); Miami-Dade Co., Miami, October 26, 1967, on *Callistemon viminalis*, J.F. Dillon (1967-038); Miami-Dade Co., Miami, March 3, 1969, on *Howea* sp., J.F. Dillon (1969-493, 3060) (2 slides); Miami-Dade Co., Miami, March 7, 1969, on *Howea* sp., J.F. Dillon (1969-3267) (4 slides); Miami-Dade Co., Miami, September 5, 1969, on *Macadamia ternifolia*, J.F. Dillon (1969-045–047) (3 slides); Miami-Dade Co., Miami, January 22, 1975, on *Callistemon viminalis*, D. Sager (1975-2885) (3 slides); Miami-Dade Co., Miami, July 27, 1978, on *Mangifera* sp., M. Corman (1978-3308) (2 slides); Miami-Dade Co., Miami, April 5, 1979, on *Kigelia pinnata*, P. Chobrda (1979-2913); Miami-Dade Co., Miami, November 5, 1979, on *Callistemon* sp., H. VonWald (1979-3003); Miami-Dade Co., Miami, April 1, 1980, on *Callistemon viminalis*, G. Webster and E. Pena (1980-014); Miami-Dade Co., Miami, April 1, 1980, on *Callistemon viminalis*, G. Webster and E. Pena (1980-2881); Miami-Dade Co., Miami, April 2, 1980, on *Santalum album*, H. Von Wald and C. Dowling (1980-2935) (2 slides); Miami-Dade Co., Miami, April 3, 1981, on *Persea americana*, K. Martin (1981-016 –020) (5 slides); Miami-Dade Co., Miami, March 3, 1981, on *Macadamia ternifolia*, W. James (1981-2934) (2 slides); Miami-Dade Co., Miami, March 25, 1981, on *Macadamia ternifolia*, W. James (1981-2984); Miami-Dade Co., Miami, February 10, 1982, on *Diospyros lotus*, H. VonWald (1982-017–019 ) (3 slides); Miami-Dade Co., Miami, April 8, 1982, on *Eucalyptus* sp., P. Perun (1982-223, 2853) (2 slides); Miami-Dade Co., Miami, April 8, 1982, on *Eucalyptus* sp., P. Perun (1982-2853); Miami-Dade Co., Miami, November 15, 1985, on *Howea forsterana*, D. Chalot (1985-3009) (2 slides); Miami-Dade Co., Miami, September 19, 29, 1986, on *Persea americana*, D. Storch (1986-021–023, 3091) (3 slides); Miami-Dade Co., Miami, January 17, 2001, *Manilkara roxburghiana*, E. Putland (2001-189) (2 slides); Miami-Dade Co., Miami, March 14, 2002, on *Persea americana*, L. Davis (2002-870); Miami-Dade Co., Miami, August 14, 2007, on *Manilkara roxburghiana*, O. Garcia (2002-5912); Miami-Dade Co., Miami, May 11, 2012, on *Laurus nobilis*, M. Figueroa (2012-3720) (2 slides); Miami-Dade Co., North Beach, January 20, 1981, on *Amyris elemifera*, E.W. Campbell and R. Kendrick (1981-2947) (2 slides); Miami-Dade Co., Opa Locka, October 5, 1977, on *Callistemon* sp., M. Corman (1977-3268, 3278) (2 slides); Miami-Dade Co., Opa Locka, May 22, 1978, on *Persea americana*, J. Hilderbrandt (1978-3313) (2 slides); Miami-Dade Co., West Miami, November 22, 1977, on *Camellia* sp., D. Martinelli (1977-2888, 2898) (2 slides); Monroe Co., Little Torch Key, April 10, 2018, on *Bidens alba*, P. Corogin, J. Hayden, E. Talamas, B. Danner, J. Farnum (2018-1780); Orange Co., Apopka, Jan 10, 2001, on *Ravenea rivularis*, K. Gonzalez (2001-116) (2 slides); Orange Co., Belle Isle, January 20, 2006, on *Garcinia livingstonei*, T. Williams (2006-268); Orange Co., Orlando, February 2013, on Theaceae, A. Puppelo (2013-1127); Orange Co., Orlando, May 27, 2008, on *Magnolia virginiana*, A. Puppelo (2008-3337); Orange Co., Winter Garden, October 31, 2008, on *Machilus thunbergii*, G. Warden (2008-7478); Orange Co., Zellwood, March 7, 2019, *Laurus nobilis*, K. Gonzalez (2019-1006) (2 slides); Palm Beach Co., Boca Raton, May 19, 1982, on *Chamaerops humilis*, D.C. Clinton (1982-487) (3 slides); Palm Beach Co., Boynton

Beach, October 10, 1973, on *Ficus* sp., K. Geyer (1973-3284) (3 slides); Palm Beach Co., Delray Beach, May 12, 1978, on *Diospyros* sp., K.C. Stolley (1978-2852) (2 slides); Palm Beach Co., Boynton Beach, June 7, 1978, on *Mimusops* sp., K. Stolley (1978-3307); Palm Beach Co., Boynton Beach, September 27, 1991, on *Camellia japonica*, E. Tannehill (1991-2906); Palm Beach Co., Boynton Beach, January 13, 1988, on *Mimusops roxburghiana*, D. Leone (1988-2880) (2 slides); Palm Beach Co., Boynton Beach, November 2, 1989, on *Sisyrinchium solstitiale*, E. Tannehill (1989-485, 3303) (2 slides); Palm Beach Co., Delray Beach, February 23, 1988, on *Melaleuca* sp., E. Tannehill and A. Hamon (1988-2851) Palm Beach Co., Jupiter, May 8, 2013, on *Magnolia* sp., L. West (2013-3217) Palm Beach Co., Lake Park, June 14, 1978, on *Chrysalidocarpus lutescens*, J. Bennet (1978-3567) (2 slides); Palm Beach Co., Lake Park, April 24, 1979, on *Chrysalidocarpus lutescens*, J.E. Bennet (1979-2920) (2 slides); Palm Beach Co., Lake Worth, March 7, 1978, on *Kentia* sp., J. Bennett (1978-3285); Palm Beach Co., Lake Worth, October 8, 1981, on *Magnolia virginiana*, J. Fellers and R. Buchholz (1981-026-027) (2 slides); Palm Beach Co., Lake Worth, July 13, 1995, on *Chrysalidocarpus lutescens*, Cook S.H., Clinton D.C. (1995-3024); Palm Beach Co., Lake Worth, July 13, 1995, on *Chrysalidocarpus lutescens*, S.H. Cook, D.C. Clinton (1995-3024); Palm Beach Co., Lake Worth, March 25, 2004, on *Calophyllum inophyllum*, L. Smith (2004-2103); Palm Beach Co., Pahokee, February 22, 1980, on *Chrysalidocarpus lutescens*, N. Miles and B. Walsh (1980-2955) (2 slides); Palm Beach Co., South Bay, November 14, 2018, on *Magnolia virginiana*, J. Farnum (2018-5955); Palm Beach Co., West Palm Beach, January 14, 1991, on *Mangifera indica*, R.T. Doll (1991-3566) (2 slides); Pinellas Co., Clearwater, January 11, 2013, on *Persea palustris*, W. Salway (2013-575) (2 slides); Pinellas Co., Indian Rocks, October 3, 1972, on *Persea americana*, K.C. Lowery (1972-2860); Pinellas Co., Largo, November 8, 1978, on *Persea* sp., P. Pullara (1978-3306); Pinellas Co., St. Petersburg, August 15, 1967, on *Persea* sp., C.K. Hickman (1967-2854) (3 slides); Pinellas Co., St. Petersburg, February 2, 2008, on *Persea borbonia*, M. Spearman (2004-724); Pinellas Co., St. Petersburg, May 28, 2009, on *Persea borbonia*, M. Spearman (2009-3632); Polk Co., Cypress Gardens, January 16, 1962, on *Tetrapanax* sp., J.N. Pott (1962-3266) (2 slides); Polk Co., Cypress Gardens, August 13, 1964, on *Magnolia* sp. W.P. Henderson (1964-2905) (2 slides); Polk Co., Lake Wales, October 25, 1962, on *Ficus* sp., Ralph E. Brown (1962-2857); Polk Co., Winter Haven, April 8, 1980, on *Persea Americana*, H.G. Schmidt (1980-2938) (2 slides); Polk Co., Winter Haven, July 26, 2018, on *Laurus nobilis*, J. Bryan (2018-4054); St. Lucie Co., Fort Pierce, March 23, 1978, on *Paurotis* sp., E.W. Campbell (1978-032-033) (2 slides); St. Lucie Co., Fort Pierce, January 17, 1979, on *Persea* sp., E.W. Campbell (1979-2893); St. Lucie Co., Fort Pierce, March 23, 1979, on *Paurotis* sp., E.W. Campbell (1979-2900); St. Lucie Co., Fort Pierce, February 24, 1984, on *Bumelia tenax*, K. Hibbard and E.W. Campbell (1984-492, 2948) (2 slides); St. Lucie Co., Fort Pierce, November 6, 1985, on *Paurotis* sp., K Hibbard and E.W. Campbell (1985-484, 2950) (2 slides); St. Lucie Co., Fort Pierce, March 13, 2003, on *Phoradendron leucarpum*, K. Hibbard (2003-927); St. Lucie Co., Fort Pierce, February 21, 2005, on *Ilex cornuta*, D. Vazquez (2005-4069); St. Lucie Co., Hutchinson, Isle, April 18, 1980, on *Eugenia simpsonii*, E.W. Campbell (1980-2990); St. Lucie Co., Port

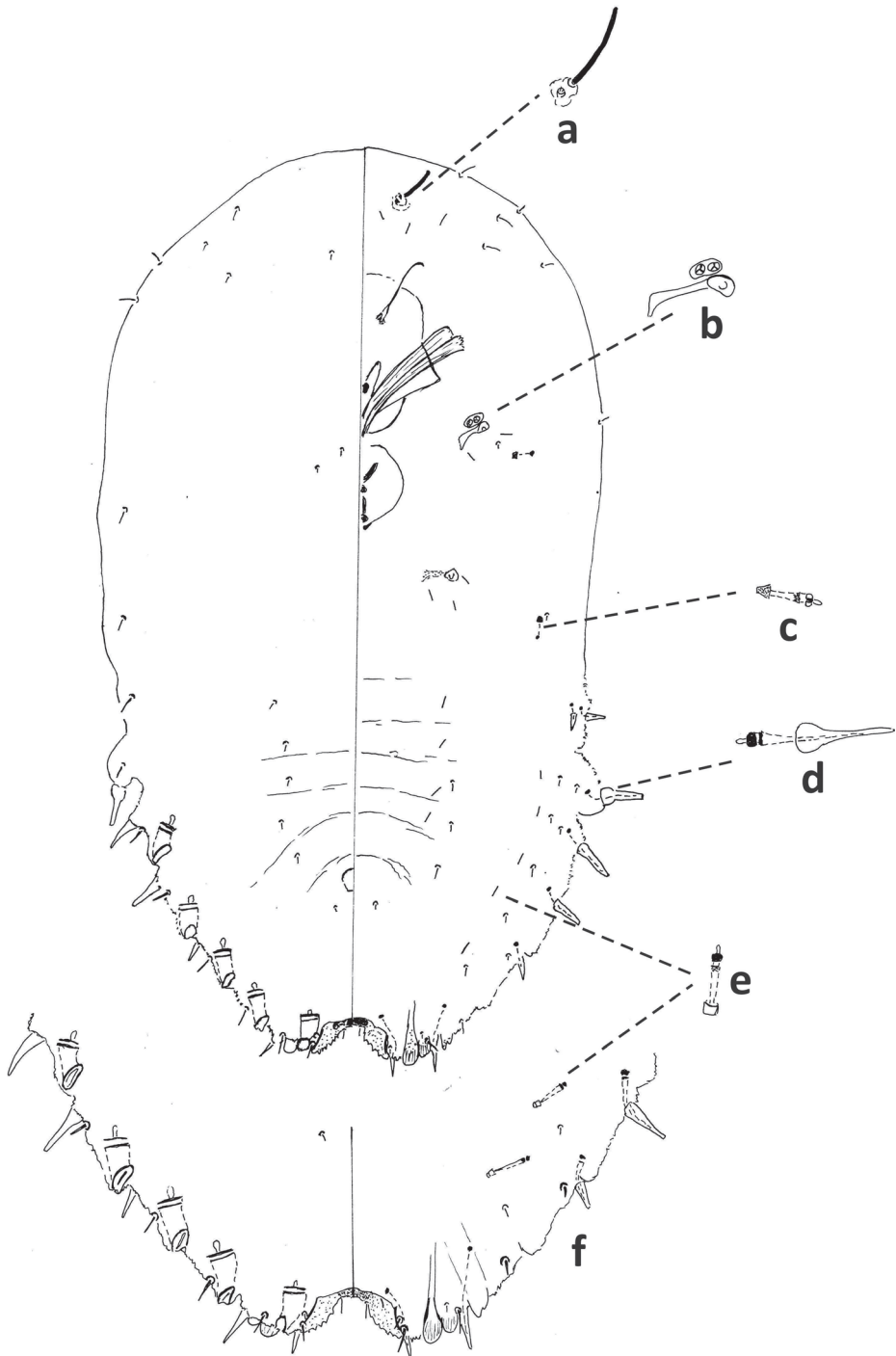


**Figure 6.** *Fiorinia fiorinia*, second-instar female, Marion Co., Ocala, August 13, 2019 on *Chamaerops humilis*, T. Gordon, (2019-4546). Abbreviations: a) antenna; b) anterior spiracle; c) microduct with sclerotized orifice; d) large gland spine; e) large microduct; f) enlargement of pygidium.

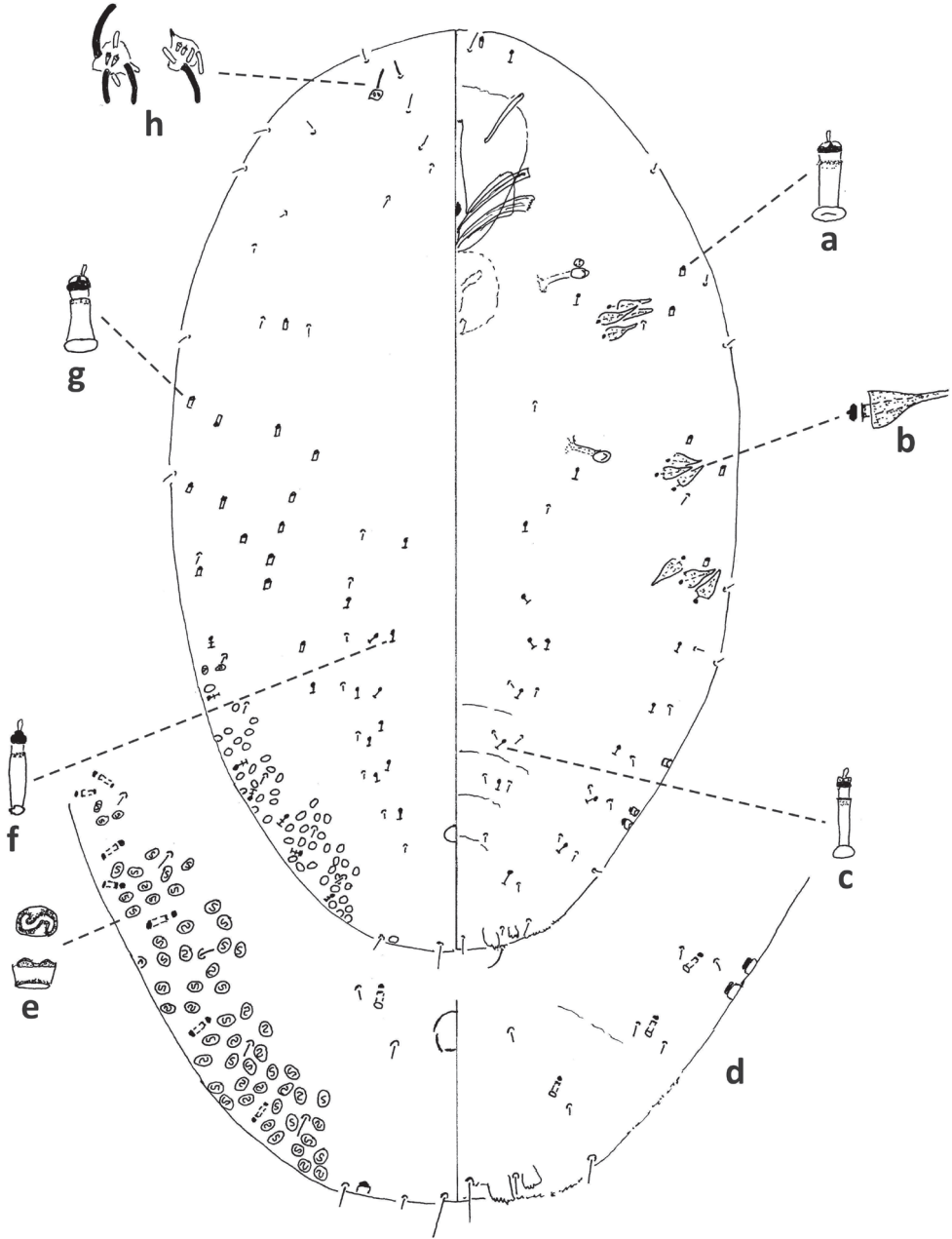


**Figure 7.** *Fiorinia foriniae*, second-instar male, Marion Co., Ocala, August 13, 2019 on *Chamaerops humilis*, T. Gordon, (2019-4546). Abbreviations: a) large microduct; b) large gland spine; c) large gland spine; d) large microduct; e) small gland c) small microduct; d) enlargement of pygidium; e) pores with S-shaped opening f) dorsal large microduct; g) dorsal large microducts; h) antennae each with several enlarged seta.

St. Lucie, May 17, 1978, on *Persea borbonia*, E.W. Campbell (1978-2858) (2 slides); St. Lucie Co., Port St. Lucie, February 20, 1980, on *Persea borbonia*, E.W. Campbell and R.H. Kendrick (1980-2989, 3008) (2 slides); St. Lucie Co., White City, May 30, 1980, on *Persea borbonia*, E.W. Campbell (1980-2961) (2 slides); Volusia Co., Allandale, March 16, 1983, on *Hedera helix*, J.N. Pott (1983-486) (2 slides); Volusia Co., Daytona Beach, August 16, 1984, on *Howea forsterina*, J.N. Pott (1984-2994); Volusia Co., Holly Hill, March 15, 1956, on *Chamaedorea* sp., C.R. Roberts (1956-2877) (3 slides); Volusia Co., New Smyrna Beach, April 8, 1985, on Palm, J.N. Pott (19852942); Volusia Co., New Smyrna Beach, September 27, 1971, on *Camellia* sp., J.N. Pott (1971-2887, 2889) (8 slides); Walton Co., Walton, February 12, 1980, on *Mangifera indica*, E.W. Campbell (1980-2946) (2 slides).

**Specimens examined for description and diagnosis.** Marion Co., Ocala, August 13, 2019 on *Chamaerops humilis*, T. Gordon, 5 2<sup>nd</sup> ♀, 5 2<sup>nd</sup> ♂, 10 ad ♀ (2019-4546).

**Other material examined from USNM.** Mexico: July 11, 1988, on *Mangifera indica*, S. Sanner 6 2<sup>nd</sup> ♀ (El Paso 032924). Peru: May 7, 1977, on *Mangifera indica*, R. Narkaus 5 2<sup>nd</sup> ♀ (Los Angeles 19190); August 21, 1972, on *Camellia* sp., E.B. Lee 1 1<sup>st</sup> ♀, 4 2<sup>nd</sup> ♀, 3 ad ♀. Portugal: Azores, August 20, 1928, on *Camellia* sp., C.A. Davis 1 1<sup>st</sup> ♀ (at Providence, Rhode Island). United States: California, San Diego, San Diego Zoo, August 19, 2002, D. Kellum, J.F. Miller, D.R. Miller, on *Camellia* sp. 3 1<sup>st</sup> ♀, 18 2<sup>nd</sup> ♀, 7 ad ♀; Georgia, Camden Co., June 14, 1969, on *Ruscus* sp., R.J. Beashear 1 1<sup>st</sup> ♀.

### *Fiorinia japonica* Kuwana, 1902

**Field characteristics.** First-instar exuviae overlapping second-instar exuviae. Without indentation or with slight indentation formed between attachment of first- and second-instar exuviae. Second-instar exuviae oval, convex marginally; medium to dark brown; longitudinal ridge inconspicuous. Posterior end of adult female within second-instar exuviae rounded. Heavily infested leaves with white secretion (Suppl. material 1: Fig. S1).

**First-instar nymph.** described in Howell (1977).

**Second-instar female.** Median lobes broad, as wide as or wider than medial lobule of second lobe, projecting ca. same distance as or further than medial lobule of second lobes. With five pairs of marginal macroducts. Swelling of body margin adjacent to macroduct usually rounded. With four large gland spines on margin of each side of body from abdominal segments II–V; usually without small gland spine on each side of abdominal segment VI; with small gland spines on margin or submargin of abdominal segment I. With one microduct on each side of head. Longitudinal line of microducts present submarginally on venter of abdominal segment II or III–VI, normally with one microduct on each side of each segment. Cicatrices absent.

**Second-instar male.** One duct cluster on each side of body, composed of several small ducts and two communal ducts. Three longitudinal lines of microducts on venter of abdomen (one medial and two submarginal). Cluster of small microducts with sclerotized orifice laterad of anterior spiracle absent. Fewer than five gland spines on each side of body between anterior and posterior spiracles. Antennae each with one enlarged seta.

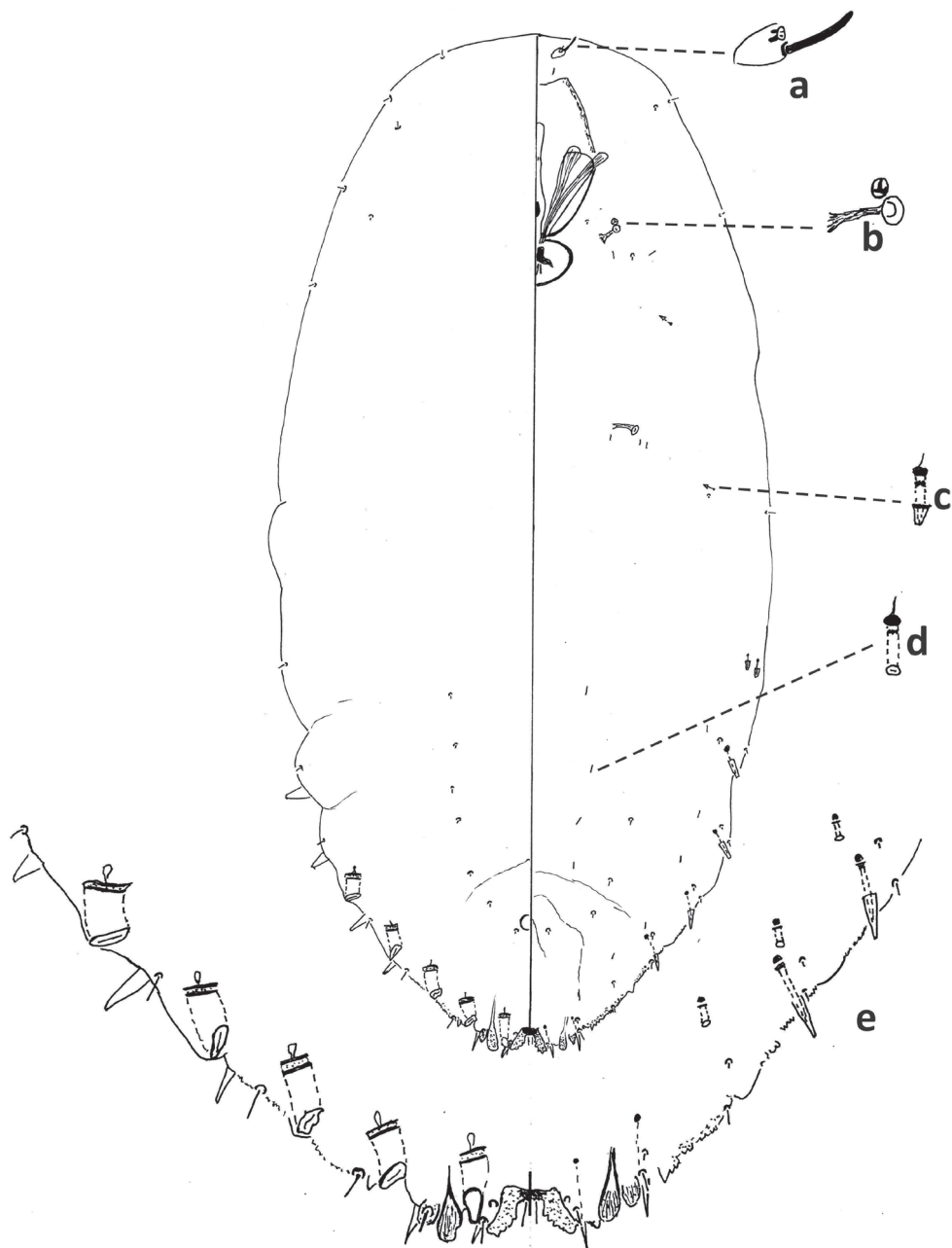


**Figure 8.** *Fiorinia japonica* second-instar female, Virginia, Chesterfield Co., Southside Nursey, July 27, 1974, on blue spruce, R. Sears. Abbreviations: a) antenna; b) anterior spiracle; c) microduct with sclerotized orifice; d) small microduct; e) enlargement of pygidium.

**Florida collection records.** *Fiorinia japonica* has not been collected in Florida.

**Specimens examined for description and diagnosis.** Virginia, Chesterfield Co., Southside Nursey, July 27, 1974, on blue spruce, R. Sears, 5 2<sup>nd</sup> ♀, 5 2<sup>nd</sup> ♂.

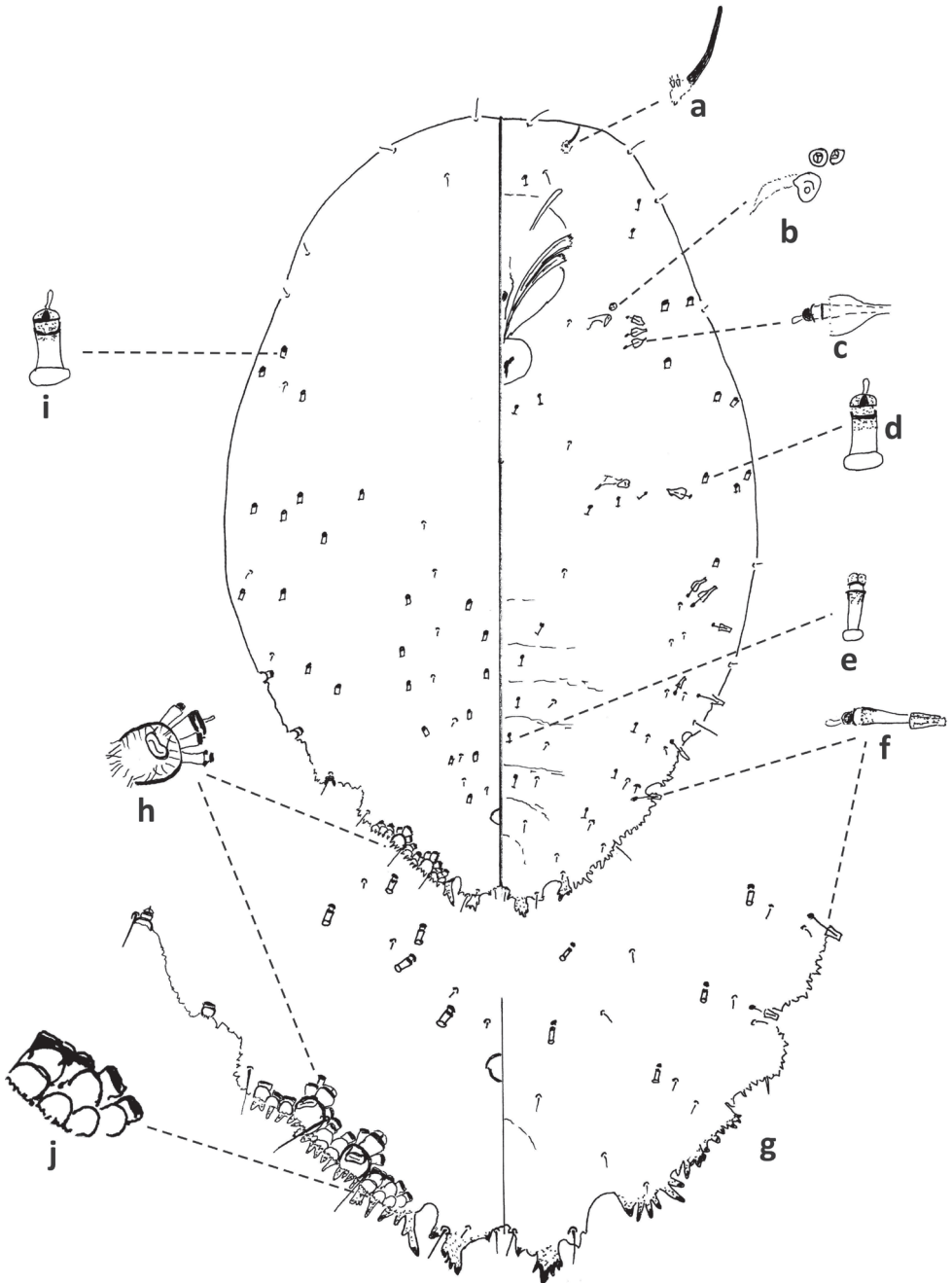


**Figure 9.** *Fiorinia japonica*, second-instar male Virginia, Chesterfield Co., Southside Nursey, July 27, 1974, on blue spruce, R. Sears. Abbreviations: a) antenna; b) anterior spiracle; c) large gland spine; d) large microduct; e) small microduct; f) small gland spine; g) enlargement of pygidium; h) enlargement of portion of duct cluster; i) large microduct; j) enlargement of communal duct.

**Other material examined from USNM.** China; “Hsifeushang” January 23, 1933, on *Pinus* sp., W.B. Wood 2 1<sup>st</sup> ♀ (JOH 55-76 F). Taiwan: Maruyama, near Taihoku, June 3, 1928, on *Pinus thunbergi*, R. Takahashi 1 1<sup>st</sup> ♂ (JOH 58-76); Taihoku, June 7, 1929, on *Pinus* sp., R. Takahashi 1 1<sup>st</sup> ♀ (JOH 54-76). United States: Virginia, Chesterfield Co., Southside Nursey, July 27, 1974, on blue spruce, R. Sears 2 1<sup>st</sup> ♀, 1 1<sup>st</sup> ♂, 5 2<sup>nd</sup> ♀, 5 2<sup>nd</sup> ♂, 4 ad ♀; Washington, D.C., August 27, 1991, on national Christmas tree, Horton 3 1<sup>st</sup> ♀, 4 2<sup>nd</sup> ♀, 3 ad ♀ (93-09742).

### *Fiorinia phantasma* Cockerell & Robinson, 1915

**Field characteristics.** First-instar exuviae overlapping second-instar exuviae. Without indentation formed between attachment of first- and second-instar exuviae. Second-instar exuviae oval, convex marginally; light to dark brown, longitudinal ridge weakly developed. Posterior end of adult female within second-instar exuviae constricted and pointed (Suppl. material 1: Fig. S1).

**First instar.** Similar to *F. fioriniae* and *F. proboscitaria* in having gland spines on abdominal segment VI at least half as long as gland spine on segment VII. *Fiorinia fioriniae* and *F. proboscitaria* differ by having (characters in parentheses are those of *P. phantasma*): pattern of derm surrounding large duct on head serpentine (globular); inner apex of large duct on head flat (rounded or mushroom like).

**Second-instar female.** Median lobes broad, as wide as or slightly narrower than medial lobule of second lobe, projecting ca. same amount or slightly less than medial lobule of second lobes. With five pairs of marginal macroducts. Swelling of body margin adjacent to macroduct usually pointed. With three large gland spines on margin of each side of body from abdominal segments II–IV, without gland spine on abdominal segment VI; with small gland spines on margin or submargin of abdominal segment I. With three microducts on each side of head. Longitudinal line of microducts absent submarginally on venter of abdomen. Cicatrices absent.

**Second-instar male.** One duct cluster on each side of body, composed of several small ducts and one communal duct. Five longitudinal lines of microducts on venter of abdomen (one medial, two mediolateral, and two submarginal), medial line sometimes incomplete. Cluster of small microducts with sclerotized orifice laterad of anterior spiracle absent. Fewer than five gland spines on each side of body between anterior and posterior spiracles. Antennae each with one enlarged seta.

**Adult female.** Body tapering at segment III to narrow pygidium. With three or four pairs of dorsal macroducts on each side of body, ducts similar in shape and size to microducts. Projection between antennae with many spicules. Antennae close together, with distinct projection.

**Florida collection records.** Miami-Dade Co., Miami, March 1, 2018, on *Phoenix canariensis*, Olga Garcia (2018-789) (3 slides); Miami-Dade Co., Coral Gables, April 2, 2018, on *Phoenix* sp., J. Farnum (2018-1499) (2 slides); Miami-Dade Co., Pincrest,

April 2, 2018, on *Phoenix* sp., J. Farnum (2018-1487, 1489, 1491, 1492, 1496, 1500, 1503, 1504, 1524, 1525) (20 slides); Miami-Dade Co., Palmetto Bay, April 2, 2018, on *Phoenix* sp., J. Farnum (2018-1488, 1493, 1498, 1501) (8 slides); Miami-Dade Co., Pinecrest, May 22, 2018, on *Phoenix* sp., J. Farnum and J. Vergel (2018-2780, 2785, 2796) (6 slides); Palm Beach Co., Boynton Beach, January 23, on *Cocos nucifera*, L. Smith (2018-304) (2 slides); Miami-Dade Co., Coral Gables, Miami-Dade Co., Palmetto Bay, May 22, 2018, on *Phoenix* sp., J. Farnum and J. Vergel (2018-2783, 2788, 2790) (6 slides); May 22, 2018, on *Dypsis lutescens*, J. Miller, H. Mayer, M.Z. Ahmed (2018-2761) (2 slides); Miami-Dade Co., Coral Gables, May 22, 2018, on *Phoenix reclinata*, H. Mayer, J. Miller, M.Z. Ahmed (2018-2767); Miami-Dade Co., Kendall, May 22, 2018, on *Phoenix* sp., J. Farnum and J. Vergel (2018-2787, 2771) (6 slides); Miami-Dade Co., Miami, May 22, 2018, on *Phoenix roebelenii*, E. Talamas, V. de Campover, C. Mannion (2018-2779); Miami-Dade Co., Miami, May 22, 2018, on *Phoenix* sp., L. Osborne, Y. Hernandez, P. Perez (2018-2794); Miami-Dade Co., Miami, May 22, 2018, on *Cycas revoluta*, L. Osborne, Y. Hernandez, P. Perez (2018-2854) (2 slides); Miami-Dade Co., Miami, May 22, 2018, on *Phoenix* sp., J. Farnum and J. Vergel (2018-2784); Miami-Dade Co., Miami, May 22, 2018, on *Phoenix* sp., L. Osborne and Y. Hernandez (2018-2785); Miami-Dade Co., Miami, May 23, 2018, on *Phoenix* sp., J. Farnum and J. Vergel (2018-2782, 2797, 2799) (6 slides); Miami-Dade Co., Miami, May 23, 2018, on *Phoenix* sp., J. Farnum, C.M. Twyford (2018-2766) (2 slides); Miami-Dade Co., Miami, May 24, 2018, on *Phoenix roebelenii*, J. Farnum and C.C. Twyford (2018-2795); Miami-Dade Co., Miami, May 24, 2018, on *Phoenix* sp., C.M. Twyford (2018-2759, 2765, 2776, 2777, 2786, 2798) (12 slides); Miami-Dade Co., Coral Gables, May 24, 2018, on *Strelitzia* sp., O. Garcia and M.Z. Ahmed (2018-2774) (2 slides); Miami-Dade Co., Coral Gables, May 24, 2018 on *Cocos nucifera*, O. Garcia and M.Z. Ahmed (2018-2773); Miami-Dade Co., Coral Gables, October 15, 2018, on *Tahina spectabilis*, C.T. Allen, J. Farnum, S. Durand, A. Roda (2018-5459) (2 slides); Miami-Dade Co., Coral Gables, October 26, 2018, on *Pittosporum tobira*, J. Farnum, C.T. Allen, A. Roda (2018-5679) (2 slides); Miami-Dade Co., Coral Gables, October 26, 2018, on *Livistona chinensis*, J. Farnum, C.T. Allen, A. Roda (2018-5680) (2 slides); Miami-Dade Co., Coral Gables, December 3, 2018, on *Sabal mexicana*, J. Farnum, L. Noblick (2018-6221) (2 slides); Miami-Dade Co., Coral Gables, December 3, 2018, on *Nypa fruticans*, J. Farnum and L. Noblick (2018-6222) (2 slides); Miami-Dade Co., Coral Gables, December 3, 2018, on *Tahina spectabilis*, J. Farnum, L. Noblick (2018-6218); Miami-Dade Co., Coral Gables, December 3, 2018, on *Howea forsteriana*, J. Farnum and L. Noblick (2018-6219) (3 slides); Palm Beach Co., Boynton Beach, February 8, 2019, on *Pandanus* sp., L. Smith (2018-481) (2 slides); Palm Beach Co., Delray Beach, March 4, 2019, on unknown host, J. Farnum and L. Smith (2018-903) (2 slides).

**Specimens examined for description and diagnosis.** Palm Beach Co., Boynton Beach, October 30, 2019, on *Wodyetia bifurcata*, L. Smith, 5 1<sup>st</sup> (2019-5998); Palm Beach Co., Boynton Beach, April 6, 2020, on *Ligustrum japonicum*, L. Smith, 10 ad ♀ (2020-1365); Palm Beach Co., Boynton Beach, November 6, 2019, on *Wodyetia bifurcata*, 5 2<sup>nd</sup> ♀ (2019-6182); Philippines, June 28, 1996 on *Plumeria* sp., 2<sup>nd</sup> ♀

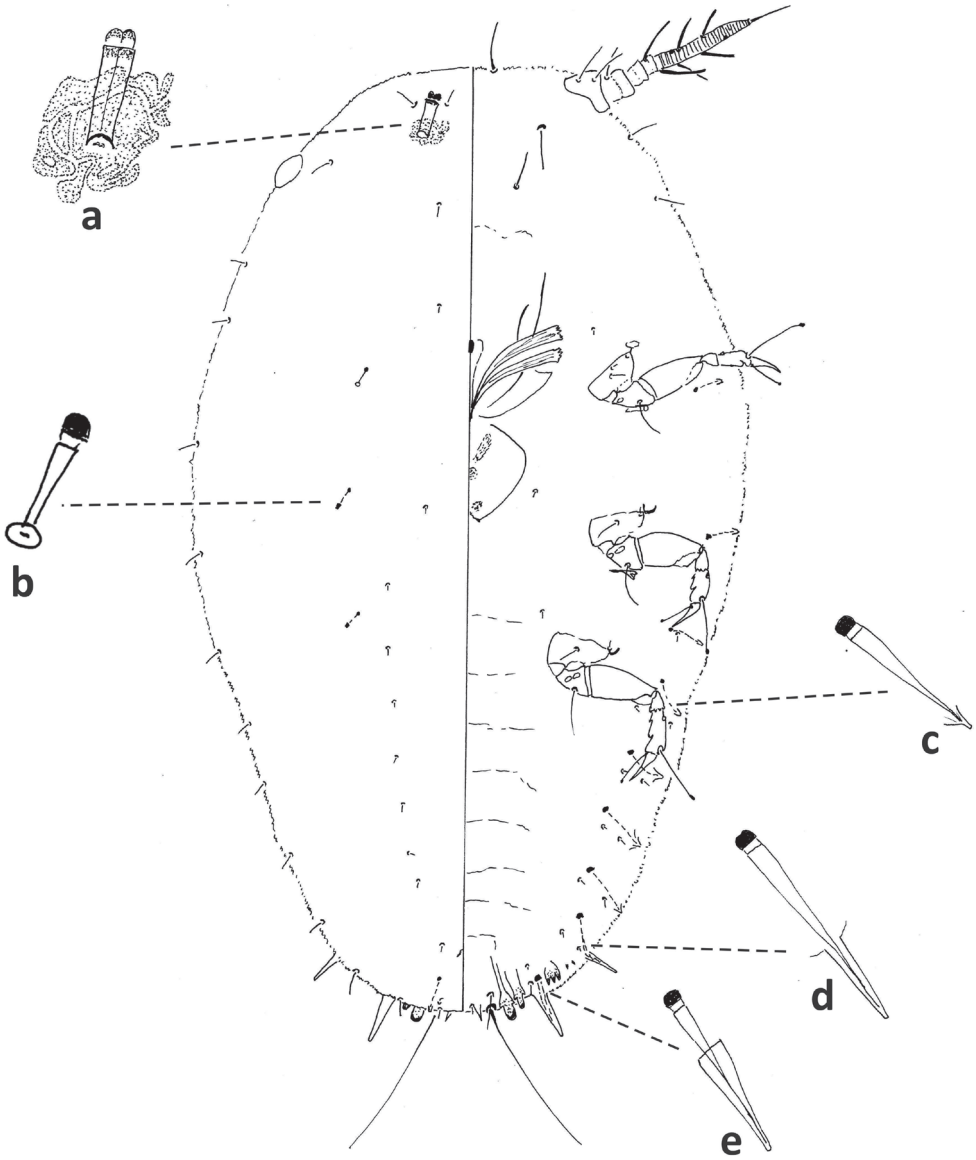


**Figure 10.** *Fiorinia phantasma*, First-instar nymph, Palm Beach Co., Boynton Beach, October 30, 2019, on *Wodyetia bifurcata*, L. Smith, (2019-5998). Abbreviations: a) large dorsal duct on head; b) small microduct; c) gland spine abdominal segment II with small projection; d) gland spine at abdominal segment VI with long projection; e) gland spine at abdominal segment VII with long projection.

(SF023635); Miami-Dade Co., Miami, November 9, 2019, on *Palmae*, O. Garcia, 5 2<sup>nd</sup> ♂ (2019-6149); Palm Beach Co., Boca Raton, December 29, 2020, on *Phoenix canariensis*, L. Smith, 10 ad ♀ (2020-4958).

**Other specimens examined from USNM.** Grenada, Calivingy Island, March 2012, on *Phoenix dactylifera*, S.W. Evans (E-2012-2099); Guam, Tamuning, June 4, 1984, on *Cocos nucifera*, R. Muniappan; Hawaii: Oahu, Kapahulu area, March 27,

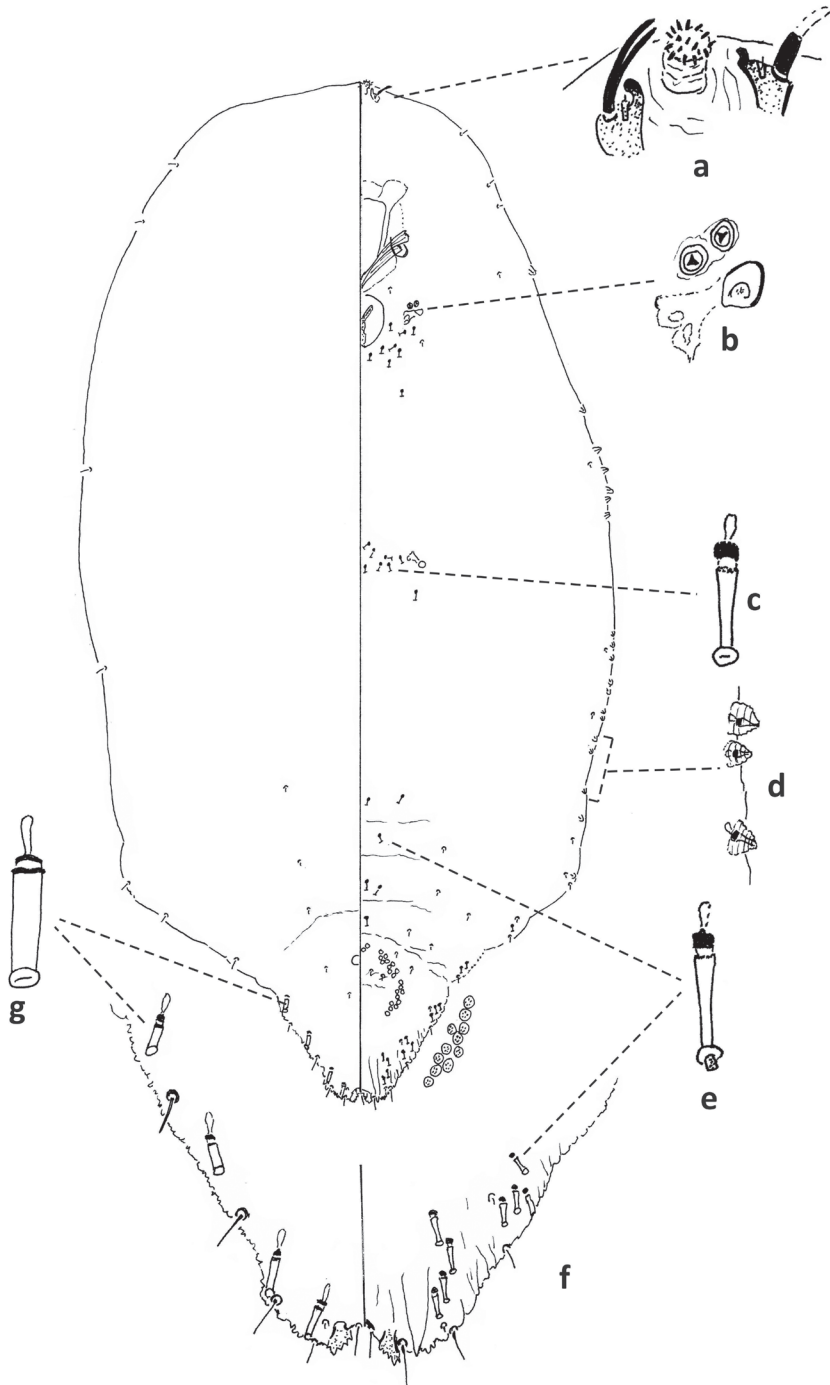


**Figure 11.** *Fiorinia phantasma* (Cockerell & Robinson); adult female, Palm Beach Co., Boynton Beach, April 6, 2020, on *Ligustrum japonicum*, L. Smith (2020-1365). Abbreviations: a) detail of antennae and inter-antennal process; b) detail of anterior spiracle; c) microducts; d) marginal duct tubercles; e) marginal microduct; f) detail of pygidium; g) marginal macroduct on pygidium.

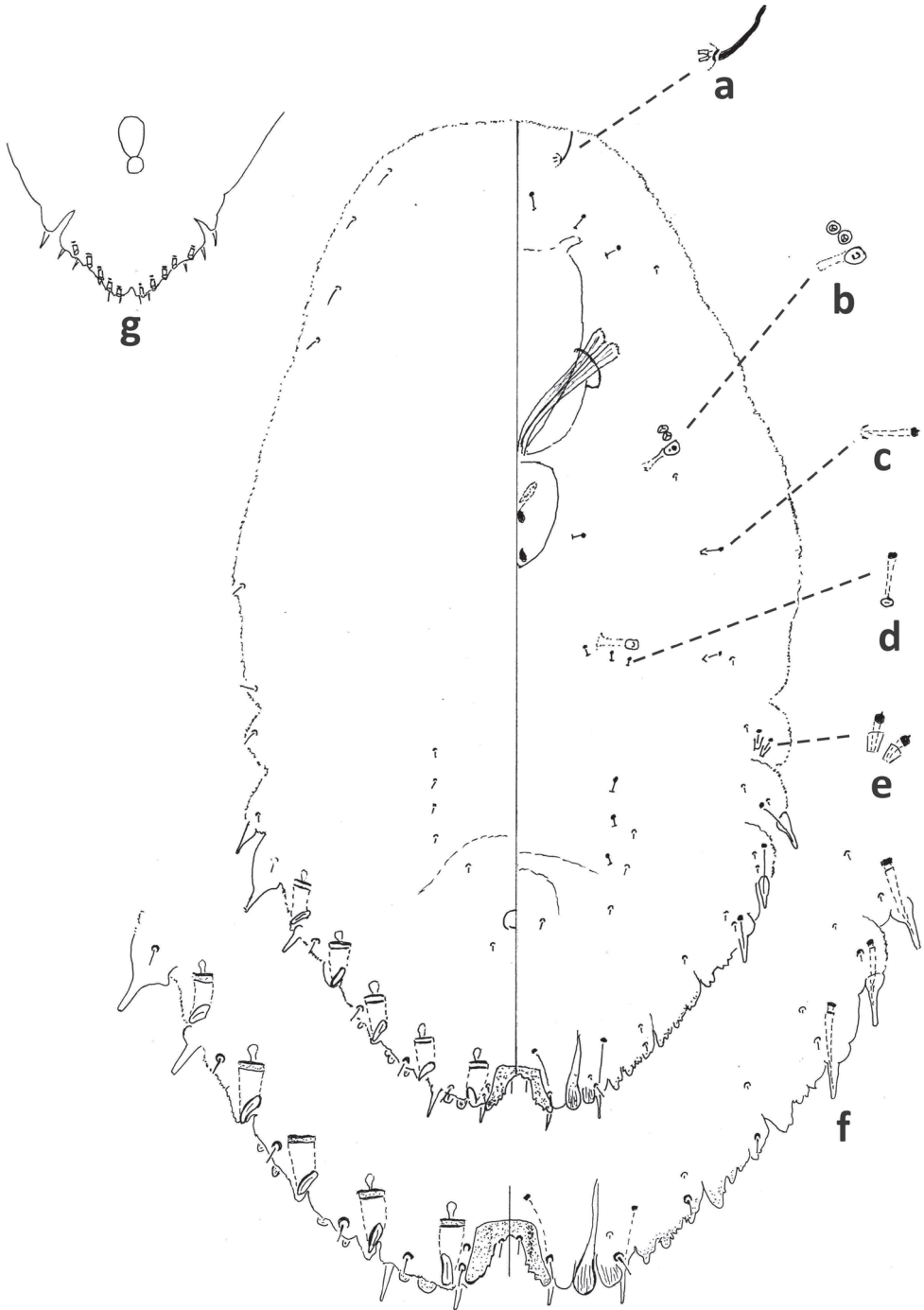


**Figure 12.** *Fiorinia phantasma*, second-instar female and second-instar female shed skin, Palm Beach Co., Boynton Beach, November 6, 2019, on *Wodyetia bifurcata*, (2019-6182). Abbreviations: a) antenna; b) anterior spiracle; c) microduct with sclerotized orifice; g) old second-instar female, Philippines, June 28, 1996 on *Plumeria* sp., 2<sup>nd</sup> ♀ (SF023635).

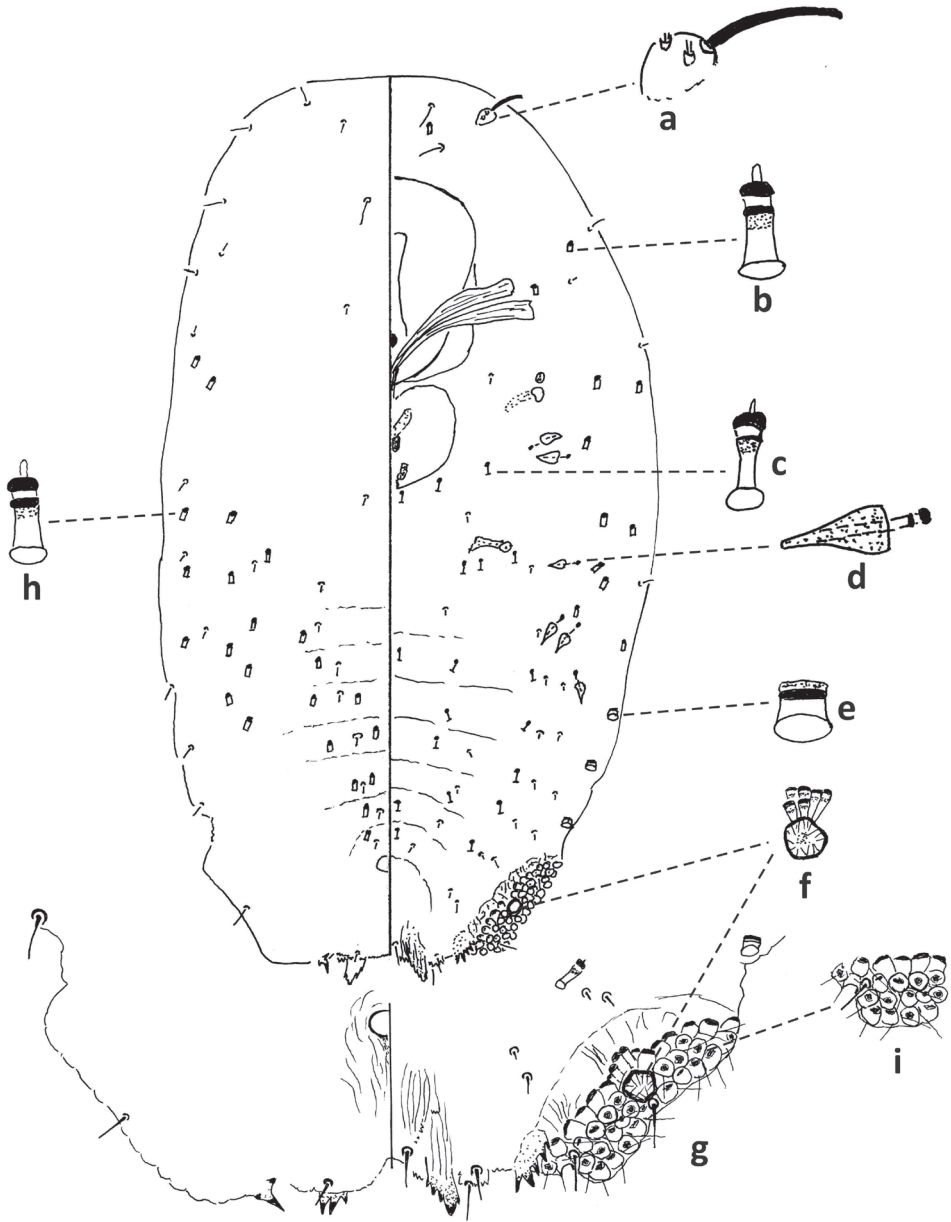


**Figure 13.** *Fiorinia phantasma*, second-instar male, Miami-Dade Co., Miami, November 9, 2019, on Palmae, O. Garcia, (2019-6149). Abbreviations: a) antenna; b) large microduct; c) small microduct; d) large gland spine; e) small macroduct; f) enlargement of communal duct; g) enlargement of pygidium; h) large microduct; j) enlargement of part of duct cluster.

2009, on *Ligustrum* sp., M. Ramadan (0904651); Hawaii, Hilo ?, date ?, on *Pittosporum* sp., B. Kumashiro 5 2<sup>nd</sup> ♀, 5 2<sup>nd</sup> ♀; Philippines, April 7, 1965, on *Cocos nucifera*, J.I. Mason; Philippines, November 15, 1971, on palm leaf, R.F. Goodall (Seattle 8910); Philippines, March 13, 1975, on *Mangifera indica*, M. Yoshinaga (Hawaii

28847); Philippines, August 26, 1975, on *Cocos nucifera*, A. Buchanan (LA 015303); Philippines, November 30, 1975, on palm leaf, Ozuka & Richardson (Hawaii 32858); Philippines, June 8, 1977, on palm leaf, Tamiya (Hawaii 39130); Philippines, August 17, 1977, on *Areca* sp., J. Sato (Honolulu 42721); Philippines, October 19, 1978, on *Areca* sp., Takeda, (Honolulu 43108); Philippines, November 4, 1978, on palm leaf, Jodoi, (Honolulu 42704); Philippines, May 26, 1981, on *Tamarindus indica*, D.O. Wienhee & F.G. Walisen (Seattle 17304); Philippines, May 12, 1985, on Philippines, *Clausenia anisum*, C. Dollopf (Chicago 009312); Philippines, June 28, 1996, on *Plumeria* sp. (SF 023635); Philippines, October 19, 1978, on *Areca* sp., Takeda (Honolulu 43108); Taiwan, May 10, 1981, on leaf, J.L. Levitt (Seattle 17328); Taiwan, April 8, 1988, on *Ficus* sp., V. McDonald (JFK 100609); Thailand, August 31, 1982, on leaf, G. Hinsdale (Anchorage 017131); Thailand, July 19, 1985, on *Murraya koenigii*, J. Alabu (LA 052785); Thailand, November 15, 1987, on *Areca* sp., J. Elridge (Atlanta 003471); Thailand, March 20, 2003, on Arecaceae, F. Hadded; Thailand, March 27, 2006, on palm, M. Hanzlik (ANC 060060); Vietnam, April 26, 2007, on *Cocos* sp., A. Coronel (LA 207977 CA); Vietnam, October 26, 2012, on unknown host, D. Gregory (SF 1301449).

**Notes.** We examined four paratype slides of *F. coronata* Williams & Watson from Guadalcanal, Solomon Islands deposited in the USNM collection at Beltsville, Maryland. Most of the specimens were punctured in the middle of the body between the posterior spiracles during the mounting process. However, we could still see that all had microducts between the posterior spiracles which were small and less numerous than specimens from elsewhere, but they definitely are there.

We also examined a paratype slide of *F. phantasma* in the same collection, but it is in such poor condition that only half of the pygidium is useful for diagnosis. It is impossible to even find the posterior spiracles, let alone microducts between them. In addition, the holotype of *F. phantasma* deposited in The Natural History Museum, London (NHMUK) was loaned to and examined by one of us (DL). It also was in poor condition; microducts close to anterior and posterior spiracles and in prepygidial abdominal segments were not visible. All of the examined specimens of *F. phantasma* that were in good condition had easily discernable microducts between the posterior spiracles.

### *Fiorinia pinicola* Maskell, 1897

**Field characteristics.** First-instar exuviae overlapping second-instar exuviae. With indentation formed between attachment of first- and second-instar exuviae. Second-instar exuviae oval, convex marginally; medium to dark brown; longitudinal ridge conspicuous. Posterior end of adult female within second-instar exuviae rounded. Heavily infested leaves with white secretion (Suppl. material 1: Fig. S1).

**First-instar nymph.** Described in Howell (1977).

**Second-instar female.** Median lobes broad, as wide as or wider than medial lobule of second lobe, projecting ca. same amount as medial lobule of second lobes. With five

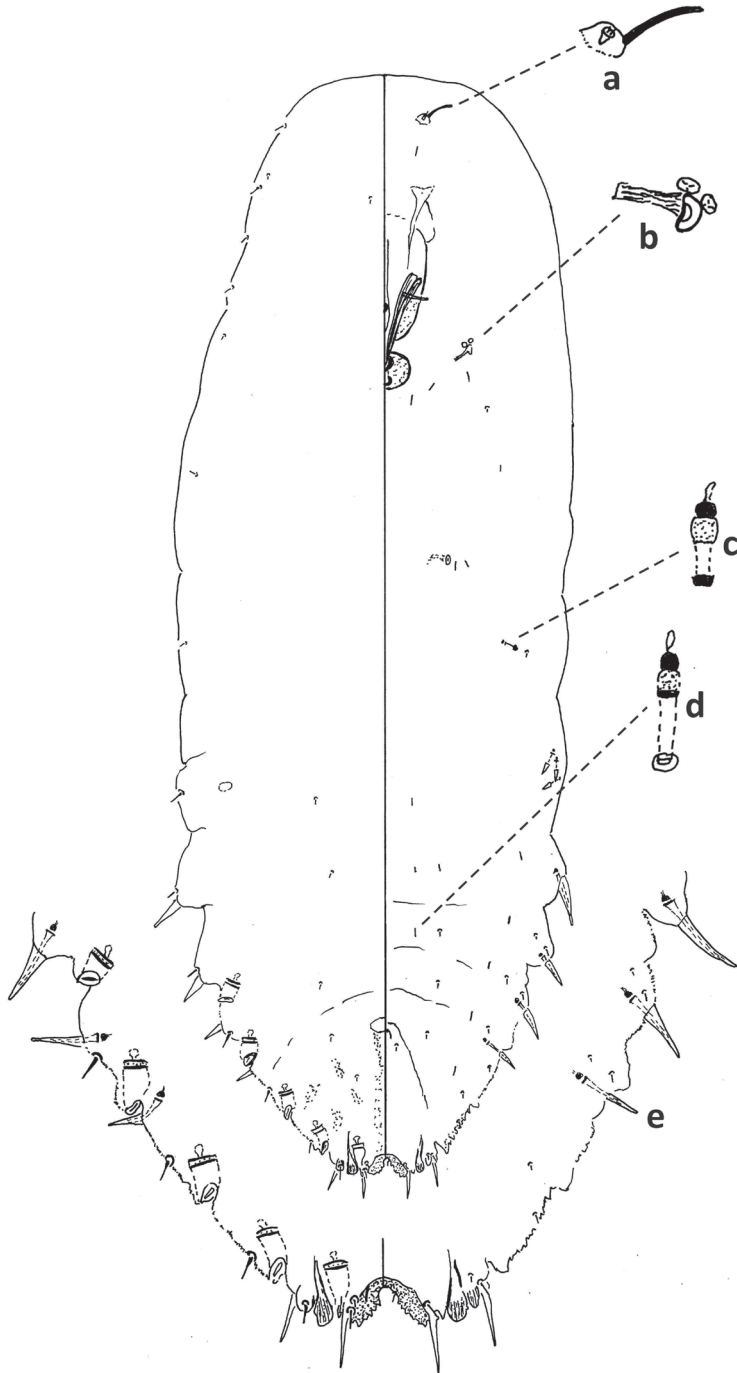


**Figure 14.** *Fiorinia pinicola*, second-instar female, Hong Kong, December 1895, on *Pinus sinensis*, A. Koebele (1529) mounted from type material. Abbreviations: a) antenna; b) anterior spiracle; c) small microduct with sclerotized orifice d) small microduct e) enlargement of pygidium. Note the blank blotches on the body margin of the pygidium enlargement.

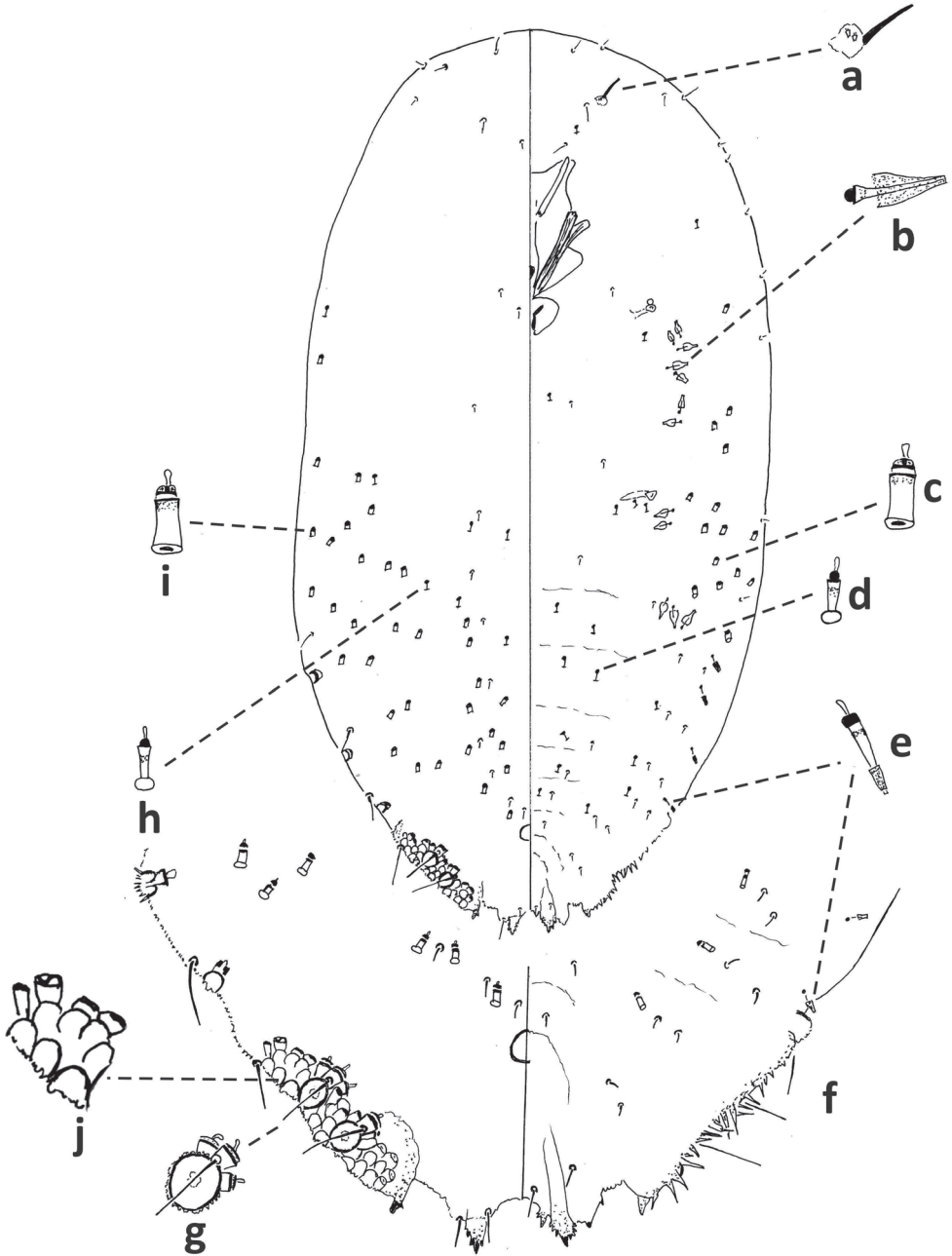


**Figure 15.** *Fiorinia pinicola*, second-instar male, Hong Kong, China, December 1895, on *Pinus sinensis*, A. Koebele (1529) mounted from type material. Abbreviations: a) antenna; b) large gland spine; c) large microduct; d) small microduct; e) small gland spine; f) enlargement of pygidium; g) enlargement of communal duct; h) small microduct; i) large microduct; j) enlargement of part of duct cluster.

pairs of marginal macroducts. Swelling of body margin adjacent to macroduct usually pointed. With four large gland spines on margin of each side of body from abdominal segments II–V; usually without small gland spine on each side of abdominal segment VI; with small gland spines on margin or submargin of abdominal segment I. With one microduct on each side of head. Longitudinal line of microducts present submarginally on venter of abdominal segments II–VI, normally with one microduct on each side of each segment. Cicatrices absent.

**Notes.** We have been unable to find characters that consistently separate second-instar females of *F. japonica* and *F. pinicola*. The swelling of the body adjacent to the abdominal macroducts is usually pointed in *F. pinicola* and is usually rounded in *F. japonica*, but we have too few specimens to understand the possible variation in this character.

**Second-instar male.** One duct cluster on each side of body, composed of several small ducts and two communal ducts. Three longitudinal lines of microducts on venter of abdomen (one medial and two submarginal). Cluster of small microducts with sclerotized orifice laterad of anterior spiracle absent. Five or more gland spines on each side of body between anterior and posterior spiracles. Antennae each with one enlarged seta.

**Specimens examined for description and diagnosis.** China, Hong Kong, December 1895, on *Pinus sinensis*, A. Koebele 2<sup>nd</sup> ♀, ♂ (1529); United States, California, Los Angeles Co., Los Angeles, August 11, 2020, on *Podocarpus macrophyllus*, N. Ellenrieder, 3 2<sup>nd</sup> ♀, 2 ad ♀ (2020-3174).

**Other specimens examined from USNM.** China, Hong Kong, December 1895, on *Pinus sinensis*, A. Koebele (1529) mounted from type material, 2 2<sup>nd</sup> ♀, 2 2<sup>nd</sup> ♂, 2 ad ♀; Japan, Yokohama, Yamashita-cho, October 15, 1941, on *Pittosporum tobira*, K. Soto 1 1<sup>st</sup> ♀, 2 2<sup>nd</sup> ♀ (Yokohama 199); Japan, November 2, 1977, on *Podocarpus* sp., 1 1<sup>st</sup> ♀, 7 ad ♀; United States, California, Orange Co., October 2002, on *Pittosporum* sp., H. Mitchell 1 1<sup>st</sup> ♂ embryo, 1 1<sup>st</sup> ♀ embryo, 7 2<sup>nd</sup> ♀, 6 ad ♀.

### *Fiorinia proboscitaria* Green, 1900

**Field characteristics.** First-instar exuviae overlapping second-instar exuviae. Without indentation formed between attachment of first- and second-instar exuviae. Second-instar exuviae oval, convex marginally or parallel sided; light to medium dark brown; longitudinal ridge conspicuous and thick. Posterior end of adult female within second-instar exuviae rounded. Heavily infested leaves with white secretion.

**First-instar nymph.** Similar to *F. fioriniae* and *F. phantasma* in having gland spines on abdominal segment VI at least half as long as gland spine on segment VII. *Fiorinia fioriniae* differs by having (characters in parentheses are those of *P. proboscitaria*): inner apex of large duct on head flat (rounded or mushroom like). *Fiorinia phantasma* differs by having (characters in parentheses are those of *F. proboscitaria*): pattern of derm surrounding large duct on head globular (serpentine); inner apex of large duct on head rounded or mushroom like (flat).

**Adult female.** Process between antennae without spicules, often clubbed. Head conical. Antennae close together. Macroducts usually 3–5 on each side of pygidium, thin, longer than wide, resembling microducts. Gland spines barely projecting from body margin. Gland tubercles nearly continuous along body margin from head to abdominal segment III. Microducts in medial areas of prepygidial segments dorsally and ventrally. Lateral margin of head with cluster of circular tubercles possibly representing eye.

**Notes.** There are a number of species with processes between the antennae; Wei et al. (2013) included 16 species in their key to the *Fiorinia* species from China. Only a few have an unusually elongate interantennal process and a conical head. *Fiorinia proboscitaria* resembles *F. biakana* Williams and Watson but differs by (characters in parentheses are those of *F. biakana*): space between median lobes less than width of median lobe (greater than width of lobe); macroducts ca. same width as gland spine ducts (wider than gland spine ducts); gland spines slightly protruding from derm surface (protruding at least half length of gland spine duct); gland tubercles continuous along body margin (grouped in clusters). This species also resembles *F. turpiniae* Takahashi but differs by (characters in parentheses are those of *F. turpiniae*): trilocular pores present near the anterior spiracle (absent); gland spines short, shorter than gland spine duct (long, longer than gland spine duct). *Fiorinia proboscitaria* differs from *F. randiae* Takahashi by (characters in parentheses are those of *F. randiae*): gland spines short, shorter than gland spine duct (long, longer than gland spine duct); median lobes nearly parallel (divergent). Florida specimens of *F. proboscitaria* are consistent with the description of Williams and Watson (1988) and Takagi (1970) except that both illustrated a lobe on each side of the head (Florida specimens lack these lobes), and that neither described the cluster of circular tubercles near the margin of the head or the ventromedial microducts anterior of the pygidium. The illustration of Takagi has small lines at the end of the lobe on the side of the head which may be the same as the circular tubercles mentioned above, but they were not discussed in the description.

**Second-instar female.** Median lobes broad, as wide as or wider than medial lobule of second lobe, projecting ca. same amount or slightly less than medial lobule of second lobes. With four pairs of marginal macroducts. Swelling of body margin adjacent to macroduct usually rounded. With three large gland spines on margin of each side of body from abdominal segments II–IV; usually with small gland spine on each side of abdominal segments V and VI; without small gland spines on abdominal segment I. With three microducts on each side of head. Longitudinal line of microducts present submarginally on venter of abdominal segments II–VI, normally with 1–5 microducts on each side of each segment. Small lobular projections on anterior of head sometimes present. Cicatrix present on dorsal submargin of abdominal segment I.

**Second-instar male.** Two duct clusters on each side of body, anterior cluster without communal duct, posterior cluster composed of communal duct without associated smaller ducts. Normally, three longitudinal lines of microducts on venter of abdomen (one medial and two submarginal) occasionally with two medially forming four longitudinal lines. Without cluster of small microducts with sclerotized orifice laterad of

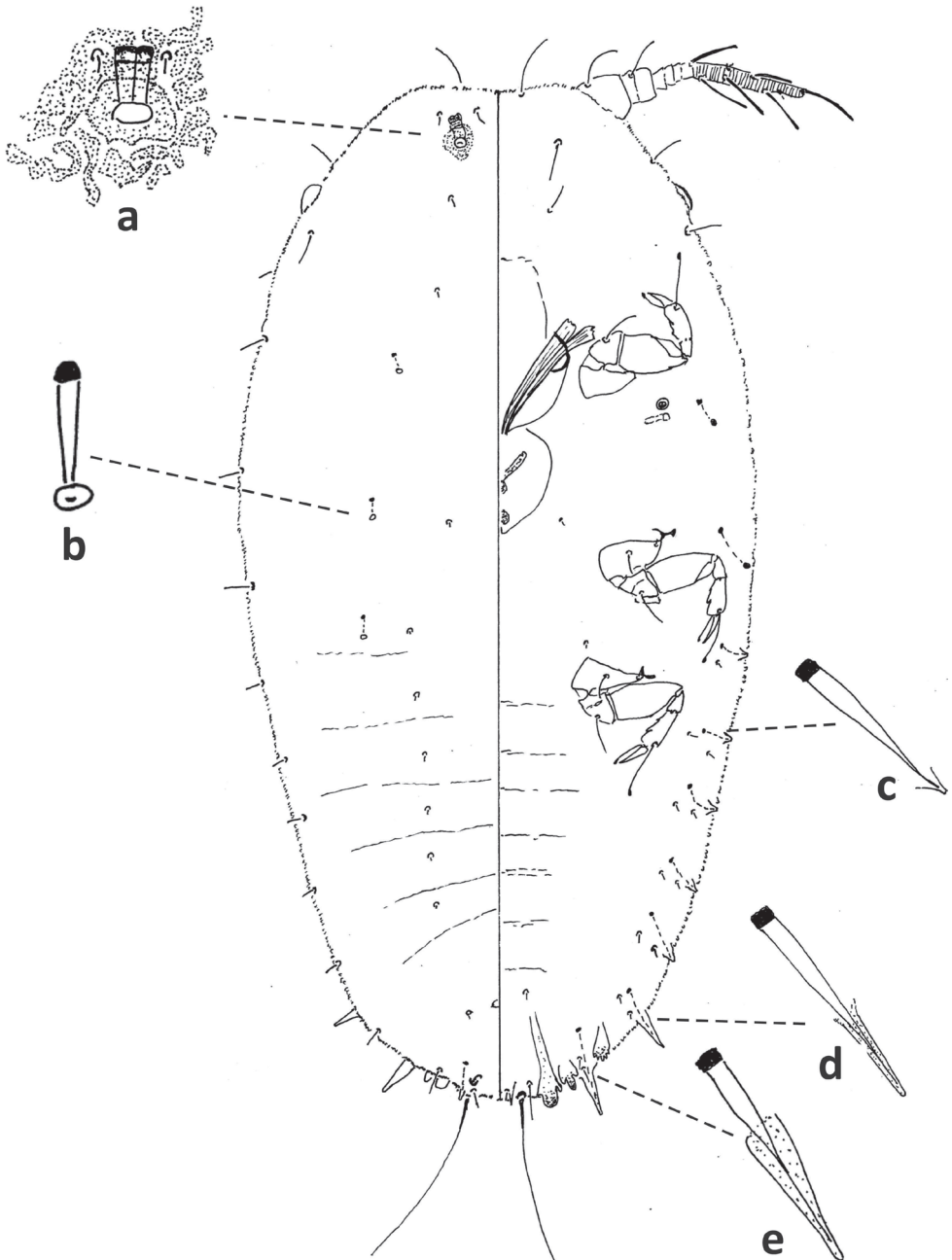


**Figure 16.** *Fiorinia proboscidea*, First-instar nymph, Putnam Co., Crescent City, October 2, 2019, on *Citrus* sp., D. Rigby, M. Cain, (2018-5548). Abbreviations: a) large duct on head; b) dorsal microduct; c) short gland spine on abdominal segment II; d) long gland spine on abdominal segment VI; e) long gland spine on abdominal segment VII.

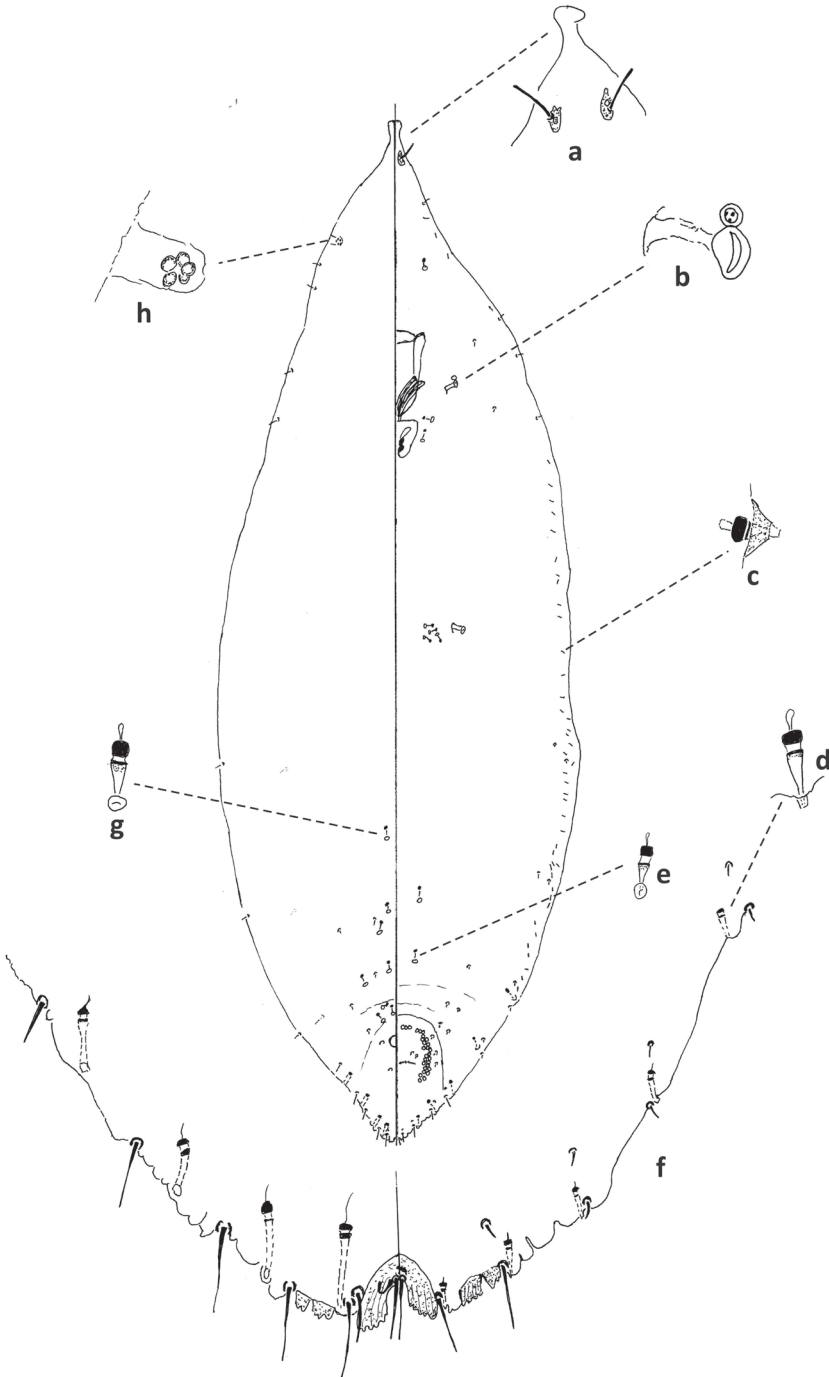


**Figure 17.** *Fiorinia proboscidea*, adult female, Hillsborough Co., Tampa, December 16, 2013, on *Citrus* sp., J. Hoffman (2013-9087). Abbreviations: a) conical head with protrusion, antennae; b) anterior spiracle; c) gland tubercle; d) gland spine with small dermal protrusion; e) small microduct; f) enlargement of pygidium; g) microduct; h) circular tubercles in invagination.

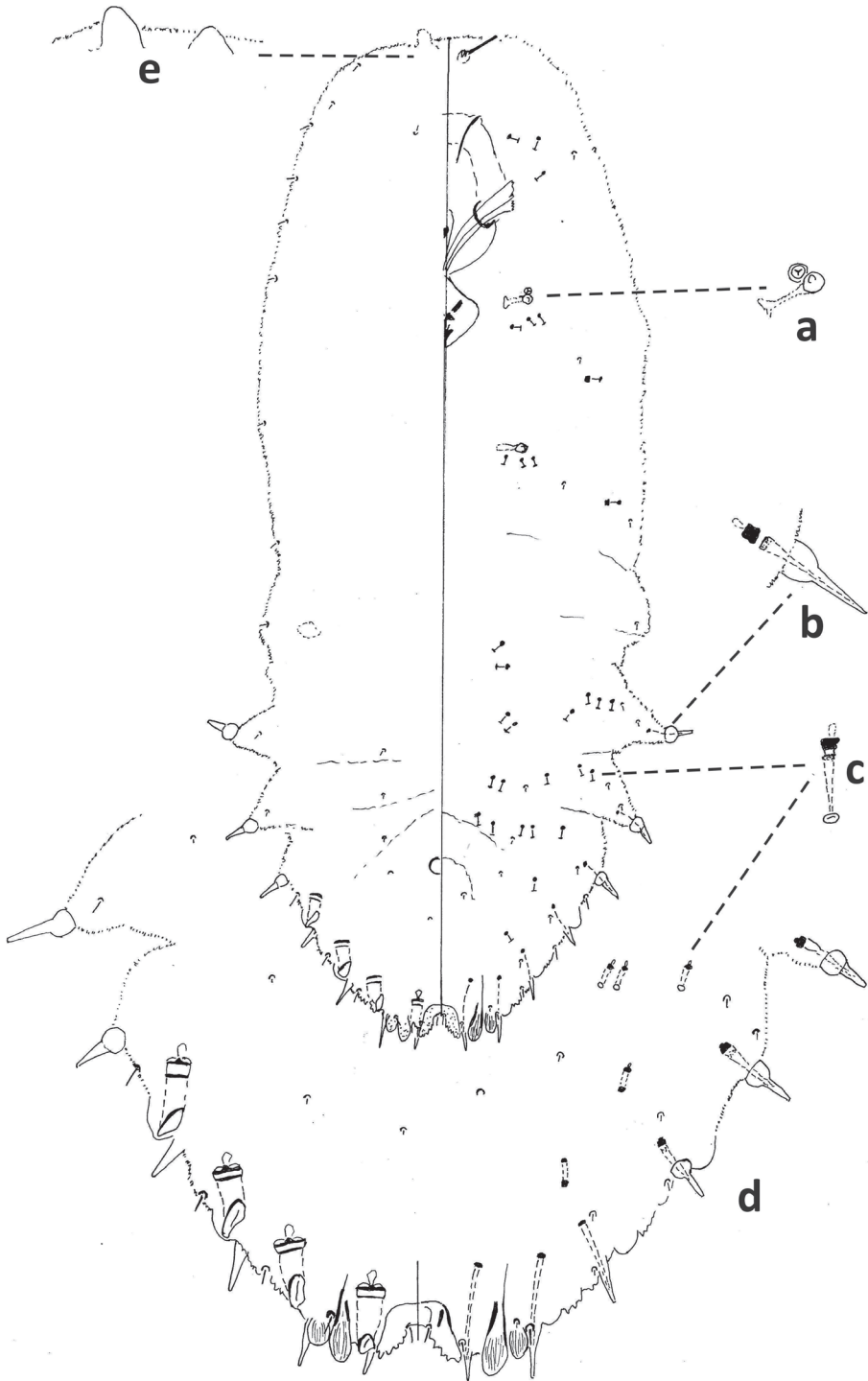


**Figure 18.** *Fiorinia proboscidaria*, second-instar female, Flagler Co., Palm Coast, June 18, 2020, on *Citrus* sp., M. Cain, (2020-2353). Abbreviations: a) anterior spiracle; b) large gland spine, c) small microduct; d) enlargement of pygidium; e) lobular projections on head.

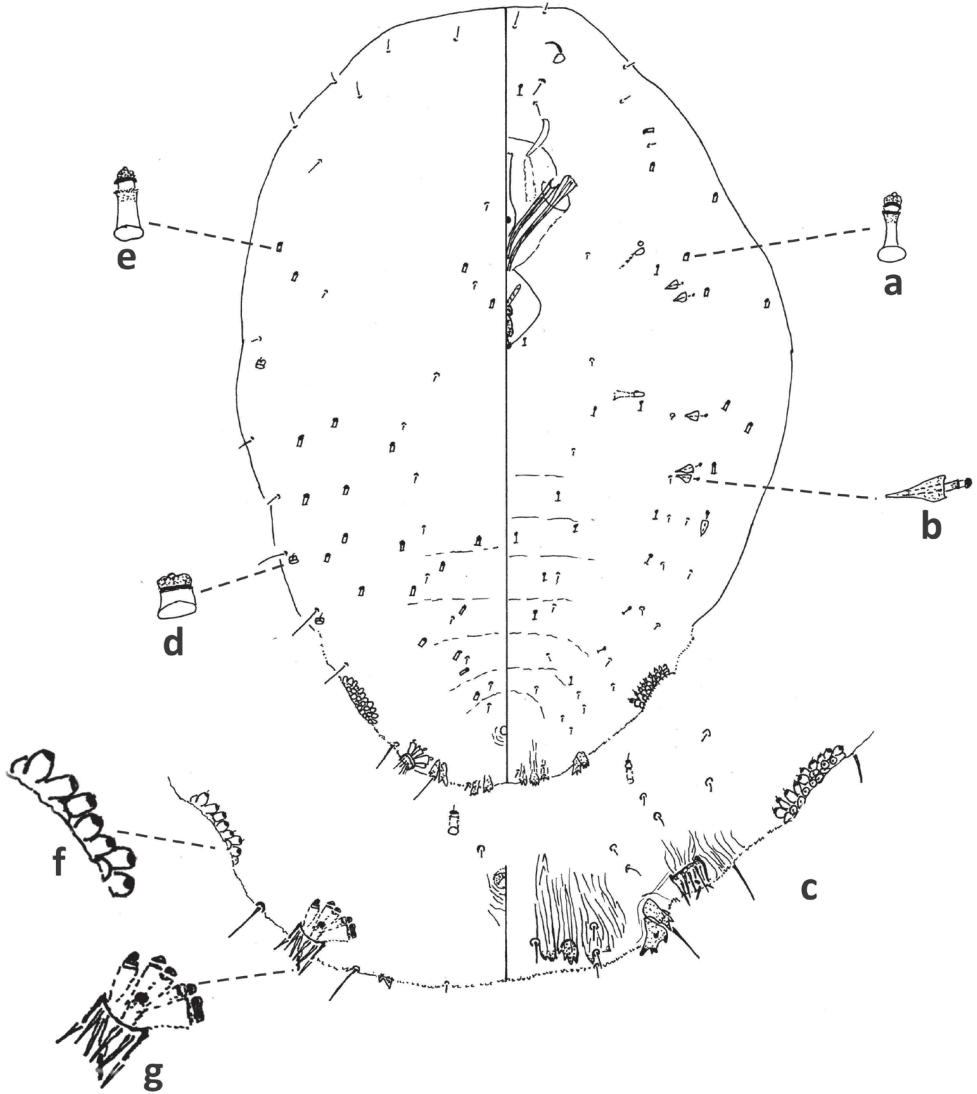


**Figure 19.** *Fiorinia proboscidea*, second-instar male, Putnam Co., Crescent City, October 2, 2019, on *Citrus* sp., D. Rigby, M. Cain, (2018-5548). Abbreviations: a) small microduct; b) large gland spine; c) enlargement of pygidium; d) small macroduct; e) large microduct; f) enlargement of part of duct cluster; g) enlargement of communal duct.

anterior spiracle. Fewer than five gland spines on each side of body between anterior and posterior spiracles. Antennae each with one enlarged seta.

**Florida collection records.** Hillsborough Co., Tampa, December 16, 2013, on *Citrus* sp., J. Hoffman (2013-9087) (7 slides); Hillsborough Co., Tampa, November 19, 2014, on *Citrus* sp., M. Briceno (2014-859) (6 slides); Hillsborough Co., Tampa, October 23, 2014, on *Citrus* sp., M. Briceno (2014-7431) (2 slides); Hillsborough Co., Tampa, October 30, 2014, on *Citrus* sp., M. Briceno (2014-7574) (7 Slides);

Hillsborough Co., Valrico, September 17, 2018, on *Citrus × paradisi*, P. Barker (2018-4907) (2 slides); Putnam Co., Palatka, October 25, 2018, on *Ilex cornuta*, M. Cain, T. Wright, and C. Hall (2018-5664) (2 slides); Santa Rosa Co., Gulf Breeze, January 3, 2014, on *Citrus* sp., M. Anderson (2014-46) (3 slides).

**Specimens examined for description and diagnosis.** Flagler Co., Palm Coast, June 18, 2020, on *Citrus* sp., M. Cain, 5 2<sup>nd</sup> ♀, (2020-2353); Hillsborough Co., Tampa, December 16, 2013, on *Citrus* sp., J. Hoffman 5 ad ♀ (2013-9087); Manatee Co., Bradenton, January 6, 2021, on *Citrus* sp., P. Kumar, 10 ad ♀ (2021-67); Pinellas Co., Palm Harbor, September 16, 2019, on *Citrus* sp. B. Rose, 2 ad ♀ (2019-5124); Putnam Co., Crescent City, October 2, 2019, on *Citrus* sp., D. Rigby, M. Cain, 5 1<sup>st</sup> (2018-5548); Putnam Co., Crescent City, October 2, 2019, on *Citrus* sp., D. Rigby, M. Cain, 5 2<sup>nd</sup> ♂ (2018-5548).

**Material examined from USNM.** China, Hong Kong, September 2, 1980, on *Podocarpus* sp., J. Dooley 1 2<sup>nd</sup> ♂, 1 prepupa, 4 ad ♀ (Los Angeles 25002). Martinique, February 8, 2000, on *Citrus aurantifolia*, K. Stewart 1 2<sup>nd</sup> ♀, 1 ad ♀ (St. Thomas 010770).

### ***Fiorinia theae* Green, 1900**

**Field characteristics.** First-instar exuviae overlapping second-instar exuviae. Without indentation between attachment of first- and second-instar exuviae. Second-instar exuviae oval, convex marginally; light gray to nearly black; longitudinal ridge conspicuous. Posterior end of adult female within second-instar exuviae rounded. Heavily infested leaves with extensive white secretion (Suppl. material 1: Fig. S1).

**First-instar nymph.** Described in Howell (1977).

**Second-instar female.** Median lobes broad, equal to or wider than width of medial lobule of second lobe, projecting ca. same amount or slightly less than medial lobule of second lobes. With four pairs of marginal macroducts. Swelling of body margin adjacent to macroduct usually rounded. With three large gland spines on margin of each side of body from abdominal segments II–IV; usually with small gland spine on each side of abdominal segments V and VI; without small gland spines on abdominal segment I. With three microducts on each side of head. Longitudinal line of microducts present submarginally on venter of abdominal segments II–VI, normally with 1–5 microducts on each side of each segment. Small lobular projections anteriorly on head sometimes present. Cicatrix present on dorsal submargin of abdominal segment I.

**Notes.** We have been unable to find characters that consistently separate second-instar females of *F. proboscidea* and *F. theae*.

**Second-instar male.** Two duct clusters on each side of body, anterior cluster without communal duct, posterior cluster composed of two communal ducts without associated smaller ducts. Five longitudinal lines of microducts on venter of abdomen (one medial, two mediolateral and two submarginal). Without cluster of small microducts with sclerotized orifice laterad of anterior spiracle (sometimes with one duct present). Fewer than five gland spines on each side of body between anterior and posterior spiracles.

cles. Antennae each with one enlarged seta. Some specimens with small protrusions that are remnants of legs.

**Florida collection records.** Alachua Co., Alachua, October 1, 2012, *Camellia* sp., C. Jones, (2012-7479) (2 slides); Alachua Co., Gainesville, February 10, 1965, on *Camellia japonica*, A.E. Graham (1965-0345); Alachua Co., Gainesville, October 16, 1973, on *Citrus mitis*, F. Collins (1973-3065); Alachua Co., Gainesville, October 25, 1979, on *Citrus* sp., R.I. Sailer (1979-1513); Alachua Co., Gainesville, March 20, 1991, on *Ilex* sp., F. Bennet (1991-2953); Alachua Co., Gainesville, March 20, 1991, on *Ilex* sp., F. Bennett (1991-001–002) (2 slides); Alachua Co., Gainesville, July 19, 1991, on *Ilex* sp., F. Bennett (1991-0383) (3 Slides); Alachua Co., Gainesville, December 3, 1991, on *Ilex* sp., F. Bennet (1991-002–003) (2 slides); Alachua Co., Gainesville, October 16, 1992, *Ilex* sp., F. Bennett (1992-001); Alachua Co., Gainesville, April 15, 1999, on *Ilex* sp., D. Strosnider (1999-383) (2 slides); Alachua Co., Gainesville, July 2011, on *Ilex cornuta*, Shirley Vogel (2011-4847); Alachua Co., Gainesville, February 2012, on *Camellia sasanqua*, D. Feiber (2012-1006) (3 slides); Alachua Co., Gainesville, January 8, 2013, on *Illicium floridanum*, M. Frank (2013-102) (2 slides); Alachua Co., Gainesville, December 1, 2013, on *Camellia* sp., T. Harris (2013-8692); Alachua Co., Hawthorne, February 26, 1971, on *Aucuba japonica*, E.W. Holder (1971-2976) (5 slides); Baker Co., Macclenny, March 14, 1968, on *Ilex latifolia*, H.W. Collins (1968-351) (2 slides); Baker Co., Macclenny, October 21, 1975, on *Ilex cornuta*, C. Webb (1975-411); Bay Co., Panama City, March 8, 1978, on *Euonymus* sp., A.E. Graham (1978-003); Brevard Co., Grant, June 15, 1962, on *Camellia* sp., H.C. Levan (1962-0388); Citrus Co., Hernando, August 15, 1979, on *Ilex cornuta*, R.H. Phillips (1979-1604) (2 slides); Collier Co., Naples, November 13, 2012, on *Ilex* sp., S. Krueger (2012-8615) (2 slides); Collier Co., Naples, November 13, 2012, on *Ilex* sp., S. Krueger (2012-8618) (2 slides); Dixie Co., Old Town, November 19, 1979, on *Euonymus* sp., F. McHenry (1979-1664) (3 slides); Dixie Co., Suwannee, May 22, 1978, on *Citrus nobilis*, A.E. Graham and A. Hamon (1978-1601) (3 slides); Duval Co., Jacksonville, February 17, 1981, on *Ilex cassine*, H. Collins (1981-0352) (2 slides); Duval Co., Jacksonville, October 13, 1981, on *Citrus sinensis*, G. Virgona (1981-0460, 3056) (3 slides); Duval Co., Jacksonville, January 25, 2005, on *Camellia japonica*, J. Smith (2005-464); Duval Co., Jacksonville, October 26, 2010, on *Ilex vomitoria*, J. Brambila (2010-6593); Duval Co., Jacksonville, October 15, 2012, on *Camellia* sp., K. Theriault (2012-7841–7842) (4 slides); Duval Co., Jacksonville, October 25, 2012, on *Citrus* sp., K. Coffey, Lisa Hassell (2012-8102) (2 slides); Duval Co., Jacksonville, April 15, 2013, on *Ilex* sp., K. Theriault (2013-2501) (2 slides); Duval Co., Jacksonville, March 26, 2014, on *Camellia sasanqua*, L. Hassel (2014-2025) (2 slides); Escambia Co., Pensacola, March 10, 1991, on *Camellia* sp., F.D. Bennett (1991-0425, 3010) (2 slides); Flagler Co., Bunnell, January 11, 2012, on *Ilex cornuta* (2012-369) (4 slides); Gadsden Co., Chattahoochee, December 13, 1990, on *Camellia* sp., F. Bennett (1990-011–013) (3 slides); Gadsden Co., Quincy, January 28, 2005, on *Ilex* sp., B. Cecil (2005-901); Gadsden Co., Quincy, March 20, 2012, on *Poncirus* sp., M. Bentley (2012-1944) (2 slides); Hillsborough Co., Brandon, May 29, 1986, on *Ilex* sp., J.

Felty (1986-0453); Hillsborough Co., Tampa, March 13, 2018, on *Citrus* × *paradisi*, M. Briceno (2018-1035) (3 slides); Indian River Co., Vero Beach, August 26, 2013, on *Ilex* sp., J. Kennedy (2013-6273); Jefferson Co., Monticello, November 29, 1973, on *Citrus* sp., W.H. Pierce (19730348) (2 slides); Lake Co., Clermont, February 7, 2012, on *Camellia* sp., H. Alred (2012-793) (3 slides); Lake Co., Eustis, January 22, 1965, on *Camellia* sp., A.L. Bentley (1965-1655) (4 slides); Lake Co., Eustis, April 29, 2010, on *Ilex* sp., M. Sellers (2010-2438) (2 slides); Lake Co., Eustis, May 3, 2018, on *Camellia japonica*, M. Sellers (2018-2334) (2 slides); Leon Co., Tallahassee October 13, 1919, on *Camellia japonica*, P.F. Robertson (1919-1619) (2 Slides); Leon Co., Tallahassee, August 8, 1976, on *Citrus* × *paradisi*, S. Beidler (1976-0423) (3 slides); Leon Co., Tallahassee, October 2, 1978, on *Euonymus* sp., Q. Anglin (1978-3073) (3 slides); Leon Co., Tallahassee, December 13, 1991, on *Camellia japonica*, F. Bennett (1991-0445) (3 slides); Leon Co., Tallahassee, April 6, 2015, on *Camellia* sp., M. Bentley (2015-1687) (3 slides); Madison Co., Pinetta, October 22, 1985, on *Poncirus trifoliata*, J. Thomas (1985-1596); Manatee Co., Duette, March 2, 2005, on *Ilex cornuta*, K. Pippenger (2005-1077); Manatee Co., Oneco, October 19, 1923, on *Camellia japonica*, D.F. Schwarts (1923-1594) (2 slides); Marion Co., Citra, March 2, 2007, on *Ilex* sp., F. McHenry (2007-1335); Marion Co., Citra, March 2, 2007, on *Ilex* sp., F. McHenry (2007-1335) (2 slides); Marion Co., November 15, 2010, on *Camellia* sp. (2010-7091); Marion Co., Reddick, November 15, 2010, on *Camellia* sp., S. Wayte (2010-7091); Martin Co., Jensen Beach, April 23, 2014, on *Ilex opaca*, L. West (2014-2807) (2 slides); Martin Co., Stuart, December 13, 1979, on *Raphiolepis umbellata*, R. Gaskalla (1979-2966) (3 slides); Miami-Dade Co., Miami, December 6, 2012, *Ilex* sp., O. Garcia (2012-9157) (2 slides); Miami-Dade Co., Surfside, March 1, 2018, on *Citrus* sp., O. Garcia (2018-788) (2 slides); Nassau Co., Fernandina Beach, November 7, 2017, on *Citrus* sp., R. Leahy (2017-4261) (2 slides); Nassau Co., Yulee, September 21, 2012, on *Ilex* sp., R. Traya (2012-7169) (2 slides); Nassau Co., Yulee, March 14, 2013, on *Ilex vomitoria*, R. Traya (2013-1586) (2 slides); Nassau Co., Yulee, July 25, 2016, on *Ilex cornuta*, R. Traya (2016-3604); Orange Co., April 30, 2002, on *Citrus reticulata*, L. Brown (2002-1644); Orange Co., Apopka, January 30, 1990, on *Ilex vomitoria*, C. Murphy (1990-0353) (4 slides); Orange Co., Apopka, November 17, 1998, on *Camellia japonica*, L. Wilber (1998-3011) (5 slides); Orange Co., Apopka, April 20, 2002, on *Citrus reticulata*, L. Brown (2002-1644) (2 slides); Orange Co., Apopka, March 8, 2012, on *Ilex* sp., K. Gonzalez (2012-1575) (2 slides); Orange Co., Orlando, February 3, 1977, on *Camellia* sp., D.A. Graddy (1977-1514) (6 slides); Orange Co., Orlando, April 19, 2010, on *Citrus reticulata*, L. Russe (2010-2055); Orange Co., Orlando, February 16, 2012, on *Ilex* sp., R. Lopez (2012-1048) (3 slides); Orange Co., Orlando, February 2013, on Theaceae, A. Puppelo (2013-1127); Orange Co., Orlando, August 20, 2014, on *Camellia japonica*, T. Lyons (2014-5856) (2 slides); Orange Co., Pine Castle, February 5, 1962, on *Camellia* sp., A.C. Crews (1962-0333) (2 slides); Orange Co., Maitland, July 30, 1970, on *Camellia japonica*, E.R. Simmons (1970-1516) (2 slides); Palm Beach Co., West Palm Beach, October 9, 1979, on *Persea americana*, N. Miles (1979-029–032) (4 slides); Palm Beach Co., West Palm Beach,

October 17, 2012, on *Citrus* sp., M. Clark (2012-7966) (2 slides); Pasco Co., Lutz, November 3, 2011, on *Citrus sinensis*, L. Osbeck (2011-8420) (2 slides); Pasco Co., Odessa, December 21, 2011, on *Ilex cornuta* (2011-9392); Pinellas Co., Clearwater, November 15, 1962, on *Senecio confusus*, C.E. Bingaman (1962-1623); Pinellas Co., Gulfport, December 14, 1977, on *Citrus aurantifolia*, K. Hickman (1977-0370) (2 slides); Pinellas Co., Oldsmar, May 5, 2005, on *Citrus* sp., D. Albritton (2005-2337); Pinellas Co., Palm Harbor, February 2012, on *Citrus maxima*, G. Campani and J. Hawk (2012-1112) (3 slides); Pinellas Co., Palm Harbor, November 16, 2010, on *Citrus limon*, J. Brownstein (2010-7134); Pinellas Co., Safety Harbor, April 11, 2012, on *Syzygium jambos*, L. Alston (2012-2672) (2 slides); Pinellas Co., St. Petersburg, May 4, 1979, on *Citrus reticulata*, K. Hickman (1979-0469) (2 slides); Pinellas Co., St. Petersburg, March 25, 2010, on *Illicium floridanum*, G. Bernard (2010-1506); Pinellas Co., Tarpon Springs, February 18, 2012, on *Citrus* sp., K. Edgerton (2012-1039) (2 slides); Pinellas Co., Tarpon Springs, March 3, 2015, on *Cinnamomum camphora*, B. Rose (2015-928) (2 slides); Polk Co., Haines City, January 22, 2013, on *Ilex* sp., S. Distelberg (2013-0328) (3 slides); Polk Co., Winter Haven, December 12, 1960, on *Camellia japonica*, A.C. McAulay and V.K. Norton (1960-0374); Polk Co., Winter Haven, September 9, 1963, on *Gardenia* sp., L.H. Heeb (1963-1653); Polk Co., Winter Haven, December 2, 2013, *Camellia* sp., C. Gibbard (2013-8729); Putnam Co., East Palaka, August 1, 2018, on *Citrus* sp., M. Cain (2018-4101) (2 slides); Putnam Co., Pomona Park, December 12, 1968, on *Euonymus americanus*, A.E. Graham (1968-0454) (6 slides); Santa Rosa Co., Bagdad, January 29, 1970, on *Eurya japonica*, R.W. Albritton (1970-1654) (7 slides); Santa Rosa Co., March 5, 2012, on *Camellia japonica*, M. Anderson (2012-1534); Seminole Co., Longwood, July 30, 1970, *Camellia japonica*, E.R. Simmons (1970-3068); Seminole Co., Oviedo, January 31, 2013, on *Cleyera japonica*, J. Krok (2013-640) (2 slides); Seminole Co., Oviedo, March 13, 2013, on *Ilex opaca*, J. Krok (2013-1691); Seminole Co., Sanford, July 16, 2012, on Myrtaceae, J. Krok, (2012-5308) (2 slides); St. Johns Co., St. Augustine, May 24, 2013, on *Ilex* sp., K. Theriault (2013-3667) (2 slides); St. Lucie Co., Ft. Pierce, February 21, 2005, on *Ilex cornuta*, D. Vazquez (2005-4069) (3 slides); Sumter Co., Bushnell, January 12, 2012, on *Camellia* sp., H. Alred (2012-377) (3 slides); Sumter Co., Bushnell, May 7, 2010, on *Camellia sasanqua*, H. Alred (2010-2501); Sumter Co., Center Hill, April 17, 2012, on *Camellia japonica*, H. Alred (2012-2752) (4 slides); Suwannee Co., Brandford, November 22, 2010, on *Camellia japonica*, W.W. Bailey (2010-7236); Suwannee Co., Live Oak, December 22, 2004, on *Camellia japonica*, Wayne Bailey (2004-8133); Suwannee Co., Live Oak, February 19, 2008, on *Camellia japonica*, W. Wayne Bailey (2008-209); Suwannee Co., Live Oak, February 28, 2012, on *Ilex cornuta*, D. Ruseell-Hughes and K. Collins (2012-1341) (3 slides); Suwannee Co., Live Oak, February 28, 2012, on *Ilex cornuta*, K. Collins (2012-1329) (2 slides); Suwannee Co., Live Oak, July 24, 2012, on Aquifoliaceae, D. Russell-Hughes (2012-5483) (2 slides); Suwannee Co., Live Oak, February 19, 2013, *Camellia* sp., W. Wayne Bailey (2013-1082); Taylor Co., November 18, 2010, on *Camellia japonica*, W. Wayne Bailey (2010-7155); Taylor Co., Perry, March 6, 1978, on

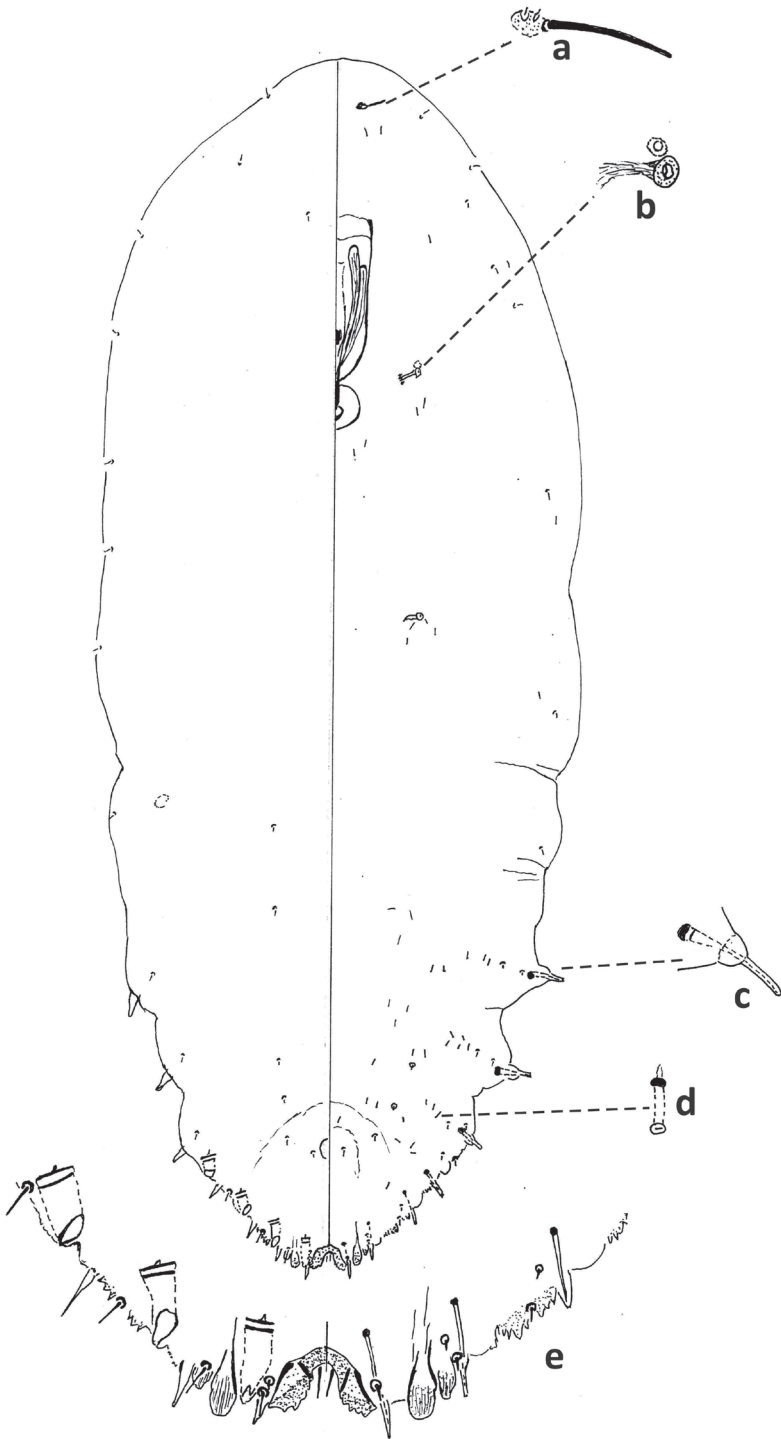


**Figure 20.** *Fiorinia theae*, second-instar female, Pulaski Co., Little Rock, Arkansas, February 15, 1972, on Bradford Holly. Abbreviations: a) antenna; b) anterior spiracle c) large gland spine; d) small microduct; e) enlargement of pygidium.

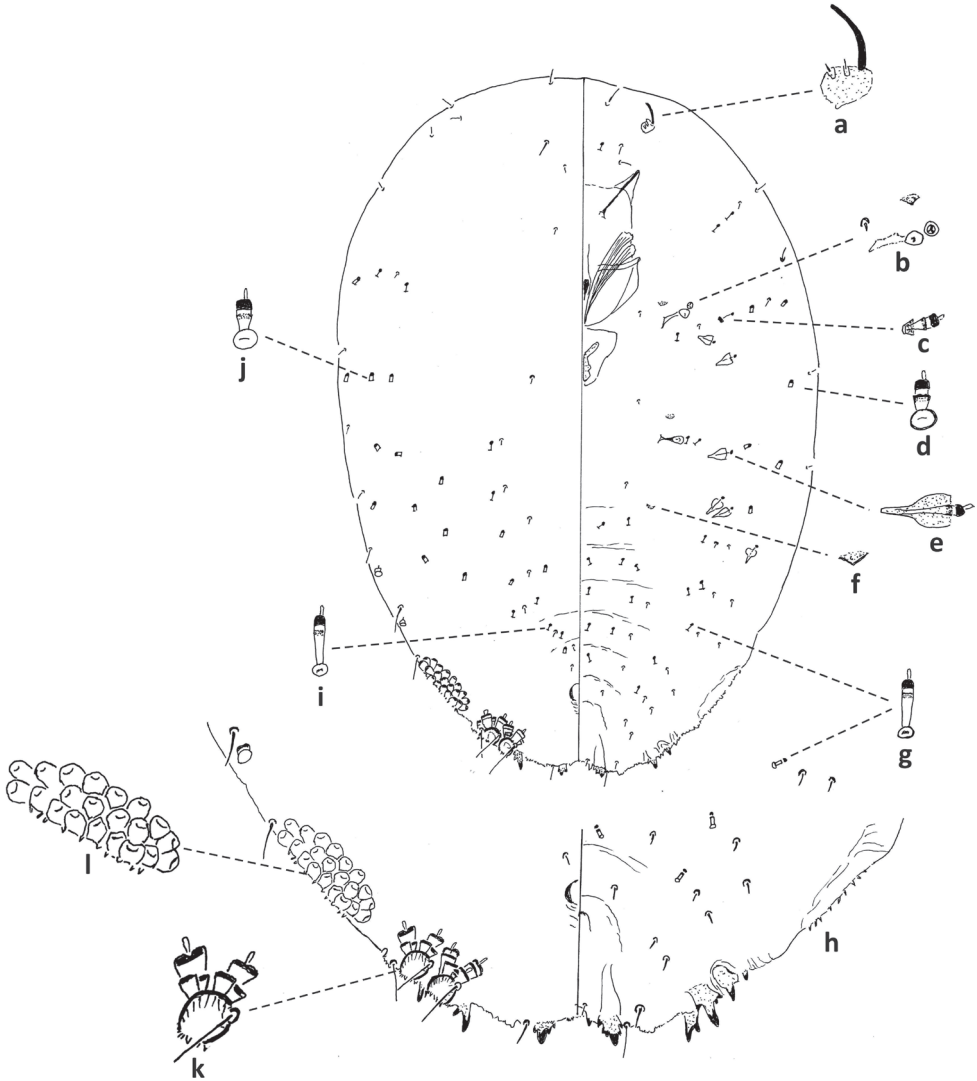


**Figure 21.** *Fiorinia theae*, second-instar male, Alachua Co., Gainesville, October 9, 2019, January 24, 2020 on *Ilex* sp., M. Borden, D. Miller (2019-5696, 2020-287). Abbreviations: a) antenna; b) anterior spiracle; c) small gland spine; d) large microduct; e) large gland spine; f) remnants of legs; g) small microduct; h) enlargement of pygidium; i) small microduct; j) large microduct; j) enlargement of part of duct cluster; k) enlargement of communal duct.

*Citrus limon*, Q. Anglin (1978-0397); Taylor Co., Perry, March 6, 1978, on *Citrus limon*, Q. Anglin (1978-034); Taylor Co., Perry, March 6, 1978, on *Citrus limon*, Q. Anglin (1978-035); Taylor Co., Perry, March 8, 1979, on *Euonymus* sp., Q. Anglin (1979-037); Taylor Co., Perry, March 8, 1979, on *Euonymus* sp., Q. Anglin (1979-1599); Taylor Co., Perry, February 7, 2007, on *Camellia japonica*, Wayne Bailey (2007-748); Taylor Co., Perry, November 18, 2010, on *Ilex cornuta*, W.W. Bailey (2010-7155); Taylor Co., Steinhatcee, May 24, 2010, on *Ilex cornuta*, W. Wayne Bailey

(2010–2993); Volusia Co., Daytona Beach, FL, March 14, 1963, on *Malpighia sp.*, J.N. Pott (1963–2963) (2 slides); Volusia Co., Orange Mills, October 6, 1964, on *Fortunella sp.*, A.E. Graham (1964–0470) (16 slides); Volusia Co., Holly Hill, November 16, 1971, on *Fortunella sp.*, J.N. Pott (1971–0366) (2 slides); Volusia Co., Daytona Beach, November 23, 1976, on *Ilex cornuta*, J.N. Pott (1976–0378) (4 slides); Volusia Co., Ormond Beach, April 18, 2008, on *Ilex cornuta*, K. Coffey (2008–2272) (3 slides); Volusia Co., Edgewater January 13, 2012, on *Ilex cornuta* (2012–263) (3 slides).

**Specimens examined for description and diagnosis.** Little Rock, Arkansas, February 15, 1972, on Bradford Holly, 2<sup>nd</sup> ♀; Alachua Co., Gainesville, October 9, 2019, January 24, 2020 on *Ilex sp.*, M. Borden, D. Miller 5 2<sup>nd</sup> ♂ (E2019–5696, E2020–287).

## Discussion

The most recent study providing taxonomic keys of first-instar nymphs of *Fiorinia* species was published more than four decades ago (Howell 1977). Our expanded version of this key includes the recently introduced species *F. phantasma* and *F. proboscitaria* and improves capabilities for the early detection of *Fiorinia* species in the USA. Our study, for the first time, generated COI barcodes of six *Fiorinia* species including *F. externa*, *F. fioriniae*, *F. phantasma*, *F. pinicola*, *F. proboscitaria*, and *F. theae*. One of the key taxonomic characters in the first-instar nymph key requires careful examination of gland spine morphology. However, gland spines can easily be damaged and are inconspicuous. Molecular identification of first-instar nymphs is recommended for *Fiorinia* species. First-instar nymphs soon molt to become second-instar nymphs (Beardsley and González 1975), and second-instar nymphs are easier to find in the field. We constructed, for the first time, a taxonomic key for second-instar females of the *Fiorinia* species occurring in the USA. Our second-instar female key successfully distinguishes three *Fiorinia* species: *F. fioriniae*, *F. externa*, and *F. phantasma*. The number of pairs of marginal macroducts were the same between *F. proboscitaria* and *F. theae*. Similarly, the ratio of the spaces between the bases of the median lobes versus the size of the medial lobule of second lobes was the same in *F. japonica* and *F. pinicola*. We suggest molecular sequencing of second-instar females for species-level identification. Contrary to second-instar females, our taxonomic key based on second-instar males distinguishes all seven *Fiorinia* species. The last taxonomic key for second-instar males of *Fiorinia* species was published ca. five decades ago by Tippins (1970) and included three *Fiorinia* species, *F. externa*, *F. pinicola*, and *F. theae*. We expanded upon it by including four more *Fiorinia* species, *F. fioriniae*, *F. japonica*, *F. phantasma*, and *F. proboscitaria*. Once a population of *Fiorinia* becomes established, adult females are usually available. They are easily observed and easier to slide-mount compared with immature stages. There are 16 *Fiorinia* species reported from the Australasian, Nearctic and Neotropical regions (Watson et al. 2015). Watson et al. (2015) provided a taxonomic key to the adult females of 12 of these species including the seven *Fiorinia* species used in this study. We

developed a key to adult females that occurs in the USA modifying the key from Watson et al. (2015). Overall, the morpho-molecular diagnostic framework developed in this study will help identify first-instar nymphs, second-instar males and females, and adult females of *Fiorinia* species and will expedite regulatory and control decisions.

Use of immature armored scales for identification is hampered by the fact that slide mounting protocols are tedious and laborious. Immature stages, especially first-instar nymphs, are very small, ca. 0.1–0.2 mm in length, and can easily be lost during the mounting process. We reexamined previously published mounting protocols (McKenzie 1957; Wilkey 1990; Watson 2002) and addressed three issues: 1) avoiding specimen loss during mounting, 2) enhancing safety by reducing the amount of chemicals needed, since the reagents can be corrosive, flammable, carcinogenic, or produce toxic fumes, and 3) saving time if possible. Our comparative analysis of different slide-mounting protocols and elaboration on their merits and drawbacks, especially for the incorporation of a mesh container during the slide-mounting protocols, enhance the potential for mounting immature armored scales.

One unexpected discovery during this project was that the morphology of second-instar males was more reliable for species recognition than any other instar, including the adult female. For example, we were unable to distinguish between second-instar females of *F. proboscitaria* and *F. theae*, but their second-instar males were easily separated using the number of communal ducts. Second-instar males of *F. fioriniae* are remarkably different from the same instar of all other species of *Fiorinia* found in the USA even though other instars are quite similar to one another. Takagi (1975) discussed having difficulty separating *F. nachiensis* Takahashi and *F. odaiensis* Takagi based on adult females. At one point he treated them as synonyms, but based on major differences between the second-instar males he concluded that they were different species. Tippins (1970) published the first key and descriptions of the second-instar males of *Fiorinia* species and was surprised by the distinctive differences among species.

Recently, Liu et al. (2020) described a new species, *F. yongxingensis* from Hainan, China. It is similar to *F. phantasma* in the number and size of the marginal macroducts, the shape of the lobes, and the shape of the pygidium. The authors based their diagnosis in part on the detailed description and illustration of *F. coronata* (Williams & Watson, 1988), a junior synonym of *F. phantasma* (see Watson et al. 2015). Characters that appeared to be diagnostic for *F. yongxingensis* compared with *F. coronata* (= *F. phantasma*) are gland tubercles on the prothorax, microducts between the posterior spiracles, a gland spine on the prepygidium, and 0–3 pores near each anterior spiracle. Unfortunately, the type series of *F. coronata* did not contain the variation that we discovered in the Florida populations of *F. phantasma*. We have seen material with or without gland tubercles on the prothorax, a gland spine on the prepygidium, and 0–3 pores near each anterior spiracle. All specimens in the Florida populations have microducts between the posterior spiracles. Based on this information it appeared that the presence of these microducts was the key diagnostic character for *F. yongxingensis*. Because we needed to know the correct identity of the species introduced to Florida, several more

steps were required. The next step was to examine the type series of *F. phantasma* and *F. coronata*. DL and JF borrowed the type specimens of *F. phantasma* from NHMUK and DRM examined another specimen from the type series deposited in USNM, but in each case the specimens were in such poor condition that it was impossible to see if microducts are present between the posterior spiracles. Type material of *F. coronata* also was studied; a type specimen deposited in the USNM has microducts between the posterior spiracles. A further step was to examine other relevant slides in the USNM. We studied slides from thirteen *F. phantasma* populations taken in quarantine from the Philippines, the type locality of *F. phantasma*, between 1965 and 1996, that are deposited in the USNM. We also examined slides taken in quarantine from Grenada, Hawaii, Thailand, Taiwan, and Vietnam. In all cases, microducts were present between the posterior spiracles, and there was overlapping variation in the other characters used to diagnose *F. yongxingensis*. We have yet to examine any adult female specimens of *F. phantasma* that lack these microducts and conclude that they are most likely a fixed character of the species.

The final step was to compare the results of multigene molecular analyses of the Florida population, the Chinese population, and two Malaysian populations (D1184 and D1185). The results clearly show that these populations are the same species. The morphological differences suggested as diagnostic of *F. yongxingensis* are within the range of variation that occurs in *F. phantasma*. Therefore, we here treat *F. yongxingensis* as a junior synonym of *F. phantasma*.

We obtained 37 5'-COI barcodes representing nine *Fiorinia* species in this study. Overall, low intraspecific genetic distances and high interspecific genetic distances ranging from 9.1% to 15.2% between *Fiorinia* species emphasize the reliability of 5'-COI barcodes in molecular diagnostics of armored scale species. Our rapid slide-mounting protocol and the morphological keys to immatures and adults can provide time- and cost-effective diagnostics of *Fiorinia* species in the USA. However, for instances where specimens are damaged and cannot be mounted and where molecular diagnostics is the only option, barcodes will help to identify the species of *Fiorinia*. All of our DNA extractions are vouchered by permanently archived specimens in FSCA. This provides the opportunity for other researchers to validate the identifications of our specimens. We found an example of apparently misidentified specimens that were submitted to Genbank: the barcode of *Aulacaspis rosarum* Borchsenius (isolate wfsys017, accession number KP981086) was placed with 35 samples of *Pseudaulacaspis cockerelli* (Cooley) in our molecular analysis. A subtler discrepancy between DNA sequence and morphological identification, also seen in Normark et al. (2019), is the placement of *F. vaccinia* Kuwana (isolate D2453A, accession number KY219617) together with three samples of *F. hymenanthis* Takagi. Our study accentuates the importance of depositing morphological voucher specimen in an accessible collection.

Three populations of *Fiorinia* species (isolates D4674F, D4778A, and D4682A), collected from Lambir Hills National Park, Malaysia, September 26, 2013 from an undetermined host, identified as *F. phantasma* by BBN, were found to be genetically different from the *F. phantasma* populations from China, Florida and Malaysia. We

reexamined the skins of the specimens used in our molecular analyses. The slides of isolates D4674F and D4778A are in poor condition and covered with fog, but we can see processes between the antennae and the shape of the pygidium, and they are consistent with the morphology of *F. phantasma*. The slide of isolate D4682A appears to have most characters of *F. phantasma* including the microducts between the posterior spiracles. This isolate is ca. 9% genetically distant from *F. phantasma* (based on COI) and is placed far from the subclade of *F. phantasma* (containing populations from China, Florida, and Malaysia) in the concatenated phylogenetic tree (Fig. 2). This may represent a cryptic species. More samples especially of second-instar males would help to confirm their identity.

Recently phylogenetic analyses in Normark et al. (2019) support the monophyly *Fiorinia* after the generic transfer of *Ichthyaspis ficicola* into the group. Our analysis agrees with the inference of Normark et al. (2019) with a few exceptions. Three *Pseudaulacaspis* MacGillivray species including *P. cockerelli*, *P. pentagona* (Targioni Tozzetti) and *P. prunicola* (Maskell) are placed in the same clade as *Fiorinia* in the case of the 5'-COI phylogenetic tree (Fig. 3, Suppl. material 1: Fig. S4). Likewise, in the case of the concatenated phylogenetic tree based on 28S, EF1- $\alpha$ , 5'-COI, 3'-COI, and COII, two samples of *Fiorinia* sp. (isolates D4815B, D4815C) fall out of the *Fiorinia* clade and placed with five *Pseudaulacaspis* species including *P. bififormis* Takagi, *P. cockerelli*, *P. momi* (Kuwana), *P. pentagona*, and *P. prunicola*, with strong clade support (Fig. 2, Suppl. material 1: Fig. S2). *Fiorinia* was rendered polyphyletic by these two isolates (*Fiorinia* sp., D4815B and D4815C). They were collected from Malaysia in 2013 and determined as *Fiorinia* sp. by BBN. Given that the pupillarial habit has been gained and lost frequently in the history of Diaspididae (Normark et al. 2019), a second origin within Fioriniina would not be surprising. These two *Fiorinia* sp. isolates along with five *Pseudaulacaspis* species were placed together with strong support in a subclade within *Fiorinia* clade in our phylogenetic analysis based on 28S gene (Suppl. material 1: Fig. S3). Therefore, the placement of these two samples out of *Fiorinia* clade could be the result of an artifact of missing data or the methodology used in multigene tree and would require additional analysis for further confirmation. There are two samples of *Lineaspis striata* (Newstead) with *P. simplex* Takagi in the sister subclade that joins the subclade of *Pseudaulacaspis*/*Fiorinia* with strong clade support (Fig. 3, Suppl. material 1: Fig. S4). Overall, the main clade of the genus *Fiorinia* joins the *Fiorinia*/*Pseudaulacaspis*/*Lineaspis* clade with strong clade support (> 90%). Borchsenius (1966) separated *Fiorinia* from *Pseudaulacaspis* and placed them in different tribes due to their pupillarial habit. However, Takagi (1969) and Howell and Tippins (1973), based on the presence of communal ducts, suggested a relationship between *Pseudaulacaspis* and *Fiorinia*. Our phylogenetic analysis suggests that additional sampling of *Fiorinia* and *Pseudaulacaspis* from Asia will further clarify the monophyly of the genus *Fiorinia*.

Field habitus of adult females, especially the character of the overlap between the first-instar and second-instar exuviae, was used for the first time in this study. For example, in the case of *F. externa*, the first-instar exuviae are barely touching the second-

instar exuviae and form a distinct indentation between the attachment of the first- and second-instar exuviae (Suppl. material 1: Fig. S1). In contrast to this, no indentation was observed in *F. phantasma*. In addition, we also compared the color and shape of the second-instar nymphs shed skins of *Fiorinia* species. Field habitus can assist growers and nursery workers in making preliminary identifications.

*Fiorinia japonica* was eradicated from California and has been rediscovered three times since its first report in 1910 (Watson 2009). The most recent reinfestation was observed in 2008 and was most likely eradicated in a subsequent year (Watson 2009). Our collaborator's attempt to collect fresh specimens of *F. japonica* in California for inclusion in this study was unsuccessful and its population has not been barcoded. It would be useful to trace its population in other states and to sequence its barcode. We also intended to include the population of *F. phantasma* from Hawaii, but efforts of our collaborators to collect it from Hawaii were unsuccessful. There have been at least two reinfestations of *F. phantasma* in Hawaii since its first report in 2004. The most recent heavy infestation was from palms reported in 2011 (Garcia 2011). Interestingly, in this most recent Hawaiian infestation, the second-instar nymph's shed cuticles had transverse brown stripes, whereas the Florida population lacks this character. It would be helpful to collect *F. phantasma* from Hawaii and to compare it with the Floridian *F. phantasma* population to determine if they are the same species. If the Hawaiian *F. phantasma* is the same as the Floridian species, that fact might imply that *F. phantasma* in Florida could follow the same pattern as it did in Hawaii and keep reappearing with heavier infestations in subsequent years. This study will facilitate regulatory and pest management decisions by enhancing morphological and molecular identification of seven adventive *Fiorinia* species occurring in the USA.

## Conclusions

There are six main conclusions of our study. 1) The utilization of molecular barcodes is highly beneficial in diagnosing species of *Fiorinia* that occur in the USA. 2) The new keys in this study demonstrate that the USA species of *Fiorinia* can be identified using immature specimens. 3) Second-instar male morphology provided a reliable suite of characters for species-level identification. 4) Based on our comparative analysis of morphological characters and multigene molecular sequencing of specimens of *F. phantasma* and *F. yongxinensis*, it is clear that the latter is a junior synonym. 5) Of the different protocols tested for mounting immature specimens of *Fiorinia*, Hoyer's mounting medium was the best for discerning delicate morphological characters but it was not desirable for permanent slide preparations. Balsam was the best for permanent mounts but did not provide the morphological clarity of Hoyer's mounts. 6) The use of a mesh container in the process of mounting immatures is an effective method for preventing the loss of specimens. Overall, the use of the morphological and molecular data provides effective methods for early detection of new infestations and assists regulators in making control decisions.

## Acknowledgements

This work was made possible, in part, by FY2019 United States Department of Agriculture Plant Protection Act Section 7721 funding. The authors thank Greg Hodges, Kate Fairbanks, Leroy Whilby, and Paul Skelly (Florida Department of Agriculture and Consumer Services, Division of Plant Industry) for administrating the grant funding. Participation by BBN was supported by the U.S. Department of Agriculture's National Institute of Food and Agriculture, and by the University of Massachusetts Amherst Biology Department and Center for Agriculture, Food, and the Environment, under project number MAS00535. Thanks to Susan Halbert and John Mcvay (FDACSDPI), for constructive reviews. The authors also thank all of our collaborators in this project including Lance Osborne (Department of Entomology & Nematology, Mid-Florida Research and Education Center, Institute of Food and Agricultural Sciences, University of Florida) and Amy Roda (Miami Laboratory, Plant Protection and Quarantine, Animal Plant Health Inspection Service, United States Department of Agriculture). This work would not be accomplished without their kind advice and field surveys. Collection in Lambir Hills National Park was conducted in collaboration with Takao Itioka (Kyoto University, Japan) and Geoff Morse (University of San Diego, California), in accordance with the Memorandums of Understanding signed between the Sarawak Forest Department (SFD, Kuching, Malaysia) and the Japan Research Consortium for Tropical Forests in Sarawak (JRCTS, Sendai, Japan) in December 2012. Thanks to Mohamad Shahbudin Sabki, Engkamat Lading, and Mohamad bin Kohdi, Paulus Meleng of SFD for help in obtaining research permission at the Lambir Hills National Park. We also thank Gillian W. Watson (The Natural History Museum, London) for helping us in tracing the type specimens of *Fiorinia phantasma*. DRM is grateful to the Division of Plant Industry including Paul Skelly and Greg Hodges for providing space and resources to conduct this research. Authors thank Natalia von Ellenrieder (California Department of Food and Agriculture) for sending us the *F. pinicola* sample. We thank technicians Chelsea Skojec, Gabi Ouwinga, and Lily Deeter (FDACSDPI) for their help in mounting slides during this study. Authors also thank Gevork Arakelian (Los Angeles County Department of Agricultural Commissioner/Weights and Measures) for providing images of *Fiorinia japonica* and Lyle Buss (University of Florida) for providing images of *Fiorinia fioriniae*, *F. theae*, *Kuwanaspis hikosani*, *Pseudaulacaspis cockerelli*, *P. pentagona*, *Poliaspis cycadis*, and *Odonaspis ruthae*. We also acknowledge the United States National Collection of Scale Insects Photographs, USDA Agricultural Research Service especially for image # UGA5111048 of *Fiorinia pinicola*.

## References

- Ahmed MZ (2018) Field detection and potential host plants of *Fiorinia phantasma* Cockerell & Robinson (Diaspididae: Hemiptera), phantasma scale, potential pest of palms and ornamental plants in Florida. Florida Department of Agriculture and Consumer Services Division of Plant Industry, FDACS-P-01917, Entomology Circular 439.

- Ahmed MZ, Stocks IC (2020) *Fiorinia proboscoidaria* Green (Hemiptera: Diaspididae), snout scale, a potential pest of Citrus in Florida. Florida Department of Agriculture and Consumer Services, Division of Plant Industry, Pest Alert, September, FDACS-P-01929.
- Ahmed, MZ, Miller DR, Rohrig E, Hodges G, Roda A, McKenzie C, Osborne L (2021) Field Report and Survey of *Fiorinia phantasma* Cockerell & Robinson (Diaspididae: Hemiptera), Phantasma Scale, Potential Pest of Palms and Ornamental Plants in the United States. Journal of Integrated Pest Management 12: 1–10. <https://doi.org/10.1093/jipm/pmab032>
- Anderson LE (1954) Hoyer's Solution as a rapid mounting medium for bryophytes. Bryologist 57: 242–244. <https://doi.org/10.2307/3240091>
- Barbecho NL, Lit I (2015) A modified sieve dish for easier preparation of microscope slide mounts for taxonomic studies of armored scale insects (Hemiptera: Diaspididae). Philippine Journal of Systematic Biology 9: 81–86.
- Beardsley JW, González RH (1975) The biology and ecology of armored scales. Annual Review of Entomology 20: 47–73. <https://doi.org/10.1146/annurev.en.20.010175.000403>
- Borchsenius NS (1966) A catalogue of the armoured scale insects (Diaspidoidea) of the world. Nauka, Moscow & Leningrad, 449 pp.
- Dowton M, Austin AD (1998) Phylogenetic relationships among the microgastroid wasps (Hymenoptera: Braconidae): Combined analysis of 16S and 28S rDNA genes and morphological data. Molecular Phylogenetics and Evolution 10: 354–366. <https://doi.org/10.1006/mpev.1998.0533>
- Edgar RC (2004) MUSCLE: multiple sequence alignment with high accuracy and high throughput. Nucleic Acids Research 32: 1792–1797. <https://doi.org/10.1093/nar/gkh340>
- FDACS-DPI Entomology Database (2021) Florida department of Agriculture and Consumer Services, Division of Plant Industry, Gainesville, FL. [Accessed on January 20, 2021. Available via Public Records Request]
- Folmer O, Black M, Hoeh W, Lutz R, Vrijenhoek R (1994) DNA primers for amplification of mitochondrial cytochrome *c* oxidase subunit I from diverse metazoan invertebrates. Molecular Marine Biology and Biotechnology 3: 294–299.
- García Morales M, Denno BD, Miller DR, Miller GL, Ben-Dov Y, Hardy NB (2016) ScaleNet: a literature-based model of scale insect biology and systematics. Database 2016: 1–5. <https://doi.org/10.1093/database/bav118>
- Garcia JN (2011) *Fiorinia phantasma* Cockerell & Robinson (Hemiptera: Diaspididae) an armored scale pest new to Hawaii. Proceedings of the Hawaiian Entomological Society 43: 59–61.
- Gill RJ (1997) The Scale Insects of California: Part 3. The Armored Scales (Homoptera: Diaspididae). California Department of Food & Agriculture Sacramento, CA, 307 pp.
- Guindon S, Dufayard JF, Lefort V, Anisimova M, Hordijk W, Gascuel O (2010) New algorithms and methods to estimate maximum-likelihood phylogenies: Assessing the performance of PhyML 3.0. Systematic Biology 59: 307–321. <https://doi.org/10.1093/sysbio/syq010>
- Hebert PDN, Penton EH, Burns JM, Janzen DH, Hallwachs W (2004) Ten species in one: DNA barcoding reveals cryptic species in the neotropical skipper butterfly *Astraptes fulgerator*. Proceedings of the National Academy of Sciences 101: 14812–14817. <https://doi.org/10.1073/pnas.0406166101>

- Hoang DT, Chernomor O, von Haeseler A, Minh BQ, Vinh LS (2018a) UFBoot2: Improving the ultrafast bootstrap approximation. *Molecular Biology and Evolution* 35: 518–522. <https://doi.org/10.1093/molbev/msx281>
- Hoang DT, Vinh LS, Flouri T, Stamatakis A, von Haeseler A, Minh BQ (2018b) MPBoot: Fast phylogenetic maximum parsimony tree inference and bootstrap approximation. *BioMed Central Evolutionary Biology* 18: e11. <https://doi.org/10.1186/s12862-018-1131-3>
- Hodges G, Evans G (2005) An identification guide to the whiteflies (Hemiptera: Aleyrodidae) of the southeastern United States. *Florida Entomologist* 88: 518–534. [https://doi.org/10.1653/0015-4040\(2005\)88\[518:AGTTW\]2.0.CO;2](https://doi.org/10.1653/0015-4040(2005)88[518:AGTTW]2.0.CO;2)
- Howell JO (1977) Description of the first instars of the North American species in the genus *Fiorinia* (Homoptera: Coccoidea: Diaspididae). *Annals of the Entomological Society of America* 70: 829–836. <https://doi.org/10.11646/zootaxa.1615.1.3>
- Howell JO, Tippins HH (1973) Immature stages of *Kuwanaspis howardi* (Homoptera: Diaspididae). *Journal of the Georgia Entomological Society* 8: 241–244.
- Kalyaanamoorthy S, Minh BQ, Wong TKF, von Haeseler A, Jermiin LS (2017) ModelFinder: fast model selection for accurate phylogenetic estimates. *Nature Methods* 14: 587–589. <https://doi.org/10.1038/nmeth.4285>
- Katoh K, Standley DM (2013) MAFFT Multiple sequence alignment software version 7: improvements in performance and usability. *Molecular Biology and Evolution* 30: 772–780. <https://doi.org/10.1093/molbev/mst010>
- Khachatryan H, Hodges AW (2012) Florida nursery crops and landscaping industry economic outlook. UF-IFAS Nursery Report, 10 pp.
- Kimura M (1980) A simple method for estimating evolutionary rates of base substitutions through comparative studies of nucleotide sequences. *Journal of Molecular Evolution* 16: 111–120. <https://doi.org/10.1007/BF01731581>
- Kumar S, Stecher G, Li M, Knyaz C, Tamura K (2018) MEGA X: Molecular Evolutionary Genetics Analysis across Computing Platforms. *Molecular Biology and Evolution* 35(5): 1547–1549. <https://doi.org/10.1093/molbev/msy096>
- Larkin MA, Blackshields G, Brown NP, Chenna R, McGettigan PA, McWilliam H, Valentin F, Wallace IM, Wilm A, Lopez R, Thompson JD, Gibson TJ, Higgins DG (2007) Clustal W and Clustal X version 2.0. *Bioinformatics* 23: 2947–2948. <https://doi.org/10.1093/bioinformatics/btm404>
- Liu D, Cai J, Feng J (2020) A new species of armored scale, *Fiorinia yongxingensis* (Hemiptera: Coccoomorpha: Diaspididae) from Hainan Province, China. *Zootaxa* 4729(3): 388–400. <https://doi.org/10.11646/zootaxa.4729.3.6>
- Maddison WP, Maddison DR (2018) Mesquite: A modular system for evolutionary analysis. Version 3.51. <http://www.mesquiteproject.org> [Accessed on January 20, 2021]
- McClure MS (1977) Resurgence of the scale, *Fiorinia externa* (Homoptera: Diaspididae), on hemlock following insecticide application. *Environmental Entomology* 6: 480–484. <https://doi.org/10.1093/ee/6.3.480>
- McKenzie H (1957) The armored scale insects of California. *Bulletin of the California Insect Survey* 5: 1–209. <https://doi.org/10.1525/9780520345775>

- Miller DR, Davidson JA (1990) A list of the armored scale insect pests. Armored Scale Insects, Their Biology, Natural Enemies and Control [Series title: World Crop Pests, Vol. 4B, 3.1.1]. Elsevier, Amsterdam, 688 pp.
- Miller DR, Davidson JA (2005) Armored Scale Insect Pests of Trees and Shrubs. Cornell University Press, Ithaca, 442 pp.
- Miller MA, Pfeiffer W, Schwartz T (2010) Creating the CIPRES Science Gateway for inference of large phylogenetic trees. In: Proceedings of the Gateway Computing Environments Workshop (GCE), 14 Nov. 2010, New Orleans, LA, 1–8. <https://doi.org/10.1109/GCE.2010.5676129>
- Minh BQ, Schmidt HA, Chernomor O, Schrempf D, Woodhams MD, von Haeseler A, Lanfear R (2020) IQ-TREE 2: New models and efficient methods for phylogenetic inference in the genomic era. *Molecular Biology and Evolution* 37: 1530–1534. <https://doi.org/10.1093/molbev/msaa015>
- Morse GE, Normark BB (2006) A molecular phylogenetic study of armoured scale insects (Hemiptera: Diaspididae). *Systematic Entomology* 31: 338–349. <https://doi.org/10.1111/j.1365-3113.2005.00316.x>
- Normark BB, Okuso A, Morse GE, Peterson DA, Itioka T, Schneider SA (2019) Phylogeny and classification of armored scale insects (Hemiptera: Coccomorpha: Diaspididae). *Zootaxa* 4616: 1–98. <https://doi.org/10.11646/zootaxa.4616.1.1>
- Nur U (1990) Parthenogenesis. Armored Scale Insects, Their Biology, Natural Enemies and Control. World Crop Pests, Vol. 4A, 1.2.2. Elsevier, Amsterdam, 384 pp.
- Palumbi SR (1996) Nucleic acids II: The polymerase chain reaction. pp 205–247. In: Hillis DM, Moritz C, Mable BK (Eds) *Molecular Systematics*. 2<sup>nd</sup> edn. Sinauer Associates, Inc. Sunderland, 655 pp.
- Park DS, Suh SJ, Oh HW, Hebert PDN (2010) Recovery of the mitochondrial COI barcode region in diverse Hexapoda through tRNA-based primers. *BioMed Central Genomics* 11: e423. <https://doi.org/10.1186/1471-2164-11-423>
- Rambaut A (2012) FigTree, version 1.4.3. Computer program distributed by the author. <http://tree.bio.ed.ac.uk/software/figtree> [Accessed on January 20, 2021]
- Ratnasingham S, Hebert PDN (2007) BOLD: The Barcode of Life Data System ([www.barcodinglife.org](http://www.barcodinglife.org)). *Molecular Ecology Notes* 7: 355–364. <https://doi.org/10.1111/j.1471-8286.2007.01678.x>
- Sirisena U, Watson G, Hemachandra K, Wijayagunasekara H (2013) A modified technique for the preparation of specimens of Sternorrhyncha for taxonomic studies. *Tropical Agricultural Research* 24: 139–149.
- Takagi S, Kawai S (1967) The genera *Chionaspis* and *Pseudaulacaspis* with a criticism on Phenacaspis (Homoptera: Coccoidea). *Insecta Matsumurana* 30: 29–43.
- Takagi S (1969) Diaspididae of Taiwan based on material collected in connection with the Japan-U.S. Co-operative Science Programme, 1965 (Homoptera: Coccoidea). Part I. *Insecta Matsumurana* 32: 1–110.
- Takagi S (1970) Diaspididae of Taiwan based on material collected in connection with the Japan-U.S. Cooperative Science Programme, 1965 (Homoptera: Coccoidea). Pt. II. *Insecta Matsumurana* 33: 1–146.

- Takagi S (1975) The Horii-group of *Fiorinia* associated with rhododendrons in East Asia (Homoptera: Coccoidea: Diaspididae). *Insecta Matsumurana (New Series)* 6: 35–61.
- Takagi S (1999) Notes on the scale insect subtribe Kuwanaspidina (Homoptera: Coccoidea: Diaspididae). *Insecta Matsumurana (New Series)* 56: 95–150.
- Tang FT (1984) Observation on the scale insects injurious to forestry of North China. Shanxi Agricultural University Press Research Publication 2: 122–133.
- Tippins HH (1970) The second instar males of three species of *Fiorinia* (Homoptera: Diaspididae). *Journal of the Georgia Entomological Society* 5: 94–99.
- Tippins HH, Howell JO (1983) Morphology and Systematics of the first instars of North American *Pseudaulacaspis*. *Journal of the Georgia Entomological Society* 18: 195–200.
- Watson GW (2002) Arthropods of economic importance: Diaspididae of the World. (Series Title: World Biodiversity Database). ETI Information Services, Expert Center for Taxonomic Identification, Amsterdam.
- Watson GW (2009) Coniferous *Fiorinia* Scale. *Entomology, California Plant Pest & Disease Report*, Gaimari S, O'Donnell D (Eds) 25: 17–18.
- Watson GW, Williams DJ, Miller DR (2015) The identity and distribution of *Fiorinia phantasma* (Cockerell & Robinson) (Hemiptera: Coccoidea: Diaspididae), with a new synonym. *Zootaxa* 4048(2): 291–300. <https://doi.org/10.11646/zootaxa.4048.2.9>
- Wei J, Zhang B, Feng JN (2013) Two new species of *Fiorinia* Targioni-Tozzetti (Hemiptera: Coccoidea: Diaspididae) from China. *Zootaxa* 3641(1): 092–100. <https://doi.org/10.11646/zootaxa.3641.1.10>
- Whiting MF, Carpenter JC, Wheeler QD, Wheeler WC (1997) The Strepsiptera problem: Phylogeny of holometabolous insect orders inferred from 18S and 28S ribosomal DNA sequences and morphology. *Systematic Biology* 46: 1–68. <https://doi.org/10.1093/sysbio/46.1.1>
- Wilkey RF (1990) Collection, preservation and microslide mounting. *Armored Scale Insects, Their Biology, Natural Enemies and Control* [Series title: World Crop Pests, Vol. 4A, 1.5.1]. Elsevier, Amsterdam, 384 pp.
- Williams DJ, Watson GW (1988) The scale insects of the tropical South Pacific region. Pt. 1. The Armoured Scales (Diaspididae). CAB International, Wallingford, 290 pp.
- Wirth W, Marston N (1968) A method for mounting small insects on microscope slides in Canada balsam. *Annals of the Entomological Society of America* 61: 783–784. <https://doi.org/10.1093/aesa/61.3.783>

## Supplementary material 1

### Figures S1–S4

Authors: Muhammad Z. Ahmed, Matthew R. Moore, Eric A. Rohrig, Cindy L. McKenzie, Di Liu, Jinian Feng, Benjamin B. Normark, Douglass R. Miller

Data type: Phylogenetic trees and images (docx. file)

Explanation note: **Figure S1.** Comparison of field habitus of first-instar exuviae overlapping second-instar exuviae of seven *Fiorinia* species occurring in the USA. **Figure S2.** Maximum likelihood bootstrap consensus tree of the subtribe Fioriniina based on 28S, EF1- $\alpha$ , 5'-COI, 3'-COI, and COII. The clade highlighted in solid red indicates a monophyletic *Fiorinia*. **Figure S3.** Maximum likelihood bootstrap consensus tree of the subtribe Fioriniina based on 28S. The clade highlighted in red contains *Fiorinia*. Red dashed line indicates two *Fiorinia* sp. isolates placed with *Pseudaulacaspis* species. Dashed black lines indicate non-*Fiorinia* species placed in the *Fiorinia* clade. Bootstrap support values equal or greater than 50 are indicated on the tree. **Figure S4.** Neighbor-joining tree of Diaspididae 5'-COI barcodes. Terminal taxa are labeled to their narrowest identification-level. Numbers in parentheses after terminal taxa indicate how many sequences are represented in each cluster. The cluster of *Fiorinia* species is highlighted in red. Bootstrap support values greater than 75 are indicated on the tree. Nodes with 100 percent bootstrap support are indicated by a “\*”.

Copyright notice: This dataset is made available under the Open Database License (<http://opendatacommons.org/licenses/odbl/1.0/>). The Open Database License (ODbL) is a license agreement intended to allow users to freely share, modify, and use this Dataset while maintaining this same freedom for others, provided that the original source and author(s) are credited.

Link: <https://doi.org/10.3897/zookeys.1065.69171.suppl1>

## Supplementary material 2

### Table S1

Authors: Muhammad Z. Ahmed, Matthew R. Moore, Eric A. Rohrig, Cindy L. McKenzie, Di Liu, Jinian Feng, Benjamin B. Normark, Douglass R. Miller

Data type: Sequences accession numbers (excel table)

Explanation note: **Table S1.** Taxa, isolates, and GenBank accessions used for phylogenetic analyses.

Copyright notice: This dataset is made available under the Open Database License (<http://opendatacommons.org/licenses/odbl/1.0/>). The Open Database License (ODbL) is a license agreement intended to allow users to freely share, modify, and use this Dataset while maintaining this same freedom for others, provided that the original source and author(s) are credited.

Link: <https://doi.org/10.3897/zookeys.1065.69171.suppl2>

### Supplementary material 3

#### Table S2. PCR primers and thermocycling conditions.

Authors: Muhammad Z. Ahmed, Matthew R. Moore, Eric A. Rohrig, Cindy L. McKenzie, Di Liu, Jinian Feng, Benjamin B. Normark, Douglass R. Miller

Data type: PCR primers and thermocycling conditions (docx. file)

Explanation note: **Table S2.** PCR primers and thermocycling conditions. All PCR reactions were performed with 2-minute denaturation at 95<sup>o</sup> C. Each subsequent cycle consists of a 30 second denaturation at 98<sup>o</sup> C, a 30 second annealing step with temperature given below, and a 45 secs extension at 72<sup>o</sup> C., end with a single 7 -minute extension at 72<sup>o</sup> C. Primer sequences are given from 5' to 3'.

Copyright notice: This dataset is made available under the Open Database License (<http://opendatacommons.org/licenses/odbl/1.0/>). The Open Database License (ODbL) is a license agreement intended to allow users to freely share, modify, and use this Dataset while maintaining this same freedom for others, provided that the original source and author(s) are credited.

Link: <https://doi.org/10.3897/zookeys.1065.69171.suppl3>

### Supplementary material 4

#### Raw data

Authors: Muhammad Z. Ahmed, Matthew R. Moore, Eric A. Rohrig, Cindy L. McKenzie, Di Liu, Jinian Feng, Benjamin B. Normark, Douglass R. Miller

Data type: fas. file

Explanation note: Raw data file containing aligned sequences used in our phylogenetic analysis.

Copyright notice: This dataset is made available under the Open Database License (<http://opendatacommons.org/licenses/odbl/1.0/>). The Open Database License (ODbL) is a license agreement intended to allow users to freely share, modify, and use this Dataset while maintaining this same freedom for others, provided that the original source and author(s) are credited.

Link: <https://doi.org/10.3897/zookeys.1065.69171.suppl4>

